PREDICTION OF EXPANSIVE CLAY ROUGHNESS IN PAVEMENTS WITH VERTICAL MOISTURE BARRIERS

PB99-157935

by

Ranasinghege Jayatilaka
Research Assistant
Texas Transportation Institute

and

Robert L. Lytton
Research Engineer
Texas Transportation Institute

Report 187-28F
Research Study Number 0-187
Research Study Title: Monitoring Moisture Barriers in Expansive Clay - Tasks 1 & 2

Sponsored by the
Texas Department of Transportation
In Cooperation with
U.S. Department of Transportation
Federal Highway Administration

October 1997

TEXAS TRANSPORTATION INSTITUTE
The Texas A&M University System
College Station, Texas 77843-3135

REPRODUCED BY: NTIS
U.S. Department of Commerce
National Technical Information Service
Springfield, Virginia 22161

IMPLEMENTATION STATEMENT

The results of this study should be implemented by using the pavement roughness program in this report when any pavement site on expansive clay is being considered for a vertical moisture barrier.

This study has developed a method of predicting the ability of vertical moisture barriers to reduce the development of roughness in pavements built on expansive clay subgrades and to predict the roughness in a given wheel path in pavements with or without vertical moisture barriers. To start with, the Texas Department of Transportation should implement the procedure on a pilot basis when the vertical moisture barriers are placed in new or existing pavements.

Data required for the program should be collected through a proper site investigation and laboratory testings. A description of a proper site investigation and the tests to determine the required soil properties is presented in Appendix E of Research Report No. 1165-2F Effectiveness of Controlling Pavement Roughness Due to Expansive Clays with Vertical Moisture Barriers. Implementation of the site investigation and test procedures recommended in that report should be used to investigate the site of the proposed moisture barrier. Life-cycle cost analysis should be carried out to decide whether the barriers are needed for a particular pavement section and to choose the barrier depth.

PROTECTED UNDER INTERNATIONAL COPYRIGHT
ALL RIGHTS RESERVED.
NATIONAL TECHNICAL INFORMATION SERVICE
U.S. DEPARTMENT OF COMMERCE

Technical Report Documentation Page

1. Report No.	2. Government Accession No.	3. Recipient's Catalog No.
FHWA/TX-98/187-28F		

4. Title and Subtitle	5. Report Date
PREDICTION OF EXPANSIVE CLAY ROUGHNESS IN PAVEMENTS WITH VERTICAL MOISTURE BARRIERS	October 1997
	6. Performing Organization Code
7. Author(s)	8. Performing Organization Report No.
Ranasinghege Jayatilaka and Robert L. Lytton	Report 187-28F
9. Performing Organization Name and Address	10. Work Unit No. (TRAIS)
Texas Transportation Institute Texas A&M University System College Station, Texas 77843-3135	11. Contract or Grant No. Study No. 0-187
12. Sponsoring Agency Name and Address	13. Type of Report and Period Covered
Texas Department of Transportation Research and Technology Transfer Office P. O. Box 5080 Austin, Texas 78763-5080	Final: September 1993- August 1997
	14. Sponsoring Agency Code

15. Supplementary Notes

Research performed in cooperation with the Texas Department of Transportation, Federal Highway Administration and the Texas Department of Transportation.

Research Study Title: Monitoring Moisture Barriers in Expansive Clay - Tasks 1 & 2

16. Abstract

This report summaries the results and conclusions of a multi-year study of the monitoring of moisture barriers in expansive soils. During the study, the surface profile measurements in ten different sites with moisture barriers were obtained using the 690D Surface Dynamics Profilometer operated by the Texas Department of Transportation. These measurements were then analyzed in terms of Serviceability Index and International Roughness Index using the computer program VERTAC. These data were fitted to appropriate models for the growth of roughness with time, and regression constants were obtained.

The development of pavement roughness due to expansive clay activity is caused by the differential movement of subgrade soil. The vertical movement at the edge of the pavement due to shrinking and swelling is higher than that of the interior of the pavement. A model was developed to predict the vertical movement in any given wheel path of a pavement as it is affected by a vertical moisture barrier at the edge of the pavement. Using this model, the vertical movement in the all wheel paths of the ten sites studies was estimated.

Another model was developed to predict the pavement roughness in terms of Serviceability Index and International Roughness Index by correlating regression constants obtained from the roughness analysis to the vertical movement estimated from the vertical movement model. The model developed calculates the roughness development due to traffic using the AASHTO model.

The vertical movement model and the roughness model developed were then assembled in the computer program PRES, which is written in FORTRAN language. The input data required for the program include the basic soil properties, climatic data, depth of a vertical moisture barrier, pavement geometry and structural properties, lateral drainage and longitudinal slope conditions, and traffic. The output will be the predicted roughness with time in any given wheel path. The program may be used to determine the depth of a moisture barrier that will meet the designers target level of pavement roughness after a selected number of years of service. Example problems demonstrate the capabilities of the program.

17. Key Words	18. Distribution Statement
Expansive Clay, Swelling Soils, Pavements, Moisture Barriers, Pavement Roughness, Suction-vs-Water Content Relations, Thornthwaite Moisture Index, Suction Compression Index, Serviceability Index, International Roughness Index, Computer Prediction	No restrictions. This document is available to the public through NTIS: National Technical Information Service 5285 Port Royal Road Springfield, Virginia 22161

19. Security Classif.(of this report)	20. Security Classif.(of this page)	21. No. of Pages	22. Price
Unclassified	Unclassified	310	

Form DOT F 1700.7 (8-72) Reproduction of completed page authorized

DISCLAIMER

The contents of this report reflect the views of the authors who are responsible for the facts and the accurate of the data presented herein. The contents do not necessarily reflect the official view or policies of the Texas Department of Transportation (TxDOT), or the Federal Highway Administration (FHWA). This report does not constitute a standard, specification, or regulation.

TABLE OF CONTENTS

Page

LIST OF FIGURES xi
LIST OF TABLES xiii
SUMMARY xix

CHAPTER
I INTRODUCTION 1
Expansive Soils 1
Pavement Roughness 2
Expansive Soil Treatment Methods 3
Problem Statement 5
Research Objectives 7
Research Approach 7
Report Organization 9

II BACKGROUND 11
Characterization of Expansive Soils 11
Pavement Roughness 23
Vertical Moisture Barriers 41

III DATA COLLECTION 45
Description of Test Sites 48
Roughness Data 55
Subgrade Soil Properties 57
Climatic Data 60

IV MODEL TO PREDICT VERTICAL MOVEMENT 63
Two Dimensional Vertical Movement Program FLODEF 64
One Dimensional Vertical Movement Program MOPREC 68
Prediction Model 80

V DEVELOPMENT OF ROUGHNESS MODEL 99
Modification to the MOPREC Program 100
Estimation of Vertical Movement at Different Wheel Paths 104
Model Development 109
Example Problems 119
Computer Program PRES 122

TABLE OF CONTENTS (continued)

VI CONCLUSIONS AND RECOMMENDATIONS 129
Conclusions 129
Recommendations 132

REFERENCES 135
APPENDIX A 145
APPENDIX B 193
APPENDIX C 211
APPENDIX D 223
APPENDIX E 225
APPENDIX F 227
APPENDIX G 229
APPENDIX H 241
APPENDIX I 279

LIST OF FIGURES

FIGURE Page

1.1 A Typical Cross Section of a Roadway with Vertical Moisture Barriers . . . 6
2.1 Chart for the Prediction of Suction Compression Index (McKeen 1980) 21
2.2 Typical Values of International Roughness Indices (Sayers et al.1986) 31
2.3 Quarter Car Model and Frequency Response to Slope Input Used for IRI (Sayers et al. 1986) 33
2.4 Fourier Amplitude Spectra of Typical Rough and Smooth Highway Profiles (Gay 1994) 38
3.1 Location Map of Test Sites 46
3.2. Arrangement of Profilometer Measurements along a Typical Interstate Highway 56
3.3 Thornthwaite Moisture Index for Texas (Wray 1978) 62
4.1 Initial Moisture Profiles over Root Depth 75
4.2 Suction Profiles for Swelling and Shrinkage Calculation 78
4.3 Vertical Movement for Different Barrier Depths 88
4.4 Vertical Movement for Different Soil Types 89
4.5 Vertical Movement for Different Thornthwaite Moisture Indices 90
4.6 Vertical Movement from FLODEF Vs. Predictive Model for Pavement Width of 9.0 m 93
4.7 Vertical Movement from FLODEF Vs. Predictive Model for Pavement Width of 12.6 m 94
4.8 Vertical Movement from FLODEF Vs. Predictive Model for Pavement Width of 16.2 m 95
4.9 Vertical Movement from FLODEF Vs. Predictive Model for Pavement Width of 23.4 m 96
4.10 Vertical Movement from FLODEF Vs. Predictive Model for Pavement Width of 34.2 m 97
4.11 Vertical Movement from FLODEF Vs. Predictive Model for Pavement Width of 45.0 m 98
5.1 Different Lateral Drainage Conditions of a Pavement 103
5.2 Frequency Distribution of B_s 112
5.3 Frequency Distribution of B_i 113
5.4 International Roughness Index Vs. Serviceability Index 118
5.5 Comparison of Measured and Predicted Serviceability Index 120
5.6 Comparison of Measured and Predicted International Roughness Index 121
5.7 Loss of Serviceability Index Vs. Time for Different Barrier Depths 123

LIST OF FIGURES (Continued)

FIGURE Page

5.8 Change in International Roughness Index Vs. Time for Different Barrier Depths 124
5.9 Comparison of AASHTO Model and New Model Using Loss of Serviceability Index 125
5.10 Comparison of AASHTO Model and New Model Using Loss of Change in International Roughness Index 126
A.1 Site Plan - San Antonio, General McMullen Drive 145
A.2 Site Plan - San Antonio, IH 410 149
A.3 Site Plan - San Antonio, IH 37 152
A.4 Site Plan - Greenville, IH 30 161
A.5 Site Plan - San Antonio, US 281 169
A.6 Site Plan - San Antonio, IH 10 172
A.7 Site Plan - Sierra Blanca, IH 182
A.8 Site Plan - Seguin, IH 10 187
A.9 Site Plan - Converse, FM 188
A.10 Site Plan - Dallas, IH 635 189
C.1 Phase Diagrams for Saturated and Field Capacity Conditions 212
C.2 A Typical Plot of Suction Vs. Gravimetric Water Content 215
C.1 Phase Diagrams for Field Capacity and Arbitrary Suction Conditions 216

LIST OF TABLES

TABLE Page

2-1 Wes Classification of Potential Swell 11
3-1 Summary Details of Moisture Barrier Sites 47
3-2 Subgrade Soil Properties - San Antonio Sites 57
3-3 Subgrade Soil Properties - Converse, FM 1516 57
3-4 Subgrade Soil Properties - Seguin, IH 10 58
3-5 Subgrade Soil Properties - Dallas, IH 635 58
3-6 Subgrade Soil Properties - Greenville, IH 30 59
3-7 Subgrade Soil Properties - Sierra Blanca, IH 10 60
3-8 Mean Thornthwaite Moisture Index of Test Sites 61
4-1 Coefficients for the Estimation of Parameters for Amplitude of Moisture Depths 71
4-2 Soil Properties Used in Developing Vertical Movement Model 81
4-3 Vertical Movements from MOPREC Program 81
4-4 Moisture Depths and Mean Matrix Suctions for Soil Type 1 82
4-5 Moisture Depths and Mean Matrix Suctions for Soil Type 2 82
4-6 Moisture Depths and Mean Matrix Suctions for Soil Type 3 83
4-7 Moisture Depths and Mean Matrix Suctions for Soil Type 4 83
4-8 Suction Profile Constants for Soil Type 1 84
4-9 Suction Profile Constants for Soil Type 2 85
4-10 Suction Profile Constants for Soil Type 3 85
4-11 Suction Profile Constants for Soil Type 4 86
5-1 Minimum Suction (pF) for Different Slope and Drainage Conditions 104
5-2 Desorption Coefficients - San Antonio Sites 105
5-3 Desorption Coefficients - Seguin, IH 10 105
5-4 Desorption Coefficients - Dallas, IH 635 106
5-5 Desorption Coefficients - Sierra Blanca, IH 10 106
5-6 Desorption Coefficients - Greenville, IH 30 107
5-7 Desorption Coefficients - Converse, FM 1516 107
5-8 Geometrical Data in Test Sections 108
A-1 Serviceability Index, San Antonio, General McMullen Drive, Section 1 145
A-2 Serviceability Index, San Antonio, General McMullen Drive, Section 2 146
A-3 Serviceability Index, San Antonio, General McMullen Drive, Section 3 146
A-4 Serviceability Index, San Antonio, General McMullen Drive, Section 4 146

LIST OF TABLES (Continued)

TABLE Page

A-5 Serviceability Index, San Antonio, General McMullen Drive, Section 5 147
A-6 Serviceability Index, San Antonio, General McMullen Drive, Section 6 147
A-7 International Roughness Index (m/km), San Antonio, General McMullen Drive, Section 1 147
A-8 International Roughness Index (m/km), San Antonio, General McMullen Drive, Section 2 148
A-9 International Roughness Index (m/km), San Antonio, General McMullen Drive, Section 3 148
A-10 International Roughness Index (m/km), San Antonio, General McMullen Drive, Section 4 148
A-11 International Roughness Index (m/km), San Antonio, General McMullen Drive, Section 5 149
A-12 International Roughness Index (m/km), San Antonio, General McMullen Drive, Section 6 149
A-13 Serviceability Index, San Antonio, IH 410, Section 1 150
A-14 Serviceability Index, San Antonio, IH 410, Section 2 150
A-15 Serviceability Index, San Antonio, IH 410, Section 3 150
A-16 Serviceability Index, San Antonio, IH 410, Section 4 151
A-17 International Roughness Index (m/km), San Antonio, IH 410, Section 1 151
A-18 International Roughness Index (m/km), San Antonio, IH 410, Section 2 151
A-19 International Roughness Index (m/km), San Antonio, IH 410, Section 3 152
A-20 International Roughness Index (m/km), San Antonio, IH 410, Section 4 152
A-21 Serviceability Index, San Antonio, IH 37, Section 1 153
A-22 Serviceability Index, San Antonio, IH 37, Section 2 153
A-23 Serviceability Index, San Antonio, IH 37, Section 3 153
A-24 Serviceability Index, San Antonio, IH 37, Section 4 154
A-25 Serviceability Index, San Antonio, IH 37, Section 5 154
A-26 Serviceability Index, San Antonio, IH 37, Section 6 154
A-27 Serviceability Index, San Antonio, IH 37, Section 7 155
A-28 Serviceability Index, San Antonio, IH 37, Section 8 155
A-29 Serviceability Index, San Antonio, IH 37, Section 9 155
A-30 Serviceability Index, San Antonio, IH 37, Section 10 156
A-31 Serviceability Index, San Antonio, IH 37, Section 11 156
A-32 Serviceability Index, San Antonio, IH 37, Section 12 156

LIST OF TABLES (Continued)

TABLE Page

A-33 International Roughness Index (m/km), San Antonio, IH 37, Section 1 157
A-34 International Roughness Index (m/km), San Antonio, IH 37, Section 2 157
A-35 International Roughness Index (m/km), San Antonio, IH 37, Section 3 157
A-36 International Roughness Index (m/km), San Antonio, IH 37, Section 4 158
A-37 International Roughness Index (m/km), San Antonio, IH 37, Section 5 158
A-38 International Roughness Index (m/km), San Antonio, IH 37, Section 6 158
A-39 International Roughness Index (m/km), San Antonio, IH 37, Section 7 159
A-40 International Roughness Index (m/km), San Antonio, IH 37, Section 8 159
A-41 International Roughness Index (m/km), San Antonio, IH 37, Section 9 159
A-42 International Roughness Index (m/km), San Antonio, IH 37, Section 10 160
A-43 International Roughness Index (m/km), San Antonio, IH 37, Section 11 160
A-44 International Roughness Index (m/km), San Antonio, IH 37, Section 12 160
A-45 Serviceability Index, Greenville, IH 30, Section 1 161
A-46 Serviceability Index, Greenville, IH 30, Section 2 162
A-47 Serviceability Index, Greenville, IH 30, Section 3 162
A-48 Serviceability Index, Greenville, IH 30, Section 4 163
A-49 Serviceability Index, Greenville, IH 30, Section 5 163
A-50 Serviceability Index, Greenville, IH 30, Section 6 164
A-51 Serviceability Index, Greenville, IH 30, Section 7 164
A-52 Serviceability Index, Greenville, IH 30, Section 8 165
A-53 International Roughness Index (m/km), Greenville, IH 30, Section 1 165
A-54 International Roughness Index (m/km), Greenville, IH 30, Section 2 166
A-55 International Roughness Index (m/km), Greenville, IH 30, Section 3 166
A-56 International Roughness Index (m/km), Greenville, IH 30, Section 4 167

LIST OF TABLES (Continued)

TABLE Page

A-57 International Roughness Index (m/km), Greenville, IH 30, Section 5 167
A-58 International Roughness Index (m/km), Greenville, IH 30, Section 6 168
A-59 International Roughness Index (m/km), Greenville, IH 30, Section 7 168
A-60 International Roughness Index (m/km), Greenville, IH 30, Section 8 169
A-61 Serviceability Index, San Antonio, US 281, Section 1 170
A-62 Serviceability Index, San Antonio, US 281, Section 2 170
A-63 International Roughness Index (m/km), San Antonio, US 281, Section 1 171
A-64 International Roughness Index (m/km), San Antonio, US 281, Section 2 171
A-65 Serviceability Index, San Antonio, IH 10, Section 1 172
A-66 Serviceability Index, San Antonio, IH 10, Section 2 173
A-67 Serviceability Index, San Antonio, IH 10, Section 3 173
A-68 Serviceability Index, San Antonio, IH 10, Section 4 174
A-69 Serviceability Index, San Antonio, IH 10, Section 5 174
A-70 Serviceability Index, San Antonio, IH 10, Section 6 175
A-71 Serviceability Index, San Antonio, IH 10, Section 7 175
A-72 Serviceability Index, San Antonio, IH 10, Section 8 176
A-73 Serviceability Index, San Antonio, IH 10, Section 9 176
A-74 Serviceability Index, San Antonio, IH 10, Section 10 177
A-75 International Roughness Index (m/km), San Antonio, IH 10, Section 1 177
A-76 International Roughness Index (m/km), San Antonio, IH 10, Section 2 178
A-77 International Roughness Index (m/km), San Antonio, IH 10, Section 3 178
A-78 International Roughness Index (m/km), San Antonio, IH 10, Section 4 179
A-79 International Roughness Index (m/km), San Antonio, IH 10, Section 5 179
A-80 International Roughness Index (m/km), San Antonio, IH 10, Section 6 180
A-81 International Roughness Index (m/km), San Antonio, IH 10, Section 7 180
A-82 International Roughness Index (m/km), San Antonio, IH 10, Section 8 181

LIST OF TABLES (Continued)

TABLE Page

A-83 International Roughness Index (m/km), San Antonio, IH 10, Section 9 181
A-84 International Roughness Index (m/km), San Antonio, IH 10, Section 10 182
A-85 Serviceability Index, Sierra Blanca, IH 10, Section 1 183
A-86 Serviceability Index, Sierra Blanca, IH 10, Section 2 183
A-87 Serviceability Index, Sierra Blanca, IH 10, Section 3 183
A-88 Serviceability Index, Sierra Blanca, IH 10, Section 4 184
A-89 Serviceability Index, Sierra Blanca, IH 10, Section 5 184
A-90 Serviceability Index, Sierra Blanca, IH 10, Section 6 184
A-91 International Roughness Index (m/km), Sierra Blanca, IH 10, Section 1 185
A-92 International Roughness Index (m/km), Sierra Blanca, IH 10, Section 2 185
A-93 International Roughness Index (m/km), Sierra Blanca, IH 10, Section 3 185
A-94 International Roughness Index (m/km), Sierra Blanca, IH 10, Section 4 186
A-95 International Roughness Index (m/km), Sierra Blanca, IH 10, Section 5 186
A-96 International Roughness Index (m/km), Sierra Blanca, IH 10, Section 6 186
A-97 Serviceability Index, Seguin, IH 10, Section 1 187
A-98 Serviceability Index, Seguin, IH 10, Section 2 187
A-99 International Roughness Index (m/km), Seguin, IH 10, Section 1 188
A-100 International Roughness Index (m/km), Seguin, IH 10, Section 2 188
A-101 Serviceability Index, Converse, FM 1516, Section 1 189
A-102 International Roughness Index (m/km), Converse, FM 1516, Section 1 189
A-103 Serviceability Index, Dallas, IH 635, Section 1 190
A-104 Serviceability Index, Dallas, IH 635, Section 2 190
A-105 International Roughness Index (m/km), Dallas, IH 635, Section 1 190
A-106 International Roughness Index (m/km), Dallas, IH 635, Section 2 191
B-1 Coefficient ξ_1 for Pavement Width of 9.0 m 193
B-2 Coefficient ξ_1 for Pavement Width of 12.6 m 194

LIST OF TABLES (Continued)

TABLE Page

B-3 Coefficient ξ_1 for Pavement Width of 16.2 m 195
B-4 Coefficient ξ_1 for Pavement Width of 23.4 m 196
B-5 Coefficient ξ_1 for Pavement Width of 34.2 m 197
B-6 Coefficient ξ_1 for Pavement Width of 45.0 m 198
B-7 Coefficient ξ_2 for Pavement Width of 9.0 m 199
B-8 Coefficient ξ_2 for Pavement Width of 12.6 m 200
B-9 Coefficient ξ_2 for Pavement Width of 16.2 m 201
B-10 Coefficient ξ_2 for Pavement Width of 23.4 m 202
B-11 Coefficient ξ_2 for Pavement Width of 34.2 m 203
B-12 Coefficient ξ_2 for Pavement Width of 45.0 m 204
B-13 Coefficient ξ_3 for Pavement Width of 9.0 m 205
B-14 Coefficient ξ_3 for Pavement Width of 12.6 m 206
B-15 Coefficient ξ_3 for Pavement Width of 16.2 m 207
B-16 Coefficient ξ_3 for Pavement Width of 23.4 m 208
B-17 Coefficient ξ_3 for Pavement Width of 34.2 m 209
B-18 Coefficient ξ_3 for Pavement Width of 45.0 m 210
C-1 data to Estimate Desorption Coefficients 219
C-2 Regression Results of Soil Suction Versus Volumetric Water Content 219
C-3 Gardner Desorption Coefficients for CH Soils 220
C-4 Gardner's Desorption Coefficients for Various Groups of Soils 221
D-1 Estimated Vertical Movements (cm) at Test Sections 223
E-1 Coefficient ρ_s 225
E-1 Coefficient ρ_i 226
F-1 Roughness Model Constants B_s and B_i 227
G-1 Predicted Roughness with Time, Converse, FM 1516 232
G-2 Vertical Movement Parameters for Different Barrier Depths (Ex 2) 233
G-3 Vertical Movement Parameters for Different Barrier Depths (Ex 3) 237

SUMMARY

The Texas Department of Transportation has engaged in a prolonged effort to seek ways to minimize damage in pavements due to expansive clay movements. Previous field testings and laboratory work have shown that the controlling subgrade moisture condition would reduce these destructive movements in expansive clays. Recognizing this, the Texas Department of Transportation has installed vertical moisture barriers with impermeable geomembranes in several pavement sections across the state which had a history of pavement distortions (roughness development) due to expansive clay movements.

The objectives of this research were to (1) collect and reduce subgrade soil data, (2) perform profilometer (roughness) measurements on selected pavement sections on a biannual basis for several years, (3) reduce profilometer data to obtain roughness coefficients such as Present Serviceability Index (PSI), and International Roughness Index (IRI), (4) devise a methodology whereby pavement engineers can predict the future effect of barriers based on data collected through site investigation, for use in pavement analysis, design, rehabilitation, and other pavement management activities.

DATA COLLECTION

The study used data collected from ten different locations in three different climatic regions in Texas. Six of the sites are located in Bexar County. Other sites are located in Guadalupe, Dallas, Hunt, and Hudspeth counties. Vertical moisture barriers have been installed in nine of the sites. In the other site, a horizontal fabric barrier has been installed. Control sections, where no moisture barriers were installed, have been designated in nine of the sites studied. During the study, the pavement surface profiles on test and control sections were obtained generally on a biannual basis for several years using the 690D Surface Dynamics Profilometer operated by the Texas Department of Transportation. These measurements were then analyzed in terms of Serviceability Index and International

Roughness Index using the computer program VERTAC. Subgrade soil properties were obtained through laboratory testing of samples collected from the sites.

FINDINGS

The differential movement of pavements due to expansive clay activity is the major source of roughness in pavements built on expansive clay subgrades. Therefore, it is obvious that the roughness development in a wheel path is directly related to the magnitude of vertical movement in that wheel path. The vertical movement at the edge of the pavement due to shrinking and swelling is higher than that of the interior of the pavement. A simple model was developed to estimate the vertical movement at any point in a pavement in order to correlate the vertical movement to the roughness measurements made in different wheel paths of the pavement sections at test sites.

Two computer programs FLODEF and MOPREC were used to develop the model. The FLODEF program is a two-dimensional finite element program capable of calculating a vertical movement profile across a pavement section with or without a vertical moisture barrier. The MOPREC program is a one-dimensional vertical movement program, and it calculates the vertical movement at the edge of the pavement using subgrade soil properties and climatic data. Both programs use the extreme dry and wet suction profiles for a particular location to estimate the vertical movement. The vertical movement model was developed by employing a nonlinear regression analysis on the vertical movements calculated from the two programs. The vertical movements in all of the wheel paths of the ten sites studied were estimated from the vertical movement model developed.

Another model was developed to predict the development of pavement roughness with time. The Serviceability Index and International Roughness Index calculated for the pavement sections at the test sites suggested that the growth of roughness with time followed a sigmoidal or "S-shaped" pattern. By fitting the roughness data to an appropriate sigmoidal model using a non linear regression analysis, the regression coefficients were obtained for

each lane in each pavement section at each test site. These coefficients were then correlated to the estimated vertical movements and an expression for a parameter that describes the roughness development due to expansive clay activity was obtained. The other parameter in the roughness model is related to the development of roughness due to traffic and is calculated from the AASHTO model. This roughness model predicts the roughness development with time in terms of Serviceability Index and International Roughness Index.

The vertical movement model and the roughness model developed were then assembled in the computer program PRES, which is written in FORTRAN language. The input file for PRES is a simple nonformatted list of the input data. The input data required for the program include the basic soil properties, climatic data, depth of a vertical moisture barrier, pavement geometry and structural properties, lateral drainage, longitudinal slope conditions, and traffic. The program calculates the roughness in terms of Serviceability Index and International Roughness Index for 20 years in one year intervals from the date of initial construction or the date of rehabilitation. It is capable of calculating roughness in any given wheel path for pavements of up to 10 lanes in width. The program can also be used to determine the depth of a moisture barrier that will meet the designers target level of pavement roughness after a selected number of years of service.

The program first estimates the total vertical movement (the total of shrinkage and swelling) in a single column of soil at the edge of the pavement using the subgrade soil properties given in the input file. Subgrade soil properties include the Atterberg limits, grain size distribution, and coefficients to describe the suction versus water content (desorption) relationship. A method of estimating desorption coefficients and typical values of desorption coefficients for various groups of soils are also presented. In estimating the vertical movement in a single column of soil, the program takes into account the variability of soil layer properties in a soil profile. The program can accommodate a maximum of 10 layers of subgrade soil. The extreme suction profiles are estimated from a climatic model using desorption relationships and the Thornthwaite Moisture Index. The vertical movement at any

given wheel path is estimated using the vertical movement estimated for a single column of soil at the edge of the pavement and a set of regression equations in the vertical movement model.

The estimated vertical movement for a particular wheel path is then used to estimate the parameter that describes the roughness development due to expansive clay activity. The other parameter in the roughness model which is related to the development of roughness due to traffic, is calculated from the AASHTO model incorporated in the program. Using these two parameters and the initial roughness given in the input file, the growth of roughness with time for a given wheel path is estimated. Running the program for different vertical moisture barrier depths, the depth of a vertical moisture barrier required to meet the designers target level of pavement roughness after a selected number of years can be estimated. The program can accommodate 10 different barrier depths in one run.

The subgrade soil properties required for input to the program needs to be collected through a proper site investigation and laboratory testings. The Thornthwaite Moisture Index for a particular location can be obtained from the maps containing the spatial distribution of Thornthwaite Moisture Index. Such a map for the state of Texas is also given in this report.

CHAPTER I

INTRODUCTION

The existence of and problems associated with expansive soils are worldwide. In the United States, approximately 20 percent of the area is underlain by moderately to highly expansive soils (Krohn and Slosson 1980). A 1972 survey of the highway departments in the 50 states, District of Columbia, and Puerto Rico indicated that 36 states have expansive soils within their jurisdictions (Snethen 1979c). They are located primarily in: (1) Texas and along the Gulf Coast states, (2) the Appalachian states, (3) the southwest, and (4) the Great Plains (Krohn and Slosson 1980). The annual cost of damage to houses, buildings, roads, and pipelines caused by expansive soils was estimated in 1973 to exceed $2.3 billion, which was more than the combined damage caused by natural catastrophes such as earthquakes, tornadoes, hurricanes, and floods (Jones and Holtz 1973). More than half of these estimated damages were attributed to highways and streets. The Texas Department of Transportation spends millions of dollars to repair the damages caused by expansive soils every year.

EXPANSIVE SOILS

Expansive soils are those clay soils which have the capacity to undergo volumetric changes when subject to variances in water content. Expansive clay minerals which, because of their natural physicochemical properties, possess a net negative electrical charge imbalance that attracts the positive pole of dipolar water molecules and cations (FHWA 1980). As a result, water molecules build the double-layer water around the clay mineral and volume change occurs. Similarly, the cations are held to the surface of the clay mineral and contribute to the double-layer water buildup through their hydration. The osmotic force which occurs when the ion concentration differs between the double-layer water and the pore water also influences the volume change.

If an expansive soil gains moisture, it swells and upward movement results. On the other hand, if it loses moisture, soil shrinks and settlement occurs. Due to the variation of moisture conditions and soil characteristics, the magnitude of volume change may be different from point to point. This condition results in differential movement of soil which is detrimental for structures built on shallow foundations, such as buildings, highway pavements, and airport pavements.

The volume change of expansive soil depends on a wide range of variables such as soil characteristics, initial moisture content, climate, vegetation, in situ density, slope of the site, and changes brought about by man's actions (Simmons 1984). The soil characteristics include the type and amount of clay, the thickness and location of potentially expansive clay layers, and the depth of the active zone. Montmorillonite (smectite) is the predominant clay mineral found in most of the highly expansive soils (Snethen et al. 1975). However, the other clay minerals such as kaolinite, illite, vermiculite, and chlorite also exhibit some degree of expansiveness. The influence of type and amount of clay on swell potential was clearly shown by Skempton (1953). He defined the clay activity as the ratio of the plasticity index to the percentage clay content (finer than 2 microns) and showed that the swell potential increases with the activity. Seed et al. (1962) have shown that percentage clay (finer than 2 microns) and Atterberg limits of a soil can be used to obtain a reasonably accurate estimate for swell potential. They also have shown that the plasticity index alone gives a good approximate estimate for swell potential. Snethen (1979c) reported that the Atterberg limits (specifically, the liquid limit and plasticity index), Bar Linear Shrinkage, and the natural soil suction were the most consistent indicators of potential swell.

PAVEMENT ROUGHNESS

Pavement roughness is an extremely important measure as it directly affects the riding quality, road safety, and vehicle operating costs. The American Society for Testing Materials has defined roughness on a traveled surface as "the deviations of a pavement surface from a true planar surface with characteristic dimensions that affect vehicle dynamics, ride quality,

dynamic loads, and drainage" (ASTM 1994). Pavement roughness is caused by a combination of traffic loading and environmental effects such as frost heave and swelling.

The most common types of distress modes observed in highway pavements built on expansive soils are as follows:

1. surface unevenness distributed over a considerable length of road,
2. longitudinal cracks, and
3. excessive deformations in locations such as pipe culverts where moisture concentration occurs.

When a pavement is built on an expansive soil, the existing moisture flow pattern will be altered. The moisture condition at the center of the pavement will remain virtually unchanged while at the edge, moisture fluctuations will occur in response to rainfall and evapotranspiration (Picornell and Lytton 1989). This moisture variation (commonly referred to as the edge moisture variation) will result in shrinking or swelling under the edges of the pavement and causes the lateral differential movement of the pavement. The differential movement is the major source of roughness development in pavements on expansive soils. The other mechanism that causes differential movement is the formation of a physiographic feature known as gilgai (Beckmann et al. 1970). Gilgai, which is a wave-like surface pattern, is developed in natural clay soils due to climatic changes over time. Lytton et al. (1976) carried out a study in two gilgai fields in Texas and found that the wave patterns observed in pavements and in adjacent gilgai fields were similar.

EXPANSIVE SOIL TREATMENT METHODS

Numerous methods of controlling volume change have been attempted in the past by transportation agencies (Snethen 1979c; Hammitt and Ahlvin 1973; Sallberg and Smith 1965; FHWA 1980; Ardani 1992). All these methods can be grouped into the following two categories:

1. alteration of expansive material by mechanical, chemical or physical means, and
2. control of subgrade moisture conditions.

Mechanical alteration includes ripping, scarifying, and then compacting the soil with moisture and/or density control. The subexcavation and replacement with granular or non-swelling or chemically treated materials can also be grouped into this category. The third method of this category is the use of fills over expansive soils in order to reduce heave as a result of the external load. The application depth of ripping or scarifying is limited to approximately 45 cm to 60 cm, while subexcavation is limited to a maximum depth of 180 cm. Ripping or scarifying is best suited for application to secondary highways. However, this method may be suited for primary highways where the swell potential is low. The use of fills over expansive soils is limited to soils exhibiting low swell potential. In the physical alteration method, expansive soil is mixed with granular or nonswelling material. The chemical alteration refers to the addition of chemical compounds to alter the characteristics of clay minerals. Lime is the most extensively used chemical for modification of expansive soils. The lime stabilization using conventional mix-in-place techniques is generally limited to approximately 20 cm to 30 cm. The use of conventional lime stabilization is well suited for fill construction using potentially expansive soils and to chemically alter backfill material in conjunction with subexcavation and replacement. For stabilizing deeper depths, pressure injection of lime slurry can be used. However, there are conflicting reports concerning the effectiveness of pressure injection treatment of expansive soils (Thompson and Robnet 1976). The pressure injection of lime may be effective only under certain circumstances.

The control of the subgrade moisture condition is achieved by prewetting the subgrade or by isolating the subgrade soil from moisture variations. The idea of prewetting or ponding a subgrade prior to the construction of a pavement is to minimize the volume change after the construction by allowing preswelling of the subgrade as a result of the increased moisture condition. Prewetting a subgrade before the pavement placement has shown promising results in improving the pavement performance (Steinberg 1977). The limitations of the ponding method are that it can only be used as a preconstruction measure and it may take many months to saturate the subgrade soil.

Since the principal problem in expansive soils is due to the moisture differential, it is obvious that by isolating subgrade soil from moisture variation, the problem can be solved. This can partly be achieved by using a physical barrier made with a waterproofing membrane. The methods of using physical barriers that have been attempted in the past are:

1. sprayed asphalt membrane over the subgrade, ditches, verge slope, and back slope,
2. full-depth asphalt pavement with a sprayed asphalt or synthetic fabric membrane beneath the ditch,
3. full-depth asphalt pavement with paved ditches in cut sections, and
4. vertical synthetic impermeable fabric membrane cutoffs.

Based on the results obtained in Arizona, Forstie et al. (1979) reported that the asphalt-rubber membrane treatment over the badly distorted highway improved the overall performance. Of all the barrier types, the vertical moisture barrier appears to be the best since it can cutoff moisture moving not only from the vicinity of the pavement but also from beyond the ditches, verge slope, or back slope. And also, a vertical moisture barrier can be used before the placement of pavement as well as after the placement of pavement. The construction of a vertical moisture barrier involves the (1) excavation of a 30 cm wide trench using a trenching machine, (2) placing of a fabric membrane, (3) backfilling the trench with sand or gravel, and (4) placing of a cement stabilized base cap over the backfill material. A typical cross section of a roadway with a vertical moisture barrier is shown in Figure 1.1.

PROBLEM STATEMENT

The Texas Department of Transportation has engaged in a prolonged effort to seek ways to minimize damage in pavements due to expansive clay movements. Previous field testings and laboratory work have shown that the controlling subgrade moisture condition would reduce these destructive movements in expansive clays. Recognizing this, the Texas Department of Transportation has installed vertical moisture barriers with impermeable geomembranes in several pavement sections across the state which had a history of pavement distortions (roughness development) due to expansive clay movements.

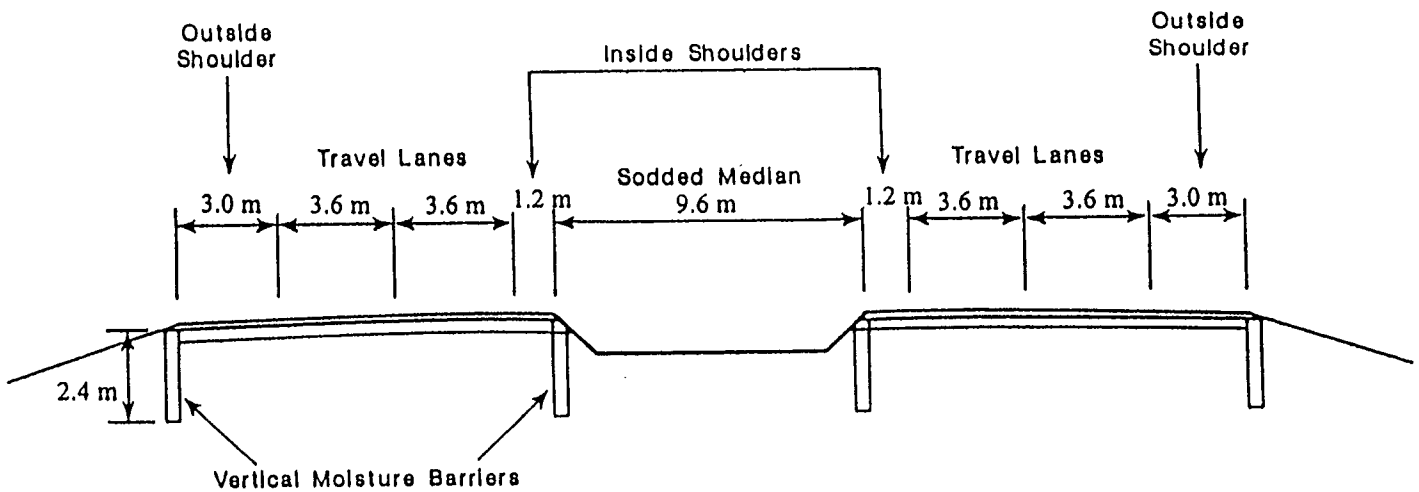

Figure 1.1. A Typical Cross Section of a Roadway with Vertical Moisture Barriers

The effectiveness of vertical moisture barriers depends upon the subgrade soil condition and the climate. With the limited resources available for the rehabilitation of pavements, decision makers are in need of a methodology to estimate the effect of a barrier on the pavement performance for a particular pavement section.

RESEARCH OBJECTIVES

The objectives of this research are to (1) collect and reduce subgrade soil data, (2) perform profilometer (roughness) measurements on selected pavement sections on a biannual basis for several years, (3) reduce profilometer data to obtain roughness coefficients such as Present Serviceability Index (PSI), and International Roughness Index (IRI), (4) devise a methodology whereby pavement engineers can predict the future effect of barriers based on data collected through site investigation, for use in pavement analysis, design, rehabilitation, and other pavement management activities.

RESEARCH APPROACH

The work plan of this project originally comprised two tasks. Task 1 was to evaluate the vertical moisture barriers in District 15 (San Antonio, Texas) at sections of IH-410, IH-37, IH-10, US 281, and General McMullen Drive. The Surface profile measurements on test and control sections were obtained using the profilometer owned by the Texas Department of Transportation. These measurements were then analyzed in terms of Present Serviceability Index (PSI), and International Roughness Index (IRI) using available computer software.

Task 2 involved similar measurements and analysis of moisture barrier sections in District 1 on IH-30 in Greenville, District 24 on IH-10 in Sierra Blanca, and the pavement sections established in another study (Project 1165) sponsored by the Texas Department of Transportation. The pavement sections in study 1165 included moisture barrier sections in District 18 on IH-635 in Dallas, in District 15 at sections of IH-10 in Seguin, and FM-1516 in Converse.

In the terminal year of this study, Task 3, Task 4, and Task 5 were added to the project. In Task 3, all the Present Serviceability Index (PSI) and International Roughness Index (IRI) data collected in Tasks 1 and 2 were analyzed and mathematical models were developed to predict the roughness with time in each lane and in each wheel path of a pavement.

The swell potential at any given point can be represented by the potential vertical movement at that point. Therefore, at first, a model to predict the vertical movement was developed in order to correlate the swell potential to the roughness development. Gay (1994) developed two computer programs , MOPREC and FLODEF, to estimate the potential vertical movement due to expansive clay activity. The computer program MOPREC is a one dimensional program and is based on a climatic model obtained from moisture balance procedure. The original program was for a single layer of soil. As part of the Task 3, the program was modified to accommodate a multi-layer soil profile. The computer program FLODEF is a two dimensional finite element program and is capable of calculating vertical movement profile across a pavement section with or without a vertical moisture barrier. However, at present, this program can be run only on the mainframe and is not feasible to use in a routine design procedure. To overcome this difficulty, the vertical movement profiles obtained from the FLODEF program for different pavement configurations, climatic conditions, and subgrade soil conditions were correlated to the vertical movements obtained from the MOPREC program and regression equations were developed. These regression equations and the modified MOPREC program are used to calculate the vertical movement at any given point in the pavement and are used in the roughness prediction model.

The final step of Task 3 was the development of a roughness prediction model. Plotting Present Serviceability Index (PSI) and the International Roughness Index (IRI) versus time, it was found that a sigmoidal or "S-shaped" curve would adequately describe the performance of pavements. Garcia-Diaz et al. (1984) also used this type of curve to describe the pavement performance and they reported that this type of curve would predict more realistic long-term behavior. The nonlinear regression technique was employed to fit the

roughness indices versus time to the sigmoidal model and regression constants were obtained for each wheel path of each lane of each test section. These constants and the estimated vertical movements for each wheel path were then used to develop the roughness prediction models.

In Task 4, a computer program was written in FORTRAN language to incorporate the models developed in Task 3. The input data to the program include the subgrade soil profile and the climatic condition at the site, cross-sectional geometry of the pavement, depth of moisture barriers to be considered, traffic, and structural properties of the pavement section. The output will be the predicted roughness with time in any selected wheel path.

Task 5 of this study was the documentation. In this task, this final report, which describes the findings and the relationships developed in this project, was prepared.

REPORT ORGANIZATION

This report consists of six chapters. The first chapter is the introduction which includes seven subsections: expansive soils, pavement roughness, expansive soil treatment methods, problem statement, research objectives, research approach, and report organization. In the second chapter, background information on characterization of expansive soils, measurement and prediction of pavement roughness in expansive soils, and vertical moisture barriers are presented. The third chapter of this report contains the data collection. This chapter includes a description of test sites, including subgrade soil conditions, pavement configurations, and barrier types. The fourth chapter is devoted to describe the development of the vertical movement model obtained by regression analysis of the data obtained from two programs MOPREC and FLODEF. In the fifth chapter, the results of nonlinear regression analysis performed to fit the roughness data to the sigmoidal models and the final roughness models are described. Finally, the sixth chapter presents the conclusions and recommendations of this study.

Eight appendices support this report. Appendix A contains Serviceability Index (PSI) and International Roughness Index data obtained for the test sites. In Appendix B, the regression coefficients obtained by fitting the vertical movements obtained for different conditions to a nonlinear model which were used to develop the vertical movement model are tabulated. Appendix C contains a procedure to estimate desorption coefficients of soil which is used to relate the water content to the soil suction, and the desorption coefficients that can be used for various groups of soils. Vertical movements estimated for test sections using the vertical movement model developed in Task 3 are given in Appendix D. In Appendix E, the regression coefficients obtained by fitting roughness data to sigmoidal models are presented. Appendix F contains the roughness model constants obtained for the test sections which were used to develop the roughness prediction model. Three example problems are solved using the roughness model developed in this study in Appendix G. Finally, in Appendix H, a complete description of the computer program developed in Task 4, its input and output and a listing of the program are presented.

CHAPTER II

BACKGROUND

CHARACTERIZATION OF EXPANSIVE SOILS

There is a considerable amount of knowledge available dealing with the nature and behavior of expansive soils as a result of many research studies performed during the last 30 years. The U.S. Army Waterways Experiment Station has produced a comprehensive series of reports which cover distribution maps of expansive soils in the USA, their geology, mineralogy, physicochemical properties, identification and classification techniques, volume change behavior, and treatment methods (Snethen et al. 1975, 1977a, 1977b; Snethen 1979a, 1979b, 1979c).

In the selection of effective treatment alternatives for a foundation in expansive soils, the two most important factors are identifying the expansive soils and estimating the potential volume change. The available methodologies of identifying expansive soils include mineralogical (x-ray diffraction, differential thermal analysis, infrared analysis, dye adsorption, cation exchange capacity), physical properties (Atterberg limits, colloid content), and soil classification systems. As an expedient methodology for identifying potentially expansive soils, Snethen (1979c) recommends the U.S. Army Corps of Engineers Waterways Experiment Station (WES) classification system which is given in Table 2-1.

Table 2-1. WES Classification of Potential Swell

Liquid Limit, %	Plasticity Index, %	Natural Soil Suction, kPa	Potential Swell
>60	>35	>383.0	High
50-60	25-35	143.6-383.0	Marginal
<50	<25	<143.6	Low

In order to quantitatively characterize the expansive soils, numerous methods have been developed in the past. As the main cause of damage to the structures built on expansive soil is due to the volume change behavior of such soils, all the methods available for quantitative characterization involve the estimation of swell pressure or percent swell. These techniques fall into three categories: (1) oedometer tests, (2) empirical or semi-empirical methodologies, and (3) soil suction tests.

Oedometer Test

In oedometer tests, estimates of volume change are obtained by applying the consolidation theory in reverse. Oedometers can be used to estimate either the swell pressure or the amount of swell depending on the structure being designed (FHWA 1980). If the applied load is large and the structure is rigid, then the swell pressure is measured. If the applied load is light and the structure is relatively flexible, then the amount of swell is measured. A large number of oedometer testing procedures have been proposed by many researchers. Two basic types of oedometer swell tests are the consolidation-swell test, and constant volume or swell pressure test (Snethen 1979c; Nelson and Miller 1992). In the consolidation-swell test, an unsaturated sample is initially loaded to a prescribed stress and then the sample is allowed to swell under that load when water is added. After swelling, the sample is further loaded until the initial void ratio is reached. Then the specimen is rebounded in decrements and the final void ratio is measured. The swell pressure is defined as the pressure required to recompress the fully swollen sample to its original volume. The amount of swell is calculated from the following relationship:

$$\frac{\Delta H}{H} = \frac{e_f - e_0}{1 + e_0} \tag{2.1}$$

where

e_0 = initial void ratio,

e_f = final void ratio,

ΔH = heave, and

H = layer thickness.

In the constant volume test, the sample is inundated while preventing the sample from swelling. The maximum applied stress required to maintain constant volume is defined as the swell pressure. The swell measurements obtained from oedometer results have been compared with the actual measured heave in the field in Sudan and Saudi Arabia (Osman et al. 1987; Dhowian et al. 1987). Both studies show that the oedometer methods overestimate the in situ heave.

Empirical Methods

The empirical or semi-empirical methods are based on the correlation between laboratory or field measurements and soil indices such as the liquid limit, plasticity index, and clay content. There are large numbers of these equations available in the literature. However, the use of such equations on a global basis is questionable. Rao and Smart (1980) evaluated four such equations using 10 different soils and showed that none of the equations considered were able to predict the swell accurately. They concluded that a strict test of similarity (geological, mineralogical, and textural) was needed in developing and using such equations. Snethen (1984) estimated the percent swell of 20 expansive soil samples using 17 published equations and compared them to the values obtained from the laboratory tests. The conclusion was that only four equations showed a balance with respect to their accuracy and conservatism. Zein (1987) applied five empirical equations to predict both swell percent and swelling pressure of nine Sudanese compacted residual black cotton soils and compared the laboratory results. He concluded that with the exception of one swell percent equation, none of the considered equations yielded acceptable predictions.

In Texas, the Potential Vertical Rise (PVR) method may be the most widely accepted empirical procedure used in the estimation of volume change behavior of expansive soils. The procedure was developed by correlating measured volumetric swell with basic soil properties (McDowell 1956). In this procedure, the family of universal curves, developed for

the relationship between volumetric swell and surcharge load and an assumed fixed relationship of one-third between linear swell and volumetric swell, are used to estimate the potential vertical movement. Also, data presented in this procedure enables the estimation of vertical movement from the plasticity index alone.

Soil Suction Method

Soil suction is a macroscopic property of soil which indicates the intensity with which a soil will attract water. The total suction consists of two components namely, matric suction and osmotic suction. Matric suction is defined as the negative gauge pressure relative to the external gas pressure on the soil water, to which a solution identical in composition with the soil water must be subjected in order to be in equilibrium through a porous permeable wall with the soil water. The osmotic suction is the negative gauge pressure to which a pool of pure water must be subjected in order to be in equilibrium through a semipermeable (i.e., permeable to water molecules only) membrane with a pool containing a solution identical in composition with the soil water (Krahn and Fredlund 1972). Methods available for measurement of suction in soil include the (1) filter paper method, (2) thermocouple psychrometer, (3) thermal moisture sensor, (4) tensiometer, (5) vacuum desiccator, and (6) pressure plate apparatus (Ridley and Wray 1995).

By evaluating available testing and prediction procedures in expansive soils, Snethen et al. (1979c) reported that the soil suction concept and associated testing and prediction procedures provided a better characterization of the behavior of expansive soils and a more reliable estimate of anticipated volume change.

Several authors have proposed models to estimate the volume change behavior in expansive soils using soil suction data. Snethen et al. (1979c) proposed the following equation to calculate the vertical movement:

$$\frac{\Delta H}{H} = \frac{C_\tau}{1 + e_0}[(A - Bw_0) - \log(\tau_{mf} + \alpha\sigma_f)] \tag{2.2}$$

where

ΔH	=	vertical movement,
H	=	stratum thickness,
C_τ	=	suction index,
e_0	=	initial void ratio,
A, B	=	constants of suction vs. water content relationship,
w_0	=	initial moisture content in percent,
τ_{mf}	=	final matric suction,
α	=	compressibility factor, and
σ_f	=	final applied pressure.

The C_τ is given by:

$$C_\tau = \frac{\alpha G_s}{100B} \tag{2.3}$$

where

G_s	=	specific gravity.

The suction versus water content is given by:

$$\log T_m^0 = A - Bw \tag{2.4}$$

where

T_m^0	=	matric soil suction without surcharge, and
w	=	water content.

The specific gravity, initial void ratio, constants A and B, initial moisture content, and compressibility factor are determined in the laboratory. The final matric suction and the final applied pressure are functions of the depth of active zone. The depth of active zone has been defined as the thickness of the layer of soil in which a moisture deficiency exists, and is

dependent upon the soil type, soil structure, topography, and climate.

Assuming the vertical strain of expansive soil is linearly proportional to the soil suction, Mitchell and Avalle (1984) presented the following equation to estimate the vertical movement:

$$\Delta H = \sum_{i=1}^{N} (I_{pt} * \Delta u * H_i) \tag{2.5}$$

where

ΔH	=	vertical movement,
N	=	number of layers to depth of active zone,
I_{pt}	=	instability index,
Δu	=	soil suction change, and
H_i	=	thickness of layer I.

The Instability Index is determined from the core shrinkage test by measuring the linear strain versus moisture change relationship and the moisture characteristic of unconfined undisturbed samples which are allowed to dry from a moisture content above the shrinkage limit. The equation to calculate Instability Index is as follows:

$$I_{pt} = \frac{\epsilon}{\Delta w} * \frac{\Delta w}{\Delta u} \tag{2.6}$$

where

ϵ	=	vertical strain,
Δw	=	amount of moisture soil gains or loses, and
Δu	=	change of soil suction expressed in pF.

Hamberg (1985) presented the following model to estimate the vertical movement:

$$\Delta H = \sum_{i=1}^{N} [\frac{H_i}{(1 + e_0)_i}] * [C_h * \Delta \log(h)]_i \tag{2.7}$$

where

ΔH	=	vertical movement,
N	=	number of layers to depth of active zone,
H_i	=	thickness of layer i,
e_0	=	initial void ratio of layer i,
C_h	=	suction index with respect to void ratio (slope of void ratio verses soil suction in logarithmic scale), and
h	=	soil suction (total or matric).

In terms of water content, the above model takes the following form (Hamberg 1985):

$$\Delta H = \sum_{i=1}^{N} [\frac{H_i}{(1 + e_0)_i}] * [(C_w * \Delta w)_i] \tag{2.8}$$

where

C_w	=	modulus ratio (slope of void ratio versus water content), and
Δw	=	change in water content.

Miller et al. (1995) presented the following equation to estimate the vertical movement:

$$\Delta H = \sum_{i=1}^{N} \frac{(C_w \Delta w)_i}{(1 + e_0)_i} H_i \tag{2.9}$$

where

ΔH	=	vertical movement,
N	=	number of layers to depth of active zone,
C_w	=	CLOD index,

Δw = change in water content,

e_0 = initial void ratio, and

H_i = thickness of layer i.

The CLOD index (C_w) is obtained from the CLOD test (McKeen 1985) developed in the New Mexico Engineering Research Institute. The slope of void ratio versus water content curve is defined as the CLOD index.

Lytton (1977) presented the following equation to estimate the volumetric strain of an elemental volume of soil.

$$\frac{\Delta V}{V} = -\gamma_h \log_{10}\left(\frac{h_f}{h_i}\right) - \gamma_\sigma \log_{10}\left(\frac{\sigma_f}{\sigma_i}\right) \tag{2.10}$$

where

ΔV = volume change,

V = initial volume,

γ_h = suction compression index,

h_i, h_f = initial and final suction,

γ_σ = compressibility constant,

σ_f = final mean principal stress, and

σ_i = initial mean principal stress above which volume change occurs. It is approximately 3 to 7 kPa.

This model was further modified as follows to separate the osmotic and matric suction components (Lytton 1995):

$$\frac{\Delta V}{V} = -\gamma_h \log_{10}\left(\frac{h_{mf}}{h_{mi}}\right) - \gamma_\sigma \log_{10}\left(\frac{\sigma_f}{\sigma_i}\right) - \gamma_\pi \log_{10}\left(\frac{\pi_f}{\pi_i}\right) \tag{2.11}$$

where

γ_h = gas law constant for volume change due to changes in matric suction,

h_{mi}, h_{mf} = initial and final matric suction,

γ_π = gas law constant for volume change due to changes in osmotic suction, and

π_i, π_f = initial and final osmotic suction.

The vertical movement can be calculated by dividing the depth of the active zone into a number of layers (N) and finding the average volumetric strain for each layer from the equation. The vertical movement is then given by the following relationship (Picornell and Lytton 1984).

$$\Delta H = \sum_{i=1}^{N} f_i \left(\frac{\Delta V}{V} \right)_i H_i \tag{2.12}$$

where

ΔH = vertical movement,

$\Delta v/v$ = volumetric strain,

H_i = thickness of layer i, and

f = factor to include the effect of lateral confinement; it ranges from 1.0 for nonfissured soil to 0.33 for highly fissured deposits.

The compressibility index (γ_σ) can be calculated from the following equation:

$$\gamma_\sigma = \frac{C_s}{1 + e_0} \tag{2.13}$$

where

C_s = pre-consolidated swelling or compression index, and

e_0 = initial void ratio.

The suction compression index (γ_h) can be estimated from Soil Conservation Service COLE test or the CLOD test. Picornell and Lytton (1984) estimated γ_h and γ_σ in the laboratory. They estimated the coefficient γ_h by a backcalculation procedure using equation 2.10 for the case of unrestricted swelling. The coefficient γ_σ was backcalculated from equation 2.10 using swell pressure (constant suction) test data.

McKeen (1980) developed an empirical procedure to calculate the Suction Compression Index (γ_h or SCI) as a function of plasticity index (PI), cation exchange capacity (CEC), and percent clay (finer than 2 micron) content. This procedure involves the calculation of the activity (Ac) and cation exchange activity (CEAc) as follows:

$$Ac = \frac{PI}{\%\ clay} \tag{2.14}$$

$$CEAc = \frac{CEC}{\%\ clay} \quad meq/100\ g \tag{2.15}$$

The percent clay content is obtained by dividing the fine clay content (finer than 2 micron) by percentage passing No. 200 sieve. For the estimation of γ_h, McKeen developed a chart which is shown in Figure 2.1. The values given in the chart are Suction Compression Index (SCI) for 100% fine clay content. The actual SCI is calculated by multiplying the values in the chart by the fine clay content of soil. The cation exchange capacity required for this procedure can be determined by a routine test procedure performed in agricultural laboratories. However, in the absence of laboratory test results, the following empirical relationships (Mojekwu 1979) can be used to obtain the cation exchange capacity:

$$\begin{aligned} CEC &= (PL)^{1.17} \quad meq/100\ g \quad ,or \\ CEC &= (LL)^{0.912} \quad meq/100\ g \end{aligned} \tag{2.16}$$

where

PL = plasticity limit , in percent, and

LL = liquid limit, in percent.

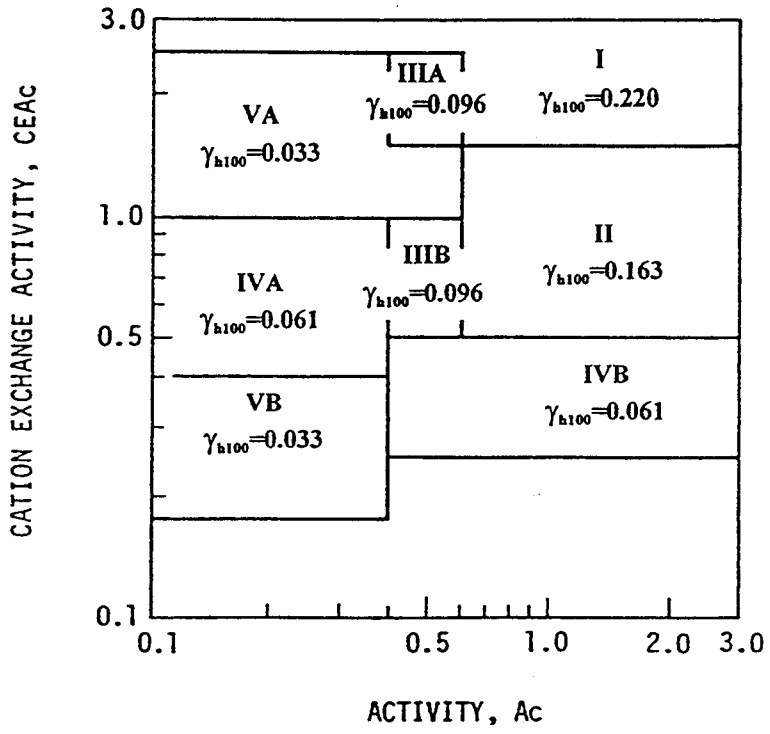

Figure 2.1. Chart for the Prediction of Suction Compression Index (McKeen 1980)

Climatic Influence on Vertical Movement

Significant areas of the earth's surface are classified as arid and semi-arid. These areas are characterized by deep groundwater tables. Soils located above the groundwater table are generally in unsaturated states. The moisture condition of the soil is controlled by the moisture balance between precipitation and evapotranspiration. Therefore, there is a wide variability in the water content of soil in the unsaturated zone with the seasonal climatic variations. The incorrect estimation of vertical movement from the oedometer type testings and empirical equations which are generally based on the oedometer type test results may be due to the difficulty in testing these unsaturated soils in oedometer. Gromko (1974) reports that upon wetting and application of load, the unsaturated soil samples tend to collapse, or otherwise heave will be overestimated. In contrast, the soil suction measurements can be made in unsaturated soils fairly accurately.

The climate has been given a scant attention if not neglected at all in the previously described oedometer type testings and empirical procedures. Many researchers have emphasized the effect of climate on vertical movement. Russam and Coleman (1961) have shown that where the water-table is present close to the surface, the moisture condition of subgrade soil is controlled by the water-table irrespective of climate and where the water-table is deeper or nonexistent, the main factors determining moisture condition in soil are rainfall and evapotranspiration. They also presented evidences of a relationship between soil suction and the Thornthwaite Moisture Index. The Thornthwaite Moisture Index is derived from a moisture balance procedure between rainfall and evapotranspiration (Thornthwaite 1948) and can be used to characterize climate. Bartelli and McCormack (1976) indicated that the predicting of swelling properties in expansive soils required the integration of soil test data and the environment of the soil. They stated that the soil moisture regimes and soil temperature regimes could be used to characterize the environment. Based on the results of 14 ground movement stations in Melbourne, Australia, Holland and Lawrence (1980) concluded that the movement of soil at the edge of a cover closely followed the evaporation minus rainfall pattern. Juca et al. (1995) studied the climatic influence on ground movements

in an unsaturated expansive clay site in Brazil. Their results indicated that there was an excellent agreement between moisture balance and vertical displacement with time. Also, the soil movements were strongly dependent upon soil suction.

Soil suction theory can be used to establish an envelope within which the soil suction vertical profile beneath a covered surface might be expected to vary as the soil becomes drier during dry seasons or wetter during wet seasons (Wray 1987). These boundaries of soil suction envelope can be used to estimate the potential vertical movement. Wray (1992) used these suction envelopes to predict the potential vertical movement in two sites in Texas and found that the predicted values compared well with the measured vertical movements.

The other important parameter in the estimation of vertical movement is the vegetation. The significance of the vegetation on vertical movement has been shown by Ward (1953), Ravina (1983), and Alonso and Loret (1995). Wray (1987) reported that during times of adequate rainfall, the vegetation did not significantly influence the vertical suction profile, and during periods of inadequate precipitation, the vegetation influenced the vertical suction profile.

From the foregoing discussion, it is evident that the methods based on soil suction theory and accurate modeling of climate and vegetation yield good predictive models for vertical movement in expansive soils.

PAVEMENT ROUGHNESS

Pavement roughness is an extremely important measure in the pavement management system. It is an indicator of road condition or riding quality of a pavement. The loss of riding quality of a pavement is not only uncomfortable for those occupying a vehicle as it travels the highway but also increases the cost of travel through increased fuel consumption and vehicle maintenance. In addition, the pavement may be subject to increased stresses and strains due to increased bouncing of vehicles on a rough roadway thus increasing the cost of

pavement maintenance. The roughness increases over time with the loss of smoothness in the pavement due to traffic loading and forces exerted by frosting or swelling of clay subgrades. The roughness is measured by taking profile measurements on a pavement. There are at least four fundamental uses of pavement surface profile measurements (Carey 1973). They are as follows:

1. construction quality control,
2. locate points where abnormal changes in pavement surface occur due to different subsurface soil or drainage conditions,
3. establish a systematic statewide basis for allocation of pavement maintenance resources, and
4. measure pavement performance.

Method of Measurement

Many instruments have been developed for measuring pavement roughness. Gillespie (1992) has presented a brief description of the history of the development of roughness measuring instruments. A sliding straightedge, known as the "viagraph" was one of the first instruments used to measure roughness. It recorded the deviation at the center point of the straight edge and was capable of measuring short wavelength profiles only. Next a rolling straightedge was developed. It recorded every bump three times and because of this, bumps of certain wavelengths recorded at twice amplitude, while others did not record at all. To overcome this problem, profilograph was subsequently developed. Profilograph consisted of an array of wheels to establish a reference plane from which the deviations of the center wheel was measured. Next, the "Via-Log" was developed by the state of New York. It recorded the suspension motion of a passenger car. Subsequently, the Bureau of Public Roads (BPR) Roughometer was developed using the same principle of "Via-Log" but with a standardized vehicle. At the time of the AASHO Road Test, the CHOLE profilometer was developed. It consisted of two small wheels 22.9 cm apart and measured the slope variance.

In the 1960's, currently used high-speed road profiling technology began and many kinds of these instruments (inertial profilers) have been manufactured since then. Early inertial profilers sensed the height of the vehicle relative to the ground using an instrumented follower wheel (Sayers and Karamihas 1996). These profilers were analog. They used electronic processors and magnetic tapes to store profiles as a continuously varying voltage. Modern profilers use noncontacting sensors to obtain the profile and are equipped with on-board digital computers.

Lu et al. (1990) quotes the FHWA classification of currently used road roughness measuring instruments. These instruments are divided into three broad categories: (1) manually operated instruments, (2) Dynamic direct profiling instruments, and (3) response-type road roughness measuring (RTRRM) systems. Manually operated instruments measure elevations at an interval of 30 cm or less and are capable of measuring shorter wavelength profiles accurately. One example of such instrument is the rod and level. The measurement interval in dynamic direct profiling instruments is less than or equal to 60 cm. These instruments can also measure shorter wavelength profiles accurately. Examples of such instruments are General Motors (GM) 690D Surface Dynamics Profilometer used by the Texas Department of Transportation, K. J. Law profilometer, and South Dakota profiler. These instruments use some kind of filtering system to remove wavelengths outside of a band of interest. Response type road roughness measuring systems are based on the assumption that the ride quality of pavement is directly related to the vehicle's vibrations. They measure and accumulate axle displacements as the vehicle traverses a test section. Examples of these instruments include the Mays Ride Meter, Cox Road-meter, Bureau of Public Roads (BPR) Roughometer, and Automatic Road Analyzer (ARAN) unit. These instruments also use a filtering system to remove wavelengths outside of a band of interest.

690D Surface Dynamics Profilometer

The Surface Dynamics Profilometer has been used for several years by the Texas Department of Transportation to measure roughness on their pavements. This instrument has

also been used as the standard reference instrument to calibrate other roughness measuring instruments, such as the Mays Ride Meter, which are less accurate and less expensive. For the current research study, this instrument was used to measure pavement roughness in all test sections. The instrument was originally designed by General Motors and built by K. J. Law Engineers in 1967 (Walker and Beck 1988). The instrument had two accelerometers and two linear potentiometers. The potentiometers were connected to road-following wheels. The accelerometers measured the amount and direction of vertical acceleration undergone by the vehicle while potentiometers and road-following wheels measured the distance between the vehicle body and the road surface. The acceleration was digitized by a profile computer and summed with the digitized potentiometer signal to obtain a profile measurement (Walker and Schuchman 1987). A high-pass filter was used to filter out long wavelength profiles. The instrument provided two separate profiles for both the left and right wheel paths.

There were two major problems with this device (Walker and Schuchman 1987). One was associated with the road following wheels and potentiometers. The measurements could be taken only at speed of about 32 kmph because at higher speeds the wheels bounced. Also, the wheels were easily damaged by rough road surfaces. The other problem was the longer time required for data processing. The profile data was written on a magnetic disk. Data processing took several days.

To overcome these problems, the profilometer was updated subsequently by replacing the potentiometer/road-following wheel combination by two noncontact Selcom laser probes, and by upgrading the on-board computer system used for the data acquisition (Walker and Schuchman 1987).

Roughness Measures

Roughness measuring instruments produce a sequence of numbers related to the profile of a line on the pavement on which they traverse. Many methods have been developed to process these data. They can be classified into three groups (Claros et al. 1985):

1. wave analysis techniques,
2. theoretical roadmeter simulation methods, and
3. indirect roadmeter simulation methods.

In wave analysis, the measured profile is treated as a complex wave made of a series of simple waves. A weighting function is used to assign the relative contribution of the simple waves to the original complex wave. Wave analysis methods include: (1) harmonic analysis, (2) power spectral density, and (3) digital filtering technique. In harmonic analysis, the measured profile is assumed to be a periodic wave. The analysis breaks down a profile record into a harmonic series of sinusoidal waves. Different pavements will have different combinations of amplitude and wave lengths. The plot of amplitude versus wavelength is used to describe the roughness. Power spectral density method treats a measured profile as a random signal. The Fast Fourier Transform method is used to obtain roughness amplitudes and spectral density estimates for a set of wave bands. These estimates are used to describe the roughness behavior on a pavement. The digital filtering technique is used to separate a measured profile by wavelengths. Highway engineers are more interested in having a single index to characterize the roughness on a pavement. The results obtained from the wave analyses can be used to estimate these indices.

In the theoretical roadmeter simulation method, the dynamic response of a vehicle is simulated to a measured profile using a set of differential equations. The characteristic parameters, such as masses, spring constants, and damping coefficients are selected so as to be representative of a real vehicle. This method allows an estimation of a single index to represent the roughness on a pavement. The Maysmeter Index, BPR Roughness Index, PCA Roughness Index, and International Roughness Index are obtained in this manner.

In the indirect road simulation method, regression models are developed to estimate a single roughness index. This method uses simple and physically meaningful functions of a measured profile as the roughness index. These techniques include slope variance (SV), root-

mean-square vertical acceleration (RMSVA), and mean absolute vertical acceleration (MAVA).

A large number of different roughness indices have been developed by many researchers. However, the Serviceability Index and the International Roughness Index may be the most widely used roughness indices at present.

Serviceability Index (PSI)

The serviceability performance concept in the design of pavements was emerged from the AASHO road test (Carey and Irick 1960). In the AASHO road rest, the serviceability of pavements was rated subjectively by a panel made up of men selected to represent many important groups of highway users. The mean of the individual ratings was defined as the Present Serviceability Rating (PSR) and it was a number between zero and five. A predictive model, the Present Serviceability Index (PSI), was developed to reproduce the PSR based on physical characteristics of the pavement surface. The physical measurements in the predictive model for flexible pavements included the percent cracking, percent patching, rut depth, and average slope variance. For rigid pavements, the parameters considered were percent cracking, percent patching, and average slope variance. The average slope variance was a profile statistic obtained from the CHOLE profilometer.

Since the AASHO road test, many improved instruments to measure pavement roughness have been developed. With the development of instruments, different roughness indices were also developed. However, the design equations developed from the AASHO road test were virtually unchanged. Therefore, these roughness indices were always correlated to Serviceability Index and relationships were obtained. The Texas Department of Transportation uses the profile statistic Root-Mean-Square Vertical Acceleration (RMSVA) to correlate pavement roughness to the Serviceability Index. The relationships developed for this purpose are as follows (Walker and Hudson 1973a; Walker and Hudson 1973b; McKenzie et al. 1982; Srinarawat 1982; Claros et al. 1985; McKenzie et al. 1986).

The serviceability index (SI) is given by:

$$SI = 5\, e^{-\left[\frac{\ln(32\ MO)}{8.4933}\right]^{9.3566}} \tag{2.17}$$

where

MO = standard Mays Ridemeter Index (in/mile).

The standard Mays Ridemeter Index (MO) is given by:

for flexible pavement,

$$MO = -24.508 + 21.597\ VAN_4 + 56.899\ VAN_{16} \tag{2.18}$$

for rigid pavement,

$$MO = -22.9 + 21.76\ VAN_4 + 55.9\ VAN_{16} \tag{2.19}$$

where

VAN_4 = RMSVA for a 4 foot (121.92 cm) base length, and

VAN_{16} = RMSVA for a 16 foot (487.68 cm) base length.

$$VAN_b = C\left[\sum_{i=k+1}^{N-k} \frac{(s_b)_i^2}{(N - 2k)}\right]^{(1/2)} \tag{2.20}$$

The RMSVA is defined as:

where

VAN_b = RMSVA for a base length b,

s = sampling interval,

k = a positive integer,

b = base length = ks,

N = total number of profile data points,

S_b = second derivative of elevations with respect to base length b, and

C = constant required for conversion of units, for a profiling speed of 50 mph (80.45 km/h) and profiles measured in feet (1 feet = 0.3048 m), C has a value of 5378 ft^2/sec^2 (499.63 m^2/sec^2).

S_b is given by:

$$(s_b)_i = (Y_{i+k} - 2Y_i + Y_{i-k}) / b^2 \tag{2.21}$$

where

Y = elevation.

The VERTAC program which uses the above relationships to calculate the Serviceability Index is used in the current research to estimate serviceability index in test sections.

International Roughness Index

The International Roughness Index (IRI) emerged from the International Road Roughness Experiment (IRRE) held in Brasilia, Brazil in 1982 (Sayers et al. 1986). The World Bank initiated the IRRE in order to find best practices appropriate for the many types of roughness measuring equipment in use. It was conducted by research teams from Brazil, England, France, the United States, and Belgium. Both profilometric methods and Response-Type Road Roughness Measuring Systems (RTRRMS) were used in the experiment and the IRI was measured from both types of instruments. The IRI is based on the roadmeter measure, called by its technical name of Average Rectified Slope (ARS) and has units of slope such as m/km or in/mile. The IRI is influenced by wavelengths ranging from 1.2 m to 30 m and is linearly proportional to roughness (Sayers and Karamihas 1996). An IRI of 0 means the profile is perfectly flat. There is no theoretical upper limit to IRI. Values of IRI for different types of pavements are shown in Figure 2.2.

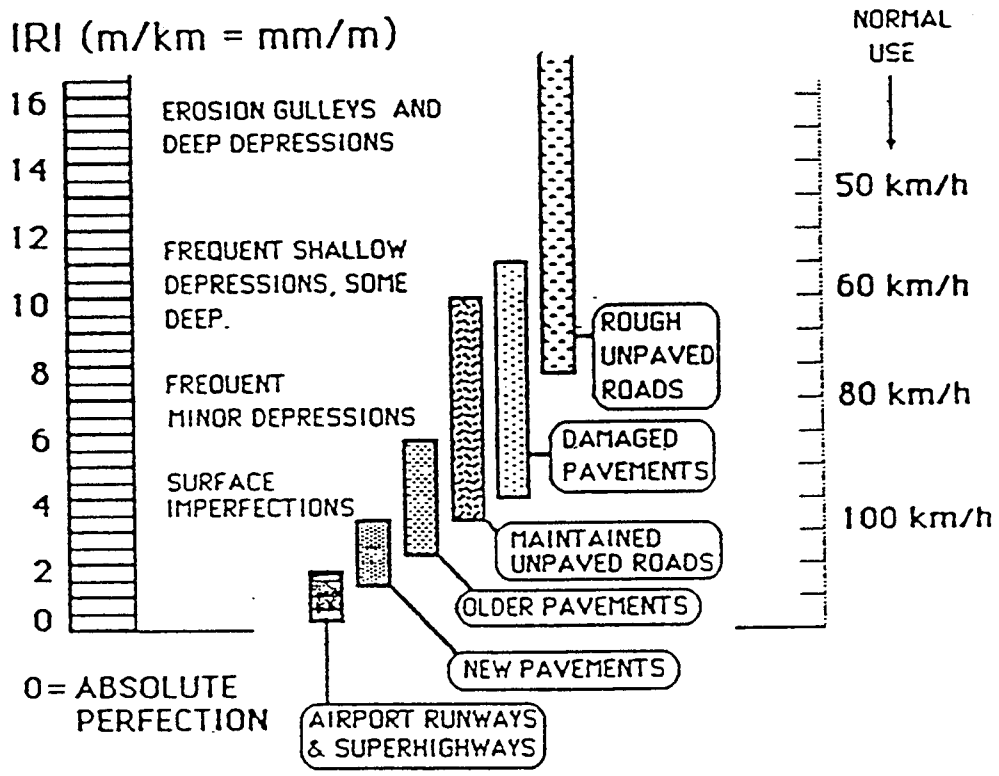

Figure 2.2. Typical Values of International Roughness Indices (Sayers et al. 1986)

The IRI is defined as a property of a single wheel-track profile and the following points fully define the IRI concept (Sayers 1995):

1. The IRI is computed from a single longitudinal profile. The sample interval should be no larger than 30 cm for accurate calculations. The required resolution depends on the roughness level, with the finer resolution being needed for smooth roads. A resolution of 0.5 mm is suitable for all conditions.
2. The profile is assumed to have a constant slope between sample elevation points.
3. The profile is smoothed with a moving average whose base length is 25 cm.
4. The smoothed profile is filtered using a quarter-car simulation, with specific parameter values, at a simulated speed of 80 km/hr. Figure 2.3 shows the quarter car model in the IRI and its frequency response to slope input.
5. The simulated suspension motion is linearly accumulated and divided by the length of the profile to yield IRI.

The quarter-car model in the IRI includes the major dynamic effects that determine how roughness causes vibrations in a vehicle. The sprung and unsprung masses and damper serve to represent the body, axle, and shock absorbers of a vehicle, respectively. The masses, springs, and dampers are defined by the following parameters (Sayers 1995):

c_s = suspension damping rate,

k_s = suspension spring rate,

k_t = tire spring rate,

m_s = sprung mass, and

m_u = unsprung mass.

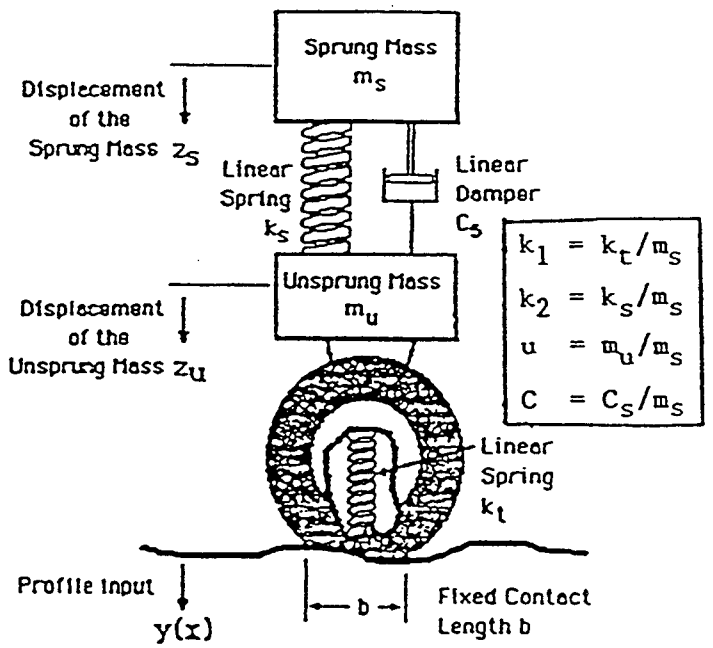

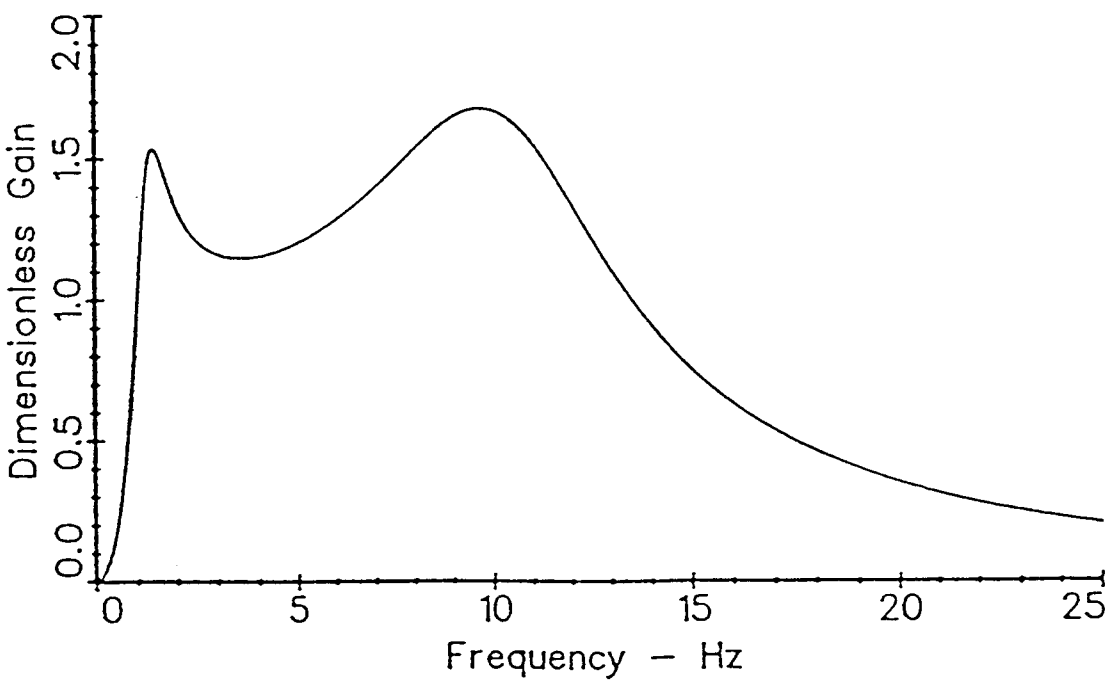

c. Frequency Response of RQCS to Slope Input

Figure 2.3. Quarter Car Model and Frequency Response to Slope Input Used for IRI (Sayers et al. 1986)

Data that are used in the IRI calculation are:

k_s / m_s = 63.3

k_t / m_s = 653

c_s / m_s = 6.0

m_u / m_s = 0.15

The quarter-car model is defined mathematically by four first-order differential equations (Sayers 1995). These can be written in matrix form:

$$\frac{dX}{dt} = AX + Bh_{ps} \tag{2.22}$$

where

$$A = \begin{pmatrix} 1 & 0 & 0 & 0 \\ -k_2 & -c & k_2 & c \\ 0 & 0 & 1 & 0 \\ \frac{k_2}{\mu} & \frac{c}{\mu} & -\frac{k_1 + k_2}{\mu} & -\frac{c}{\mu} \end{pmatrix} \tag{2.23}$$

$$X = \begin{pmatrix} z_s \\ \frac{dz_s}{dt} \\ z_u \\ \frac{dz_u}{dt} \end{pmatrix} \tag{2.24}$$

where

h_{ps} = smoothed profile elevation,

z_s = height (vertical coordinate) of sprung mass,

z_u = height (vertical coordinate) of unsprung mass, and

X = array of state variables.

Time t is given by:

$$t = \frac{x}{V} \tag{2.25}$$

where

x	=	horizontal distance, and
V	=	simulated forward velocity (80 km/hr for IRI calculation), V should be length/sec, where the units of length match with those of x.

The International Roughness Index (IRI) statistic is then obtained from:

$$IRI = \frac{1}{L} \int_0^{L/V} \left| \frac{dz_s}{dt} - \frac{dz_u}{dt} \right| dt \tag{2.26}$$

where

L	=	length of the profile.

Prediction of Roughness in Expansive Soils

The American Association of State Highway and Transportation officials' guide for design of pavement structures (AASHTO 1993) presents a procedure to estimate the serviceability loss due to expansive soils. In this procedure, the serviceability loss is calculated from a plot of serviceability loss versus time which is generated using three estimated parameters. The three parameters are: (1) swell rate constant, (2) potential vertical rise, and (3) swell probability. The swell rate constant estimates the rate at which swelling will take place. This value varies from 0.04 to 0.20 depending on the moisture supply and the soil crack fabric at the site. The Potential Vertical Rise (PVR) is estimated from a laboratory test, empirical procedure, or by experience and it represents the amount of swell that can occur due to the presence of expansive clay in the subgrade. The swell probability represents the percentage of the project length that is subject to swell. If the plasticity index

of the subgrade soil exceeds 30 and the layer thickness exceeds 60 cm or if the PVR exceeds 0.5 cm, the swell probability is taken as 100 percent. The serviceability loss due to expansive soils (ΔPSI_{sw}) is calculated from the following relationship:

$$\Delta PSI_{sw} = 0.00335 * PVR * P_s * (1 - e^{-\theta t}) \tag{2.27}$$

where

PVR	=	potential vertical rise (in),
P_s	=	swell probability,
θ	=	swell rate constant, and
t	=	time (years).

Also, the AASHTO guide provides nomographs to estimate swell rate constant, PVR, and the serviceability loss.

Lytton et al. (1976) studied the development of roughness in two gilgai fields in Texas and found that the cracking patterns in soil determined the roughness pattern and suggested that the roughness could be predicted from the mineralogical and pedologic properties of a clay deposit. Wave analysis using the Fast Fourier Transformation technique was performed on the profilometer data collected from those sites and they developed the following relationship between Serviceability Index (SI), wave length (λ), and amplitude (a):

$$SI = 5.00 + 0.1774\lambda - a\,(126.4 - 0.1665\lambda^2) + a^2\,(1684.4 - 21.99\lambda) \tag{2.28}$$

They concluded that the field amplitude-wavelength relations were a practical upper limit of the roughness that would develop on a pavement.

Velasco and Lytton (1981) used a similar procedure to analyze profilometer data collected in 23 pavement sections in Texas and the graphs of half amplitude versus frequency were fitted by the following equation:

$$\frac{a}{2} = cf^{n} \tag{2.29}$$

where

a	=	mean amplitude, in inches,
f	=	frequency, in cycles/foot, and
c, n	=	regression constants.

A typical plot of half amplitude versus frequency for rough and smooth profiles is shown in Figure 2.4. The values of two constants, c and n, were found to depend upon the composite flexural stiffness of the pavement, time, climatic measures, and several physicochemical soil properties. They developed two empirical models to predict c and n and then these were correlated to the Serviceability Index reduction (ΔPSI). In developing the equation for ΔPSI, it was assumed that the initial serviceability index for all pavement sections was 5.0 and the serviceability loss measured was totally due to expansive clay activity. The relationships developed were as follows:

$$c = 0.0004 * DEPTH^{-0.81} * TIME^{0.49} * AC^{-1.20} * ESP^{0.12} \tag{2.30}$$

$$n = -0.79 * DEPTH^{0.09} * CEC^{-0.16} * CLAY^{0.40} * RANGE^{-0.16} \tag{2.31}$$

$$\Delta PSI = 2675.41 * c^{1.09} * |n|^{7.62} \tag{2.32}$$

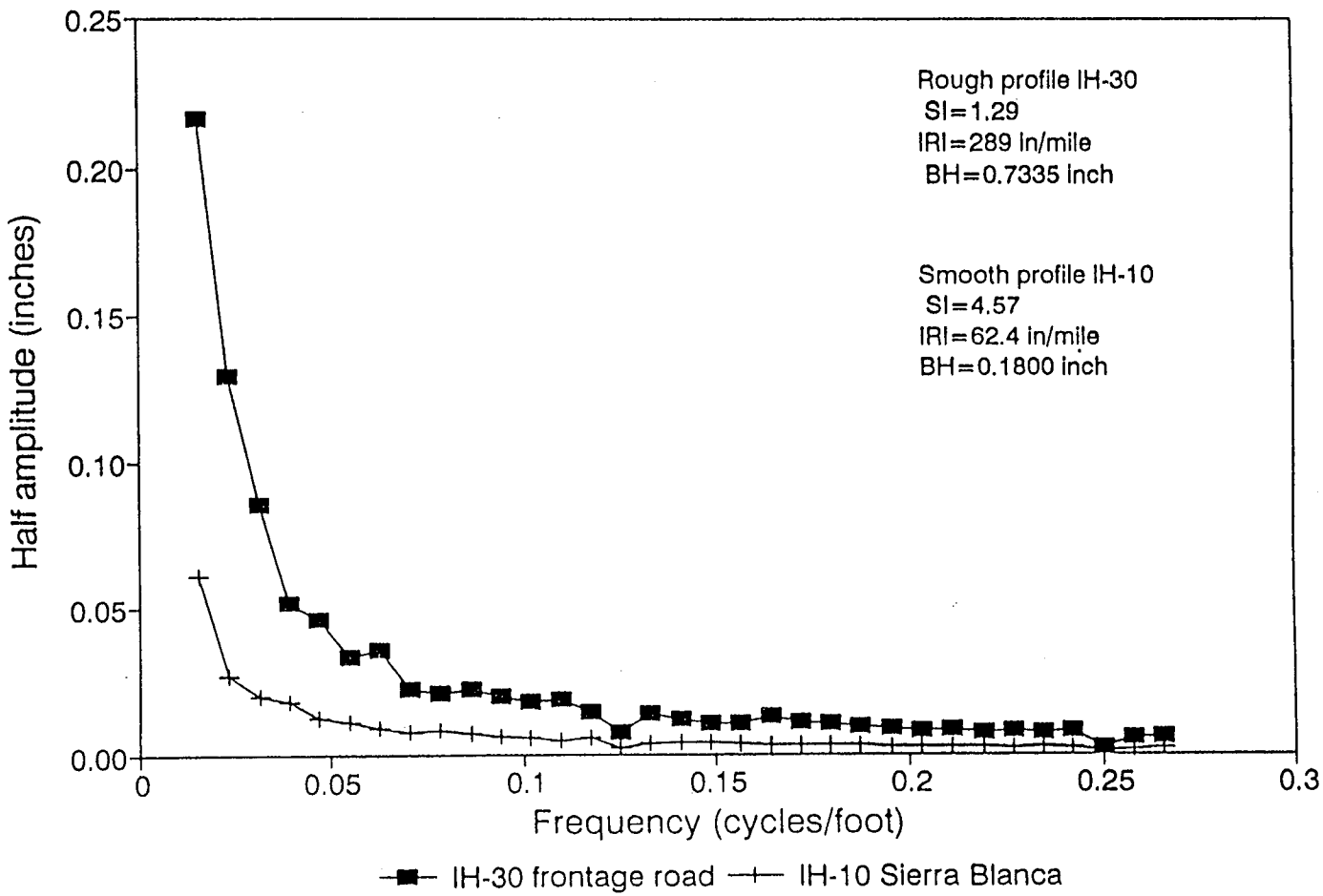

Figure 2.4. Fourier Amplitude Spectra of Typical Rough and Smooth Highway Profiles (Gay 1994)

where

DEPTH	=	effective depth of pavement, in inches,
TIME	=	time since construction or last rehabilitation, in years,
AC	=	activity,
ESP	=	exchange sodium percentage,
CEC	=	cation exchange capacity, in meq/100 g,
CLAY	=	percent clay (less than 2 micron), and
RANGE	=	range of values of Thorntwaite Moisture Index for a 20-year period.

The pavement sections in that study contained five rigid pavements. Omitting these rigid pavements and assuming an initial serviceability index of 4.2, Rauhut and Lytton (1984) performed a new regression analysis for the data and proposed the following model to predict the serviceability loss:

$$\Delta PSI = 39396\ c^{1.544}\ |n|^{9.59} \tag{2.33}$$

McKeen (1985) used the procedure proposed by Velasco and Lytton (1981) to analyze the roughness pattern on airport pavements and to develop a thickness design procedure for airport pavements using a mathematical model for an elastic beam on a deformed foundation. The parameters used to model the roughness pattern were the weighted amplitude and characteristic wavelength.

Gay (1994) studied the development of pavement roughness in expansive soils with and without vertical moisture barriers and developed the following models to predict the rate of change of roughness:

the change in SI/year, dR/dt is given by:

$$\frac{dR}{dt} = \beta_1 \Delta H + \beta_2 \tag{2.34}$$

where for category,

A moisture barriers with paved medians

$\beta_1 = 0.02176 \quad \beta_2 = 0.03226$

B moisture barriers with sodded medians

$\beta_1 = 0.03430 \quad \beta_2 = 0.07269$

C control sections with and without medians

$\beta_1 = 0.04418 \quad \beta_2 = 0.12461$

the mean rate of change of IRI (in/mile/yr), dR/dt is given by the same form as in Equation 2.34 but with following constants:

A moisture barriers with paved medians

$\beta_1 = 0.61939 \quad \beta_2 = 1.2954$

B moisture barriers with sodded medians

$\beta_1 = 1.5825 \quad \beta_2 = 2.0105$

C control sections with and without medians

$\beta_1 = 2.7014 \quad \beta_2 = 4.0146$

the mean rate of change of Bump Height (in/yr), dR/dt is given by:

$$\frac{dR}{dt} = \beta_1 + \beta_2 e^{\beta_3 \Delta H} \tag{2.35}$$

where for category,

A moisture barriers with paved medians

$\beta_1 = 0.011 \quad \beta_2 = 0.012 \quad \beta_3 = 0.216$

B moisture barriers with sodded medians

$\beta_1 = 0.010 \quad \beta_2 = 0.011 \quad \beta_3 = 0.305$

C control sections with and without medians

$\beta_1 = 0.000 \quad \beta_2 = 0.018 \quad \beta_3 = 0.302$

Nyangaga (1996) fitted the International Roughness Index (IRI) and Serviceability Index data (PSI) with data collected from the sites studied under current study to sigmoidal curves and estimated regression coefficients. The relationships were obtained for the regression coefficients as a function of vertical movement and the roughness prediction models for 1-lane, 2-lane, and 3-lane highways were developed. He used the VOLFLO program to calculate the vertical movement. Both Gay (1994) and Nyangaga (1996) considered that the roughness developed on the pavements was totally due to expansive clay activity.

VERTICAL MOISTURE BARRIERS

The Texas Department of Transportation has been using vertical moisture barriers for several years in pavement sections where repeated maintenance work due to expansive clay activity has been reported. However, this treatment method has not been used extensively elsewhere mainly due to construction difficulties and higher cost.

The first vertical moisture barrier on a Texas highway was installed on Interstate Highway Loop 410 in the Valley Hi Drive Interchange area in southwestern San Antonio in 1979 (Steinberg 1981). In the following year, the second vertical moisture barrier was placed on Interstate Highway 37 in southeast San Antonio. Both sites showed a lesser roughness development over time than their companion control sections (Steinberg 1985). Since then many more pavement sections in Texas were protected with vertical moisture barriers. Site descriptions and construction details of these barrier sections have been reported by Steinberg (1980; 1985; 1989; 1992).

Picornell et al. (1984) assessed the effectiveness of the vertical moisture barrier placed on Interstate Highway 37 by evaluating the subgrade moisture condition inside the barrier and roughness development on the pavement. They measured in situ matric potential using thermal block sensors and found that the barrier kept the moisture in the subgrade soil underneath the pavement at a reasonably constant condition. The profilometer measurements were analyzed through a Fast Fourier Transform Algorithm and the roughness development on test and control sections were compared using the procedure presented by Velasco et al. (1981). They also compared the bump height index and serviceability index on test and control sections. They showed that the barrier was effective in controlling roughness.

Gay (1994) studied the development of roughness on pavements with and without moisture barriers and found that the barriers were effective in reducing roughness. Jayatilaka et al. (1993) used the vertical movement estimated from a finite element program to study the effectiveness of moisture barriers. They found that the barriers were effective only when the medium cracked soils were present in the subgrade. Also, in extremely dry climates and in semi-arid climates under "ponded" drainage conditions, the moisture barriers were ineffective even if the medium cracked soils were present.

Most of the barriers placed on Texas highways were placed to a depth of 244 cm based on previous observations that the depth of active zone in the area was around this depth. Picornell (1985) developed a procedure to determine the depth of a barrier needed for a particular site based on its climatic condition and the subsoil characteristics. He assumed that the barrier performs different roles depending on the moisture condition of the subsoil at the time of installation of the barrier. Two basic assumptions made in this procedure were: (1) if the soil is at an advanced stage of desiccation, the barrier will prevent the access of free water to the shrinkage crack fabric, and (2) if the subsoil is initially very wet, the crack fabric is closed and it does not allow the movement of water and the role of the barrier in this condition is to prevent excessive drying of the soil under the edges of the pavement.

From both points of view, the worst condition that governs the design is associated with the worst intensity of the drought that seems possible at a particular site. A statistical analysis of existing records of meteorological data was carried out to evaluate the worst drought condition of a particular site for a return period equal to the design life of a pavement. Since the pavements are essentially impermeable, the rainfall that falls on the pavement runs off towards the uncovered ground surface between the shoulder and the drainage ditch. The effect of this extra supply of water available for infiltration was taken into account by increasing the direct rainfall by multiplying it by a Rainfall Multiplying Factor (RMF). The coefficient RMF varied from 1 to 5 and was chosen based on the relative width of the pavement and the uncovered soil profile adjacent to the pavement edge, and the geometric characteristics of the roadway cross section. The finite element method was used in the modeling of moisture flow and in the analysis of nonlinear elastic deformation of the soil.

This procedure allows the determination of the depth of a barrier for a particular climatic environment and site condition by two criteria, namely the edge distortion criterion and the maximum crack depth criterion. In the edge distortion criterion, the barrier depth is chosen as the smaller depth that would maintain an angular distortion of 1/360 or less at the edge of the pavement. In the crack depth criterion, the barrier is placed to the maximum crack depth expected with the hydrologic regime imposed by the pavement or to the crack depth existing at the time of construction, whichever is larger. Picornell suggests that the edge distortion criterion be used to determine the depth of a barrier if the initial soil conditions are at its equilibrium condition or wetter than the equilibrium condition. The crack depth criterion is suggested when the initial moisture condition is drier than the equilibrium condition. Based on the results of this study, Picornell and Lytton (1987) suggested that a barrier be placed to the depth of the roots in order to stop longitudinal cracking and about 25 percent deeper than the rooting depth to stop the development of roughness. The crack depth in expansive soils can be measured using the surface wave propagation technique (Picornell and Lytton 1989).

Abd Rahim et al. (1989) developed a computer program to predict the behavior of different barrier alternatives. They consider that the subsurface soil is divided into parallelepipeds of different sizes and the moisture movement into the soil domain takes place within the soil entirely through cracks between soil blocks. The program performs a water balance for the unpaved soils on the side of the pavement and a second water balance for the soils underneath the pavement. Through trial runs from this program, they have shown that the moisture barrier can cause faster swelling under the pavement than that for the surrounding soils if the pavement surface has cracks and joints that allow water infiltration. This program requires some information about the sizes of the soil blocks in order to form the shrinkage crack fabric. They have reported that this data was not readily available in the literature for the typical subsurface soil conditions in Texas.

CHAPTER III

DATA COLLECTION

The current research study uses data collected from ten different locations in three different climatic regions in Texas. Six of the sites are located in Bexar county. Other sites are located in Guadalupe, Dallas, Hunt, and Hudspeth counties. The general locations of these sites are shown in Figure 3.1. Vertical moisture barriers have been installed in nine of the sites. A horizontal fabric barrier has been installed in General McMullen Drive in San Antonio. Roughness data has been collected from all these sites generally on a biannual basis for several years. Subgrade soil properties have been obtained through laboratory testing of samples collected from the sites. In addition to data from moisture barrier sections, data has also been collected from designated control sections where no moisture barriers were installed. Control sections have been designated in all sites except for Converse, FM 1516 in Bexar County.

Many research studies have been performed using roughness and subgrade soil data collected from these sites. Data required for this study was extracted mainly from the previous studies performed by Steinberg (1980; 1981; 1985; 1989; 1992), Gay and Lytton (1988), Jayatilaka et al. (1993), Gay (1994), and Nyangaga (1996). Subgrade soil properties not available in the literature were obtained from the soil survey reports prepared by the Soil Conservation Service of the Department of Agriculture (USDA 1966; 1981). The locations of test sites and details of moisture barriers installed in the test sites are given in Table 3-1. A brief description of test sites and data collected from these sites is presented in the following paragraphs of this chapter.

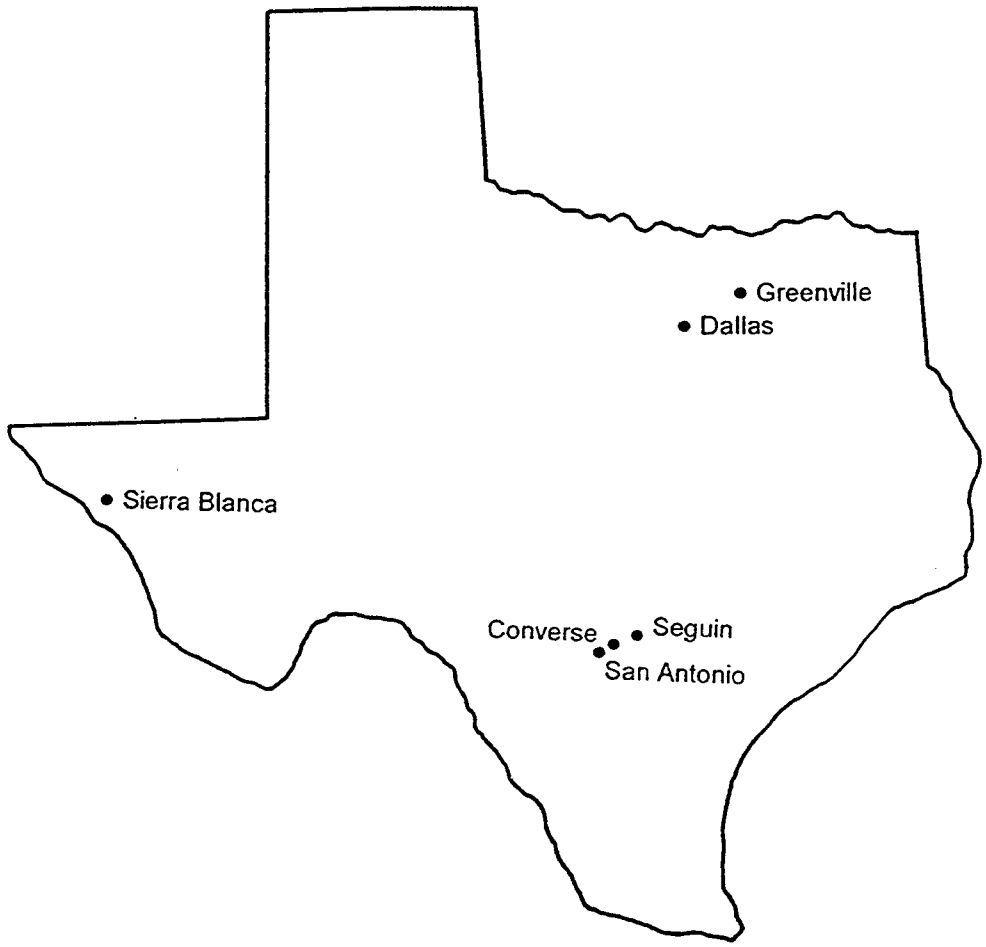

Figure 3.1. Location Map of Test Sites

Table 3-1. Summary Details of Moisture Barrier Sites

Test Site	County	Type of Barrier	Length of Barrier (m)	Date of Barrier Installation	Date of Last Rehabilitation
San Antonio, General McMullen	Bexar	Horizontal Fabric	183	May, 1977	August, 1989
San Antonio, IH 410	Bexar	244 cm Vertical Fabric	800	March, 1979	December, 1987
San Antonio, IH 37	Bexar	244 cm Vertical Fabric	3400	December, 1980	December, 1980
Greenville, IH 30	Hunt	244 cm Vertical Fabric	343	December, 1983	August, 1986
		183 cm Vertical Fabric	305	December, 1983	August, 1986
		244 cm Lime	305	December, 1983	August, 1986
		244 cm Lime Fly Ash	305	December, 1983	August, 1986
San Antonio, US 281	Bexar	244 cm Vertical Fabric	762	January, 1984	November, 1986
San Antonio, IH 10	Bexar	244 cm Vertical Fabric	2400	May, 1985	August, 1987
Sierra Blanca, IH 10	Hudspeth	244 cm Vertical Fabric	305	December, 1985	December, 1985
Seguin, IH 10	Guadalupe	244 cm Vertical Fabric	4000	November, 1988	November, 1988
Converse, FM 1516	Bexar	244 cm Vertical Fabric	2200	November, 1989	November, 1989
Dallas, IH 635	Dallas	244 cm Vertical Fabric	183	September, 1990	September, 1990

DESCRIPTION OF TEST SITES

San Antonio, General McMullen Drive

General McMullen Drive in Southwest San Antonio was the first Texas Department of Transportation geomembrane project (Steinberg 1992). This section of roadway comprises a dual traveledway of three 3.4 m lanes in each direction separated by a 4.3 m wide raised paved median (Gay 1994). The pavement section ends in sidewalk curbs in both directions. Sidewalk is approximately 1.8 m wide.

DuPont Typar geomembrane was placed horizontally across the full width of the prepared subgrade to a street length of 183 m in 1977. The pavement section comprises 15 cm of flexible base, 27.9 cm of asphalt stabilized base, and 3.8 cm wearing course. Two 183 m long adjacent sections to the north and south of the test section were designated as control sections.

In the summer of 1989, a major rehabilitation, which included a level-up and overlay, was carried out at this site.

San Antonio, IH 410

The first vertical moisture barrier installed on a Texas highway is located on Interstate Highway Loop 410 in the Valley Hi Drive interchange area in Southwestern San Antonio (Steinberg 1981). This section of highway was originally built in 1960 as a 4-lane (two lanes in each direction) divided highway. The width of driving lanes, outside and inside shoulders, were 3.7 m, 3.0 m, and 1.2 m, respectively. A 13.4 m wide sodded median separated the northbound and southbound traveledways. The pavement section consisted of 40.6 cm of foundation course, 22.9 cm of flexible base, 7.6 cm of Type A asphaltic concrete, and 5.1 cm of Type C asphaltic concrete (Steinberg 1985). At the section where the moisture barrier was placed, the roadway begins at natural ground level, traverses a cut section of about 6 m below original ground, and then returns to natural ground level.

As part of a rehabilitation project of Loop 410, a 244 cm deep vertical moisture barrier was installed along the inside and outside shoulders of a 0.8 km long section of the northbound traveledway in the Valley Hi Drive area in 1979 (Steinberg 1985). The adjacent southbound lane was designated as the control section. Rehabilitation work of Loop 410 included an asphalt seal coat, a Type C asphaltic level-up, and a 1.9 cm Type D finish asphaltic concrete surface. The thickness of asphaltic concrete level-up varied from 2.5 cm to 30 cm. A spun-bonded polypropylene membrane coated with ethyl vinyl acetate (DuPont Typar T-063) was used for the vertical barrier.

In another rehabilitation project carried out between October 1985 and October 1989, a barrier was placed in the previously designated control section on the southbound traveledway resulting in loss of the control section (Steinberg 1992). Also, an extra lane was added to both the northbound and southbound traveledways at the Valley Hi overpass (Gay 1994). This altered the configuration of the test section. The moisture barrier on the northbound traveledway is now located between the new inside lane and the center lane (previous inside lane).

San Antonio, IH 37

The second Texas vertical moisture barrier site is located on Interstate Highway 37 in southeast San Antonio between Fair Avenue and Pecan Valley Drive. This pavement section was originally constructed in 1968 (Steinberg 1985). The original roadway configuration consisted of two northbound and two southbound lanes separated from a sodded median of 8.5 m to 11 m wide. The driving lanes were 3.7 m wide and outside and inside shoulders were 3.0 m and 1.8 m wide, respectively. The pavement section comprised 15.2 cm of lime-stabilized subgrade, 20.3 cm of cement-stabilized base, and 20.3 cm of concrete pavement. This test section is in a cut section of about 7 m below natural ground.

In a major rehabilitation project carried out between October 1979 and December 1980, a 244 cm deep vertical moisture barrier was installed along the outside shoulders of the

southbound and northbound traveledways (Steinberg 1985). DuPont Typar T-063 was used as the vertical geomembrane. The length of the barrier was 3.4 km. The median was reconstructed by removing the ditch and paving the median to establish a positive drainage towards the outside shoulders. Rehabilitation work included a rubberized asphalt seal, an asphaltic concrete level-up, and overlay. The control sections are located immediately to the north and south of barrier sections.

In March 1984, an asphaltic concrete level-up was applied to the north control section of the northbound lanes (Gay 1994).

Greenville, IH 30

This moisture barrier site is located on IH 30 near Greenville in northeast Texas. The highway was constructed in the 1950's with a 25.4 cm concrete pavement over 15.2 cm of cement-stabilized subgrade (Steinberg 1992). Subsequently, the pavement was overlaid with asphaltic concrete in depths varying from 10.2 cm to 55.9 cm. This pavement section comprised two 3.7 m travel lanes, 3.0 m outside shoulder, and 1.2 m inside shoulder in both eastbound and westbound traveledways. A 9.8 m sodded median separated the eastbound and westbound traveledways (Gay 1994).

A rehabilitation project carried out in 1983 included the installation of moisture barriers in two different locations approximately 4.5 km apart (Gay and Lytton 1988). Moisture barriers were constructed on the eastbound traveledway. The unprotected adjacent westbound traveledway was designated as control sections. Four types of barriers were installed at this site. At one location, two ethyl vinyl acetate (EVA) coated fabric barriers were installed at a depth of 244 cm and 183 cm. The 244 cm and 183 cm deep barriers were placed to a length of 343 m and 305 m, respectively. In the other location, two 244 cm deep barriers each to a length of 305 m were installed with injected lime slurry and lime-fly ash slurry. The barriers were constructed by injecting slurry in three staggered rows, parallel to the roadway centerline at 30.5 cm intervals. The rehabilitation work included rotomilling

and planing of rough spots and overlaying the pavement with 6.4 cm thick hot mix asphaltic concrete.

As part of the planned stage construction of the new surface on this site, 1.9 cm open-graded friction course was placed in August 1986.

San Antonio, US 281

This vertical moisture barrier site is located in the north-central section of San Antonio (Steinberg 1985). The roadway was originally built between 1970 and 1975 and comprised three northbound and three southbound lanes separated by a paved median (Gay 1994). The width of driving lanes, outside and inside shoulders were 3.7 m, 3.0 m, and 3.4 m, respectively. The pavement section consisted 15.2 cm of lime stabilized subgrade, 15.2 cm of base, an asphaltic seal coat, and 20.3 cm of concrete pavement. At the section where the moisture barrier was placed, the pavement elevations vary from natural grade to approximately 6.1 m below natural grade.

A 244 cm deep vertical moisture barrier was installed along inside and outside shoulders of the southbound traveledway of this pavement section in 1984 (Steinberg 1985). Mirafi MCF 500 was used as the vertical geomembrane. The moisture barrier begins approximately 381 m south of the North Loop 410 and extends to a length of 762 m. Rehabilitation work included applying an asphaltic seal coat, an asphaltic concrete level-up, and a finish course on the southbound traveledway. The adjacent northbound traveledway was used as the control section.

Both test and control sections were upgraded with a 2.5 cm asphaltic concrete overlay in November 1986 (Gay 1994). In addition, an asphaltic seal coat was applied to the southbound outside and merge lanes of the Airport Boulevard intersection in 1989.

San Antonio, IH 10

The San Antonio IH 10 moisture barrier site is located in the southeastern area of San Antonio and it extends from Pine Street to Amanda Street. This section of highway was originally built in 1968 as a 6-lane (three lanes in each direction) divided highway (Steinberg 1985). Eastbound and westbound traveledways were separated by a sodded median. The pavement section consisted of 15.2 cm of lime-stabilized subgrade, 15.2 cm of lime-stabilized flexible base, an asphalt seal coat, an 20.3 cm of continuously reinforced concrete pavement. The moisture barrier section is primarily in a cut section of about 6 m below natural ground.

As part of a major rehabilitation project, 244 cm deep vertical moisture barriers were installed along the outside shoulders of the eastbound and westbound traveledways. Rehabilitation work included a rubber asphalt seal, an asphaltic concrete level-up, and a finish course (Steinberg 1985). Mirafi MCF 500 was used for the geomembrane. The rehabilitation of this section was completed in May 1985 with a section configuration similar to that of the San Antonio IH 37 site. The barrier was constructed in two parts in both traveledways. Total length of the barrier was 2.5 km. A total of four control sections were selected for this site. Two control sections were selected in between the barrier sections in the eastbound and westbound traveledways. The other two control sections are located to the west of the barrier section in the eastbound traveledway and to the east of the barrier section in the westbound traveledway.

As part of a planned rehabilitation project, an asphaltic concrete overlay was placed on this pavement section in August 1987 (Gay 1994).

Sierra Blanca, IH 10

This vertical moisture barrier site is located along Interstate Highway 10 approximately 130 km east of El Paso and 4 km west of the town of Sierra Blanca (Gay 1994). The roadway was originally constructed in the 1950's and was comprised of two eastbound and

two westbound lanes separated by a 9.8 m wide sodded median. The width of driving lanes, outside and inside shoulders were 3.7 m, 3 m, and 1.2 m, respectively. The pavement section included a 15.2 cm flexible base and a 14 cm hot mix asphaltic concrete surface.

A 244 cm deep vertical moisture barrier was constructed along inside and outside shoulders of eastbound and westbound traveledways in 1985. Barriers in both directions were constructed to a length of 305 m. A DuPont Typar 3358 EVA coated polypropylene type geomembrane was used for the vertical barriers. The control sections were selected at either side of the barrier sections in both eastbound and westbound traveledways.

Seguin, IH 10

This moisture barrier site is located on the westbound Interstate Highway 10 in Guadalupe county approximately 33 miles east of San Antonio (Jayatilaka et al. 1993). The barrier section extends from the intersection of FM 725 to the intersection of FM 465. This section of roadway was originally constructed in the early 1960's and comprised two eastbound and two westbound traffic lanes separated by a 20 m wide sodded median. The traffic lanes were 3.7 m wide and outside shoulders were 3.0 m wide. The width of the inside shoulder varied from 1.2 m to 1.8 m. The pavement section consisted of a flexible base and a hot mix asphalt concrete surface.

In a rehabilitation project carried out in 1988, a vertical moisture barrier was installed along the inside and outside shoulders of the westbound traveledway. The barrier was constructed in four separate segments with a total length of 4.0 km on both sides of the roadway. A Remag geomembrane (formerly DuPont Typar) was used for the vertical moisture barrier (Steinberg 1992). Rehabilitation work included a seal coat, asphalt concrete level-up, and a 7.6 cm asphalt concrete surface. An adjacent unprotected section to the west of the test section was designated as the control section.

Converse, FM 1516

This moisture barrier test section extends from the intersection of Interstate Highway 10 to approximately 500 m north of Peaceful Drive in Farm to Market 1516 in Bexar county (Jayatilaka et al. 1993). This rural highway is a 2-lane, 2-way road. The original roadway did not have paved shoulders and the lane width was 3.4 m.

In a major rehabilitation and modification project carried out in 1989, the highway was widened and a 244 cm deep vertical moisture barrier was installed. The barrier was constructed in three separate segments with a total length of 2.2 km on either side of the roadway. The geomembrane used was a Phillips fiber (Steinberg 1992). The present roadway consists of two 3.7 m wide traffic lanes and 2.4 m wide paved shoulders on both sides of the roadway (Jayatilaka et al.). The rehabilitation work included the placement of a 22.9 cm thick asphalt stabilized base on an existing 30.5 cm thick flexible base, and a 7.6 cm thick asphalt concrete surface course.

Dallas, IH 635

This moisture barrier site is located on the westbound IH 635 in Dallas county approximately four miles west of the intersection of IH 35E (Jayatilaka et al. 1993). The roadway is a 6-lane divided highway with paved shoulders. The eastbound and westbound roadways are separated by a 36 m wide sodded median. Each roadway comprises three 3.7 m wide traffic lanes, 3.7 m wide outside shoulder, and a 3.0 m wide inside shoulder. The pavement section comprised 20.3 cm lime stabilized subgrade, 10.2 cm of asphalt stabilized base, and 22.9 cm of continuously reinforced concrete pavement.

In a rehabilitation project carried out in 1990, a 244 cm deep vertical moisture barrier was placed to a length of 183 m along the inside and outside shoulders of the roadway. The geomembrane used was a Phillip's Petromat. The rehabilitation work included rotomilling and asphalt concrete level-up and overlay. The control section for this site is located immediately to the east of the barrier section.

ROUGHNESS DATA

The 690D Surface Dynamics Profilometer owned by the Texas Department of Transportation was used to obtain relative elevation profiles of the road surface in all of the test sites. The profilometer records relative elevations along the right and left wheel paths of the surface when it traverses on a roadway. The measurements are obtained at 15.24 cm intervals and saved in a computer file. The relative elevations of right and left wheel paths are recorded in two columns in units of thousandths of an inch (1 inch = 2.54 cm). This computer file is used as the input file for the computer programs that are used to obtain profile statistics. In a multi-lane two way road, the profilometer is normally driven beginning with the outside lanes and ending with the inside lanes as illustrated in Figure 3.2. The profile statistics, International Roughness Index (IRI), and Serviceability Index (SI) are used in this study to develop roughness prediction models. The computer program VERTAC (McKenzie et al. 1986) was used to obtain IRI and SI of all of the pavement sections.

VERTAC Program

The present version of VERTAC is capable of calculating both an International Roughness Index (IRI) and a Serviceability Index (SI). The Serviceability Index is calculated from the profile measurements using two regression equations between Serviceability Index and Mays Ridemeter Index (MO), and Mays Ridemeter Index and Root Mean Square Vertical Acceleration (RMSVA) at baselengths of 121.92 cm and 487.68 cm. The procedure is described in Chapter II and the relevant relationships are shown in Equations 2.17 through 2.21. The International Roughness Index is calculated from the International Roughness Index algorithm incorporated in this program. The length of the roadway section that was used in the program depended on the lengths of barrier and control sections. The Serviceability Indices and International Roughness Indices obtained from this program were used in the development of roughness prediction models. In addition, these data were used to develop a relationship between the International Roughness Index and the Serviceability Index. The details of the analysis are described in Chapter V. The International Roughness Indices and Serviceability Indices obtained for each site are given in Appendix A.

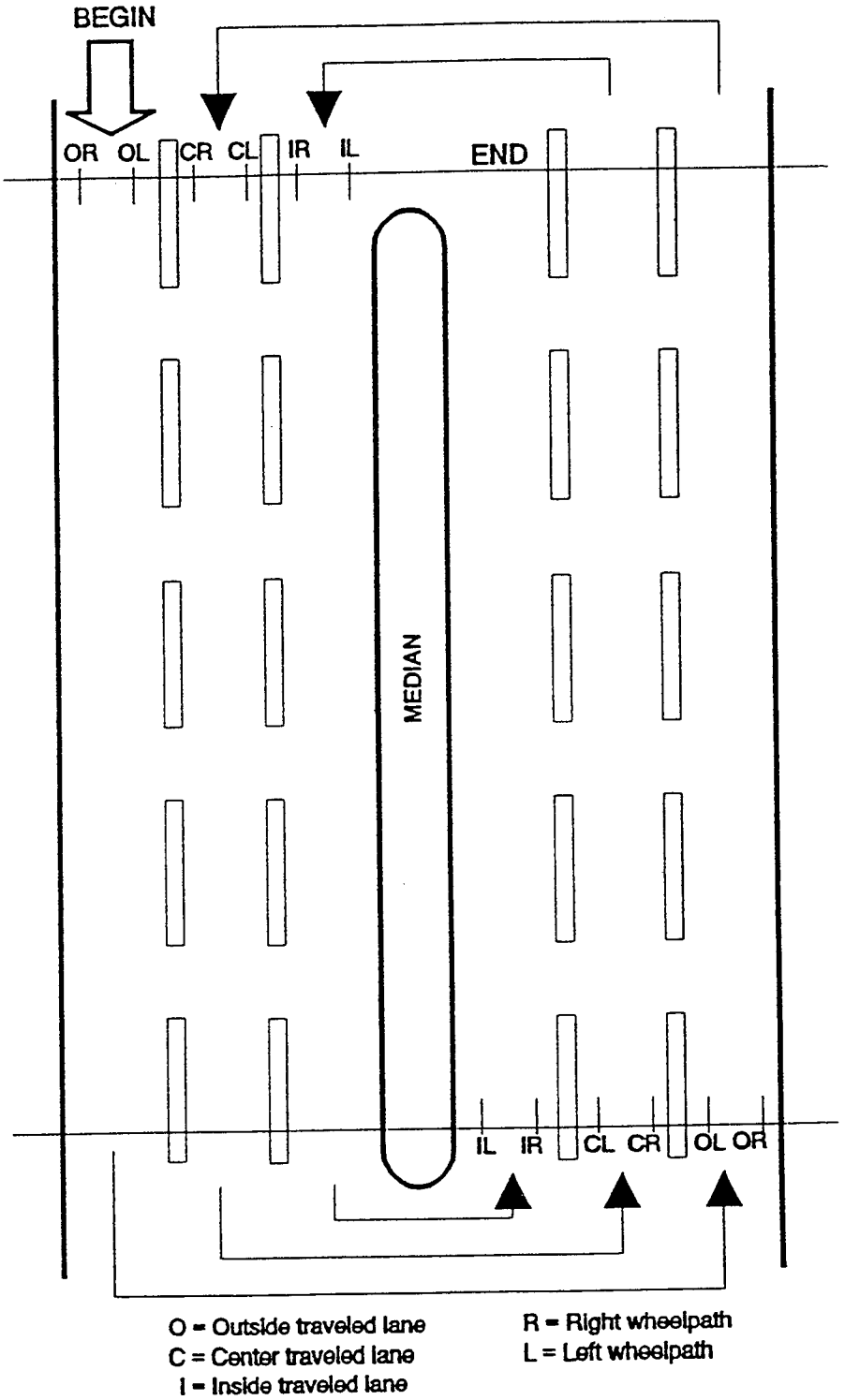

Figure 3.2. Arrangement of Profilometer Measurements Along a Typical Interstate Highway (Gay 1994)

SUBGRADE SOIL PROPERTIES

Subgrade soil properties which are required in the development of roughness prediction model are compiled in this section. Most of the data required were extracted from Steinberg (1980; 1981; 1985), Jayatilaka et al. (1993), and Gay (1994). Subgrade soil properties not available in the literature were obtained from the soil survey reports prepared by the Soil Conservation Service of the Department of Agriculture (USDA 1966; 1981). Tables 3-2 through 3-7 show the soil properties that are used in this study.

Table 3-2. Subgrade Soil Properties - San Antonio Sites

Test Site	Depth (cm)	Liquid Limit (%)	Plasticity Index (%)	Passing #200 (%)	Fine Clay (%)
San Antonio, General McMullen	0.0-244.0	64.0	41.0	85.0	50.0
San Antonio, IH 410	0.0-244.0	71.0	45.0	85.0	50.0
San Antonio, IH 37	0.0-244.0	86.0	54.0	85.0	50.0
San Antonio, US 281	0.0-244.0	64.0	41.0	85.0	50.0
San Antonio, IH 10	0.0-244.0	70.0	45.0	85.0	50.0

Table 3-3. Subgrade Soil Properties - Converse, FM 1516

Pavement Section	Depth (cm)	Liquid Limit (%)	Plasticity Index (%)	Passing #200 (%)	Fine Clay (%)
Barrier Section	0.0-91.5	50.4	31.6	83.4	40.6
	91.5-152.5	83.4	54.0	89.8	48.0
	152.5-213.5	72.9	49.4	89.4	46.7
	213.5-244.0	80.0	51.3	90.3	52.3

Table 3-4. Subgrade Soil Properties - Seguin, IH 10

Pavement Section	Depth (cm)	Liquid Limit (%)	Plasticity Index (%)	Passing #200 (%)	Fine Clay (%)
Barrier Section	0.0-106.7	66.3	40.7	91.0	43.3
	106.7-182.9	57.6	33.3	91.3	42.3
	182.9-244.0	75.4	42.7	93.0	51.2
Control Section	0.0-122.0	66.4	41.4	82.2	49.1
	122.0-244.0	49.7	28.8	85.6	42.2

Table 3-5. Subgrade Soil Properties - Dallas, IH 635

Pavement Section	Depth (cm)	Liquid Limit (%)	Plasticity Index (%)	Passing #200 (%)	Fine Clay (%)
Barrier Section	0.0-106.7	73.9	43.9	99.1	59.4
	106.7-213.4	73.6	46.0	99.0	57.7
	213.4-244.0	75.9	47.7	99.1	63.3
Control Section	0.0-152.4	77.9	48.2	97.0	55.5
	152.4-244.0	73.5	44.6	99.4	54.7

Table 3-6. Subgrade Soil Properties - Greenville, IH 30

Pavement Section	Depth (cm)	Liquid Limit (%)	Plasticity Index (%)	Passing #200 (%)	Fine Clay (%)
Vertical Fabric Barrier Sections	0.0-61.0	27.5	4.0	85.0	16.0
	61.0-91.5	43.5	30.0	85.0	38.0
	91.5-122.0	41.1	25.2	85.0	33.0
	122.0-183.0	86.4	58.4	85.0	23.0
	183.0-244.0	81.4	56.4	85.0	38.0
Lime and Lime-Fly Ash Barrier Sections	0.0-61.0	24.1	15.0	85.0	35.0
	61.0-122.0	39.1	21.9	85.0	50.0
	122.0-183.0	35.1	19.6	85.0	48.0
	183.0-244.0	36.3	18.9	85.0	48.0
Control Sections to Vertical Fabric Barriers	0.0-61.0	41.0	28.2	85.0	43.0
	61.0-122.0	61.7	31.2	90.0	51.5
	122.0-183.0	70.0	30.1	90.0	60.0
	183.0-244.0	73.2	36.8	90.0	22.0
Control Sections to Lime and Lime-Fly Ash Barrier Sections	0.0-61.0	26.7	15.0	85.0	27.5
	61.0-122.0	31.2	21.0	85.0	7.5
	122.0-183.0	49.3	31.7	85.0	13.5
	183.0-244.0	77.8	38.3	90.0	58.0

Table 3-7. Subgrade Soil Properties - Sierra Blanca, IH 10

Pavement Section	Depth (cm)	Liquid Limit (%)	Plasticity Index (%)	Passing #200 (%)	Fine Clay (%)
Eastbound Barrier Section	0.0-76.2	25.0	7.0	10.0	1.0
	76.2-213.4	47.0	24.0	74.0	47.0
	213.4-244.0	65.3	24.5	74.0	47.0
Westbound Barrier Section	0.0-137.2	25.0	7.0	10.0	1.0
	137.2-213.4	47.0	24.0	74.0	47.0
	213.4-244.0	65.3	24.5	74.0	47.0
Control Sections	0.0-244.0	12.0	4.0	5.0	1.0

CLIMATIC DATA

Thornthwaite Moisture Index (Thornthwaite 1948) is used to characterize the climate in the test sites. The Thornthwaite Moisture Index can be calculated by a water balance procedure which involves: (1) determination of monthly potential evapotranspiration, (2) allocation of available water to storage, deficit, and runoff on a monthly basis, and (3) summation of monthly runoff moisture depth, deficit moisture depth, and evapotranspiration to obtain annual values. Then the Thornthwaite Moisture Index (TMI) is given by:

$$TMI = \frac{100R - 60DEF}{E_p} \tag{3.1}$$

where

R = runoff moisture depth,

DEF = deficit moisture depth, and

E_p = evapotranspiration.

Historical mean of TMI is available through maps containing spatial distributions of TMI. For all the sites except Greenville and Sierra Blanca, the TMI was obtained from the TMI map of Texas produced by Wray (1978). This map is shown in Figure 3.3. For Greenville and Sierra Blanca sites, the TMI estimated by Gay (1994) are used. The TMI values used for each site are given in Table 3-8.

Table 3-8. Mean Thornthwaite Moisture Index of Test Sites

Test Site	Mean Thorntwaite Moisture Index
San Antonio, General McMullen	-13.75
San Antonio, IH 410	-13.75
San Antonio, IH 37	-13.75
Greenville, IH 30	16.20
San Antonio, US 281	-13.75
San Antonio, IH 10	-13.75
Sierra Blanca, IH 10	-37.80
Seguin, IH 10	-11.50
Converse, FM 1516	-12.50
Dallas, IH 635	0.00

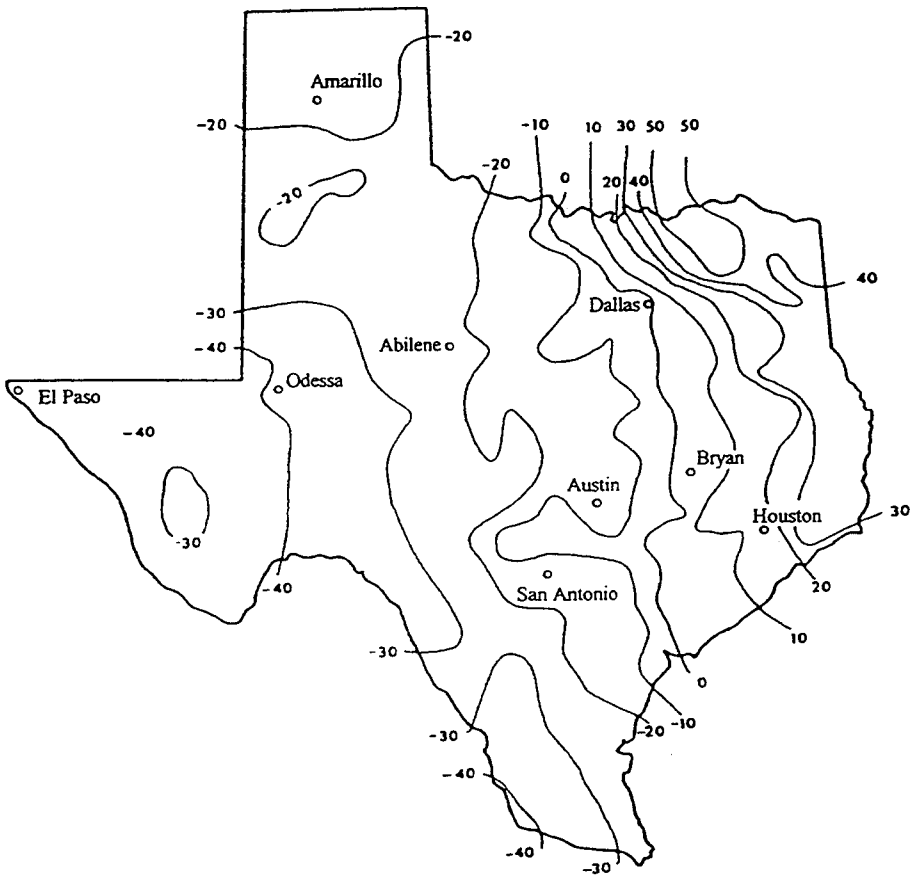

Figure 3.3. Thornthwaite Moisture Index for Texas (Wray 1978)

CHAPTER IV

MODEL TO PREDICT VERTICAL MOVEMENT

The development of pavement roughness due to expansive clay activity is caused by the differential movement of subgrade soil. Therefore, it is obvious that the roughness development is directly related to the magnitude of vertical movement of a pavement structure. Various methods of estimating vertical movement in expansive soils are available in the literature. These methods were reviewed in Chapter II. Many of those methods are calculating one dimensional vertical movement.

The magnitude of vertical movement in a pavement structure is not uniform everywhere even when the subgrade soil properties are the same. The moisture fluctuation at the edge of a pavement is higher than the interior of the pavement since the edge is directly exposed to the environment as opposed to the interior of the pavement which is covered by a nearly impermeable pavement surface. Since the amount of volume change in expansive soils is directly related to the changes in moisture content or soil suction, the maximum potential vertical movement at the edge of a pavement should be higher than that of the interior of the pavement. Therefore, two dimensional analysis of vertical movement is required for the correlation of vertical movement to the roughness that develops in different wheel paths of a pavement.

Gay (1994) studied the expansive soil deformation in a two dimensional domain and developed the computer program FLODEF. This program is a two dimensional finite element program and is capable of calculating vertical movement profile across a pavement section with or without a vertical moisture barrier. However, the use of this program is limited because many parameters are needed to run the program and they are not readily available. In addition, this program needs an enormous amount of computer memory and

time. Therefore, at present, this program can be run only on the mainframe computer.

In this kind of circumstance, there are two options available. One is the producing of design charts or tables from the results obtained from a two dimensional analysis. The second option is the developing of regression equations. With the first option, large numbers of charts or tables are required to include many parameters that are involved in the calculation of vertical movement. Hence, this option was not preferred in this research study. The use of a one dimensional vertical movement program in a design procedure is relatively easy. It is also possible to develop good regression equations by correlating two dimensional vertical movement with one dimensional vertical movement and other parameters that are involved in the calculation of vertical movement. Hence, in this research study, a model to estimate vertical movement in a two dimensional domain is developed using a one dimensional vertical movement program in conjunction with a set of regression equations developed from the results obtained from the FLODEF program.

The one dimensional vertical movement program MOPREC developed by Gay (1994) uses a climatic model based on the frequency analysis of precipitation and evapo-transpiration. The basic climatic data are the only data required for this climatic model. This kind of program allows a convenient way of estimating vertical movement. In this research study, the MOPREC program is used as the one dimensional vertical movement program in the development of regression equations for the estimation of vertical movement in a two dimensional domain.

TWO DIMENSIONAL VERTICAL MOVEMENT PROGRAM FLODEF

The FLODEF program (Gay 1994) computes the transient unsaturated moisture flow and deformation in an expansive clay domain using a sequential analysis of flow and deformation. Unsaturated moisture flow is modelled through a model developed by Mitchell (1980) by converting the nonlinear partial differential equation given in the modified Darcy's law into an ordinary partial differential equation. The partial differential equation that

describes the unsaturated moisture flow in the modified Darcy's law is given by:

$$C(\phi)\frac{\partial\phi}{\partial t} = \frac{\partial}{\partial x_i}\left[K_{ij}(\phi)\left(\frac{\partial\phi}{\partial x_j} + \frac{\partial z}{\partial x_j}\right)\right] - Q(\phi, x_i, t) \qquad i, j = 1, 2 \tag{4.1}$$

where

$C(\phi)$	=	the slope of the desorption curve,
K_{ij}	=	the permeability tensor, and
$Q(\phi, x_i, t)$	=	a source or sink term that may be described as a variable function of matric potential ϕ, spatial coordinates, and time.

The two main assumptions made by Mitchell in the conversion of the nonlinear partial differential equation into an ordinary differential equation are: (1) the unsaturated permeability is linearly related to the reciprocal of total suction, and (2) the desorption relationship is linear when the suction is expressed in terms of pF. These assumptions can be expressed as:

$$K = K_0\frac{h_0}{h} \tag{4.2}$$

$$C = \frac{\Delta mc}{\Delta u} \tag{4.3}$$

where

K	=	permeability of soil at suction h,
K_0	=	saturated permeability,
h_0	=	total suction at saturation which is approximately 100 cm,
C	=	slope of desorption curve,
Δmc	=	change in moisture content of soil, and
Δu	=	change of soil suction expressed as pF.

Mitchell (1980) defined the rate of moisture flow through an unsaturated soil as:

$$V = -K_0 \frac{h_0}{h} \frac{dh}{dx} \tag{4.4}$$

Soil suction (u) in logarithmic units of pF is defined as:

$$u = \log_{10} h \tag{4.5}$$

This can be written as:

$$u = \frac{1}{\log_e 10} \log_e h \tag{4.6}$$

Differentiating both sides with respect to x this becomes:

$$\frac{du}{dx} = \frac{0.434}{h} \frac{dh}{dx} \tag{4.7}$$

Combining Equations 4.4 and 4.7, the rate of moisture flow through an unsaturated soil is given by:

$$V = -P \frac{du}{dx} \tag{4.8}$$

where

$$p = \frac{k_0 h_0}{0.434} \tag{4.9}$$

The parameter p is termed the unsaturated permeability.

Applying the continuity equation to Equation 4.9, Mitchell (1980) obtained the following ordinary partial differential equation:

$$\frac{\partial^2 u}{\partial x^2} + \frac{\partial^2 u}{\partial y^2} + \frac{\partial^2 u}{\partial z^2} + \frac{f(x,y,z,t)}{p} = \frac{1}{\alpha}\frac{\partial u}{\partial t} \tag{4.10}$$

The coefficient α is given by:

$$\alpha = \frac{\gamma_w\, p}{\gamma_d\, C} \tag{4.11}$$

where

γ_w = density of water, and

γ_d = dry density of soil.

Equation 4.10 is a diffusion equation defining the movement of moisture through unsaturated soil, and is similar in form to the equation of consolidation for saturated soils and the heat conduction equation. The coefficient α is the diffusion coefficient of the soil.

In the FLODEF program, the climate is modelled through a function describing the time dependant variation of matric potential at the exposed soil surface. The functions that can be used in the program are sinusoidal, step, and combination of sinusoidal and step.

Mitchell (1980) modelled the climate by a sinusoidal function in the following form:

$$u(0,t) = U_e + U_0 \cos 2\pi n t \tag{4.12}$$

where

$u(0,t)$ = matric suction at the surface,

U_e = equilibrium matric potential,

U_0 = amplitude of matric potential, and

n = frequency.

Solving the diffusion equation for this boundary condition, Mitchell (1980) obtained the following equation to describe the suction u (y,t) at any time t and depth y:

$$u(y,t) = U_e + U_0 \exp\left[-\left(\frac{n\pi}{\alpha}\right)^{0.5} y\right] \cos\left[2\pi nt - \left(\frac{n\pi}{\alpha}\right)^{0.5} y\right] \tag{4.13}$$

In the FLODEF program, a linear elastic finite element approach based on quadratic isoparametric elements is used to model the two dimensional soil deformation. The changes in matric potential are modelled in a manner similar to the changes in temperature that are modelled in an elastic medium. The volumetric strain of an element is calculated through the swelling coefficient method presented by Lytton (1977) which is given in Equation 2.10 in Chapter II.

ONE DIMENSIONAL VERTICAL MOVEMENT PROGRAM MOPREC

The vertical movement program MOPREC developed by Gay (1994) estimate the vertical movement in expansive soils in a one dimensional domain. The major components of the program are: (1) climatic modelling, (2) estimation of suction profiles, and (3) estimation of vertical movement.

Climatic Model

The Climatic model for the MOPREC program was developed employing a frequency analysis of monthly mean rainfall and potential evapotranspiration of 12 different sites in the state of Texas for periods of time varying 20 to 52 years (Gay 1994). The selected sites covered the full range of climatic conditions prevailing in the state of Texas.

This climatic model allows the estimation of extreme dry and wet moisture depths, mean moisture depth, and mean matric suction for a soil profile at a particular location. The moisture depth is defined as the volume of water stored in a volume of soil profile having a unit cross-sectional area and a depth equal to the depth of the rooting zone of the vegetation at a particular location. Moisture depth of a soil profile varies in response to rainfall and

evapotranspiration. Since the rainfall and evapotranspiration at a particular location is stochastic in nature, the moisture depth should also be stochastic. The Thornthwaite Moisture Index (TMI) is a convenient parameter that can be used in lieu of both rainfall and evapotranspiration. In this climatic model, a relationship for the moisture depth has been obtained as a function of TMI and the depth of available moisture of the soil. The depth of available moisture refers to the quantity of water that the soil is capable of storing for use by plants and it depends on soil properties that affect the retention of water and the depth of the root zone (USDA 1981). To include the stochastic nature of rainfall and evapotranspiration in the climatic model, a relationship to estimate the variability of TMI has also been developed.

Estimation of Moisture Depths

The mean, dry, and wet moisture depths and mean matric suction for a particular climatic environment can be estimated using the relationships that have been developed in the climatic model. The procedure is described in the following steps.

Step 1: The distribution of TMI at a particular location follows the normal probability distribution. The frequency distribution of the TMI is obtained by using a historical mean of TMI (T_{mean}) at the site and obtaining the standard deviation of TMI from the following equation:

$$\sigma_{TMI} = 0.2833 T_{mean} + 17.73 \tag{4.14}$$

where,

σ_{TMI} = standard deviation, and

T_{mean} = mean Thornthwaite Moisture Index at the location. This can be obtained from maps containing spatial distribution of TMI such as that shown in Figure 3.2.

Step 2: The extreme values of the mean TMI for a dry year and a wet year (T_{wet} and T_{dry}) for a specific return period are then estimated from the following relationships:

$$TMI_{wet} = T_{mean} + \sigma_{TMI} Z \tag{4.15}$$

$$TMI_{dry} = T_{mean} - \sigma_{TMI} Z \tag{4.16}$$

where

Z = standard normal variable corresponding to the return period.

Step 3: The mean moisture depth for a particular year is defined as the average monthly moisture storage in the soil profile over the year. Mean annual moisture depths (d_{mean}, d_{dry}, and d_{wet}) corresponding to T_{mean}, T_{wet}, and T_{dry} are estimated from the following equation by substituting T_{mean}, T_{wet},and T_{dry} in place of TMI in the equation.

$$d = \frac{d_{am}}{\left[1 + \frac{d_{am} - d_1}{d_1\left(\frac{T}{T_1}\right)^{\gamma}}\right]} \tag{4.17}$$

where

d = mean annual moisture depth,

T = TMI + 60,

d_{am} = available moisture depth,

γ = 0.039337 d_{am} + 1.357033,

d_1 = 0.449079 d_{am} + 0.304560, and

T_1 = 0.062651 d_{am} + 59.53593.

Step 4: The amplitude of moisture depth (a_{dm}) describes the variability of moisture depth over a year at a specific site. This is calculated from the following equation:

$$a_{dm} = a_1 \exp\left[-\left(\frac{T_{mean} - a_2}{a_3}\right)^2\right] + a_4 \tag{4.18}$$

where

a_{dm}	=	amplitude of moisture depth,
T_{mean}	=	mean TMI at the site, and
a_1,a_2,a_3,a_4	=	regression coefficients.

Regression coefficients a_1,a_2,a_3,a_4 are given by:

$$a_i = \beta_{i,4} + \beta_{i,1} d_{am} - \beta_{i,2} \exp\left(-\left(\beta_{i,3} d_{am}\right)\right) \tag{4.19}$$

where

$\beta_{i,j}$ = regression coefficients for parameter a_i, i,j=1,4. These parameters are given in Table 4-1.

Table 4-1. Coefficients for the Estimation of Parameters for Amplitude of Moisture Depths

a_i	$\beta_{i,1}$	$\beta_{i,2}$	$\beta_{i,3}$	$\beta_{i,4}$
a_1	0.007327	17.601	0.057207	16.10400
a_2	-0.000100	-19.000	0.010000	-7.00000
a_3	-0.236260	-52.811	0.130077	39.55800
a_4	0.034308	0.000	0.000000	1.54771

Step 5: The extreme moisture depths are estimated from the following equations:

$$d_{max} = d_{wet} + a_{dm} \tag{4.20}$$

$$d_{min} = d_{dry} - a_{dm} \tag{4.21}$$

If the estimated value of d_{max} exceeds d_{am}, the value of d_{am} is used for d_{max}, and if the estimated d_{min} goes below zero, zero is used for d_{min}.

Estimation of Mean Matric Suction

Mean volumetric moisture content (θ_m) for a soil at a given location is expressed as functions of TMI and d_{am} as:

$$\theta_m = \frac{\dfrac{d_{am}}{Z_c}}{\left[1 + \dfrac{d_{am} - d_1}{d_1\left(\dfrac{T}{T_1}\right)^{Y}}\right]} + \theta_{dry} \tag{4.22}$$

where

Z_c = characteristic soil depth, and

θ_{dry} = volumetric moisture content at the driest soil state.

The characteristic soil depth is the minimum depth of soil over which the available moisture depth d_{am} may be stored. Z_c is given by:

$$Z_c = \frac{d_{am}}{\theta_{fc} - \theta_{dry}} \tag{4.23}$$

where

θ_{fc} = volumetric moisture content at field capacity.

θ_{fc} is given by:

$$\theta_{fc} = 0.88\ \theta_s \tag{4.24}$$

A relationship between volumetric moisture content and matric suction of a given soil exists through the desorption curve of that soil. Many forms of desorption relationships can be found in the literature. The MOPREC program developed by Gay (1994) uses the Nieber's equation which is given by:

$$|h| = \left[A \left(\frac{\theta_s - \theta_r}{\theta - \theta_r} - 1 \right) \right]^{\frac{1}{B}} \tag{4.25}$$

where

h = matric suction in cm,

θ_s = saturation volumetric moisture content,

θ_r = residual volumetric moisture content,

θ = volumetric moisture content, and

A, B = constants obtained by fitting this expression to measured data.

Given the desorption relationship for a site, the mean matric suction can be obtained by substituting the mean volumetric moisture content (θ_m) for θ in the above expression.

Estimation of Suction Profiles

The maximum, minimum, mean soil moisture depths, and mean matric suction for a given location is obtained from the previously described climatic model. In order to estimate the vertical movement due to changes in moisture content, it is necessary to develop suction variation with depth corresponding to the maximum, minimum, and mean soil moisture depths.

The wet suction profile for a particular location is obtained by using the maximum moisture depth estimated for that location and the desorption relationship. The procedure is described in the following steps.

1. Assume a triangular distribution of volumetric water content from the surface of the soil profile to the depth of root zone as shown in Figure 4.1 and estimate the volumetric moisture content at the surface (θ_{max}) from the following expression:

$$\frac{(\theta_{max} - \theta_m)}{2} Z_r = d_{max} - d_m \tag{4.26}$$

where

θ_m = mean volumetric moisture content from Equation 4.22,

Z_r = depth of root zone,

d_{max} = maximum moisture depth from Equation 4.20, and

d_m = mean moisture depth from Equation 4.17.

If the value of θ_{max} is less than or equal to the field capacity (θ_{fc}) of the soil, the assumed triangular distribution is used as the wet moisture profile.

2. If the value of θ_{max} exceeds the field capacity of soil, a trapezoidal distribution of volumetric water content from the surface of the soil profile to the depth of root zone as shown in Figure 4.1 is assumed and the depth of soil layer (Z_f) of which the volumetric moisture content is equal to the field capacity of soil is determined from the following expression:

$$(\theta_{fc} - \theta_m)Z_f + \frac{(\theta_{fc} - \theta_m)(Z_r - Z_f)}{2} = d_{max} - d_m \tag{4.27}$$

In this case, the trapezoid gives the wet moisture profile.

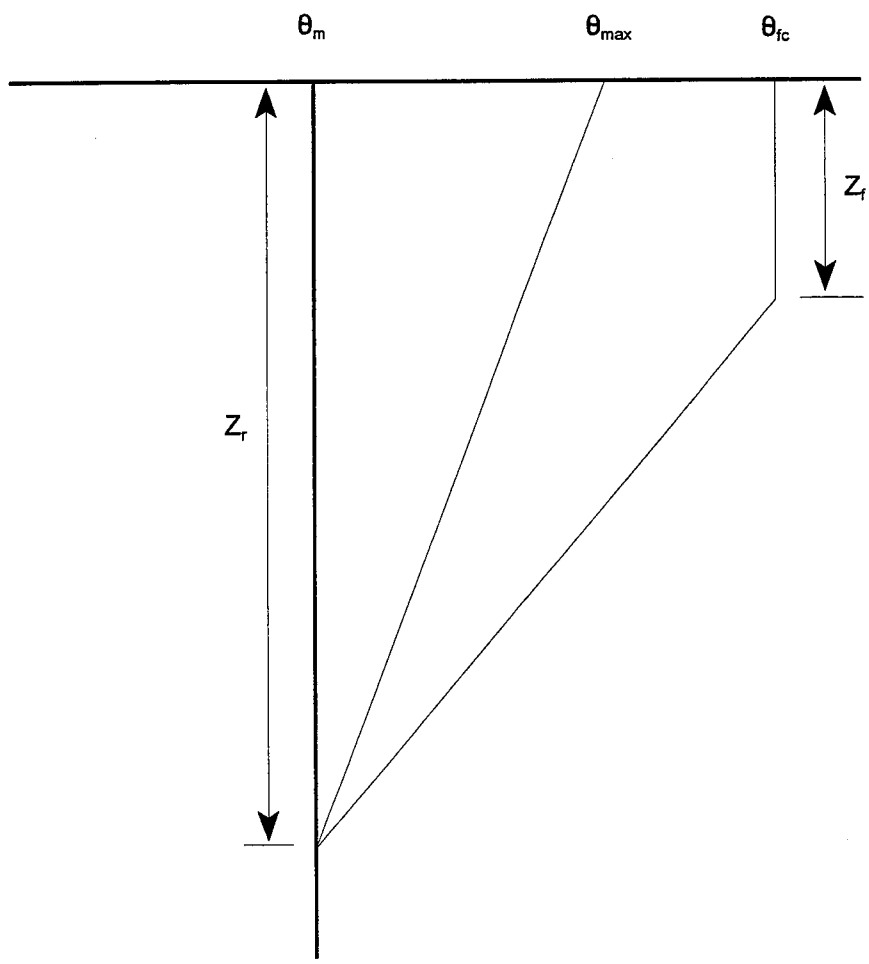

Figure 4.1. Initial Moisture Profiles over Root Depth

3. Using the desorption relationship in the form of Equation 4.25 and the wet moisture profile determined from Steps 1 or 2, the wet suction profile is obtained.

The equilibrium and dry moisture profiles are obtained by dividing the depth of root zone into several layers and extracting water from the soil profile using the following root extraction model (Prasad 1988):

$$S = \alpha \frac{2T_p}{Z_r}\left((z_2 - z_1) - \frac{z_2^2 - z_1^2}{2Z_r}\right) \tag{4.28}$$

where

S	=	depth of moisture extracted from the sublayer for one time step,
α	=	dimensionless parameter that is a function of matric suction,
T_p	=	plant transpiration rate,
z_1	=	depth to the top of the layer, and
z_2	=	depth to the bottom of the layer.

The values of α used in the model are as follows:

α	=	1	$100 \text{ cm} < h \leq 300 \text{ cm}$
α	=	0	$h > 31{,}622 \text{ cm}$
α	=	$(31{,}622 - h)/(31{,}622 - 300)$	$300 \text{ cm} < h \leq 31{,}622 \text{ cm}$

where

h	=	matric suction in cm of water.

The equilibrium moisture profile is obtained by extracting moisture until the extracted moisture depth is equal to $d_{max} - d_m$. By extracting moisture until the extracted moisture depth is equal to $d_{max} - d_{min}$, the dry moisture profile is obtained. The equilibrium and dry suction profiles are obtained through the desorption relationship of the soil.

Estimation of Vertical Movement

The volume change of a layer in the soil profile is calculated using the model proposed by Lytton (1977) which is given in Equation 2.10 in Chapter II. In this calculation, the estimated wet, equilibrium, and dry suction profiles which were explained in the previous section of this chapter are used. The swelling and shrinkage are calculated using wet and equilibrium suction profiles, and equilibrium and dry suction profiles, respectively (see Figure 4.2). The procedure of estimating total vertical movement is described below.

The volumetric strain for the ith layer due to swelling is given by:

$$\left(\frac{\Delta V}{V}\right)_{swell} = -\gamma_h \log_{10}\left(\frac{h_{wi}}{h_{ei}}\right) - OBC_i \tag{4.29}$$

The volumetric strain for the ith layer due to shrinkage is given by:

$$\left(\frac{\Delta V}{V}\right)_{shrink} = -\left[-\gamma_h \log_{10}\left(\frac{h_{di}}{h_{ei}}\right) + OBC_i\right] \tag{4.30}$$

where

$(\Delta V/V)_{swell}$	=	volumetric strain due to swelling,
$(\Delta V/V)_{shrink}$	=	volumetric strain due to shrinkage,
γ_h	=	suction compression index,
h_{wi}	=	extreme wet suction in cm of water,
h_{ei}	=	equilibrium suction in cm of water,
h_{di}	=	extreme dry suction in cm of water, and
OBC_i	=	overburden correction.

The overburden correction for the depth of 40 cm below the soil surface is neglected. For the depth greater than 40 cm, the overburden correction is given by:

$$OBC_i = \gamma_\sigma \log_{10}\left(\frac{\sigma_{fi}}{\sigma_i}\right) \tag{4.31}$$

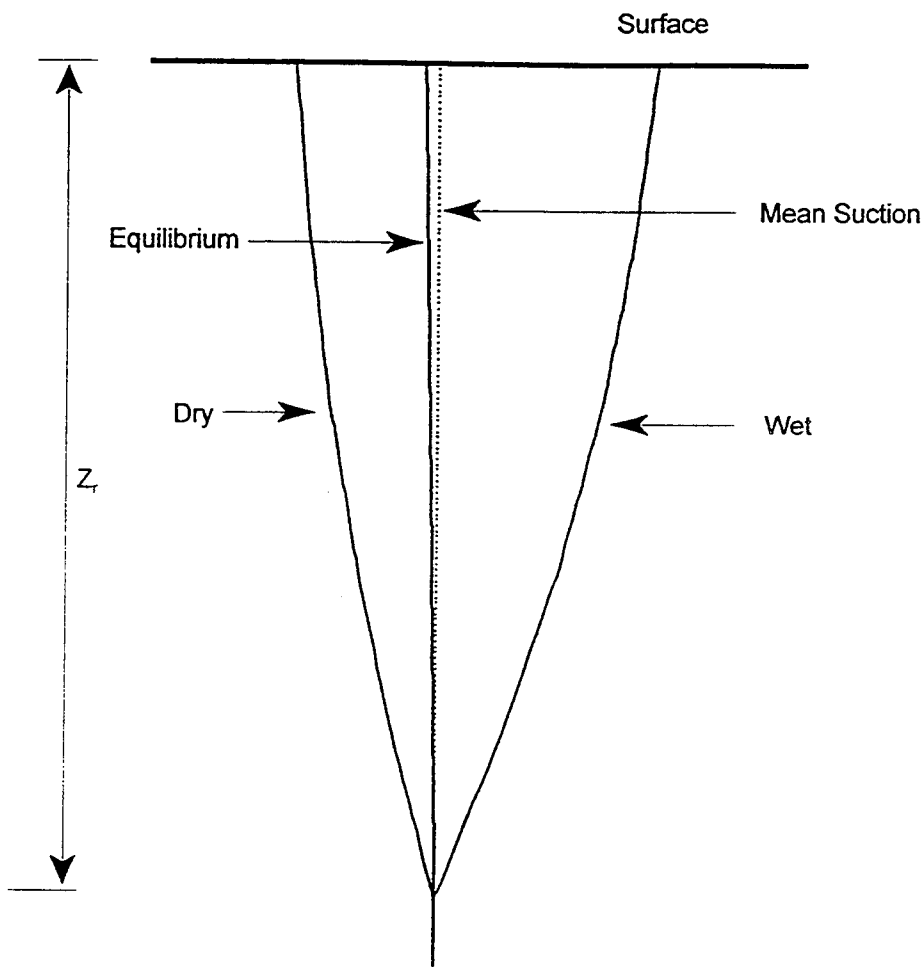

Figure 4.2. Suction Profiles for Swelling and Shrinkage Calculation

where

γ_σ = compressibility constant, assumed to be 1.2 times γ_h,

The value of σ_i is given by:

$$\sigma_i = 40\ \gamma_t \tag{4.32}$$

The value of σ_{fi} is given by:

$$\sigma_{fi} = \frac{z_i \gamma_t\ (1 + 2K_0)}{3} \tag{4.33}$$

where

γ_t = density of soil,

z_i = depth to the middle of ith layer from the soil surface in cm, and

K_0 = lateral earth pressure coefficient.

The lateral earth pressure coefficient is assumed as:

K_0	=	1.0	$pF \leq 3.0$
K_0	=	0	$pF \geq 4.5$
K_0	=	1- (pF-3)/1.5	$4.5 > pF > 3.0$

where

pF = average soil suction in pF scale,

pF = $(\log_{10} h_{wi} + \log_{10} h_{ei})/2$, for swelling, and

pF = $(\log_{10} h_{di} + \log_{10} h_{ei})/2$, for shrinkage.

When σ_{fi}/σ_i is less than zero, the overburden correction is taken as zero. Also, if the calculated values of $(\Delta V/V)_{swell}$, and $(\Delta V/V)_{shrink}$ are negative, the volumetric strains are taken as zero.

The total vertical swelling and shrinkage for the soil profile is calculated as follows:

$$\Delta H_{swell} = f_{swell} \sum_{i=1}^{N} \left(\frac{\Delta V}{V} \right)_{swell} \Delta z_i \tag{4.34}$$

$$\Delta H_{shrink} = f_{shrink} \sum_{i=1}^{N} \left(\frac{\Delta V}{V} \right)_{shrink} \Delta z_i \tag{4.35}$$

where

Δz_i = thickness of the ith layer, and

f_{swell} = lateral confinement factor for swelling, and

f_{shrink} = lateral confinement factor for shrinkage.

The values of f_{swell} and f_{shrink} are taken as 0.8 and 0.5, respectively (Lytton 1994). The maximum expected vertical movement is obtained by summing the vertical shrinkage and swelling.

PREDICTION MODEL

In order to develop a regression model to estimate vertical movement in a two dimensional domain, vertical movements for similar conditions were estimated from both the MOPREC and FLODEF computer programs. In this respect, vertical movements are estimated for four types of soils in five different climatic conditions. Five climatic conditions were represented by mean Thornthwaite Moisture Indices of -46.5, -21.3, -11.3, 14.8, and 26.8. The soil properties of the four soil types that were used in the analysis are shown in Table 4-2. The desorption parameters given in the table are for the desorption relationship of the form of Nieber's expression given in Equation 4.25. The other data that were common to both the MOPREC and FLODEF programs were the root depth of 240 cm and the return period of 25 years.

Table 4-2. Soil Properties Used in Developing Vertical Movement Model

No.	Suction Compression Index	Depth of Available Moisture (cm)	Desorption Parameters			
			θ_s	θ_r	B	A
1	0.04	25	0.54	0.054	0.3663	35.12
2	0.06	30	0.57	0.057	0.4036	41.70
3	0.08	34	0.59	0.059	0.4408	49.49
4	0.10	39	0.62	0.062	0.4781	58.76

Vertical Movement from MOPREC Program

The vertical movements for each case explained in the previous section were determined from the MOPREC program by dividing the root zone into layers 5 cm thick. Table 4-3 shows the estimated vertical movements from the MOPREC program.

Table 4-3. Vertical Movements from MOPREC Program

Thornthwaite Moisture Index	Total Vertical Movement (cm)			
	Soil Type 1	Soil Type 2	Soil Type 3	Soil Type 4
-46.5	1.32	1.73	2.11	2.44
-21.3	4.33	6.15	7.79	9.43
-11.3	5.57	8.36	10.46	12.48
14.8	4.65	7.00	9.07	11.18
26.8	4.50	6.76	8.76	10.76

In addition to the vertical movements, extreme dry and wet moisture depths (d_{min} and d_{max}), mean moisture depths (d_m), and mean matric suctions for each case considered were estimated from the MOPREC program. They are shown in Tables 4-4 through 4-7.

Table 4-4. Moisture Depths and Mean Matric Suctions for Soil Type 1

Thornthwaite Moisture Index	d_m	d_{max}	d_{min}	Mean Matric Suction (pF)
-46.5	0.61	5.32	0.00	4.45
-21.3	5.68	19.69	0.00	4.04
-11.3	8.37	25.00	0.00	3.82
14.8	14.47	25.00	0.00	3.28
26.8	16.52	25.00	0.00	3.09

Table 4-5. Moisture Depths and Mean Matric Suctions for Soil Type 2

Thornthwaite Moisture Index	d_m	d_{max}	d_{min}	Mean Matric Suction (pF)
-46.5	0.54	5.28	0.00	4.46
-21.3	6.25	22.09	0.00	4.06
-11.3	9.61	29.66	0.00	3.83
14.8	17.50	30.00	0.00	3.26
26.8	20.14	30.00	0.00	3.05

Table 4-6. Moisture Depths and Mean Matric Suctions for Soil Type 3

Thornthwaite Moisture Index	d_m	d_{max}	d_{min}	Mean Matric Suction (pF)
-46.5	0.47	5.22	0.00	4.47
-21.3	6.60	23.90	0.00	4.07
-11.3	10.51	32.66	0.00	3.83
14.8	19.96	34.00	0.00	3.24
26.8	23.11	34.00	0.00	3.02

Table 4-7. Moisture Depths and Mean Matric Suctions for Soil Type 4

Thornthwaite Moisture Index	d_m	d_{max}	d_{min}	Mean Matric Suction (pF)
-46.5	0.40	5.15	0.00	4.47
-21.3	6.92	26.04	0.00	4.09
-11.3	11.51	36.32	0.00	3.84
14.8	23.07	39.00	0.00	3.21
26.8	26.92	39.00	0.00	2.98

Vertical Movement from FLODEF Program

The two dimensional vertical movement profiles for different pavement configurations were obtained using the FLODEF program for the same cases of climatic and soil types that were considered in the estimation of vertical movements using the MOPREC program. Six different pavement configurations were used. The widths of pavement sections considered were 9.0 m, 12.6 m, 16.2 m, 23.4 m, 34.2 m, and 45.0 m. The vertical movements were calculated for pavements with and without vertical moisture barriers. The different barrier

depths considered were 90 cm, 150 cm, and 240 cm. Pavement sections considered consisted of a 45 cm thick combined subbase and surface layer and a 315 cm thick subgrade soil layer.

The initial subgrade moisture condition is given to the FLODEF program in the form of Equation 4.13. Therefore, a suction profile given in the form of this equation, which corresponds to the moisture depth, can be used to represent the initial moisture condition of the soil. For this computation, it is assumed that the matric potential varies in the range of 2.0-4.5 pF. Assuming trial dry and wet suction profiles, a numerical integration is carried out to estimate the soil moisture depth between dry and wet suction profiles in the root zone of subgrade soil. The suction profiles that yield the moisture depths between dry and wet suction profiles equal to (d_{max} - d_{min}) were selected to represent the initial dry and wet suction profiles. The equilibrium matric potentials and amplitudes of matric potential that describe the initial suction profiles through Equation 4.13 for the different cases considered are listed in Tables 4-8 through 4-11.

Table 4-8. Suction Profile Constants for Soil Type 1

Thornthwaite Moisture Index	Dry Profile (pF)		Wet Profile (pF)	
	U_e	U_0	U_e	U_0
-46.5	4.45	0.05	4.45	0.30
-21.3	4.04	0.46	4.04	1.34
-11.3	3.82	0.68	3.82	1.82
14.8	3.28	1.22	3.28	1.28
26.8	3.09	1.41	3.09	1.09

Table 4-9. Suction Profile Constants for Soil Type 2

Thornthwaite Moisture Index	Dry Profile (pF)		Wet Profile (pF)	
	U_e	U_0	U_e	U_0
-46.5	4.46	0.04	4.46	0.31
-21.3	4.06	0.44	4.06	1.36
-11.3	3.83	0.67	3.83	1.83
14.8	3.26	1.24	3.26	1.26
26.8	3.05	1.45	3.05	1.05

Table 4-10. Suction Profile Constants for Soil Type 3

Thornthwaite Moisture Index	Dry Profile (pF)		Wet Profile (pF)	
	U_e	U_0	U_e	U_0
-46.5	4.47	0.03	4.47	0.32
-21.3	4.07	0.43	4.07	1.37
-11.3	3.83	0.67	3.83	1.83
14.8	3.24	1.26	3.24	1.24
26.8	3.02	1.48	3.02	1.02

Table 4-11 Suction Profile Constants for Soil Type 4

Thornthwaite Moisture Index	Dry Profile (pF)		Wet Profile (pF)	
	U_e	U_0	U_e	U_0
-46.5	4.47	0.03	4.47	0.32
-21.3	4.09	0.41	4.09	1.39
-11.3	3.84	0.66	3.84	1.84
14.8	3.21	1.29	3.21	1.21
26.8	2.98	1.52	2.98	0.98

The swelling and shrinkage profiles for the pavement sections for each type of soil were obtained through the FLODEF program using the initial conditions listed in Tables 4-8 through 4-11. The analysis was carried out for 20 years using a constant surface suction at the exposed boundary which was equal to the mean matric potential for the respective case. Mean matric potentials are listed in Tables 4-4 through 4-7. The total vertical movements were calculated by summing the swelling and shrinkage.

Model Development

The estimated vertical movements from the two programs MOPREC and FLODEF suggest a model of the following form:

$$\frac{VM_{2D}}{VM_{1D}} = \xi_1 \exp\left[\left(\xi_2 \frac{d}{D}\right)^{\xi_3}\right] \tag{4.36}$$

where

VM_{2D} = vertical movement from the FLODEF program,

VM_{1D} = vertical movement from the MOPREC program,

d	=	distance from the center of the pavement to the point where the vertical movement needs to be calculated,
D	=	half width of the pavement, and
ξ_1, ξ_2, ξ_3	=	regression coefficients.

Typical plots of vertical movement profile across a pavement section for different conditions considered are shown in Figures 4.3 through 4.5.

The nonlinear regression analysis was carried out for the vertical movement data obtained from the two computer programs using the NLIN procedure in the statistical analysis software package developed by SAS Institute Inc. The regression coefficients obtained from this analysis are tabulated in Appendix B.

In order to develop predictive equations for the parameters ξ_1, ξ_2, and ξ_3, a multiple linear regression analysis was carried out using the same statistical analysis software package used in the nonlinear regression. The regression equations developed are as follows:

for pavement width less than 18.0 m,

$$\begin{aligned}\xi_1 = {} & 2.0144 - 0.0238(VM_{1D}) - 0.000892(DB) - 0.1611(\log_e a_{dm}) - \\ & 0.1936(\log_e D) + 0.4016\left(\frac{VM_{1D}}{a_{dm}}\right) + 0.00005336(VM_{1D} * TMI) + \\ & 0.00004112(a_{dm} * DB) \\ & n = 240 \qquad R^2 = 0.88\end{aligned} \tag{4.37}$$

$$\begin{aligned}\xi_2 = {} & -1.2924 + 0.0332(VM_{1D}) + 0.004651(TMI) - 0.002591(DB) + \\ & 0.321(\log_e D) + 0.000006077(DB^2) - 0.2634\left(\frac{VM_{1D}}{a_{dm}}\right) - \\ & 0.001172(VM_{1D} * TMI) + 0.00005722(a_{dm} * DB) \\ & n = 240 \qquad R^2 = 0.92\end{aligned} \tag{4.38}$$

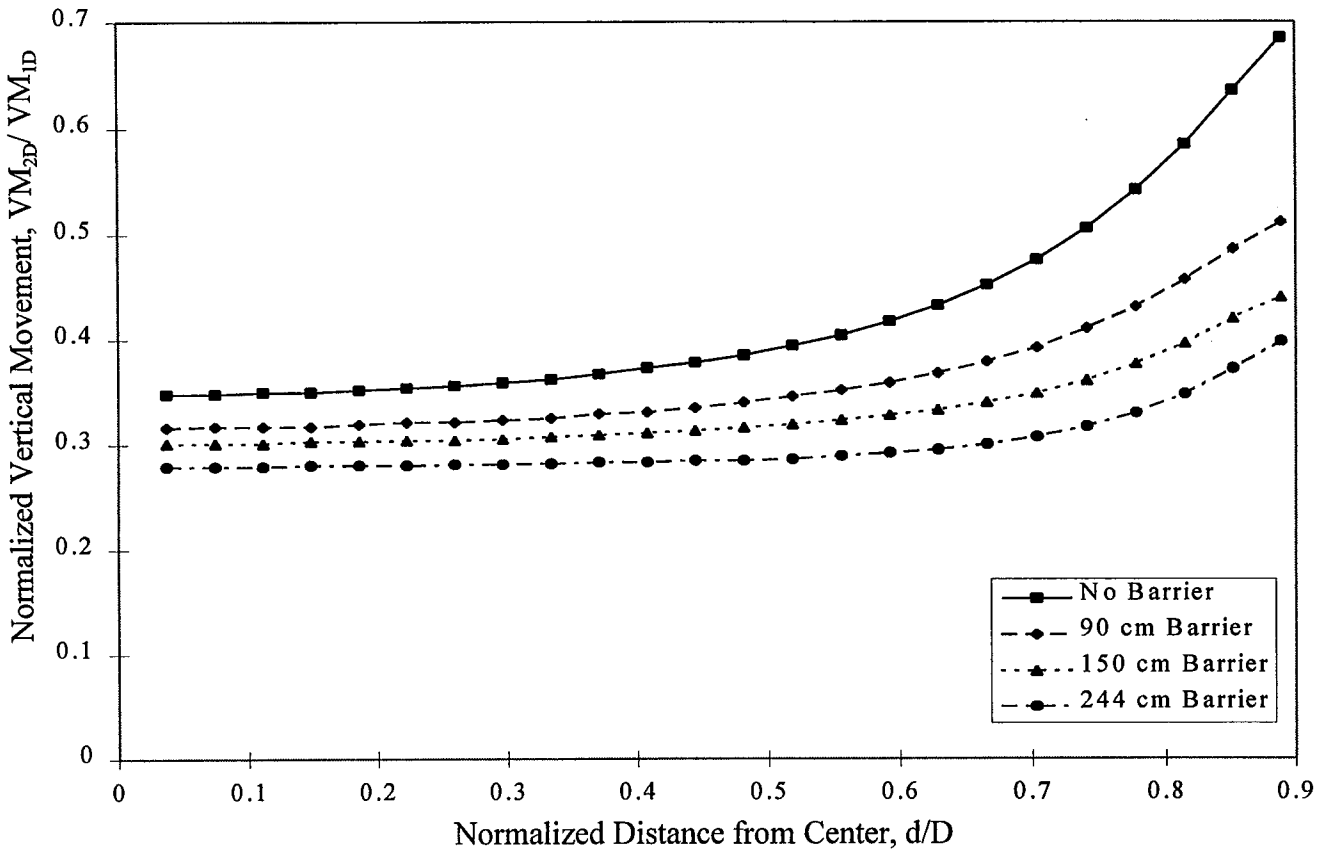

Figure 4.3. Vertical Movement for Different Barrier Depths

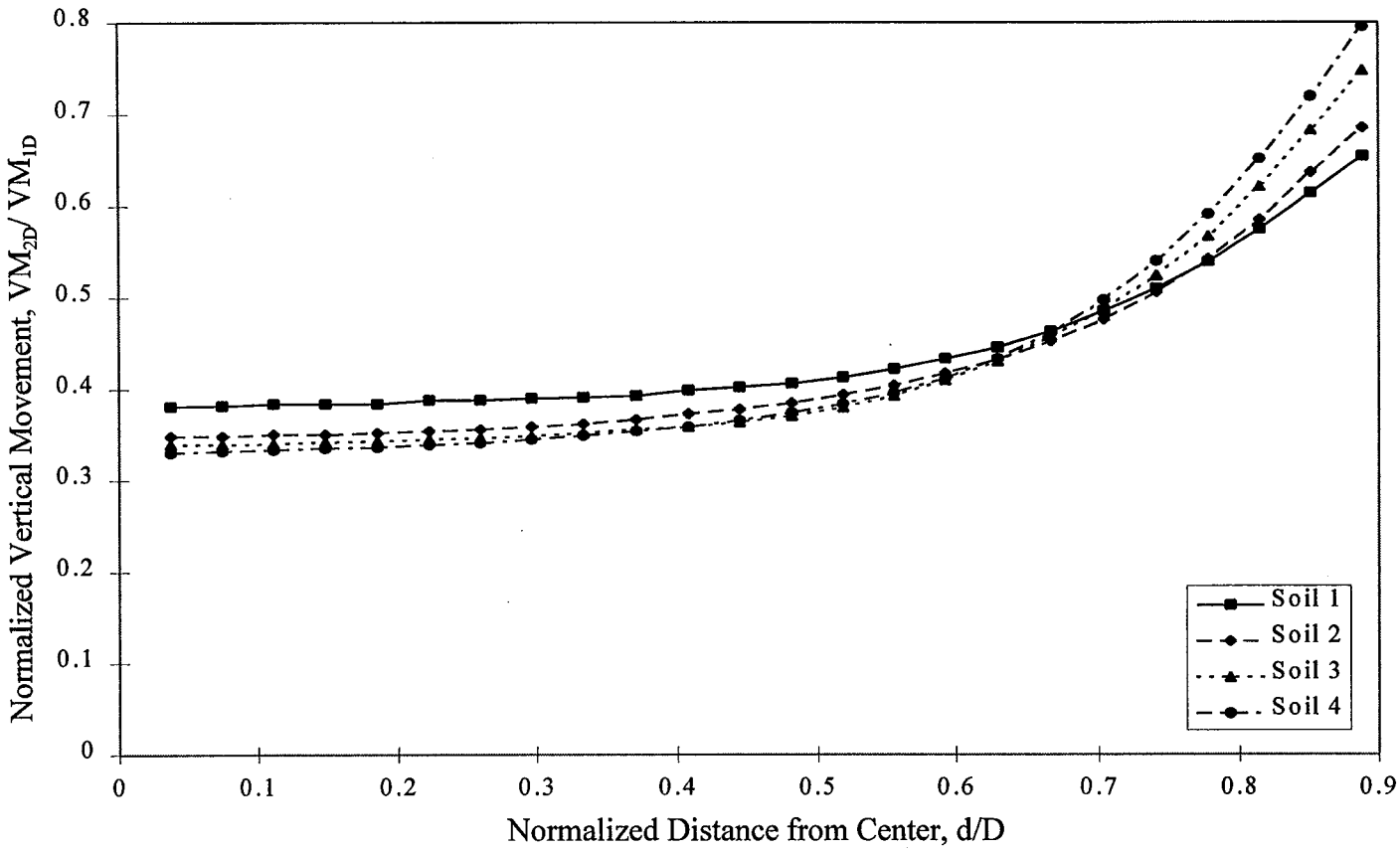

Figure 4.4. Vertical Movement for Different Soil Types

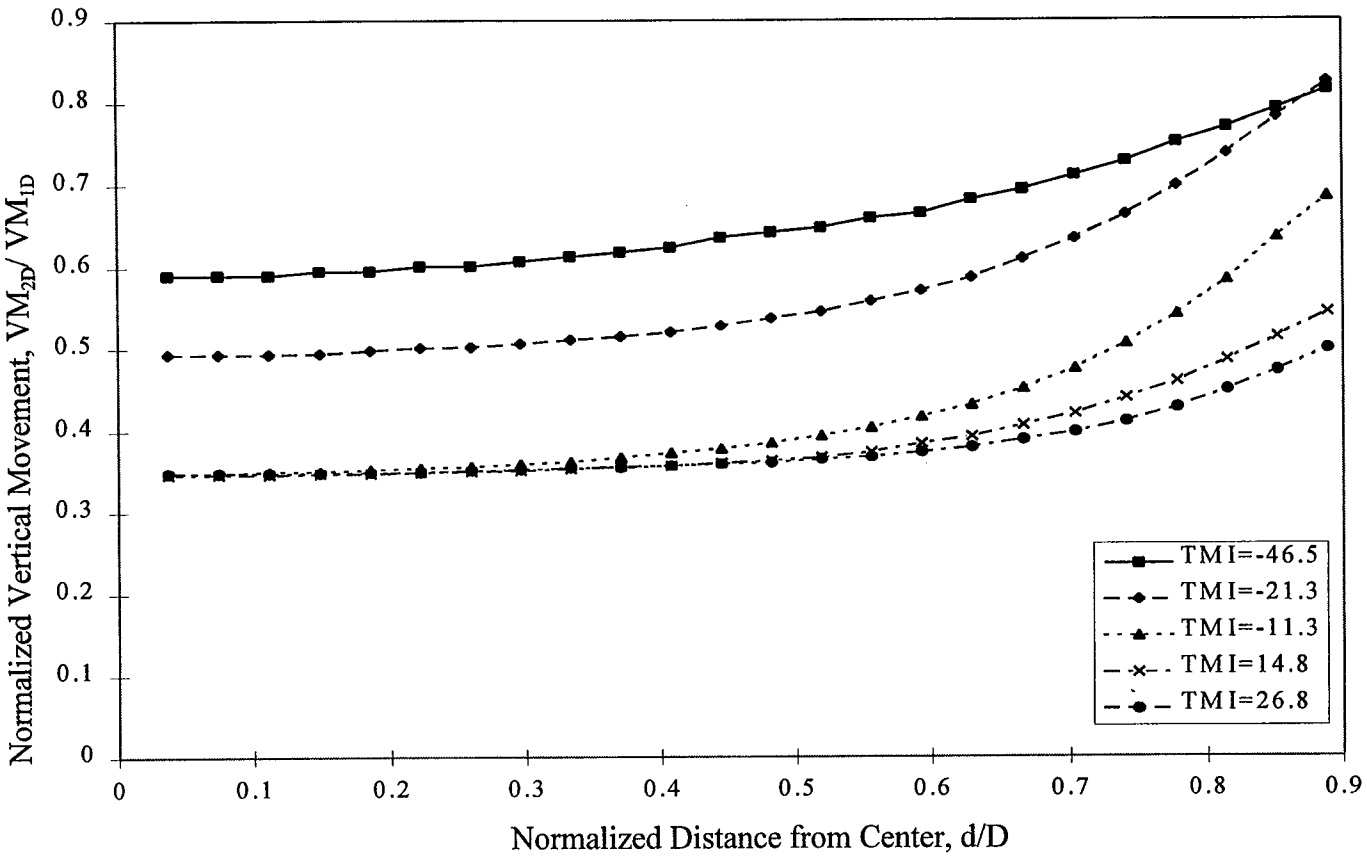

Figure 4.5. Vertical Movement for Different Thornthwaite Moisture Indices

$$\xi_3 = \exp(1.0725 - 0.07346(VM_{1D}) + 0.008762(TMI) - 0.003529(DB) + 0.00000852(DB^2) - 0.001458(VM_{1D} * TMI) + 0.000121(VM_{1D} * D) + 0.000156(a_{dm} * DB))$$

$$n = 240 \qquad R^2 = 0.83 \tag{4.39}$$

for pavement widths greater than 22.0 m,

$$\xi_1 = 0.9061 - 0.03515(VM_{1D}) - 0.00015(DB) - 0.04483(\log_e a_{dm}) - 0.0924(\log_e D) + 0.3332\left(\frac{VM_{1D}}{a_{dm}}\right) + 0.00005867(VM_{1D} * TMI) + 0.000006405(a_{dm} * DB)$$

$$n = 240 \qquad R^2 = 0.86 \tag{4.40}$$

$$\xi_2 = -0.4083 + 0.02936(VM_{1D}) - 0.002136(TMI) - 0.001454(DB) + 0.1701(\log_e D) + 0.000002259(DB^2) - 0.1412\left(\frac{VM_{1D}}{a_{dm}}\right) - 0.000186(VM_{1D} * TMI) + 0.00002022(a_{dm} * DB)$$

$$n = 240 \qquad R^2 = 0.85 \tag{4.41}$$

$$\xi_3 = \exp(1.4566 - 0.08179(VM_{1D}) + 0.0175(TMI) - 0.002933(DB) + 0.000008001(DB^2) - 0.003066(VM_{1D} * TMI) + 0.00002585(VM_{1D} * D) + 0.00009203(a_{dm} * DB))$$

$$n = 240 \qquad R^2 = 0.75 \tag{4.42}$$

where

VM_{1D}	=	vertical movement from 1-D program,
DB	=	depth of barrier,
a_{dm}	=	amplitude of moisture depth,

D	=	half width of pavement, and
TMI	=	Thornthwaite Moisture Index.

For pavement widths between 18 m and 22 m, the parameters ξ_1, ξ_2, and ξ_3 are estimated from the following equation:

$$\xi = \frac{[\xi_{18}(2200 - D) + \xi_{22}(D - 1800)]}{400} \tag{4.43}$$

where

ξ	=	parameter ξ_1, ξ_2, or ξ_3 for the pavement width of D,
ξ_{18}	=	parameter ξ_1, ξ_2, or ξ_3 estimated from the equations for the pavement widths less than 18 m (Equation 4.37, 4.38, or 4.39), and
ξ_{22}	=	parameter ξ_1, ξ_2, or ξ_3 estimated from the equations for the pavement widths greater than 22 m (Equation 4.40, 4.41, or 4.42).

Equations 4.36 through 4.43 give the complete predictive model for the vertical movement in a two dimensional domain. Figures 4.6 through 4.11 show the plots of vertical movement estimated from the FLODEF program versus vertical movements estimated from the predictive model.

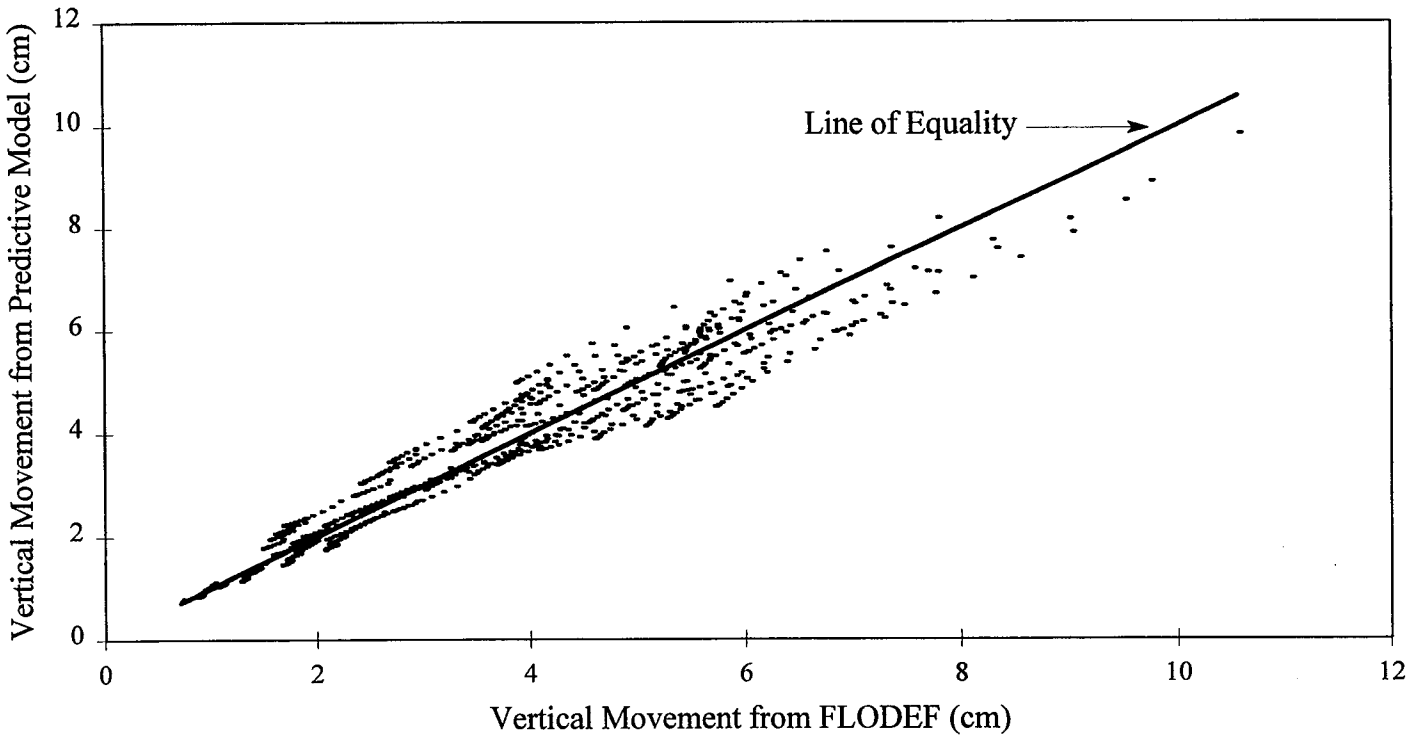

Figure 4.6. Vertical Movement from FLODEF Vs. Predictive Model for Pavement Width of 9.0 m

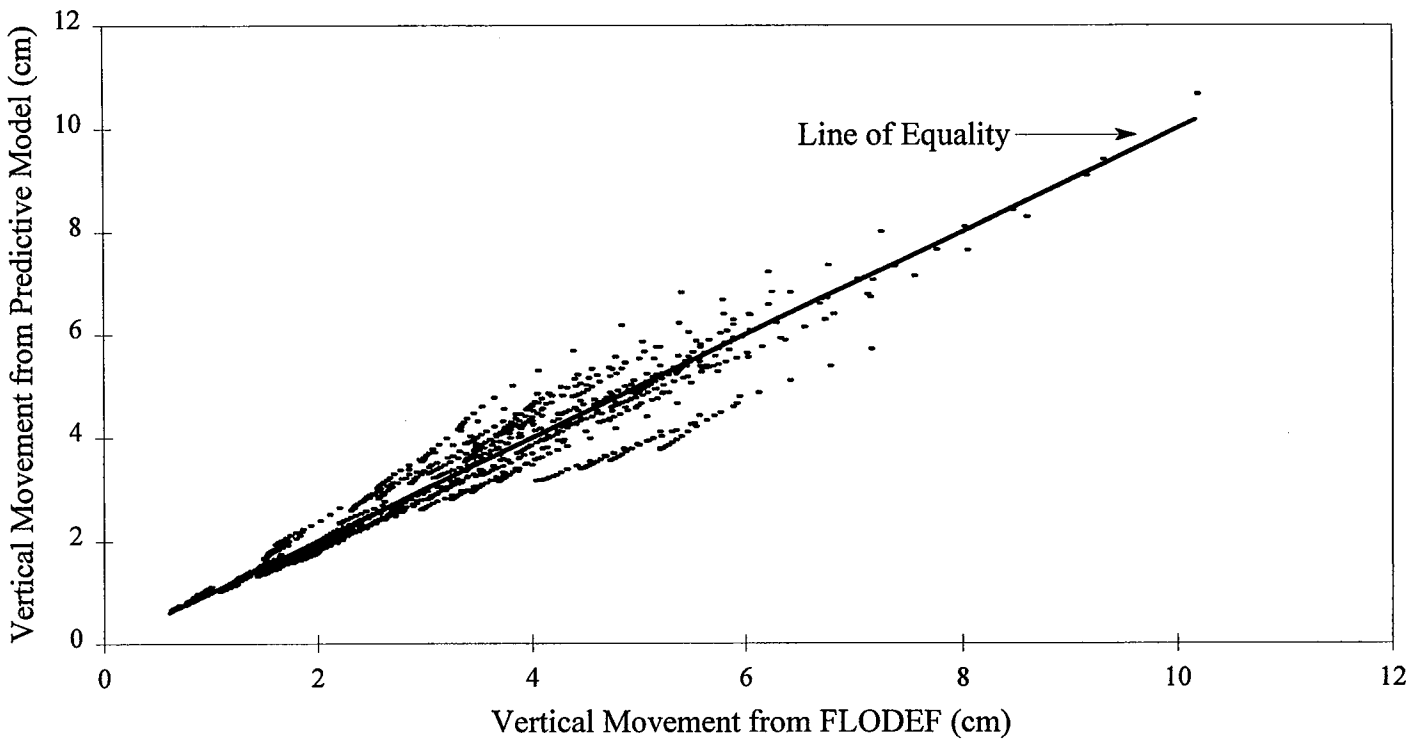

Figure 4.7. Vertical Movement from FLODEF Vs. Predictive Model for Pavement Width of 12.6 m

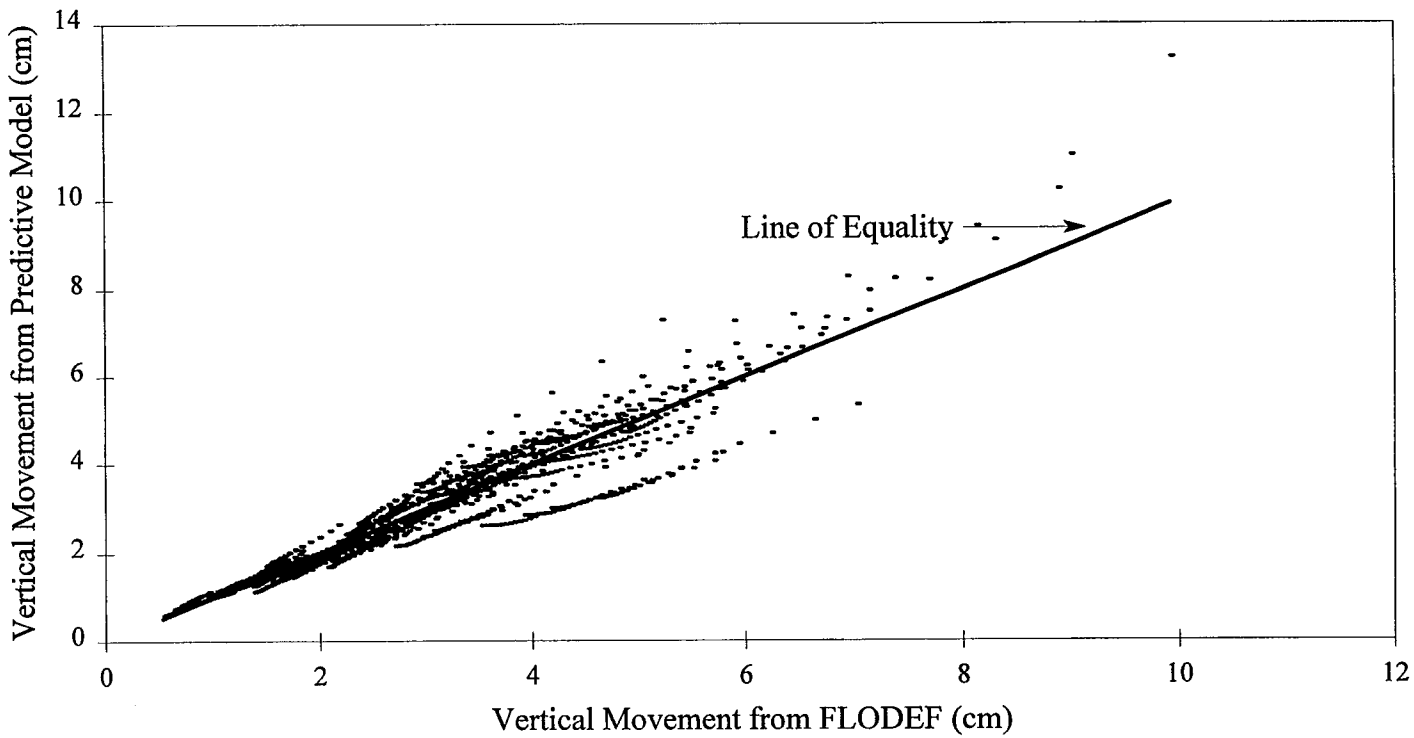

Figure 4.8. Vertical Movement from FLODEF Vs. Predictive Model for Pavement Width of 16.2 m

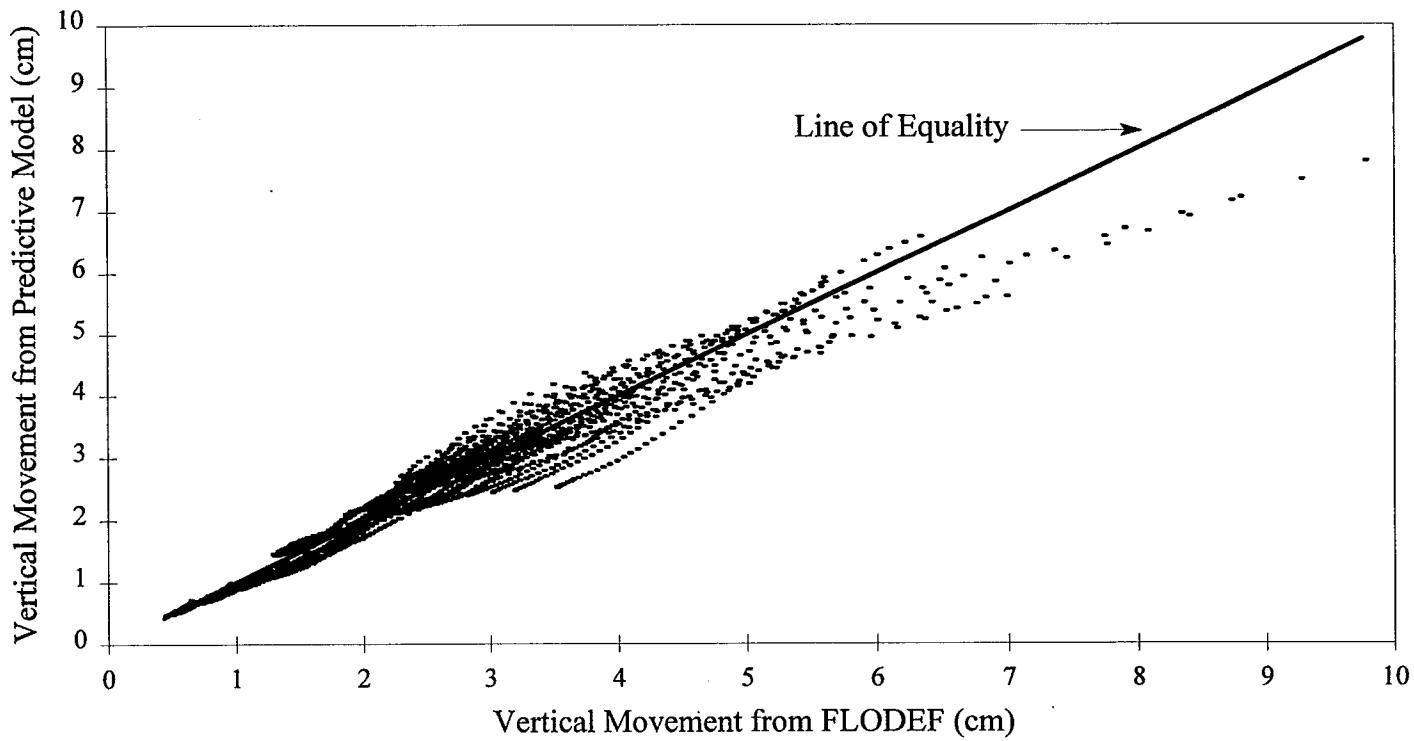

Figure 4.9. Vertical Movement from FLODEF Vs. Predictive Model for Pavement Width of 23.4 m

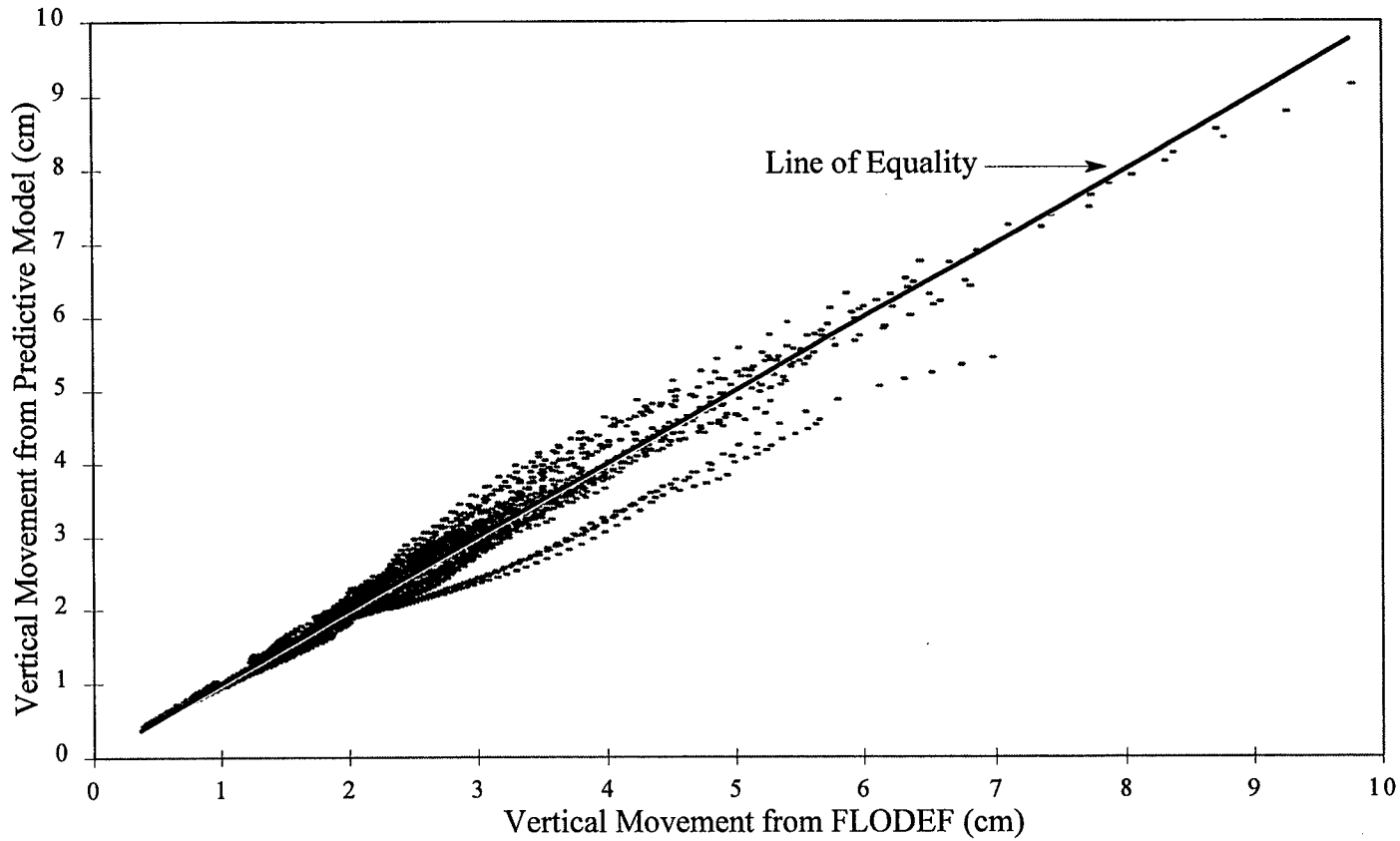

Figure 4.10. Vertical Movement from FLODEF Vs. Predictive Model for Pavement Width of 34.2 m

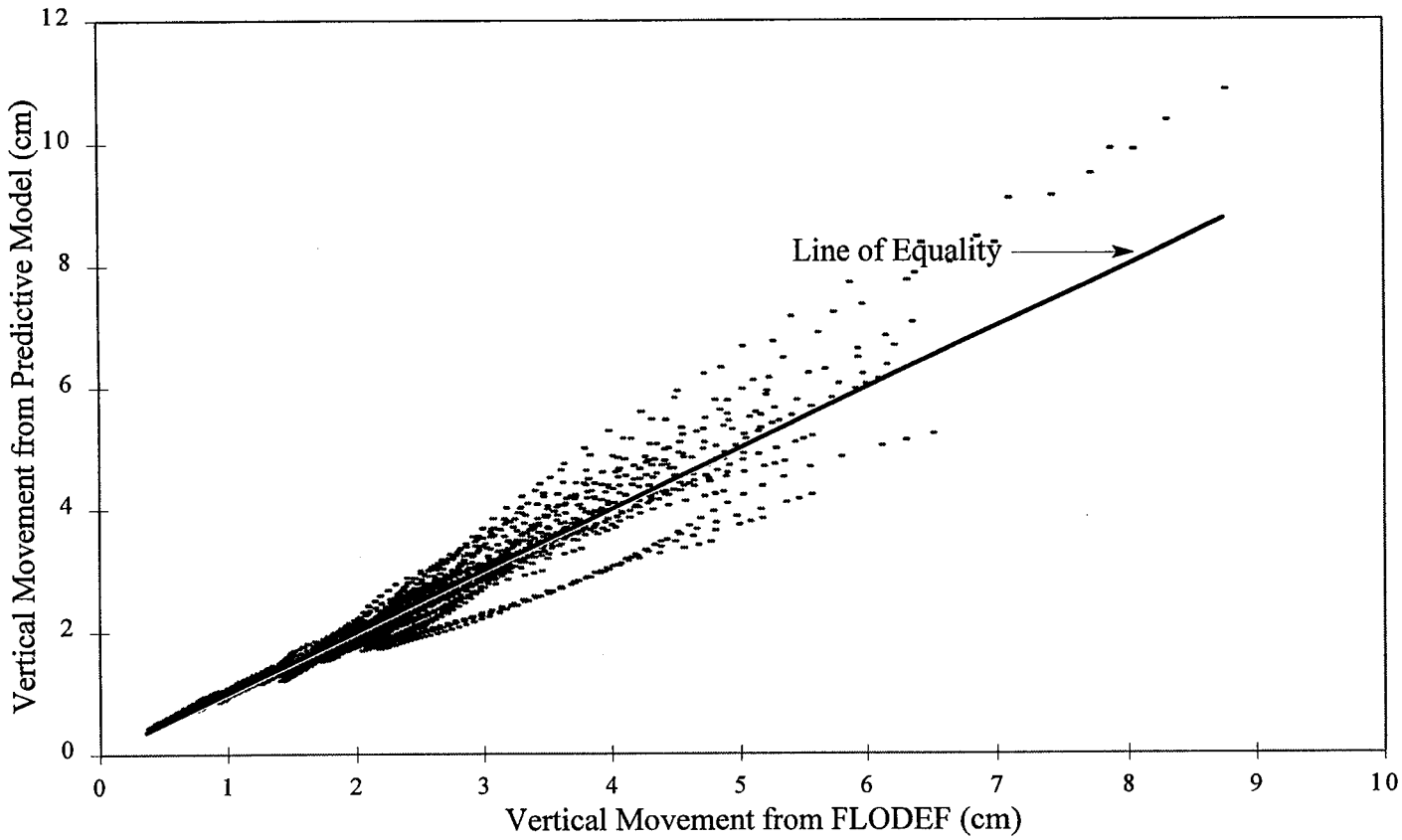

Figure 4.11. Vertical Movement from FLODEF Vs. Predictive Model for Pavement Width of 45.0 m

CHAPTER V

DEVELOPMENT OF ROUGHNESS MODEL

The development of roughness on pavements with time is caused by the combination of traffic loading applied on the pavement and the environmental effects such as frost heave in cold regions and swelling of subgrade soil where the pavements are built on expansive clay subgrades. In Texas, the major causes of roughness are the traffic loading and the activity of expansive clay subgrades. In this chapter, a model is developed to predict the roughness development on pavements built on expansive clay subgrades based on roughness data collected from several highway pavement sections in Texas. Data collected are described in Chapter III of this report.

The pavement sections considered in this research study were originally constructed during different periods of time in the past, long before the testing program began. Over the years, many rehabilitations on these pavement sections have been performed. As a result, the current structure of these pavements is very complex. Layer thicknesses and properties vary dramatically throughout the pavement sections. Hence, a reliable estimation of roughness development due to traffic loading is not possible and the component of roughness due to swelling clay activity of an individual data point cannot be isolated. This prohibits the development of a model that predicts the roughness development due solely to the expansive clay activity. Therefore, the model developed in this chapter needs to be used with a model that predicts the roughness due to traffic.

The roughness model is developed by fitting the roughness data to appropriate models, estimating parameters, and by correlating these parameters to the vertical movements predicted through the vertical movement model described in Chapter IV. This vertical movement model uses the one dimensional vertical movement estimated for a soil column

using the MOPREC program to estimate the vertical movement at different points of a pavement cross section. The original MOPREC program developed by Gay (1994) allows only a single layer of subgrade soil. In nature, the subgrade soil profile may consist of many layers of soil with different properties. The arrangement of these soil layers controls the amount of vertical movement that the pavement will experience. In order to account for the variability of properties in a soil profile, the MOPREC program was modified to accommodate a multilayer subgrade soil profile with different soil properties in each layer. In the preceding sections of this chapter, the modifications to the MOPREC program and the development of the roughness prediction models are described.

MODIFICATION TO THE MOPREC PROGRAM

Depth of Available Moisture

The input data to the MOPREC program developed by Gay (1994) include the Suction Compression Index (SCI), parameters of the desorption relationship, and depth of available moisture. Assuming the suction at the field capacity and the wilting point of soil are 2.0 pF and 4.5 pF, respectively, the depth of available moisture is estimated from the following relationship:

$$d_{am} = 0.5 Z_r (\theta_1 - \theta_2) \tag{5.1}$$

where

d_{am} = depth of available moisture,

Z_r = depth of root zone,

θ_1 = volumetric moisture content corresponding to the field capacity of soil obtained through the desorption relationship, and

θ_2 = volumetric moisture content corresponding to the wilting point of soil obtained through the desorption relationship.

Desorption Relationship

The MOPREC program requires parameters for the Nieber's desorption relationship in order to estimate suction profiles from moisture profiles. These parameters need to be estimated from laboratory testings since the parameters for different types of soils are not readily available. However, many researchers have used Gardner's desorption relationship to describe the suction and water content relationship for soils. They have also estimated parameters for different types of soils. Therefore, the MOPREC program is modified to include the Gardner's desorption relationship in lieu of Nieber's equation. The Gardner's expression for the desorption relationship is as follows:

$$\theta = \frac{n}{1 + a|h|^x} \tag{5.2}$$

where

θ	=	volumetric moisture content,
n	=	porosity of the soil,
h	=	soil suction in cm of water, and
a, x	=	soil constants.

The parameters required to describe this desorption relationship can either be estimated from laboratory testing or obtained from data available in the literature. Appendix C presents the procedure of estimating these parameters from laboratory results, parameters estimated for 14 different expansive clay soil samples of CH soil group of Unified Soil Classification System, and parameters for other groups of soils which were extracted from the existing literature.

Suction Compression Index

A subroutine to the MOPREC program was added to calculate the SCI using basic soil parameters. The SCI is calculated for each layer of soil from the chart method proposed by McKeen (1980) which is explained in detail in Chapter II. Data required for the estimation of SCI are plasticity index, percentage clay (% finer than 2 micron), and cation exchange capacity. When the cation exchange capacity is not available, the program estimates the

cation exchange capacity from the empirical equation developed by Mojekwu (1979) which is given in Equation 2.16 in Chapter II. The original MOPREC program used a single suction compression index for the soil profile. The program was modified to use the suction compression index of each layer in the estimation of vertical movement.

Moisture Depths and Extreme Suction Profiles

The average available moisture depth for the soil profile is estimated from Equation 5.1 by using average desorption parameters n, a, and x that are calculated as follows:

$$P = \frac{1}{Z_r}\sum_{i=1}^{N} P_i t_i \tag{5.3}$$

where

P	=	average desorption parameter,
Z_r	=	depth of root zone,
N	=	no. of layers from the surface to the depth of root zone,
P_i	=	desorption parameter for the ith layer, and
t_i	=	thickness of the ith layer.

The average available moisture depth estimated in this manner is used in Equations 4.17 through 4.23 to calculate the mean, maximum, and minimum moisture depths(d_{mean}, d_{max}, and d_{min}), and the mean volumetric moisture content (θ_m). Mean matric potential for the site is estimated by using average desorption parameters and substituting θ_m for θ in Equation 5.2 and solving for h. An extreme wet soil moisture profile for a particular location is obtained by distributing moisture in a soil profile by a triangular or trapezoidal distribution as explained in Chapter IV and using average desorption parameters. In the original MOPREC program, the minimum suction at the surface was considered as the suction corresponding to the field capacity of soil (see Figure 4.1). The program was modified to accommodate the longitudinal slope and lateral drainage conditions of the pavement. The slope conditions used are flat, hill, and valley. The lateral drainage conditions used are negative, zero, and positive drainage as shown in Figure 5.1. The minimum suction at the surface for different

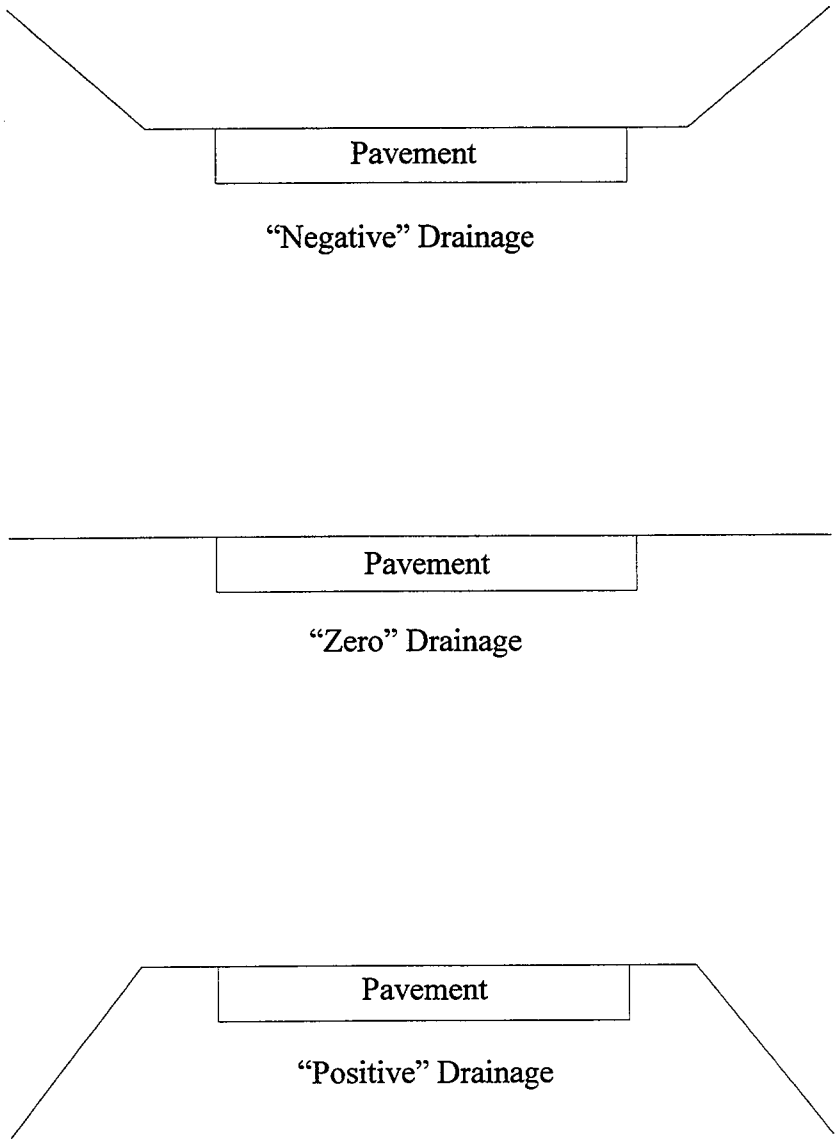

Figure 5.1. Different Lateral Drainage Conditions of a Pavement

slope and drainage conditions are given in Table 5.1.

Table 5-1. Minimum Suction (pF) for Different Slope and Drainage Conditions

Longitudinal Slope	Lateral Drainage		
	Negative	Zero	Positive
Flat	2.0	2.2	2.3
Hill	2.3	2.5	2.6
Valley	2.0	2.2	2.3

Note: For Thornthwaite Moisture Index (TMI) greater than +10.0, the values in the table are used. For $-20.0 \leq TMI < 10.0$, 0.2 is added to the values in the table. For TMI less than -20.0, 0.4 is added to the values in the table.

ESTIMATION OF VERTICAL MOVEMENT AT DIFFERENT WHEEL PATHS

In Chapter IV, a model was developed to estimate the vertical movement at different points of a pavement cross section. Data required for this model include 1-D vertical movement, depth of barrier, Thornthwaite Moisture Index, amplitude of moisture depth, half width of pavement, and distance from the center of pavement to the point where the vertical movement needs to be estimated. The modified MOPREC program explained in the previous section was used to estimate the 1-D vertical movement. Desorption coefficients used in the modified MOPREC program are given in Tables 5.2 through 5.7. Other data used in the program are given in Chapter III. Amplitude of moisture depth was calculated from Equation 4.18. Widths of pavement sections and distance from the center of pavement to each wheel path are shown in Table 5-8. Vertical movements estimated from the model for each wheel path are given in Appendix D.

Table 5-2. Desorption Coefficients - San Antonio Sites

Test Site	Depth (cm)	a	x	n
San Antonio, General McMullen	0.0-244.0	0.0290	0.3836	0.5940
San Antonio, IH 37	0.0-244.0	0.0299	0.3705	0.6230
San Antonio, US 281	0.0-244.0	0.0290	0.3836	0.5940
San Antonio, IH 10	0.0-244.0	0.0297	0.3638	0.6040

Table 5-3. Desorption Coefficients - Seguin, IH 10

Pavement Section	Depth (cm)	a	x	n
Barrier Section	0.0-106.7	0.0290	0.3836	0.5940
	106.7-182.9	0.0300	0.3902	0.5430
	182.9-244.0	0.0305	0.3683	0.6110
Control Section	0.0-122.0	0.0290	0.3836	0.5940
	122.0-244.0	0.0040	0.4740	0.4930

Table 5-4. Desorption Coefficients - Dallas, IH 635

Pavement Section	Depth (cm)	a	x	n
Barrier Section	0.0-106.7	0.0296	0.3661	0.6060
	106.7-213.4	0.0297	0.3638	0.6040
	213.4-244.0	0.0292	0.3668	0.6120
Control Section	0.0-152.4	0.0292	0.3668	0.6120
	152.4-244.0	0.0297	0.3638	0.6040

Table 5-5. Desorption Coefficients - Sierra Blanca, IH 10

Pavement Section	Depth (cm)	a	x	n
Eastbound Barrier Section	0.0-76.2	0.0310	0.7220	0.3760
	76.2-213.4	0.0180	0.5230	0.4520
	213.4-244.0	0.0290	0.3836	0.5940
Westbound Barrier Section	0.0-137.2	0.0310	0.7220	0.3760
	137.2-213.4	0.0180	0.5230	0.4520
	213.4-244.0	0.0290	0.3836	0.5940
Control Sections	0.0-244.0	0.0310	0.7220	0.3760

Table 5-6. Desorption Coefficients - Greenville, IH 30

Pavement Section	Depth (cm)	a	x	n
Vertical Fabric Barrier Sections	0.0-61.0	0.0310	0.7220	0.3760
	61.0-91.5	0.0040	0.6100	0.4400
	91.5-122.0	0.0040	0.6100	0.4400
	122.0-183.0	0.0277	0.3709	0.6740
	183.0-244.0	0.0299	0.3705	0.6230
Control Sections to Vertical Fabric Barriers	0.0-61.0	0.0040	0.6100	0.4400
	61.0-122.0	0.0290	0.3836	0.5940
	122.0-183.0	0.0297	0.3638	0.6040
	183.0-244.0	0.0726	0.2838	0.6090
Control Sections to Lime and Lime-Fly Ash Barrier Sections	0.0-61.0	0.0640	0.2470	0.2930
	61.0-122.0	0.0240	0.3590	0.3410
	122.0-183.0	0.0280	0.3440	0.4930
	183.0-244.0	0.0299	0.3705	0.6230

Table 5-7. Desorption Coefficients - Converse, FM 1516

Pavement Section	Depth (cm)	a	x	n
Barrier Section	0.0-91.5	0.0278	0.3952	0.5210
	91.5-152.5	0.0299	0.3705	0.6230
	152.5-213.5	0.0297	0.3638	0.6040
	213.5-244.0	0.0299	0.3705	0.6230

Table 5-8. Geometrical Data in Test Sections

Test Site	Pavement Width (cm)	Distance from Center of Pavement to Wheel Path (cm)					
		Outside Lane		Center Lane		Inside Lane	
		Right	Left	Right	Left	Right	Left
San Antonio, General McMullen	2865	1158	975	823	640	488	305
San Antonio, IH 37	4145	1676	1494	1311	1128	945	762
Greenville, IH 30	1158	183	0	-	-	183	366
San Antonio, US 281	3536	1372	1189	1006	823	640	457
San Antonio, IH 10	4145	1676	1494	1311	1128	945	762
Sierra Blanca, IH 10	1158	183	0	-	-	183	366
Seguin, IH 10	1189	198	15	-	-	168	351
Converse, FM 1516	1219	274	91	-	-	-	-
Dallas, IH 635	1768	427	244	61	122	305	488

MODEL DEVELOPMENT

By plotting the Present Serviceability Index (PSI) and the International Roughness Index (IRI) obtained for the barrier and control sections by the data reduction procedures described in Chapter III with the time elapsed from the last rehabilitation of the pavement sections, it was found that the pavement performance can be modelled through a sigmoidal type curve. In this research study, the following sigmoidal models with respect to PSI and IRI are used in modelling pavement roughness with time.

With respect to PSI

$$PSI = PSI_0 - (PSI_0 - 1.5)\exp\left[-\left(\frac{\rho_s}{t}\right)^{\beta_s}\right] \tag{5.4}$$

With respect to IRI

$$IRI = IRI_0 + (4.2 - IRI_0)\exp\left[-\left(\frac{\rho_i}{t}\right)^{\beta_i}\right] \tag{5.5}$$

where

PSI_0	=	initial serviceability index of the pavement,
t	=	time in months,
IRI_0	=	initial IRI in m/km, and
ρ_s, β_s, ρ_i, β_i	=	roughness parameters.

To estimate the roughness parameters, ρ_s, β_s, ρ_i, β_i, for each wheel path, the nonlinear regression analysis was carried out for the roughness data using the NLIN procedure in the statistical analysis software package developed by SAS Institute Inc. Out of 10 sites studied in this research study, only six sites were used in the development of roughness models. Four other sites were not used due to the following reasons.

1. San Antonio, IH 410 - After the barriers were placed, the pavement section was modified and an extra lane was added to both the northbound and

southbound traveled ways. The moisture barrier on the northbound traveled way is now located between the new inside lane and the center lane (previous inside lane).

2. San Antonio, IH 37 - The barrier in this pavement section was constructed in 1968, and the latest rehabilitation was carried out in 1979. Roughness data was not collected at this site until 1987. Due to the unavailability of roughness data during the first eight years, it is not possible to accurately fit the roughness data to the models.
3. San Antonio, General McMullen Drive - A horizontal barrier has been placed at this site. Also, there is no appreciable roughness development since the last rehabilitation.
4. San Antonio, US 281 - No appreciable roughness development since the last rehabilitation. Since the variability of roughness measurements are higher than the roughness developed in the pavement sections, data cannot be used to fit the roughness models.

From the results of nonlinear regression, it was found that a single value for each of the parameters, β_s and β_i, could be used to describe the roughness development with time. In order to estimate the single values for these roughness constants, the nonlinear regression was performed using different values for β_s and β_i. From this analysis, the best values for β_s, and β_i were found to be 0.6 and 0.55, respectively. Using these values for β_s and β_i, the final nonlinear regression analysis was performed for the data in all test sections and the roughness parameters ρ_s and ρ_i were estimated. The estimated values of ρ_s and ρ_i are tabulated in Appendix E.

Since the development of roughness is caused by both traffic loading and expansive behavior of subgrade soil, the parameters ρ_s and ρ_i should take the following form:

$$\rho_s = A_s - B_s \Delta H \tag{5.6}$$

$$\rho_i = A_i - B_i \Delta H \tag{5.7}$$

where

ΔH	=	vertical movement,
A_s, A_i	=	parameters that are functions of traffic, structural number (SN) of pavement section, and resilient modulus of subgrade soil (M_r), and
B_s, B_i	=	constants.

Since SN, M_r, and traffic are the same in a single lane of a pavement section, the two wheel paths of a single lane should have the same A_s and A_i values. Using this property, two simultaneous equations with two unknowns were obtained for each lane of a pavement section. The unknowns are either A_s and B_s, or A_i and B_i. Two simultaneous equations were solved for each lane and values of B_s and B_i were estimated for all the pavement sections considered for the development of roughness models. In a very few pavement sections, the roughness development in the wheel path with lower vertical movement was found to be higher than that of the wheel path with higher vertical movement. This type of behavior may be due to a structural failure of the pavement or other property that is not considered in this study. These pavement sections are not used in the model development. The estimated values of B_s and B_i are given in Appendix F. The mean values of B_s and B_i were found to be 162.87 and 306.66, respectively. The standard deviations of B_s and B_i are 40.99 and 72.83, respectively. The frequency distribution of B_s and B_i is shown in Figures 5.2 and 5.3. These plots suggest that the estimated values of B_s and B_i follow a near normal distribution. Hence, the values of B_s and B_i can be found for a site by assigning a reliability and using the following relationships:

$$B_s = 162.87 + 40.99Z \tag{5.8}$$

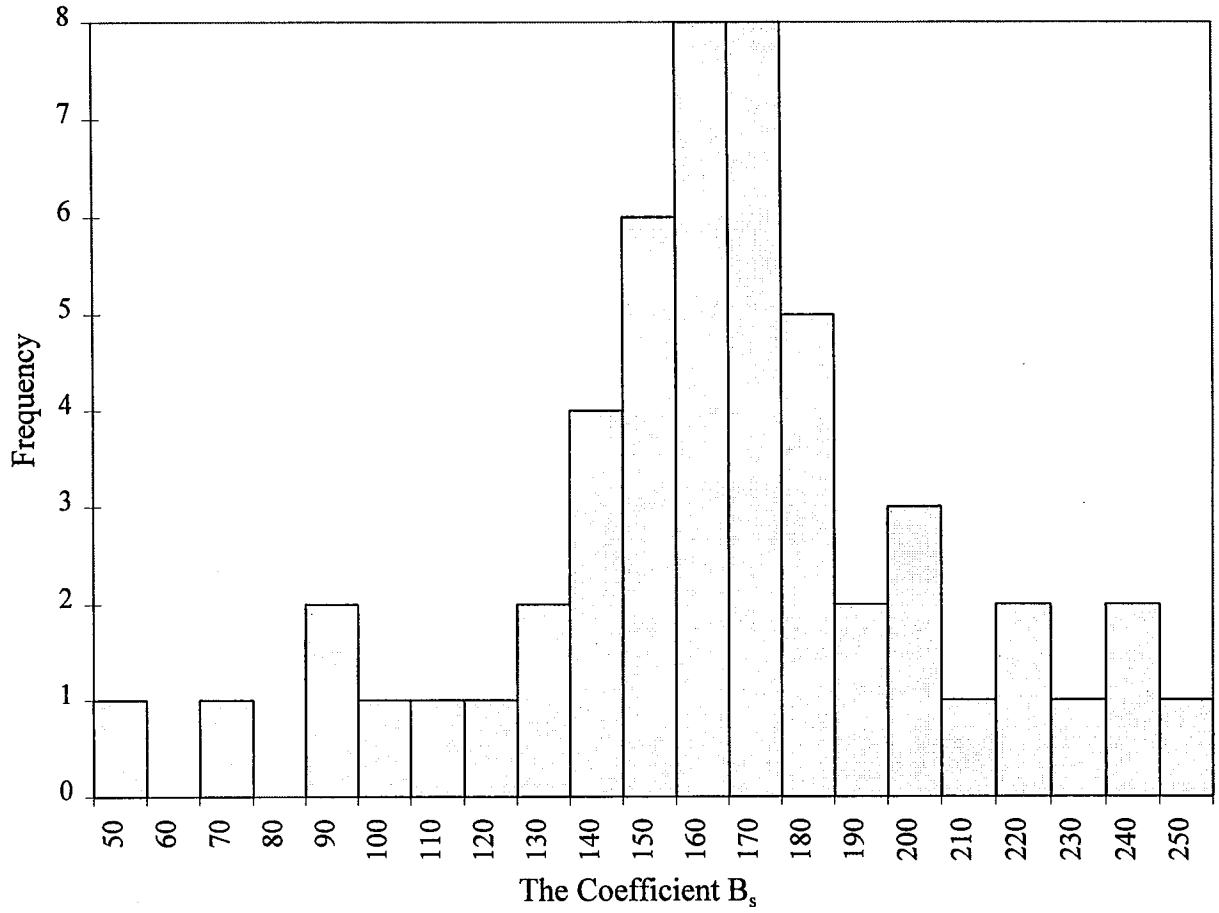

Figure 5.2. Frequency Distribution of B_s

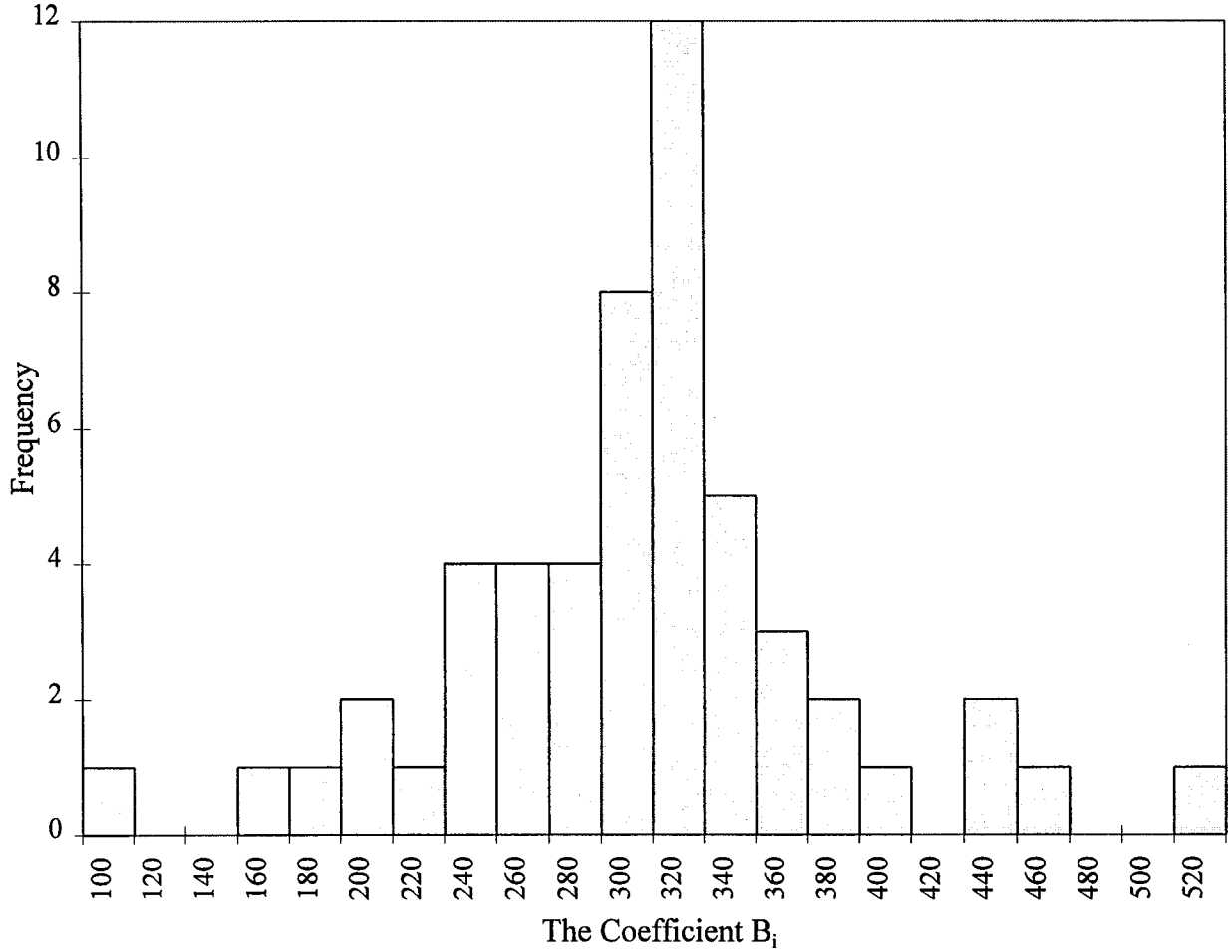

Figure 5.3. Frequency Distribution of B_i

$$B_i = 306.66 + 72.83Z \quad (5.9)$$

where

Z = standard normal variable corresponding to the assigned reliability. For example, for 95 percent reliability, Z is equal to 1.645.

The parameters A_s and A_i can also be estimated from the two simultaneous equations used in the estimation of B_s and B_i. Theoretically, relationships could be obtained for A_s and A_i as functions of traffic, SN, and M_r. However, for this purpose, exact traffic counts, SN, and M_r in each lane should be known. The traffic counts in each lane have not been recorded for the pavement sections studied in this research study. Also, these pavement sections have had many overlays applied on the original pavements over the years of their service period. As a result, layer thicknesses and material properties in these pavement sections vary dramatically throughout the pavement sections. Therefore, an accurate estimate of SN cannot be obtained. This precludes the development of relationships to estimate values of A_s and A_i. However, these parameters can be estimated using existing models that predict the roughness development due to traffic alone. In the next section, equations are derived to estimate A_s and A_i using the AASHTO design equation (AASHTO 1993) for flexible pavements.

Roughness Parameter, A_S

The AASHTO design procedure is based on the results of the AASHO road test conducted in Ottawa, Illinois, in the late 1950's and early 1960's. The design equation for the flexible pavement is as follows:

$$\log_{10} W_{18} = -ZS_0 + 9.36\log_{10}(SN+1) - 0.20 + \frac{\dfrac{\log_{10}(\Delta PSI_w)}{(PSI_0 - 1.5)}}{0.4 + \dfrac{1094}{(SN+1)^{5.19}}} + 2.32\log_{10} M_r - 8.07 \tag{5.10}$$

where

W_{18}	=	80 kN (18 kip) single-axle load applications,
Z	=	standard normal variable,
S_0	=	standard deviation which is equal to 0.35,
SN	=	structural number of pavement, in inches,
ΔPSI_w	=	loss of serviceability due to traffic,
ΔPSI_0	=	initial serviceability, and
M_r	=	resilient modulus of subgrade soil, in lbf/in^2.

The 80 kN single-axle load applications can be calculated from the following traffic equation used by the Texas Department of Transportation:

$$W_{18} = \frac{N_c}{C(r_0 + r_c)}\left[2r_0 t_k + \left(\frac{r_c - r_0}{C}\right) t_k^2\right] \tag{5.11}$$

where

C	=	analysis period,
t_k	=	time in years,
r_0	=	average daily traffic (ADT) in one direction when $t_k = 0.0$,
r_c	=	average daily traffic (ADT) in one direction when $t_k = C$, and
N_c	=	W_{18} at $t = C$.

Rearranging Equation 5.10,

$$\log_{10}\left[\frac{\Delta PSI_w}{(PSI_0 - 1.5)}\right] = \lambda \tag{5.12}$$

where λ is given by:

$$\lambda = \left[0.4 + \frac{1094}{(SN + 1)^{5.19}}\right]\left[\log_{10} W_{18} - 9.36\log_{10}(SN + 1) + 8.27 - 2.32\log_{10} M_r + ZS_0\right] \tag{5.13}$$

Rearranging Equation 5.12,

$$\Delta PSI_w = (PSI_0 - 1.5)\,10^{\lambda} \tag{5.14}$$

From Equation 5.4, the total serviceability loss (ΔPSI_t) is given by:

$$\Delta PSI_t = (PSI_0 - 1.5)\exp\left[-\left(\frac{\rho_s}{t}\right)^{0.6}\right] \tag{5.15}$$

When the vertical movement (ΔH) is equal to zero, from Equation 5.6, $\rho_s = A_s$. Then, the total loss of serviceability calculated from Equation 5.15 is equal to the serviceability loss due to traffic (ΔPSI_w) as follows.

$$\Delta PSI_w = (PSI_0 - 1.5)\exp\left[-\left(\frac{A_s}{t}\right)^{0.6}\right] \tag{5.16}$$

Solving Equations 5.14 and 5.16, A_s is given by:

$$A_s = t\left[\log_e(10^{-\lambda})\right]^{\left(\frac{1}{0.6}\right)} \tag{5.17}$$

In the development of the vertical movement model, the two dimensional vertical movement from the FLODEF program was calculated by adding shrinkage and swelling. Both shrinkage and swelling were calculated for a 20-year period which corresponds to the vertical movement for a 40-year period. Therefore, the time in Equation 5.17 is taken as 40 years

(t = 480). The value of λ is also calculated for a 40-year period.

Roughness Parameter, A_i

Since the AASHTO design equation is not available in terms of IRI, the parameter A_i cannot be estimated directly as in the case of A_s. In order to use the AASHTO design equation in calculating the parameter A_i, a regression relationship between PSI and IRI was developed using PSI and IRI values calculated for all the pavement sections studied in this research study. The PSI and IRI values were calculated using the VERTAC program and are tabulated in Appendix A. A plot of IRI versus PSI and the fitted model is shown in Figure 5.4. The relationship developed is as follows:

$$IRI = 8.4193 \exp(-0.4664 PSI) \qquad n = 2020 \qquad R^2 = 0.90 \tag{5.18}$$

where IRI is in m/km.

A relationship for A_i is developed using Equation 5.18 and assuming an initial serviceability of 4.2 for new flexible pavements. From Equation 5.14, the PSI at any time is given by:

$$PSI = PSI_0 - (PSI_0 - 1.5)10^{\lambda} \tag{5.19}$$

Since $PSI_0 = 4.2$, this equation is reduced to:

$$PSI = 4.2 - 2.7(10^{\lambda}) \tag{5.20}$$

From Equation 5.18, the corresponding IRI is given by:

$$IRI = 8.4193 \exp\left[-0.4664\left(4.2 - 2.7(10^{\lambda})\right)\right] \tag{5.21}$$

From Equation 5.18, the initial IRI which corresponds to PSI of 4.2 is estimated to be 1.19. Then the change in IRI due to traffic (ΔIRI_w) is given by:

$$\Delta IRI_w = 8.4193 \exp\left[-0.4664\left(4.2 - 2.7(10^{\lambda})\right)\right] - 1.19 \tag{5.22}$$

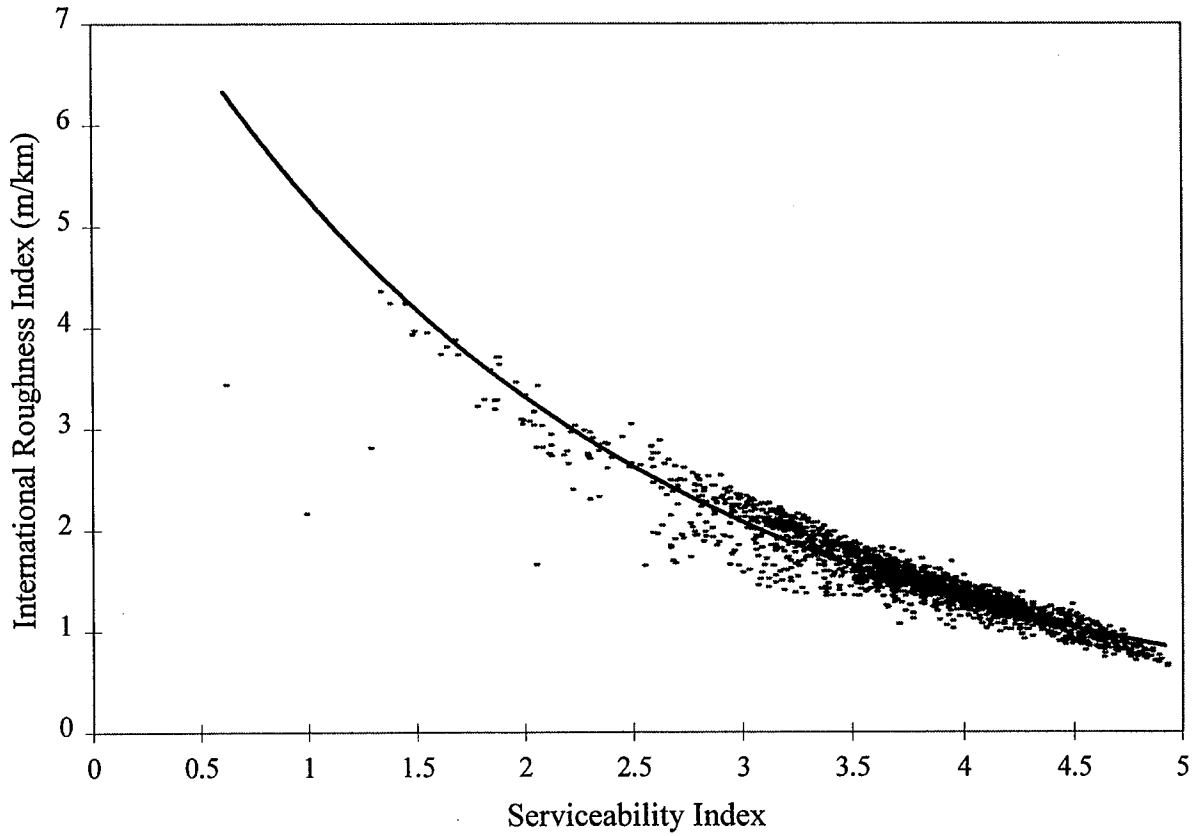

Figure 5.4. International Roughness Index Vs. Serviceability Index

From Equation 5.5, the total change in IRI (ΔIRI_t) is given by:

$$\Delta IRI_t = (4.2 - 1.19)\exp\left[-\left(\frac{\rho_i}{t}\right)^{0.55}\right] \tag{5.23}$$

When the vertical movement (ΔH) is equal to zero, from Equation 5.7, $\rho_i = A_i$. Then, the total change in IRI calculated from Equation 5.23 is equal to the change in IRI due to traffic (ΔPSI_w) as follows.

$$\Delta IRI_w = 3.01\exp\left[-\left(\frac{A_i}{t}\right)^{0.55}\right] \tag{5.24}$$

Solving Equations 5.22 and 5.24, A_i is given by:

$$A_i = t\left[\log_e\left(\frac{3.01}{8.4193\exp(-0.4664(4.2 - 2.7(10^{\lambda}))) - 1.19}\right)\right]^{\left(\frac{1}{0.55}\right)} \tag{5.25}$$

As in the case of PSI, t is taken as 480 and λ is estimated for 40 years.

EXAMPLE PROBLEMS

Using the roughness model developed in the previous section, solutions for three example problems are given in Appendix G. In Example 1, the roughness parameters A_s, B_s, A_i, and B_i are calculated for the test site at Converse, FM 1516 using the models developed in the previous section. Roughness development with time was then calculated. The plots of measured and calculated PSI and IRI versus time are shown in Figures 5.5 and 5.6. In Figure 5.5, the trends are similar. However, at the end of the 60-month monitoring period, the measured serviceability index is accelerating downward whereas the predicted serviceability index is decelerating. This is the effect of traffic. The same observation may be made concerning the IRI trends in Figure 5.6.

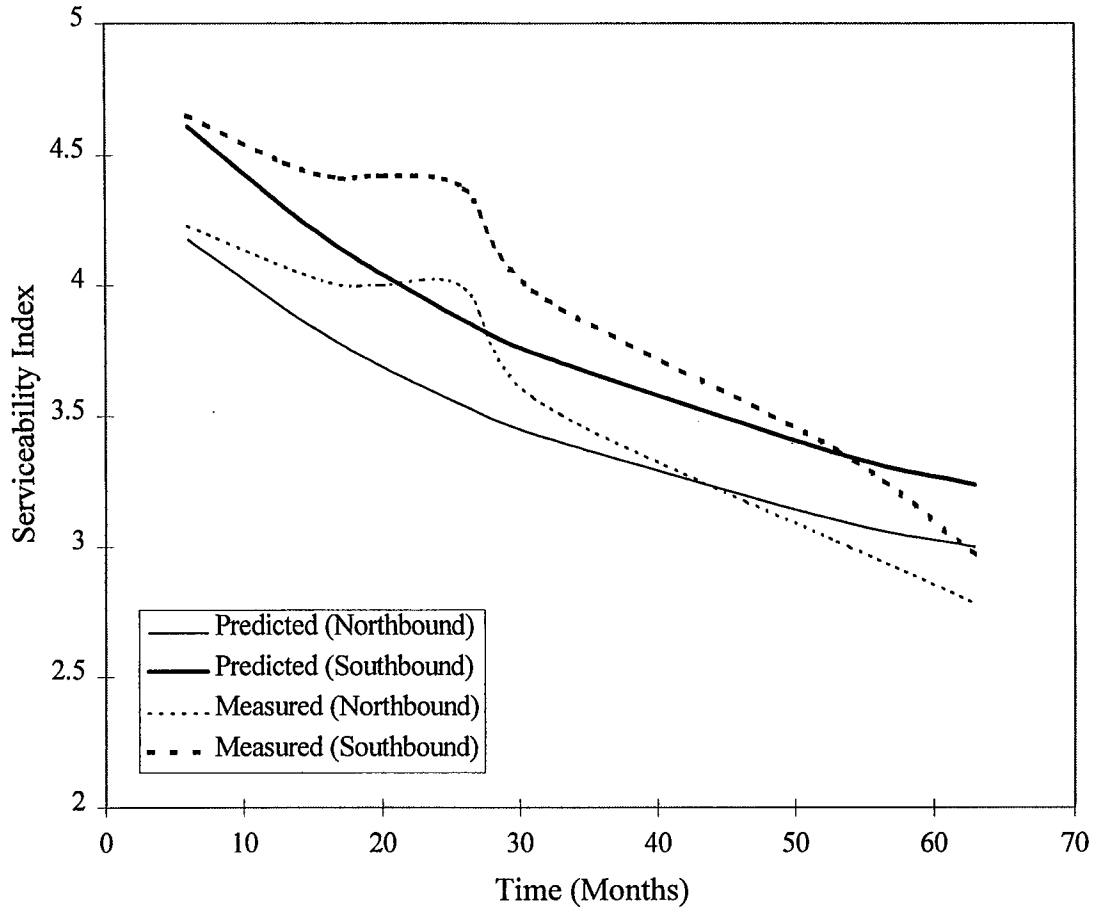

Figure 5.5. Comparison of Measured and Predicted Serviceability Index

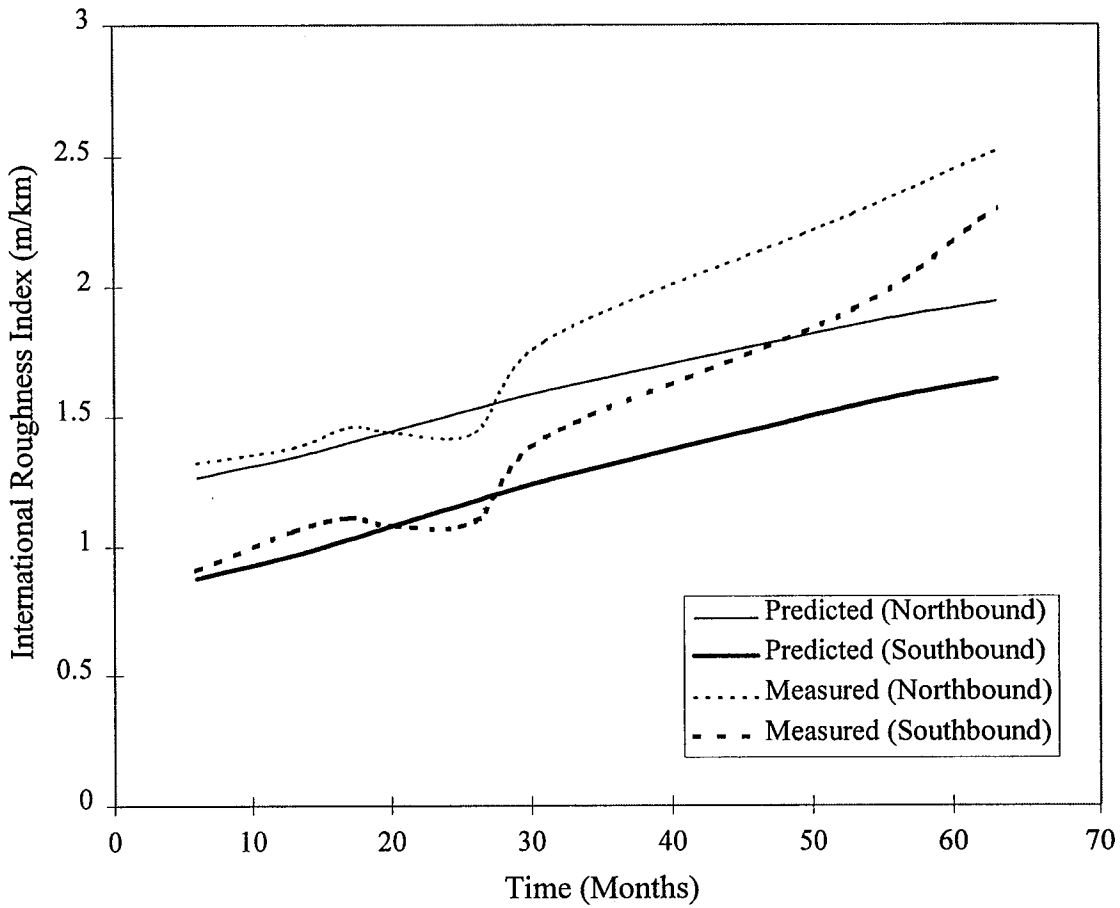

Figure 5.6. Comparison of Measured and Predicted International Roughness Index

In Example 2, the effect of vertical moisture barriers on pavement roughness is evaluated. The roughness development with time is calculated for the following four conditions:

1. No vertical moisture barrier,
2. 91 cm deep vertical moisture barrier,
3. 152 cm deep vertical moisture barrier, and
4. 244 cm deep vertical moisture barrier.

Also, for the no barrier condition, the roughness development with time is calculated using the AASHTO model. The plots of roughness development versus time for different vertical moisture barrier depths are shown in Figures 5.7 and 5.8. The comparison between roughness development calculated using AASHTO model and the models developed in the previous section is shown in Figures 5.9 and 5.10.

Example 3 shows how this model can be used in the design of pavement structures in expansive soils. In this example, the minimum vertical moisture barrier depth required in order for not exceed the assigned terminal serviceability in a pavement in a specified time is calculated. The allowable terminal serviceability after 10 years is considered 3.5. Using the roughness model developed, the serviceability after 10 years is calculated for nine different barrier depths. The barrier depths considered were 0 cm, 30 cm, 60 cm, 90 cm, 120 cm, 150 cm, 180 cm, 210 cm, and 240 cm. For the pavement section considered in Example 3, the barrier depth required is 180 cm.

COMPUTER PROGRAM PRES

The Vertical movement model developed in Chapter IV and the roughness models developed in this chapter are assembled in the computer program PRES. The program is written in Fortran language. The input file for PRES is a simple nonformatted list of the input data. Data required in the input file include the following:

1. Depth of root zone. A typical value of 244 cm can be used for the pavements in the state of Texas,

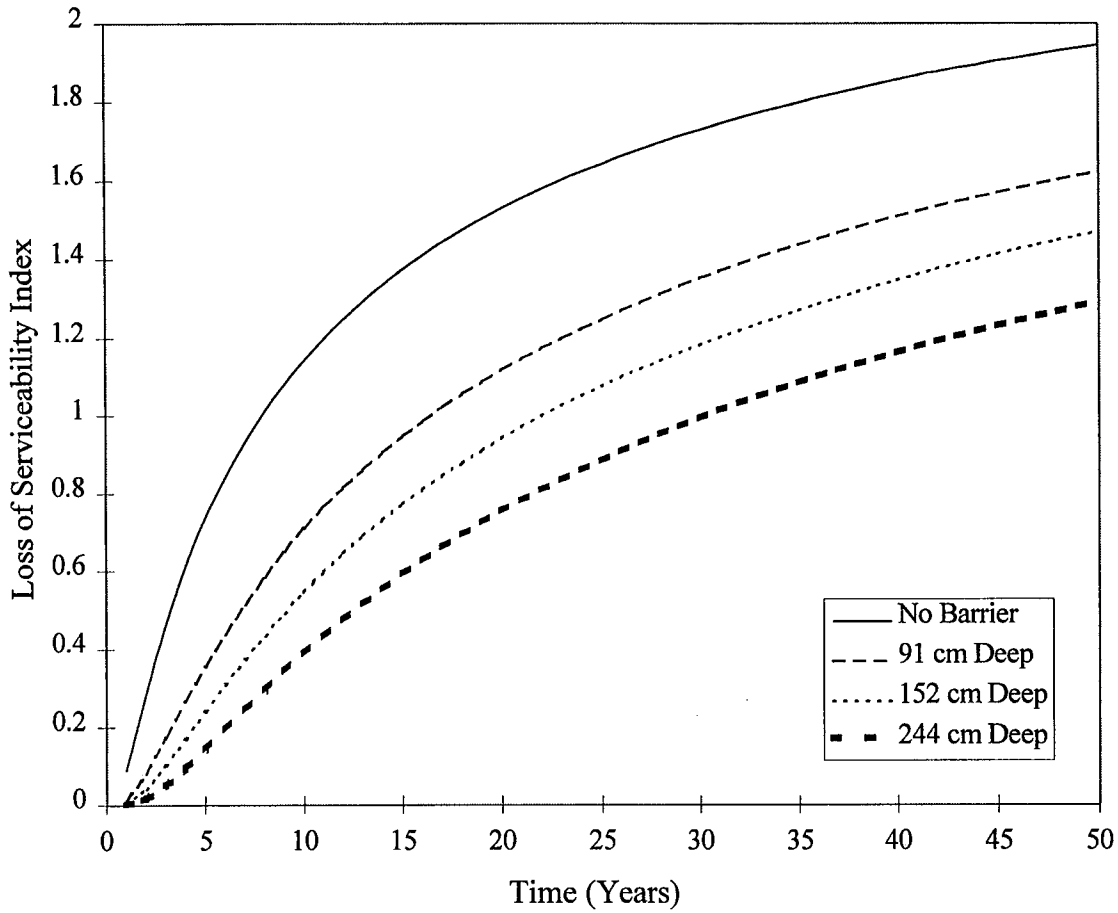

Figure 5.7. Loss of Serviceability Index Vs. Time for Different Barrier Depths

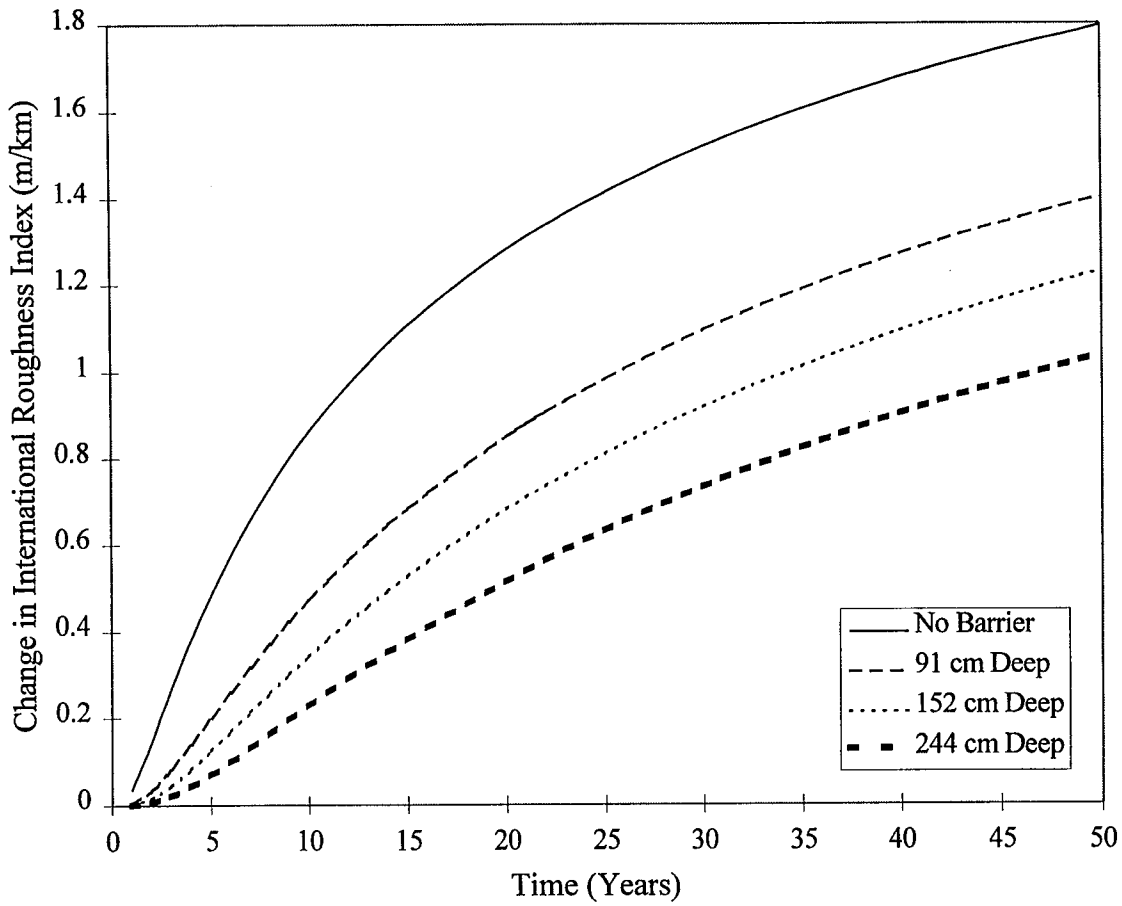

Figure 5.8. Change in International Roughness Index Vs. Time for Different Barrier Depths

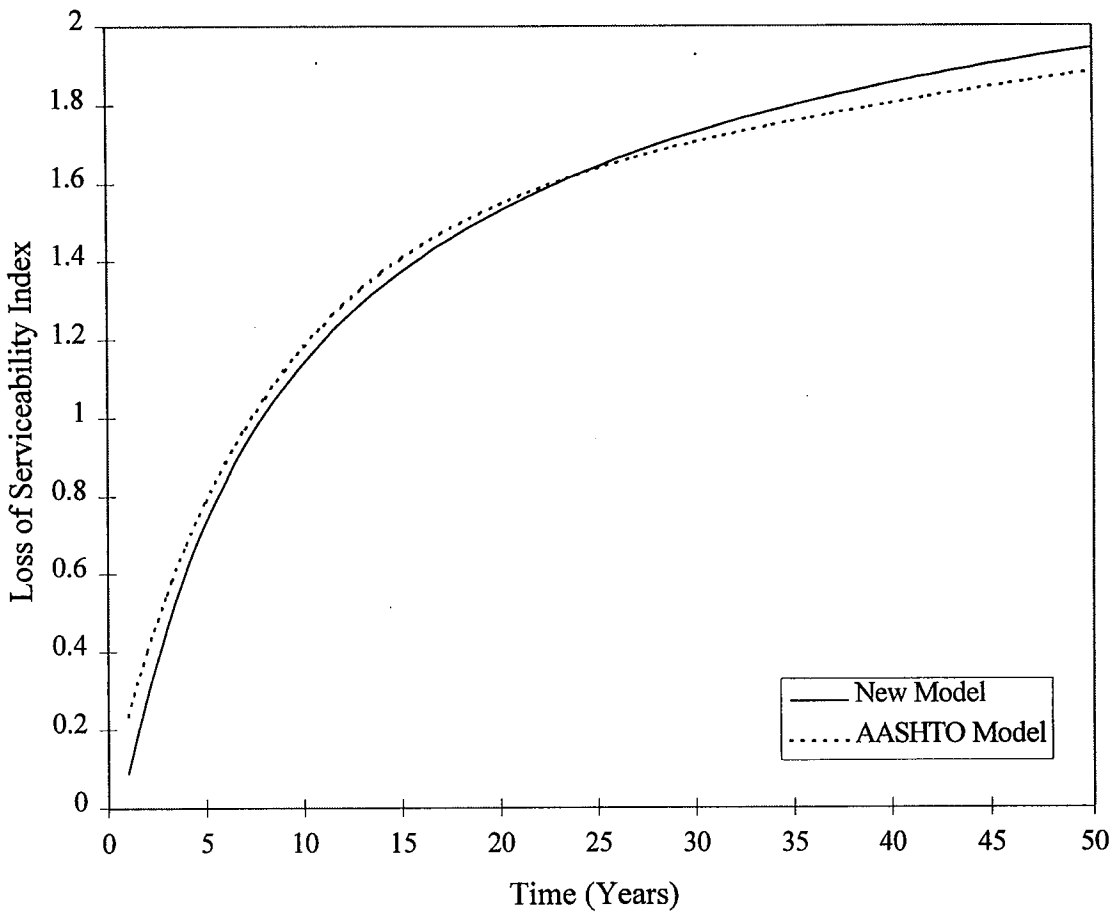

Figure 5.9. Comparison of AASHTO Model and New Model Using Loss of Serviceability Index

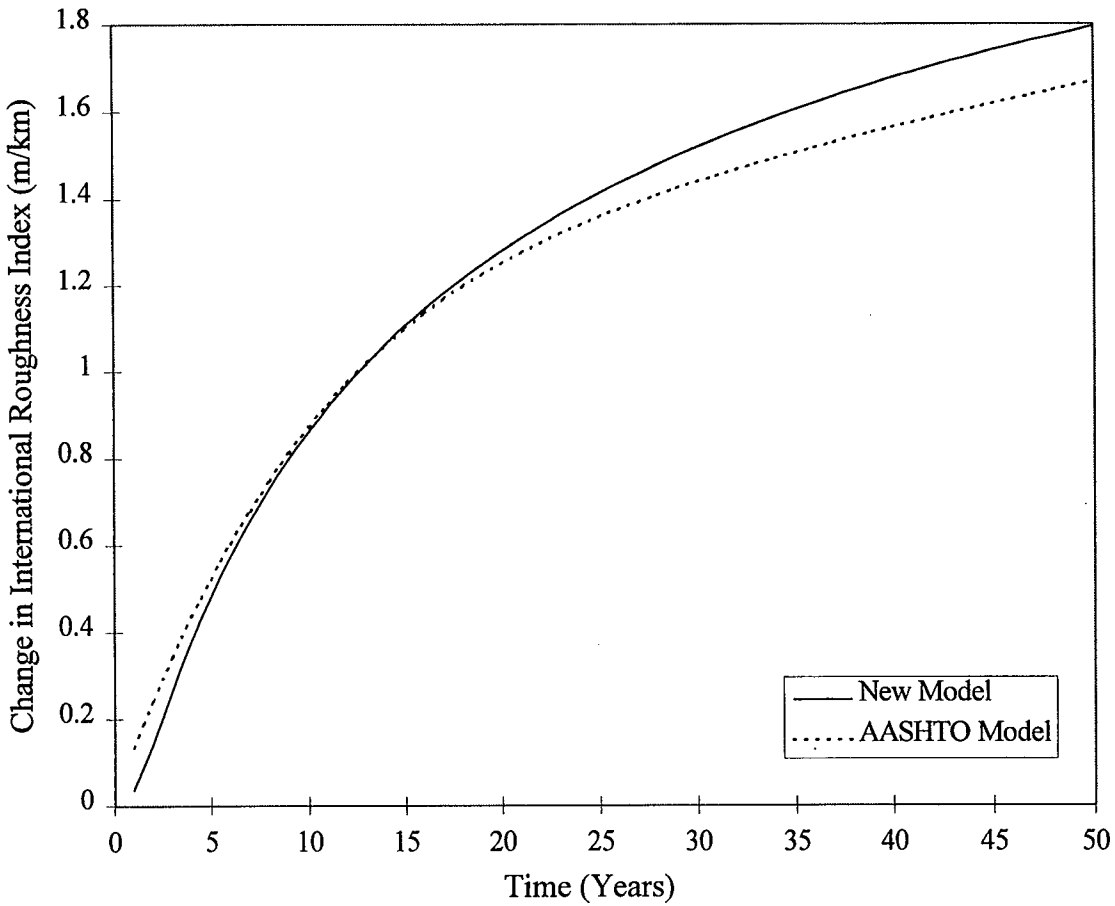

Figure 5.10. Comparison of AASHTO Model and New Model Using Change in International Roughness Index

2. Number of soil layers to the depth of root zone. This information should be obtained through site investigation,
3. Layer thickness, liquid limit, plasticity index, % clay, and % fine clay. These data can be obtained from laboratory testing on samples collected from the pavement sections,
4. Desorption parameters. Desorption parameters can be estimated from the method presented in Appendix C or can be directly obtained from the tables in Appendix C. In order to use these tables, the porosity of the soil sample should be known. The porosity can be estimated from Equation C.26 in Appendix C,
5. Thornthwaite Moisture Index as taken from the map in Figure 3.1,
6. Width of pavement,
7. Distance to wheel paths from the center of pavement,
8. Initial roughness (PSI and/or IRI) soon after the construction or rehabilitation. Typical values for PSI and IRI for flexible pavements are 4.2 and 1.19 m/km, respectively,
9. Traffic data. This can be obtained from the planning division of the Texas Department of Transportation,
10. Structural number (SN) of the pavement section estimated as per the AASHTO guide (AASHTO 1993),
11. Resilient modulus of subgrade soil through laboratory testing, and
12. Depths of vertical moisture barriers.

The output file gives a list of input data and, PSI and IRI with time for each wheel path. A complete description of the program, its input and output, are described in Appendix H.

CHAPTER VI

CONCLUSIONS AND RECOMMENDATIONS

CONCLUSIONS

This research project is a part of continuing efforts by the Texas Department of Transportation to seek ways to reduce damage in pavements due to expansive clay movements. Its basic objectives are to evaluate the vertical moisture barrier effect on reducing the development of roughness and to develop models to predict the roughness development in pavements with or without vertical moisture barriers.

The work plan of this project comprised five tasks. These are explained in detail in Chapter I. Chapter II presents the background information on expansive soils, pavement roughness, and vertical moisture barriers. Data collected over several years in the pavement sections studied are explained and presented in Chapter III and in Appendix A. The differential movement of pavements due to expansive clay activity is the major source of roughness in pavements built on expansive clay subgrades. A simple model to predict the vertical movement at different locations of a pavement section has been developed. Chapter IV of this report explains this vertical movement model. Data required to use this model are the basic soil properties, climatic data, and pavement geometry. Of the soil properties that are needed in the estimation of vertical movement, the desorption coefficients may be the most difficult data to collect. A method of estimating desorption coefficients from laboratory testing and a list of coefficients for various groups of soils are presented in Appendix C. Models have been developed to predict the pavement roughness. This has been achieved by employing regression analysis on roughness data collected from the pavement sections and the vertical movements calculated from the vertical movement model. These models predict the roughness development with time in terms of Serviceability Index and International Roughness Index. Chapter V explains these roughness models. Three example problems are

solved using these models in Appendix G. The vertical movement model and the roughness models are assembled in the computer program PRES which is written in Fortran language. The input data required for the program include the basic soil properties, climatic data, pavement geometry and structural properties, and traffic. A description of the program is provided in Appendix H. The following conclusions can be drawn based on this study.

1. The vertical moisture barriers are effective in reducing the development of roughness in pavements on expansive soils.
2. The main factors determining moisture condition in soil are rainfall and evapotranspiration. Besides the potential expansive characteristics of a soil, the vertical movement in expansive soils depends on how much moisture is gained or lost from the soil. Hence, the climate is an important parameter in the estimation of potential vertical movement in expansive soils. Wet, dry, and equilibrium suction profiles can be estimated using the climatic model presented in this report.
3. The vertical suction profiles can effectively be used in the estimation of vertical movement.
4. Simple and reliable estimates of vertical movement in a two dimensional domain can be obtained from the vertical movement model presented. Data required to apply the model can easily be collected. The model can estimate vertical movement in a soil profile having many layers of soil with different properties.
5. The data points used in the vertical movement model development were between the center of the pavement and 0.90 m inside the edge of the pavement. Hence, the reliable estimates of vertical movement are expected only in this region. Usually, all the wheel paths lie within this region and, therefore, the model can be applied for almost all the cases encountered.
6. The Suction Compression Index is a powerful tool in characterizing expansive soils and in estimating vertical movement in such soils. The estimation of this parameter from the chart method presented in the report is relatively simple.
7. The amount of vertical movement controls the amount of roughness development in

pavements on expansive soils. Higher vertical movement causes a higher roughness development.

8. The maximum vertical movement in a pavement occurs at the edge and decreases toward the center of the pavement. Increasing the shoulder width of the pavement decreases the potential vertical movement in the travel lanes and hence decreases the roughness development.
9. A paved median decreases the roughness development in the inside lane of a pavement.
10. Vertical moisture barriers reduce the development of roughness, with the deeper barriers arresting more than the shallower barriers. The amount of roughness reduction by barriers warrants their application in many places where there is an expansive clay activity.
11. The roughness prediction model developed in this research study is a versatile tool in determining the effectiveness of a vertical moisture barrier at a particular location. The model can be used in estimating the roughness development in any wheel path of a pavement.
12. In current design practices, the critical lane of a pavement is generally considered to be the outside lane as the traffic is expected to be higher at the outside lane. However, in pavements where there is an expansive clay activity, this may not be true. Depending on the amount of traffic, shoulder widths, and the expansive clay movement, the roughness development in the inside lane may be higher than that of the outside lane. The roughness prediction model can be used to find the most critical lane if the amount of traffic is known for each lane.
13. Estimating the roughness development in each wheel path may not be required at the initial construction stage. However, this may be useful in planning subsequent rehabilitation work of the pavement.
14. The roughness data used to develop the model were collected in pavements that were in service for many years before the testing program began. Layer thicknesses and properties vary dramatically throughout the pavement sections. This prevented the development of an independent model that takes into account the traffic, expansive

clay properties, and structural properties of a pavement. The models presented in this report use the AASHTO model to predict the roughness due to traffic.

15. The swelling clay model presented in the AASHTO guide (AASHTO 1993) can predict roughness due to expansive clay activity in the outside wheel path when there are no barriers present.
16. The computer program PRES is expected to be a versatile tool in the estimation of roughness development in expansive soils. The program can be used to find whether the barriers are effective in a particular environment. Also, it can be used to estimate the depth of the barrier required to achieve the desired roughness reduction in a given wheel path. Data required for the program are relatively easy to collect.
17. The computer program PRES is valid for all soils that lie on the McKeen chart in Figure 2.1. All soils sampled in this project and other related expansive soil projects in Texas were found to lie on the McKeen chart. If soil properties which fall off of the McKeen Chart are entered into the program, the program will respond with the error message "Error in soil properties or soil properties out of range." Also, the program can work only when the constants ρ_s and ρ_i in Equations 5.6 and 5.7 are greater than zero. Therefore, the pavement section and the barrier depths should be selected so that ρ_s and ρ_i are greater than zero.

RECOMMENDATIONS

This study has developed a methodology to evaluate the effectiveness of vertical moisture barriers in reducing the development of roughness in pavements built on expansive clay subgrades and to predict the roughness in a given wheel path in pavements with or without vertical moisture barriers. It is recommended that life cycle cost analysis be carried out to decide whether the barriers are needed for a particular pavement section and to choose the barrier depth.

The roughness prediction model developed in this study used data collected from different pavement sections at six different locations in the state of Texas. These pavement

sections have been constructed at different times in the past. The pavement sections have undergone many overlays during their service life. As a result, the current pavement sections at these locations are very complex. Therefore, developing an independent model to predict the total roughness was not possible due to traffic and expansive clay activity. Also, the daily traffic volumes in most of these pavement sections are very high. Therefore, as the pavement sections became rougher with time, the maintenance repairs were carried out. This prevented a continuous record of roughness with time. It is recommended that the pavement sections with fairly constant structure in areas where a relatively high level of roughness can be tolerated be selected for the research in this nature. Moreover, it is advantageous to collect traffic data in all the lanes in these pavement sections.

A database containing desorption relationships for different types of soils should be formed. Each additional soil that is added will make the use of the existing program more comprehensive and generally useful in the design of pavements on expansive soils. Maps containing the spatial distribution of extreme suction envelopes may be developed and can be used in the estimation of vertical movement at a given location. These, in turn, may be used to select the depth of moisture barriers that is consistent with the envisioned life-cycle of the pavement. These data can be used in improving the existing models that predict the vertical movement and roughness development of pavements on expansive soils.

REFERENCES

AASHTO (1993). *AASHTO Guide for Design of Pavement Structures*. American Association of State Highway and Transportation Officials, Washington, D.C.

Abd Rahim, and M. A. B., Picornell. M. (1989). "Moisture Movement under the Pavement Structure." *Research Report 1165-1*, Center for Geotechnical and Highway Research, University of Texas at El Paso, El Paso, Texas.

Alonso, E. E., and Loret, A. (1995). "Settlement of a 12 Storey Building due to Dessication Induced by Trees: a Case Study." *Proc., First International Conference on Unsaturated Soils*, Paris, France, 2, 935-943.

Ardani, A. (1992). "Expansive Soil Treatment Methods in Colorado." *Report CDOT-DTD-R-92-2*, Colorado Department of Transportation, Denver, Colorado.

ASTM (1994). *Compilation of ASTM Standard Definitions, 8th edition, ASTM Publication 03-001094-42*. American Society for Testing and Materials, Philadelphia, Pensylvania.

Bartelli, L. J., and McCormack, D. E. (1976). "Morphology and Pedologic Classification of Swelling Soils." *Transportation Research Record 568*, TRB, National Research Council, Washington, D.C., 01-08.

Beckmann, G. G., Hubble, G. D., and Thompson, C. H. (1970). "Gilgai Forms, Distribution and Soil Relationships in North-Eastern Australia." *Proc., Symposium on Soils and Earth Structures in Arid Climates*, Institution of Engineers (Australia), Adelaide, Australia, 88-93.

Carey Jr., W. N. (1973). "Uses of Surface Profile Measurements." *Special Report 133,* Highway Research Board, National Research Council, Washington, D.C., 05-07.

Carey Jr., W. N., and Irick, P. E. (1960). "The Pavement Serviceability-Performance Concept.", *Bulletin 250*, Highway Research Board, National Research Council, Washington, D.C., 40-58.

Claros, G. J., Hudson, W. R., and Lee, C. E. (1985). "Performance of the Analog and the Digital Profilometer with Wheels and with Non-Contact Transducers." *Research Report 251-3F*, Center for Transportation Research, The University of Texas at Austin, Austin, Texas.

Dhowian, A., Erol, A. O., and Youssef, A. (1987). "Assessment of Oedometer Methods for Heave Prediction." *Proc. Sixth International Conference on Expansive Soils*, New Delhi, India, 99-104.

FHWA (1980). "Expansive Soils in Highway Subgrades: Summary." *Report FHWA-TS-80-236*, U.S. Department of Transportation, Washington, D.C.

Forstie, D., Walsh, H., and Way, G. (1979). "Membrane Technique for Control of Expansive Clays." *Transportation Research Record 705*, TRB, National Research Council, Washington, D.C., 49-53.

Garcia-Diaz, A., Riggins, M., and Liu, S. J. (1984). "Development of Performance Equations and Survivor Curves for Flexible Pavements." *Research Report 284-5*, Texas Transportation Institute, Texas A&M University, College Station, Texas.

Gay, D. A. (1994). "Development of a Predictive Model for Pavement Roughness on Expansive Clay," PhD dissertation, Texas A&M University, College Station, Texas.

Gay, D. A., and Lytton, R. L. (1988). "Moisture Effects on Pavement Roughness," in Measured Performance of Shallow Foundations, *Geotechnical Special Publication No. 15*, American Society of Civil Engineers, New York, New York.

Gillespie, T. D. (1992). "Everything You Always Wanted to Know About the IRI, But Were Afraid to Ask!" *Presentation at the Fourth Annual Road Profile Users Group Meeting*, Lincoln, Nebraska.

Gromko, G. J. (1974). "Review of Expansive Soils." *Journal of the Geotechnical Engineering Division*, American Society of Civil Engineers, New York, New York, 100(GT6), 667-687.

Hamberg, D. J. (1985). "A Simplified Method for Predicting Heave in Expansive Soils," MS thesis, Colorado State University, Fort Collins, Colorado.

Hammitt, G. E., and Ahlvin, R. G. (1973). "Membranes and Encapsulation of Soils for Control of Swelling." *Proc., Workshop on Expansive Clays and Shales in Highway Design and Construction*, Federal Highway Administration, U.S. Department of Transportation, Washington, D.C., 2, 80-95.

Holland, J. E., and Lawrence, C. E. (1980). "Seasonal Heave of Australian Clay Soils." *Proc., Fourth International Conference on Expansive Soils*, Denver, Colorado, 1, 302-321.

Jayatilaka, R., Gay, D. A., Lytton, R. L., and Wray, W. K. (1993). "Effectiveness of Controlling Pavement Roughness Due to Expansive Clays with Vertical Moisture Barriers." *Research Report 1165-2F*, Texas Transportation Institute, Texas A&M University, College Station, Texas.

Jones, D. E., and Holtz,W. G. (1973). "Expansive Soils - The Hidden Disaster." *Journal of Civil Engineering*, American Society of Civil Engineers, New York, New York, 43(8), 49-51.

Juca, J. F. T., Da Silva, J. M. J., Filho, J. A. G., and Bastos, E. G. (1995). "Laboratory and Field Tests on an Unsaturated Expansive Clay." *Proc., First International Conference on Unsaturated Soils*, Paris, France, 2, 877-884.

Krahn, J., and Fredlund, D. G. (1972). "On Total, Matrix and Osmotic Suction." *Soil Science*, 114(5), 339-348.

Krohn, J. P., and Slosson, J. E. (1980). "Assessment of Expansive Soils in the United States." *Proc., Fourth International Conference on Expansive Soils*, Denver, Colorado, 1, 596-608.

Lu, J., Bertrand, C., and Hudson, W. R. (1990). "Speed Effect Analysis and Canceling Model of a Response-Type Road Roughness Measuring System." *Transportation Research Record 1260*, TRB, National Research Council, Washington, D.C., 125-134.

Lytton, R. L. (1977). "The Characterization of Expansive Soils in Engineering." *Presentation at the Symposium on Water Movement and Equilibria in Swelling Soils*, American Geophysical Union, San Francisco, California.

Lytton, R. L. (1994). "Prediction of Movement in Expansive Clay." *Geotechnical Special Publication No. 40*, American Society of Civil Engineers, New York, New York.

Lytton, R. L. (1995). "Foundations and Pavements on Unsaturated Soils." *Proc., First International Conference on Unsaturated Soils*, Paris, France, 3, 1201-1220.

Lytton, R. L., Boggess, R. L., and Spotts, J. W. (1976). "Characteristics of Expansive Clay Roughness of Pavements." *Transportation Research Record 568*, TRB, National Research Council, Washington, D.C., 9-23.

Lytton, R. L., Pufahl, D. E., Michalak, C. H., Liang, H. S., and Dempsey, B. J. (1989). "An Integrated Model of the Climatic Effects on Pavements." *Final Report*, Federal Highway Administration, Offices of Research & Development, Washington, D.C.

McDowell, C. (1956). "Interrelationship of Load, Volume Change, and Layer Thickness of Soils to the Behavior of Engineering Structures." Proc., Highway Research Board, 35, 754-770.

McKeen, R. G. (1980). "Field Studies of Airport Pavements on Expansive Clay." *Proc., Fourth International Conference on Expansive Soils*, Denver, Colorado, 1, 242-261.

Mckeen, R. G. (1985). "Validation of Procedures for Pavement Design on Expansive Soils." *Report DOT/FAA/PM-85/15*, U.S. Department of Transportation, Federal Aviation Administration, Washington, D.C.

McKenzie, D. W., Hudson, W. R., and Lee, C. E. (1982). "The Use of Road Profile Statistics for Maysmeter Calibration." *Research Report 251-1*, Center for Transportation Research, The University of Texas at Austin, Austin, Texas.

McKenzie, D. W., Riddle, P., and Crandell, J. (1986). *VERTAC, a Vertical Acceleration Program for the Calculation of Serviceability Index, Version 6.0* (Software), Center for Transportation Research, The University of Texas at Austin, Austin, Texas.

Miller D. J., Durkee, D. B., Chao, K. C., and Nelson, J. D. (1995). "Simplified Heave Prediction for Expansive Soils." *Proc., First International Conference on Unsaturated Soils*, Paris, France, 2, 891-897.

Mitchell, P. W. (1980). "The Concepts Defining the Rate of Swell of Expansive Soils." *Proc., Fourth International Conference on Expansive Soils*, Denver, Colorado, 1, 106-116.

Mitchell, P. W., and Avalle, D. L. (1984). "A Technique to Predict Expansive Soil Movements." *Proc., Fifth International Conference on Expansive Soils*, Adelaide, Australia, 124-130.

Mojekwu, E. C. (1979). "A Simplified Method for Identifying the Predominant Clay Mineral," MS thesis, Texas Tech University, Lubbock, Texas.

Nelson, J. D., and Miller, D. J. (1992). *Expansive Soils Problems and Practice in Foundation and Pavement Engineering*. John Wiley & Sons, New York, New York.

Nyangaga, F. N. (1996). "Developing a Model to Predict Pavement Roughness Development on Expansive Soils," PhD dissertation, Texas A&M University, College Station, Texas.

Picornell, M. (1985). "The Development of Design Criteria to Select the Depths of a Vertical Moisture Barrier," PhD dissertation, Texas A&M University, College Station, Texas.

Picornell, M., and Lytton, R. L. (1984). "Modelling the Heave of a Heavily Loaded Foundation." *Proc., Fifth International Conference on Expansive Soils*, Adelaide, Australia, 104-108.

Picornell, M. and Lytton, R. L. (1987). "Behavior and Design of Vertical Moisture Barriers." *Transportation Research Record 1137*, TRB, National Research Council, Washington, D.C., 71-81.

Picornell, M. and Lytton, R. L. (1989). "Field Measurement of Shrinkage Crack Depth in Expansive Soils." *Transportation Research Record 1219*, TRB, National Research Council, Washington, D.C., 121-130.

Picornell, M., Lytton, R. L., and Steinberg, M. L. (1984). "Assessment of the Effectiveness of a Vertical Moisture Barrier." *Proc., Fifth International Conference on Expansive Soils*, Adelaide, Australia, 354-358.

Prasad, R. (1988). "A Linear Root Water Uptake Model." Journal of Hydrology, Vol. 99, 297-306.

Osman, M. A., and Sharief, A. M. E. (1987). "Field and Laboratory Observations of Expansive Soil Heave." *Proc. Sixth International Conference on Expansive Soils*, New Delhi, India, 105-110.

Rao, R. R., and Smart, P. (1980). "Significance of Particle Size Distribution Similarity in Prediction of Swell Properties." *Proc. Fourth International Conference on Expansive Soils*, Denver, Colorado, 1, 96-105.

Rauhut, B. and Lytton, R. L. (1984). "Serviceability Loss Due to Roughness Caused by Volume Change in Expansive Clay Subgrades." *Transportation Research Record 993*, TRB, National Research Council, Washington, D.C., 12-18.

Ravina, I. (1983). "The Influence of Vegetation on Moisture and Volume Changes." *Geotechnique*, 33(2), 151-157.

Ridley, A. M., and Wray, W. K. (1995). "Suction Measurement: a Review of Current Theory and Practices." *Proc., First International Conference on Unsaturated Soils*, Paris, France, 3, 1293-1322.

Russam, K., and Coleman, J. D. (1961). "The Effect of Climatic Factors on Subgrade Moisture Conditions." *Geotechnique*, 2(1), 22-28.

Sallberg, J. R., and Smith, P. C. (1965). "Pavement Design over Expansive Clays: Current Practices and Research in the United States." *Proc., International Research and Engineering Conference on Expansive Clay Soils*, Texas A&M University, College Station, Texas, 208-230.

Sayers, M. W. (1995). "On the Calculation of International Roughness Index from Longitudinal Road Profile." *Transportation Research Record 1501*, TRB, National Research Council, Washington, D.C., 01-12.

Sayers, M. W., and Karamihas, S. M. (1996). "The Little Book of Profiling." Transportation Research Institue, University of Michigan, Ann Arbor, Michigan.

Sayers, M. W., Gillespie, T. D., and Querioz, C. A. V. (1986). "The International Road Roughness Experiment: Establishing Correlation and a Calibration Standard for Measurements." *Technical Paper 45*, World Bank, Washington, D.C.

Seed, H. B., Woodward, R. J., and Lundgren, R. (1962). "Prediction of Swelling Potential for Compacted Clays." *Journal of the Soil Mechanics and Foundation Division*, American Society of Civil Engineers, New York, New York, 53-87.

Simmons, M. E. (1984). "Predicted and Actual Performance of a Structure in Expansive Soils." *Miscellaneous Paper GL-84-20*, Foundations and Materials Branch, U.S. Army Engineer District, Fort Worth, Texas.

Skempton, A. W. (1953) "The Colloidal Activity of Clays." *Proc., Third International Conference on Soil Mechanics and Foundation Engineering*, Zurich, Switzerland, 1, 57-61.

Snethen, D. R. (1979a). "An Evaluation of Methodology for Prediction and Minimization of Detrimental Volume Change of Expansive Soils in Highway Subgrades, Vol. I", *Report FHWA-RD-79-49*, Federal Highway Administration, U.S. Department of Transportation, Washington, D.C.

Snethen, D. R. (1979b). "An Evaluation of Methodology for Prediction and Minimization of Detrimental Volume Change of Expansive Soils in Highway Subgrades, Vol. II" *Report FHWA-RD-79-50*, Federal Highway Administration, U.S. Department of Transportation, Washington, D.C.

Snethen, D. R. (1979c). "Technical Guidelines for Expansive Soils in Highway Subgrades." *Report FHWA-RD-79-51*, Federal Highway Administration, U.S. Department of Transportation, Washington, D.C.

Snethen, D. R. (1984). "Evaluation of Expedient Methods for Identification and Classification of Potentially Expansive Soils." *Proc. Fifth International Conference on Expansive Soils*, Adelaide, Australia, 22-26.

Snethen, D. R., Townsend, F. C., Johnson, L. D., Patrick, D. M., and Vedros, P. J. (1975). "A Review of Engineering Experiences with Expansive Soils in Highway Subgrades." *Report FHWA-RD-75-48*, Federal Highway Administration, U.S. Department of Transportation, Washington, D.C.

Snethen, D. R., Johnson, L. D., and Patrick, D. M. (1977a). "An Investigation of the Natural Microscale Mechanisms that Cause Volume Changes in Expansive Clays." *Report FHWA-RD-77-75*, Federal Highway Administration, U.S. Department of Transportation, Washington, D.C.

Snethen, D. R., Johnson, L. D., and Patrick, D. M. (1977b). "An Evaluation of Expedient Methodology for Identification of Potentially Expansive Soils." *Report FHWA-RD-77-94*, Federal Highway Administration, U.S. Department of Transportation, Washington, D.C.

Srinarawat, M. (1982). "A Method to Calibrate and Correlate Road Roughness Devices Using Road Profiles," PhD dissertation, The University of Texas at Austin, Austin, Texas.

Steinberg, M. L. (1977). "Ponding an Expansive Clay Cut: Evaluations and Zones of Activity." *Transportation Research Record 641*, TRB, National Research Council, Washington, D.C., 61-66.

Steinberg, M. L. (1980). "Deep Vertical Fabric Moisture Seals." *Proc., Fourth International Conference on Expansive Soils*, Denver, Colorado, 1, 383-400.

Steinberg, M. L. (1981). "Deep-Vertical-Fabric Moisture Barriers in Swelling Soils." *Transportation Research Record 790*, TRB, National Research Council, Washington, D.C., 87-94.

Steinberg, M. L. (1985). "Controlling Expansive Soil Destructiveness by Deep Vertical Geomembranes on Four Highways." *Transportation Research Record 1032*, TRB, National Research Council, Washington, D.C., 48-53.

Steinberg, M. L. (1989). "Further Monitoring of Twelve Geomembrane Sites in Texas." *Report DHT-18*, Departmental Information Exchange, State Department of Highways and Public Transportation, Austin, Texas.

Steinberg, M. L. (1992). "Controlling Expansive Soils: Twenty Texas Highway Projects." *Proc., Seventh International Conference on Expansive Soils*, Dallas, Texas, 1, 392-397.

Thompson, M, R., and Robnet, Q., L. (1976). "Pressure-Injected Lime for Treatment of Swelling Soils." *Transportation Research Record 568*, TRB, National Research Council, Washington, D.C., 24-34.

Thornthwaite, C. W. (1948). "An Approach Toward a Rational Classification of Climate." *Geographical Review*, 54-94.

USDA (1966). *Soil Survey of Bexar County, Texas*. United States Department of Agriculture, Soil Conservation Service in Cooperation with Texas Agricultural Experiment Station, Washington, D.C.

USDA (1981). *Soil Survey of Hunt County, Texas*. United States Department of Agriculture, Soil Conservation Service in Cooperation with Texas Agricultural Experiment Station, Washington, D.C.

Velasco, M. O., and Lytton, R. L. (1981). "Pavement Roughness on Expansive Clays." *Research Report 284-2*, Texas Transportation Institute, Texas A&M University, College Station, Texas.

Walker, R. S., and Beck, R. (1988). "Field Implementation of Non-Contact Profiling and Road Roughness Equipment." *Research Report 394-1F*, The University of Texas at Arlington, Arlington, Texas.

Walker, R. S., and Hudson, W. R. (1973a). "A Correlation Study of the Mays Road Meter with the Surface Dynamics Profilometer." *Research Report 156-1*, Center for Highway Research, The University of Texas at Austin, Austin, Texas.

Walker, R. S., and Hudson, W. R. (1973b). "The Use of Spectral Estimates for Pavement Charaterization." *Research Report 156-2*, Center for Highway Research, The University of Texas at Austin, Austin, Texas.

Walker, R. S., and Schuchman, J. S. (1987). "Upgrade of 690D Surface Dynamics Profilometer for Non-Contact Measurements." *Research Report 494-1F*, The University of Texas at Arlington, Arlington, Texas.

Ward, W. H. (1953). "Soil Movement and Weather." *Proc., Third International Conference on Soil Mechanics and Foundation Engineering*, Zurich, Switzerland, 1, 477-482.

Wray, W. K. (1978). "Development of a Design Procedure for Residential & Light Commercial Slabs-On-Ground Constructed over Expansive Soils," PhD dissertation, Texas A&M University, College Station, Texas.

Wray, W. K. (1987). "Evaluation of Static Equilibrium Soil Suction Envelopes for Predicting Climate-induced Soil Suction Changes Occuring Beneath Covered Surfaces." *Proc., Sixth International Conference on Expansive Soils*, New Delhi, India, 235-240.

Wray, W. K. (1992). "Comparison of Predicted Heave to Field Measurements." *Proc., Seventh International Conference on Expansive Soils*, Dallas, Texas, 1, 331-336.

Zein, A. K. M. (1987). "Comparison of Measured and Predicted Swelling Behavior of a Compacted Black Cotton Soil." *Proc. Sixth International Conference on Expansive Soils*, New Delhi, India, 121-126.

APPENDIX A

ROUGHNESS DATA

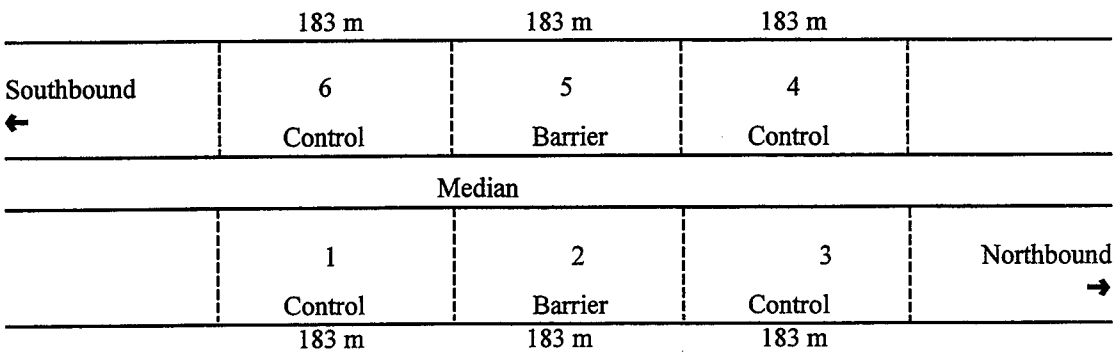

Figure A.1. Site Plan - San Antonio, General McMullen Drive

Table A-1. Serviceability Index, San Antonio, General McMullen Drive, Section 1

Date	Time (Months)	Outside Lane Right	Outside Lane Left	Center Lane Right	Center Lane Left	Inside Lane Right	Inside Lane Left
Oct-89	2	3.34	2.77	4.28	4.36	4.25	4.10
Mar-90	7	3.29	3.05	3.96	3.91	3.07	2.69
Nov-90	15	2.86	3.32	3.65	3.98	4.13	3.85
Mar-91	19	3.39	2.71	4.09	4.04	4.06	4.01
Sep-91	25	3.16	2.95	4.22	4.21	4.19	4.04
Feb-92	30	3.46	2.60	4.16	4.27	4.06	3.95
Jun-92	34	3.40	2.58	4.14	4.14	4.03	4.08
Apr-94	56	3.10	2.78	3.90	3.89	4.01	4.00
Feb-95	66	3.19	2.81	4.04	4.11	4.05	3.95

Table A-2. Serviceability Index, San Antonio, General McMullen Drive, Section 2

Date	Time (Months)	Outside Lane Right	Outside Lane Left	Center Lane Right	Center Lane Left	Inside Lane Right	Inside Lane Left
Oct-89	2	3.29	3.79	3.83	4.04	3.57	3.92
Mar-90	7	3.05	3.39	4.21	4.15	4.24	4.28
Nov-90	15	2.37	3.25	3.67	4.18	3.93	3.82
Mar-91	19	3.13	3.59	3.86	3.90	3.79	3.80
Sep-91	25	3.07	3.67	4.22	4.02	3.83	3.92
Feb-92	30	3.23	3.68	4.34	3.91	3.78	3.86
Jun-92	34	3.19	3.74	4.22	3.93	3.86	3.91
Apr-94	56	2.76	3.55	3.97	3.78	3.89	3.68
Feb-95	66	3.10	3.77	4.31	4.05	3.85	4.05

Table A-3. Serviceability Index, San Antonio, General McMullen Drive, Section 3

Date	Time (Months)	Outside Lane Right	Outside Lane Left	Center Lane Right	Center Lane Left	Inside Lane Right	Inside Lane Left
Oct-89	2	3.12	3.83	4.08	4.06	3.73	3.68
Mar-90	7	3.60	3.81	3.54	3.83	3.62	3.49
Nov-90	15	1.54	1.85	2.82	2.90	3.64	3.56
Mar-91	19	1.83	3.66	3.52	4.05	3.86	3.91
Sep-91	25	1.86	3.36	3.53	3.91	3.53	3.57
Feb-92	30	2.05	3.39	3.36	3.94	3.57	3.69
Jun-92	34	1.87	3.14	3.13	3.88	3.46	3.57
Apr-94	56	1.37	2.82	2.75	3.65	3.59	3.72
Feb-95	66	1.33	2.68	2.67	3.92	3.51	3.62

Table A-4. Serviceability Index, San Antonio, General McMullen Drive, Section 4

Date	Time (Months)	Inside Lane Left	Inside Lane Right	Center Lane Left	Center Lane Right	Outside Lane Left	Outside Lane Right
Oct-89	2	3.69	3.95	4.00	3.53	3.28	2.72
Mar-90	7	3.84	4.07	4.05	3.92	3.26	2.57
Nov-90	15	3.98	4.07	4.11	4.03	2.97	3.36
Mar-91	19	3.80	4.01	3.91	3.57	3.23	2.77
Sep-91	25	3.82	4.11	3.98	3.81	3.35	2.77
Feb-92	30	3.90	4.07	3.99	3.74	3.36	2.81
Jun-92	34	3.86	4.08	3.99	3.72	3.48	2.94
Apr-94	56	3.65	3.88	3.94	3.55	3.31	2.81
Feb-95	66	3.93	4.12	4.03	3.76	3.38	2.78

Table A-5. Serviceability Index, San Antonio, General McMullen Drive, Section 5

Date	Time (Months)	Inside Lane Left	Inside Lane Right	Center Lane Left	Center Lane Right	Outside Lane Left	Outside Lane Right
Oct-89	2	3.70	3.87	4.20	3.89	3.35	2.30
Mar-90	7	3.65	3.76	4.23	3.82	3.30	2.33
Nov-90	15	3.78	3.61	3.91	4.24	3.65	3.17
Mar-91	19	3.77	3.92	4.22	3.55	3.18	2.26
Sep-91	25	3.78	3.94	4.12	3.51	3.34	2.63
Feb-92	30	3.89	3.98	4.14	3.60	3.20	2.36
Jun-92	34	3.71	3.87	4.21	3.57	3.24	2.57
Apr-94	56	3.73	3.86	4.07	3.87	3.20	2.22
Feb-95	66	3.73	3.88	4.13	3.53	3.22	2.29

Table A-6. Serviceability Index, San Antonio, General McMullen Drive, Section 6

Date	Time (Months)	Inside Lane Left	Inside Lane Right	Center Lane Left	Center Lane Right	Outside Lane Left	Outside Lane Right
Oct-89	2	3.38	3.32	2.72	2.94	1.77	1.48
Mar-90	7	3.50	3.43	2.66	3.12	2.03	1.60
Nov-90	15	3.65	3.60	3.85	3.70	3.69	1.95
Mar-91	19	3.37	3.61	3.30	2.91	1.86	1.44
Sep-91	25	3.56	3.95	3.80	3.18	2.11	1.63
Feb-92	30	3.49	3.85	3.61	3.22	2.11	1.67
Jun-92	34	3.52	3.93	3.81	3.41	2.17	1.68
Apr-94	56	3.31	3.65	3.51	3.37	2.03	1.47
Feb-95	66	3.45	3.84	3.64	3.40	1.97	1.44

Table A-7. International Roughness Index (m/km), San Antonio, General McMullen Drive, Section 1

Date	Time (Months)	Outside Lane Right	Outside Lane Left	Center Lane Right	Center Lane Left	Inside Lane Right	Inside Lane Left
Oct-89	2	2.01	1.98	1.20	1.14	1.27	1.27
Mar-90	7	1.88	1.86	1.31	1.37	2.00	2.25
Nov-90	15	2.30	1.83	1.49	1.41	1.28	1.54
Mar-91	19	1.86	1.95	1.25	1.35	1.39	1.31
Sep-91	25	2.03	1.79	1.13	1.19	1.30	1.31
Feb-92	30	1.80	1.96	1.15	1.16	1.30	1.37
Jun-92	34	1.86	1.97	1.21	1.20	1.38	1.28
Apr-94	56	2.09	1.95	1.39	1.43	1.46	1.35
Feb-95	66	1.94	1.89	1.25	1.22	1.33	1.29

Table A-8. International Roughness Index (m/km), San Antonio, General McMullen Drive, Section 2

Date	Time (Months)	Outside Lane Right	Outside Lane Left	Center Lane Right	Center Lane Left	Inside Lane Right	Inside Lane Left
Oct-89	2	2.11	1.52	1.45	1.31	1.42	1.25
Mar-90	7	2.24	1.71	1.22	1.25	1.25	1.11
Nov-90	15	2.84	2.00	1.43	1.20	1.38	1.46
Mar-91	19	2.18	1.62	1.36	1.41	1.44	1.35
Sep-91	25	2.25	1.56	1.22	1.36	1.39	1.30
Feb-92	30	2.10	1.55	1.01	1.41	1.46	1.29
Jun-92	34	2.12	1.51	1.17	1.41	1.36	1.26
Apr-94	56	2.56	1.79	1.34	1.55	1.37	1.45
Feb-95	66	2.16	1.53	1.06	1.33	1.35	1.19

Table A-9. International Roughness Index (m/km), San Antonio, General McMullen Drive, Section 3

Date	Time (Months)	Outside Lane Right	Outside Lane Left	Center Lane Right	Center Lane Left	Inside Lane Right	Inside Lane Left
Oct-89	2	2.08	1.51	1.32	1.32	1.67	1.69
Mar-90	7	1.71	1.42	1.58	1.46	1.58	1.58
Nov-90	15	3.95	3.19	2.27	1.94	1.64	1.78
Mar-91	19	3.58	1.56	1.47	1.31	1.61	1.54
Sep-91	25	3.71	1.68	1.41	1.35	1.71	1.56
Feb-92	30	3.42	1.72	1.51	1.35	1.67	1.51
Jun-92	34	3.71	1.84	1.65	1.40	1.82	1.61
Apr-94	56	4.24	2.07	1.73	1.50	1.78	1.63
Feb-95	66	4.36	1.90	1.70	1.33	1.72	1.60

Table A-10. International Roughness Index (m/km), San Antonio, General McMullen Drive, Section 4

Date	Time (Months)	Inside Lane Left	Inside Lane Right	Center Lane Left	Center Lane Right	Outside Lane Left	Outside Lane Right
Oct-89	2	1.62	1.42	1.40	1.60	1.95	2.62
Mar-90	7	1.54	1.34	1.31	1.31	1.94	2.82
Nov-90	15	1.29	1.36	1.27	1.26	1.85	1.93
Mar-91	19	1.61	1.42	1.42	1.54	1.88	2.38
Sep-91	25	1.57	1.29	1.38	1.36	1.83	2.44
Feb-92	30	1.55	1.35	1.43	1.38	1.85	2.38
Jun-92	34	1.53	1.31	1.40	1.38	1.73	2.21
Apr-94	56	1.74	1.48	1.48	1.54	1.88	2.41
Feb-95	66	1.48	1.25	1.32	1.39	1.78	2.43

Table A-11. International Roughness Index (m/km), San Antonio, General McMullen Drive, Section 5

Date	Time (Months)	Inside Lane Left	Inside Lane Right	Center Lane Left	Center Lane Right	Outside Lane Left	Outside Lane Right
Oct-89	2	1.50	1.45	1.17	1.34	1.88	2.90
Mar-90	7	1.54	1.51	1.16	1.37	1.91	2.84
Nov-90	15	1.42	1.58	1.43	1.12	1.58	2.19
Mar-91	19	1.47	1.42	1.17	1.48	2.08	2.98
Sep-91	25	1.49	1.37	1.18	1.53	1.95	2.65
Feb-92	30	1.42	1.40	1.22	1.48	2.02	2.86
Jun-92	34	1.47	1.36	1.17	1.42	2.00	2.70
Apr-94	56	1.56	1.47	1.35	1.44	2.06	3.03
Feb-95	66	1.49	1.39	1.24	1.52	2.02	2.96

Table A-12. International Roughness Index (m/km), San Antonio, General McMullen Drive, Section 6

Date	Time (Months)	Inside Lane Left	Inside Lane Right	Center Lane Left	Center Lane Right	Outside Lane Left	Outside Lane Right
Oct-89	2	1.95	1.90	1.92	2.12	3.22	3.97
Mar-90	7	1.82	1.84	1.84	2.02	3.03	3.74
Nov-90	15	1.56	1.69	1.40	1.43	1.54	3.46
Mar-91	19	1.93	1.72	1.83	2.25	3.28	4.24
Sep-91	25	1.77	1.49	1.44	1.98	2.83	3.81
Feb-92	30	1.78	1.54	1.56	1.91	2.94	3.88
Jun-92	34	1.76	1.51	1.42	1.79	2.73	3.73
Apr-94	56	2.02	1.74	1.58	1.93	3.16	3.94
Feb-95	66	1.85	1.55	1.55	1.79	3.09	4.25

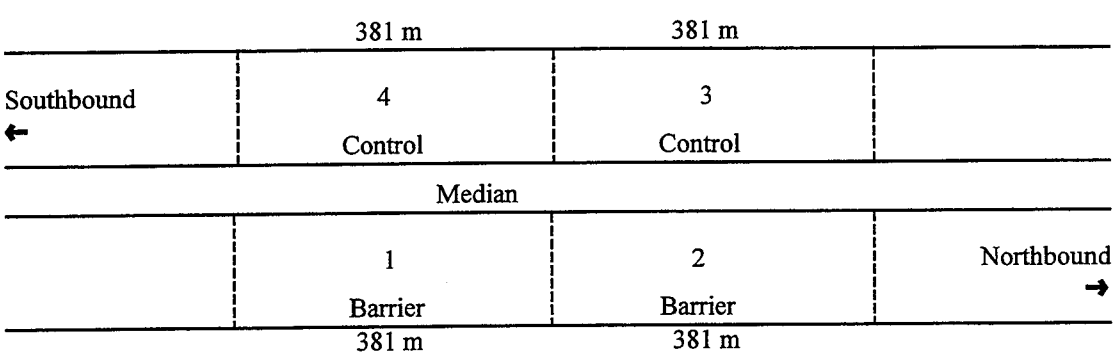

Figure A.2. Site Plan - San Antonio, IH 410

Table A-13. Serviceability Index, San Antonio, IH 410, Section 1

Date	Time (Months)	Outside Lane Right	Outside Lane Left	Center Lane Right	Center Lane Left	Inside Lane Right	Inside Lane Left
Oct-89	22	3.84	3.88	3.76	3.55		
Nov-90	35	3.98	4.35	4.33	4.39	3.58	3.83
Mar-91	39	3.81	4.17	4.17	4.23	3.55	3.77
Aug-91	44	3.95	4.30	4.34	4.40	3.62	3.87
Feb-92	50	3.83	3.89	3.80	3.70	3.56	3.74
Jun-92	54	3.96	4.37	4.34	4.39	3.58	3.78
Apr-94	76	3.59	3.81	3.83	3.60	3.82	3.58
Feb-95	86	3.79	3.98	3.94	3.84	3.43	3.80

Table A-14. Serviceability Index, San Antonio, IH 410, Section 2

Date	Time (Months)	Outside Lane Right	Outside Lane Left	Center Lane Right	Center Lane Left	Inside Lane Right	Inside Lane Left
Oct-89	22	3.83	3.97	4.40	4.44		
Nov-90	35	3.63	3.86	3.55	3.77	3.99	3.82
Mar-91	39	3.59	3.87	3.54	3.85	3.97	3.80
Aug-91	44	3.67	3.83	3.60	3.79	4.12	3.90
Feb-92	50	3.64	3.86	3.68	3.97	3.70	3.93
Jun-92	54	3.67	3.85	3.60	3.78	4.11	3.93
Apr-94	76	3.56	3.70	3.73	3.94	3.72	3.87
Feb-95	86	3.68	3.95	3.81	4.10	3.79	4.08

Table A-15. Serviceability Index, San Antonio, IH 410, Section 3

Date	Time (Months)	Inside Lane Left	Inside Lane Right	Center Lane Left	Center Lane Right	Outside Lane Left	Outside Lane Right
Oct-89	22			4.54	4.40	4.40	3.97
Nov-90	35	3.67	3.62	3.63	3.86	3.74	3.76
Mar-91	39	3.62	3.32	3.60	3.79	3.69	3.69
Aug-91	44	3.74	3.80	3.63	3.86	3.86	3.81
Feb-92	50	3.84	3.68	4.38	4.38	4.37	3.92
Jun-92	54	3.76	3.70	3.64	3.69	3.88	3.76
Apr-94	76	3.67	3.53	4.37	4.24	4.06	3.67
Feb-95	86	3.54	3.50	4.13	4.11	4.23	3.81

Table A-16. Serviceability Index, San Antonio, IH 410, Section 4

Date	Time (Months)	Inside Lane Left	Inside Lane Right	Center Lane Left	Center Lane Right	Outside Lane Left	Outside Lane Right
Oct-89	22			3.73	3.51	3.73	3.59
Nov-90	35	4.48	4.40	4.27	4.24	3.72	3.66
Mar-91	39	4.38	4.33	4.22	4.14	3.64	3.53
Aug-91	44	4.14	4.20	4.00	4.14	3.68	3.79
Feb-92	50	3.93	4.01	3.82	3.58	3.96	3.61
Jun-92	54	3.98	3.69	4.02	3.64	3.90	3.65
Apr-94	76	3.85	4.09	3.74	3.55	3.55	3.50
Feb-95	86	4.00	4.22	3.98	3.65	3.92	3.65

Table A-17.International Roughness Index (m/km), San Antonio, IH 410, Section 1

Date	Time (Months)	Outside Lane Right	Outside Lane Left	Center Lane Right	Center Lane Left	Inside Lane Right	Inside Lane Left
Oct-89	22	1.46	1.41	1.53	1.69		
Nov-90	35	1.46	1.11	1.08	1.06	1.77	1.56
Mar-91	39	1.62	1.21	1.20	1.17	1.80	1.60
Aug-91	44	1.47	1.15	1.05	1.05	1.72	1.52
Feb-92	50	1.45	1.42	1.46	1.59	1.59	1.51
Jun-92	54	1.47	1.09	1.08	1.05	1.78	1.62
Apr-94	76	1.69	1.50	1.53	1.74	1.53	1.72
Feb-95	86	1.49	1.35	1.45	1.50	1.75	1.53

Table A-18. International Roughness Index (m/km), San Antonio, IH 410, Section 2

Date	Time (Months)	Outside Lane Right	Outside Lane Left	Center Lane Right	Center Lane Left	Inside Lane Right	Inside Lane Left
Oct-89	22	1.39	1.28	1.02	0.99		
Nov-90	35	1.52	1.37	1.50	1.43	1.27	1.33
Mar-91	39	1.51	1.34	1.55	1.36	1.26	1.40
Aug-91	44	1.44	1.41	1.50	1.40	1.19	1.33
Feb-92	50	1.50	1.39	1.44	1.28	1.36	1.32
Jun-92	54	1.54	1.42	1.53	1.41	1.21	1.35
Apr-94	76	1.59	1.51	1.46	1.36	1.42	1.41
Feb-95	86	1.44	1.33	1.32	1.17	1.28	1.20

Table A-19. International Roughness Index (m/km), San Antonio, IH 410, Section 3

Date	Time (Months)	Inside Lane Left	Inside Lane Right	Center Lane Left	Center Lane Right	Outside Lane Left	Outside Lane Right
Oct-89	22			0.97	1.03	1.07	1.47
Nov-90	35	1.56	1.55	1.61	1.42	1.44	1.47
Mar-91	39	1.62	1.79	1.63	1.48	1.48	1.51
Aug-91	44	1.49	1.40	1.65	1.46	1.40	1.44
Feb-92	50	1.55	1.68	1.06	1.04	1.09	1.51
Jun-92	54	1.50	1.51	1.62	1.57	1.41	1.45
Apr-94	76	1.70	1.80	1.12	1.17	1.35	1.63
Feb-95	86	1.58	1.66	1.16	1.20	1.11	1.46

Table A-20. International Roughness Index (m/km), San Antonio, IH 410, Section 4

Date	Time (Months)	Inside Lane Left	Inside Lane Right	Center Lane Left	Center Lane Right	Outside Lane Left	Outside Lane Right
Oct-89	22			1.48	1.63	1.52	1.60
Nov-90	35	0.98	0.99	1.02	1.02	1.32	1.42
Mar-91	39	1.04	1.01	1.06	1.07	1.39	1.53
Aug-91	44	1.38	1.21	1.33	1.37	1.59	1.43
Feb-92	50	1.31	1.29	1.37	1.51	1.31	1.56
Jun-92	54	1.27	1.38	1.25	1.47	1.37	1.46
Apr-94	76	1.47	1.23	1.50	1.61	1.63	1.68
Feb-95	86	1.32	1.12	1.31	1.44	1.30	1.51

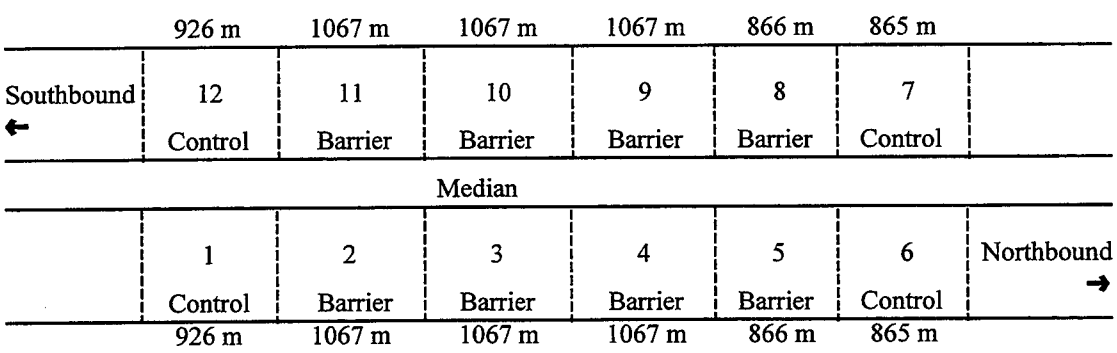

Figure A.3. Site Plan - San Antonio, IH 37

Table A-21. Serviceability Index, San Antonio, IH 37, Section 1

Date	Time (Months)	Outside Lane Right	Outside Lane Left	Center Lane Right	Center Lane Left	Inside Lane Right	Inside Lane Left
Oct-89	109	3.13	3.21	3.13	3.14	3.30	3.03
Mar-90	114	3.16	3.23	3.05	3.23	3.27	3.15
Nov-90	122	3.81	3.88	3.89	3.92	3.59	3.78
Mar-91	126	3.09	3.27	3.14	3.08	3.21	2.96
Sep-91	132	3.13	3.06	3.05	2.85	3.32	2.94
Jan-92	136	2.98	2.94	3.03	2.75	3.05	2.64
Jul-92	142	3.19	3.40	2.93	2.76	3.27	2.82
Apr-94	163	4.17	4.06	4.29	4.08	4.40	3.89
Feb-95	173	4.47	4.38	4.47	4.27	4.52	4.22

Table A-22. Serviceability Index, San Antonio, IH 37, Section 2

Date	Time (Months)	Outside Lane Right	Outside Lane Left	Center Lane Right	Center Lane Left	Inside Lane Right	Inside Lane Left
Oct-89	109	3.87	4.04	3.82	3.81	3.82	3.90
Mar-90	114	3.71	3.85	3.68	3.72	3.67	3.80
Nov-90	122	3.42	3.39	3.34	3.49	3.38	3.66
Mar-91	126	3.60	3.75	3.56	3.55	3.49	3.63
Sep-91	132	3.66	3.81	3.65	3.62	3.66	3.70
Jan-92	136	3.76	3.97	3.77	3.75	3.62	3.71
Jul-92	142	3.74	3.88	3.76	3.70	3.62	3.70
Apr-94	163	3.69	3.62	3.55	3.37	3.35	3.27
Feb-95	173	4.56	4.42	4.64	4.29	4.65	4.11

Table A-23. Serviceability Index, San Antonio, IH 37, Section 3

Date	Time (Months)	Outside Lane Right	Outside Lane Left	Center Lane Right	Center Lane Left	Inside Lane Right	Inside Lane Left
Oct-89	109	3.60	3.75	3.59	3.66	3.74	3.80
Mar-90	114	3.37	3.56	3.32	3.41	3.54	3.67
Nov-90	122	3.13	3.20	3.18	3.17	3.11	3.47
Mar-91	126	3.13	3.41	3.21	3.25	3.42	3.52
Sep-91	132	3.15	3.38	3.24	3.27	3.48	3.56
Jan-92	136	3.16	3.35	3.19	3.22	3.37	3.49
Jul-92	142	3.05	3.24	3.13	3.14	3.40	3.49
Apr-94	163	3.15	3.21	3.29	3.25	3.23	3.00
Feb-95	173	4.24	4.26	4.38	4.14	4.52	4.04

Table A-24. Serviceability Index, San Antonio, IH 37, Section 4

Date	Time (Months)	Outside Lane Right	Outside Lane Left	Center Lane Right	Center Lane Left	Inside Lane Right	Inside Lane Left
Oct-89	109	2.97	3.03	3.08	3.27	3.20	3.31
Mar-90	114	2.98	3.04	2.92	3.12	3.04	3.14
Nov-90	122	3.40	3.46	3.24	3.26	3.28	3.41
Mar-91	126	3.02	3.11	3.16	3.20	3.25	3.26
Sep-91	132	3.22	3.33	3.27	3.22	3.48	3.46
Jan-92	136	3.16	3.29	3.24	3.23	3.31	3.23
Jul-92	142	3.12	3.27	3.10	3.11	3.31	3.21
Apr-94	163	3.31	3.17	3.09	2.97	3.10	2.80
Feb-95	173	4.35	4.18	4.49	4.09	4.44	3.89

Table A-25. Serviceability Index, San Antonio, IH 37, Section 5

Date	Time (Months)	Outside Lane Right	Outside Lane Left	Center Lane Right	Center Lane Left	Inside Lane Right	Inside Lane Left
Oct-89	109	2.97	3.03	3.08	3.27	3.20	3.31
Mar-90	114	2.98	3.04	2.92	3.12	3.04	3.14
Nov-90	122	3.40	3.46	3.24	3.26	3.28	3.41
Mar-91	126	3.02	3.11	3.16	3.20	3.25	3.26
Sep-91	132	3.22	3.33	3.27	3.22	3.48	3.46
Jan-92	136	3.16	3.29	3.24	3.23	3.31	3.23
Jul-92	142	3.12	3.27	3.10	3.11	3.31	3.21
Apr-94	163	3.31	3.17	3.09	2.97	3.10	2.80
Feb-95	173	4.35	4.18	4.49	4.09	4.44	3.89

Table A-26. Serviceability Index, San Antonio, IH 37, Section 6

Date	Time (Months)	Outside Lane Right	Outside Lane Left	Center Lane Right	Center Lane Left	Inside Lane Right	Inside Lane Left
Oct-89	67	3.07	3.67	3.38	3.94	4.41	4.25
Mar-90	72	3.55	3.81	3.14	3.70	4.37	4.25
Nov-90	80	2.91	3.42	3.17	3.01	3.16	2.86
Mar-91	84	3.90	3.97	4.19	4.53	4.87	4.75
Sep-91	90	3.69	3.91	4.03	4.17	4.24	4.06
Jan-92	94	2.99	3.11	3.17	3.85	4.18	3.94
Jul-92	100	3.77	3.89	4.10	4.02	4.24	4.11
Apr-94	121	3.82	3.76	2.54	3.06	4.10	3.87
Feb-95	131	3.63	3.71	3.95	3.86	4.15	4.09

Table A-27. Serviceability Index, San Antonio, IH 37, Section 7

Date	Time (Months)	Inside Lane Left	Inside Lane Right	Center Lane Left	Center Lane Right	Outside Lane Left	Outside Lane Right
Oct-89	109	3.83	3.64	4.04	3.92	4.30	3.89
Mar-90	114	3.80	3.44	4.01	3.87	4.14	3.76
Nov-90	122	2.72	3.16	3.14	3.17	3.12	2.93
Mar-91	126	3.70	3.40	3.88	3.47	3.97	3.58
Sep-91	132	3.74	3.46	3.86	3.37	4.15	3.81
Jan-92	136	3.69	3.41	3.14	3.24	3.23	3.17
Jul-92	142	3.72	3.63	3.94	3.85	4.09	3.93
Apr-94	163	3.62	3.69	3.78	3.81	3.03	3.78
Feb-95	173	3.90	3.79	4.03	3.98	3.97	3.93

Table A-28. Serviceability Index, San Antonio, IH 37, Section 8

Date	Time (Months)	Inside Lane Left	Inside Lane Right	Center Lane Left	Center Lane Right	Outside Lane Left	Outside Lane Right
Oct-89	109	3.82	3.53	3.82	3.42	3.81	3.38
Mar-90	114	3.80	3.47	3.70	3.20	3.61	3.25
Nov-90	122	3.64	3.64	3.59	3.81	3.89	3.81
Mar-91	126	3.62	3.34	3.60	3.38	3.70	3.53
Sep-91	132	3.69	3.41	3.66	3.43	3.77	3.48
Jan-92	136	3.53	3.36	3.18	3.40	3.59	3.32
Jul-92	142	3.66	3.33	3.59	3.43	3.74	3.47
Apr-94	163	3.51	3.33	3.53	3.36	3.69	3.47
Feb-95	173	3.83	3.77	3.97	3.85	3.72	3.45

Table A-29. Serviceability Index, San Antonio, IH 37, Section 9

Date	Time (Months)	Inside Lane Left	Inside Lane Right	Center Lane Left	Center Lane Right	Outside Lane Left	Outside Lane Right
Oct-89	109	3.54	3.24	3.21	3.13	3.33	3.30
Mar-90	114	3.43	3.09	3.28	3.17	3.24	3.18
Nov-90	122	3.58	3.47	3.25	3.29	3.41	3.26
Mar-91	126	3.42	3.29	3.18	3.20	3.16	3.27
Sep-91	132	3.40	3.32	3.20	3.32	3.21	3.29
Jan-92	136	3.28	3.17	3.18	3.28	3.19	3.24
Jul-92	142	3.25	3.22	3.13	3.24	3.13	3.22
Apr-94	163	2.83	2.95	2.79	2.93	2.88	3.03
Feb-95	173	4.08	4.46	4.31	4.41	4.10	4.36

Table A-30. Serviceability Index, San Antonio, IH 37, Section 10

Date	Time (Months)	Inside Lane Left	Inside Lane Right	Center Lane Left	Center Lane Right	Outside Lane Left	Outside Lane Right
Oct-89	109	3.68	3.43	3.47	3.47	3.60	3.53
Mar-90	114	3.66	3.40	3.44	3.36	3.40	3.31
Nov-90	122	3.32	3.17	3.00	2.97	3.08	2.86
Mar-91	126	3.33	3.12	3.13	3.11	3.27	3.23
Sep-91	132	3.36	3.13	3.17	3.19	3.38	3.37
Jan-92	136	3.32	3.08	3.13	3.14	3.28	3.30
Jul-92	142	3.30	3.09	3.06	3.11	3.21	3.19
Apr-94	163	2.84	2.78	2.80	2.85	2.87	2.99
Feb-95	173	3.93	4.27	4.06	4.19	4.27	4.31

Table A-31. Serviceability Index, San Antonio, IH 37, Section 11

Date	Time (Months)	Inside Lane Left	Inside Lane Right	Center Lane Left	Center Lane Right	Outside Lane Left	Outside Lane Right
Oct-89	109		3.67		3.65		3.77
Mar-90	114		3.74		3.54		3.57
Nov-90	122		3.47		3.48		3.49
Mar-91	126		3.39		3.24		3.34
Sep-91	132		3.61		3.57		3.60
Jan-92	136		3.52		3.54		3.56
Jul-92	142		3.57		3.53		3.47
Apr-94	163		3.47		3.51		3.60
Feb-95	173	4.24	4.61		4.69		4.62

Table A-32. Serviceability Index, San Antonio, IH 37, Section 12

Date	Time (Months)	Inside Lane Left	Inside Lane Right	Center Lane Left	Center Lane Right	Outside Lane Left	Outside Lane Right
Oct-89	109	2.98	3.14	3.12	2.97	3.32	2.88
Mar-90	114	3.03	3.12	3.30	3.03	3.19	2.79
Nov-90	122	4.15	4.32	3.98	4.07	3.89	3.78
Mar-91	126	2.93	3.07	3.12	3.16	3.31	2.85
Sep-91	132	2.87	3.09	3.09	2.95	3.22	2.68
Jan-92	136	2.76	2.98	2.89	2.80	3.12	2.73
Jul-92	142	2.69	3.03	2.98	3.01	3.13	2.70
Apr-94	163	3.59	3.86	4.13	4.18	3.68	3.36
Feb-95	173	3.92	4.30	4.26	4.17	4.33	4.21

Table A-33. International Roughness Index (m/km), San Antonio, IH 37, Section 1

Date	Time	Outside Lane		Center Lane		Inside Lane	
	(Months)	Right	Left	Right	Left	Right	Left
Oct-89	109	2.06	1.70	2.01	1.85	1.81	2.08
Mar-90	114	2.04	1.66	1.94	1.82	1.85	2.09
Nov-90	122	1.46	1.40	1.41	1.45	1.50	1.40
Mar-91	126	2.07	1.70	2.01	1.96	1.92	2.23
Sep-91	132	2.03	1.74	2.00	2.01	1.79	2.20
Jan-92	136	2.08	1.76	2.01	2.06	1.91	2.34
Jul-92	142	2.02	1.71	2.06	2.03	1.82	2.25
Apr-94	163	1.07	1.14	1.11	1.21	1.02	1.42
Feb-95	173	0.97	0.98	0.99	1.06	0.92	1.20

Table A-34. International Roughness Index (m/km), San Antonio, IH 37, Section 2

Date	Time	Outside Lane		Center Lane		Inside Lane	
	(Months)	Right	Left	Right	Left	Right	Left
Oct-89	109	1.49	1.37	1.50	1.61	1.51	1.48
Mar-90	114	1.54	1.44	1.57	1.63	1.60	1.53
Nov-90	122	1.79	1.75	1.80	1.76	1.82	1.57
Mar-91	126	1.64	1.52	1.68	1.77	1.74	1.63
Sep-91	132	1.57	1.48	1.59	1.70	1.61	1.56
Jan-92	136	1.61	1.44	1.57	1.64	1.65	1.58
Jul-92	142	1.58	1.49	1.56	1.67	1.64	1.58
Apr-94	163	1.57	1.62	1.67	1.85	1.77	1.79
Feb-95	173	0.93	1.02	0.87	1.16	0.83	1.25

Table A-35. International Roughness Index (m/km), San Antonio, IH 37, Section 3

Date	Time	Outside Lane		Center Lane		Inside Lane	
	(Months)	Right	Left	Right	Left	Right	Left
Oct-89	109	1.68	1.59	1.78	1.70	1.59	1.58
Mar-90	114	1.84	1.72	1.94	1.83	1.69	1.64
Nov-90	122	2.08	2.03	2.03	2.08	2.09	1.79
Mar-91	126	2.05	1.86	2.09	2.02	1.84	1.80
Sep-91	132	2.04	1.89	2.04	1.98	1.77	1.79
Jan-92	136	2.01	1.87	2.07	2.02	1.88	1.86
Jul-92	142	2.08	1.95	2.09	2.07	1.85	1.85
Apr-94	163	1.90	1.87	1.91	1.93	2.00	2.13
Feb-95	173	1.10	1.10	1.04	1.21	0.96	1.37

Table A-36. International Roughness Index (m/km), San Antonio, IH 37, Section 4

Date	Time	Outside Lane		Center Lane		Inside Lane	
	(Months)	Right	Left	Right	Left	Right	Left
Oct-89	109	2.24	2.28	2.26	2.02	1.99	1.92
Mar-90	114	2.21	2.24	2.36	2.08	2.10	2.02
Nov-90	122	1.79	1.77	1.94	1.94	1.87	1.80
Mar-91	126	2.29	2.26	2.21	2.13	2.05	1.98
Sep-91	132	2.13	2.07	2.14	2.10	1.84	1.80
Jan-92	136	2.17	2.09	2.16	2.06	1.97	1.98
Jul-92	142	2.19	2.12	2.25	2.12	1.98	2.01
Apr-94	163	1.95	2.08	2.07	2.12	2.04	2.23
Feb-95	173	1.13	1.18	1.01	1.26	1.00	1.32

Table A-37. International Roughness Index (m/km), San Antonio, IH 37, Section 5

Date	Time	Outside Lane		Center Lane		Inside Lane	
	(Months)	Right	Left	Right	Left	Right	Left
Oct-89	109	1.57	1.69	1.48	1.39	1.38	1.36
Mar-90	114	1.62	1.67	1.67	1.44	1.36	1.35
Nov-90	122	1.85	1.67	1.88	1.85	1.87	1.63
Mar-91	126	1.56	1.68	1.63	1.58	1.56	1.54
Sep-91	132	1.52	1.74	1.53	1.45	1.59	1.55
Jan-92	136	1.48	1.73	1.59	1.49	1.48	1.45
Jul-92	142	1.54	1.76	1.50	1.48	1.41	1.38
Apr-94	163	1.48	1.77	1.52	1.60	1.48	1.54
Feb-95	173	1.12	1.37	1.23	1.25	1.14	1.25

Table A-38. International Roughness Index (m/km), San Antonio, IH 37, Section 6

Date	Time	Outside Lane		Center Lane		Inside Lane	
	(Months)	Right	Left	Right	Left	Right	Left
Oct-89	67	1.51	1.34	1.42	1.02	0.96	0.97
Mar-90	72	1.39	1.28	1.48	1.07	0.99	0.96
Nov-90	80	2.25	1.65	2.07	2.01	1.93	2.15
Mar-91	84	1.26	1.14	1.25	0.88	0.71	0.74
Sep-91	90	1.42	1.28	1.33	1.07	1.05	1.12
Jan-92	94	1.58	1.43	1.50	1.23	1.02	1.10
Jul-92	100	1.38	1.26	1.36	1.23	1.02	1.05
Apr-94	121	1.34	1.40	1.65	1.45	1.11	1.20
Feb-95	131	1.34	1.28	1.40	1.23	0.99	1.04

Table A-39. International Roughness Index (m/km), San Antonio, IH 37, Section 7

Date	Time	Inside Lane		Center Lane		Outside Lane	
	(Months)	Left	Right	Left	Right	Left	Right
Oct-89	109	1.35	1.52	1.37	1.38	1.20	1.40
Mar-90	114	1.36	1.56	1.39	1.41	1.27	1.44
Nov-90	122	2.19	1.80	1.82	1.95	1.62	1.96
Mar-91	126	1.44	1.57	1.46	1.55	1.34	1.56
Sep-91	132	1.42	1.55	1.43	1.48	1.29	1.39
Jan-92	136	1.44	1.57	1.55	1.45	1.42	1.50
Jul-92	142	1.43	1.50	1.47	1.40	1.33	1.37
Apr-94	163	1.56	1.52	1.58	1.45	1.49	1.47
Feb-95	173	1.30	1.39	1.33	1.31	1.33	1.38

Table A-40. International Roughness Index (m/km), San Antonio, IH 37, Section 8

Date	Time	Inside Lane		Center Lane		Outside Lane	
	(Months)	Left	Right	Left	Right	Left	Right
Oct-89	109	1.48	1.73	1.56	1.79	1.53	1.71
Mar-90	114	1.44	1.75	1.58	1.74	1.58	1.75
Nov-90	122	1.56	1.59	1.70	1.50	1.47	1.53
Mar-91	126	1.57	1.86	1.70	1.81	1.57	1.74
Sep-91	132	1.53	1.81	1.69	1.77	1.52	1.76
Jan-92	136	1.58	1.84	1.79	1.74	1.55	1.78
Jul-92	142	1.55	1.88	1.71	1.74	1.57	1.80
Apr-94	163	1.63	1.89	1.77	1.80	1.64	1.77
Feb-95	173	1.34	1.38	1.32	1.33	1.41	1.45

Table A-41. International Roughness Index (m/km), San Antonio, IH 37, Section 9

Date	Time	Inside Lane		Center Lane		Outside Lane	
	(Months)	Left	Right	Left	Right	Left	Right
Oct-89	109	1.78	2.01	2.04	2.10	1.92	1.96
Mar-90	114	1.85	2.10	1.97	2.05	1.98	2.02
Nov-90	122	1.75	1.78	1.99	1.94	1.82	1.89
Mar-91	126	1.92	2.01	2.15	2.11	2.11	2.05
Sep-91	132	1.93	1.98	2.13	1.99	2.04	2.02
Jan-92	136	2.00	2.16	2.16	1.99	2.04	2.05
Jul-92	142	2.02	2.07	2.20	2.07	2.11	2.08
Apr-94	163	2.23	2.19	2.32	2.22	2.22	2.11
Feb-95	173	1.24	1.00	1.15	1.09	1.23	1.11

Table A-42. International Roughness Index (m/km), San Antonio, IH 37, Section 10

Date	Time	Inside Lane		Center Lane		Outside Lane	
	(Months)	Left	Right	Left	Right	Left	Right
Oct-89	109	1.56	1.80	1.86	1.82	1.73	1.77
Mar-90	114	1.54	1.80	1.82	1.87	1.84	1.85
Nov-90	122	1.88	1.99	2.17	2.27	2.12	2.29
Mar-91	126	1.84	2.01	2.06	2.10	1.97	1.95
Sep-91	132	1.79	1.99	2.05	2.02	1.88	1.84
Jan-92	136	1.78	2.01	2.04	2.07	1.97	1.89
Jul-92	142	1.81	2.01	2.12	2.10	2.02	2.00
Apr-94	163	2.12	2.27	2.33	2.30	2.32	2.20
Feb-95	173	1.40	1.13	1.22	1.11	1.13	1.09

Table A-43. International Roughness Index (m/km), San Antonio, IH 37, Section 11

Date	Time	Inside Lane		Center Lane		Outside Lane	
	(Months)	Left	Right	Left	Right	Left	Right
Oct-89	109		1.71		1.72		1.63
Mar-90	114		1.66		1.78		1.73
Nov-90	122		1.65		1.72		1.65
Mar-91	126		1.94		2.00		1.89
Sep-91	132		1.76		1.79		1.74
Jan-92	136		1.84		1.80		1.77
Jul-92	142		1.79		1.80		1.79
Apr-94	163		1.93		1.83		1.77
Feb-95	173	1.20	0.91		0.80		0.92

Table A-44. International Roughness Index (m/km), San Antonio, IH 37, Section 12

Date	Time	Inside Lane		Center Lane		Outside Lane	
	(Months)	Left	Right	Left	Right	Left	Right
Oct-89	109	2.14	2.09	1.95	2.19	1.78	2.28
Mar-90	114	2.06	2.08	1.83	2.13	1.83	2.43
Nov-90	122	1.03	0.99	1.15	1.30	1.34	1.38
Mar-91	126	2.14	2.00	1.91	2.04	1.70	2.28
Sep-91	132	2.15	2.06	1.93	2.16	1.84	2.33
Jan-92	136	2.36	2.14	2.12	2.17	1.83	2.41
Jul-92	142	2.38	2.13	2.08	2.09	1.86	2.50
Apr-94	163	1.42	1.26	1.16	1.19	1.26	1.57
Feb-95	173	1.18	1.01	1.01	1.03	1.01	1.14

	343 m	305 m		305 m	305 m	
Westbound ←	8 Control	7 Control		6 Control	5 Control	
			Median			
	1 244 cm Bar.	2 183 cm Bar.		3 Lime	4 Flyash	Eastbound →
	343 m	305 m		305 m	305 m	

Figure A.4. Site Plan - Greenville, IH 30

Table A-45. Serviceability Index, Greenville, IH 30, Section 1

Date	Time (Months)	Outside Lane Right	Outside Lane Left	Inside Lane Right	Inside Lane Left
May-87	9	4.36	4.37	3.88	4.05
Aug-88	24	3.57	3.81	4.06	3.61
Mar-89	31	3.65	3.92	4.03	3.86
Apr-90	44	3.76	4.01	4.01	3.81
Nov-90	51	3.65	3.41	4.41	4.51
Mar-91	55	3.81	4.28	3.64	4.17
Jul-91	59	4.40	3.88	3.99	4.19
Jan-92	65	3.89	3.82	4.41	4.25
Jul-92	71	4.22	3.65	3.68	4.26
Apr-94	92	4.10	3.54	3.76	4.07
Oct-94	98	3.97	3.14	3.59	4.21
Apr-95	104	4.22	3.40	3.77	4.27

Table A-46. Serviceability Index, Greenville, IH 30, Section 2

Date	Time (Months)	Outside Lane Right	Outside Lane Left	Inside Lane Right	Inside Lane Left
May-87	9	4.82	4.83	4.52	4.26
Aug-88	24	4.62	4.34	4.13	3.64
Mar-89	31	4.50	4.43	4.15	3.88
Apr-90	44	4.45	4.30	3.92	3.65
Nov-90	51	4.09	3.68	3.75	3.50
Mar-91	55	3.64	3.26	3.73	3.37
Jul-91	59	4.26	3.74	3.91	3.40
Jan-92	65	4.10	4.03	4.00	3.99
Jul-92	71	4.03	3.20	3.52	3.08
Apr-94	92	3.86	3.08	3.35	2.66
Oct-94	98	3.61	2.58	3.24	2.93
Apr-95	104	4.07	3.26	3.69	3.37

Table A-47. Serviceability Index, Greenville, IH 30, Section 3

Date	Time (Months)	Outside Lane Right	Outside Lane Left	Inside Lane Right	Inside Lane Left
May-87	9	4.86	4.83	4.87	4.81
Aug-88	24	4.78	4.43	4.72	4.35
Mar-89	31	4.59	4.38	4.70	4.58
Apr-90	44	4.67	4.43	4.67	4.61
Nov-90	51	4.68	4.42	4.69	4.55
Mar-91	55	4.68	4.06	4.68	4.56
Jul-91	59	4.69	4.13	4.63	4.52
Jan-92	65	4.49	3.85	4.57	4.46
Jul-92	71	4.59	3.33	4.57	4.50
Apr-94	92	3.20	1.98	4.45	4.43
Oct-94	98	2.79	2.79	4.17	4.33
Apr-95	104	3.31	3.03	4.44	4.47

Table A-48. Serviceability Index, Greenville, IH 30, Section 4

Date	Time (Months)	Outside Lane Right	Outside Lane Left	Inside Lane Right	Inside Lane Left
May-87	9	4.59	4.51	4.58	4.54
Aug-88	24	4.03	3.83	4.17	3.90
Mar-89	31	4.12	4.14	4.45	4.39
Apr-90	44	3.98	3.23	4.06	4.29
Nov-90	51	3.86	3.73	4.01	3.99
Mar-91	55	3.28	3.16	3.63	3.52
Jul-91	59	3.21	2.87	3.78	3.50
Jan-92	65	3.02	2.82	3.65	3.60
Jul-92	71	2.97	2.33	3.65	3.61
Apr-94	92	2.07	1.99	3.76	3.36
Oct-94	98	1.85	1.87	3.50	3.55
Apr-95	104	2.18	2.19	3.66	3.66

Table A-49. Serviceability Index, Greenville, IH 30, Section 5

Date	Time (Months)	Inside Lane Left	Inside Lane Right	Outside Lane Left	Outside Lane Right
May-87	9	4.62	4.68	4.19	4.38
Aug-88	24	4.02	4.39	3.86	4.22
Mar-89	31	4.49	4.60	4.15	4.33
Apr-90	44	2.04	0.98	4.05	4.11
Nov-90	51	4.19	4.39	3.88	4.10
Mar-91	55	4.27	4.42	3.82	3.85
Jul-91	59	4.16	4.34	3.76	3.91
Jan-92	65	4.15	3.60	3.92	4.12
Jul-92	71	4.12	4.23	3.65	3.71
Apr-94	92	4.00	4.10	3.50	3.74
Oct-94	98	3.94	3.89	3.34	3.38
Apr-95	104	4.14	4.27	3.67	3.81

Table A-50.Serviceability Index, Greenville, IH 30, Section 6

Date	Time (Months)	Inside Lane Left	Inside Lane Right	Outside Lane Left	Outside Lane Right
May-87	9	4.33	4.27	4.44	4.58
Aug-88	24	3.86	4.10	4.00	4.41
Mar-89	31	4.33	4.46	4.18	4.34
Apr-90	44	4.13	4.13	4.24	4.31
Nov-90	51	4.02	4.03	3.98	4.16
Mar-91	55	4.06	4.12	4.10	4.15
Jul-91	59	4.05	4.03	4.01	4.20
Jan-92	65	4.34	4.45	3.78	4.37
Jul-92	71	3.98	4.01	4.00	4.01
Apr-94	92	3.97	4.01	3.86	3.83
Oct-94	98	3.95	3.68	3.74	3.58
Apr-95	104	4.11	4.04	4.13	4.16

Table A-51. Serviceability Index, Greenville, IH 30, Section 7

Date	Time (Months)	Inside Lane Left	Inside Lane Right	Outside Lane Left	Outside Lane Right
May-87	9	3.20	3.15	4.19	4.24
Aug-88	24	2.93	2.82	3.35	3.47
Mar-89	31	3.03	2.87	3.63	3.52
Apr-90	44	0.61	1.28	4.18	4.14
Nov-90	51	2.69	2.62	3.80	3.82
Mar-91	55	2.70	2.67	3.77	3.65
Jul-91	59	2.37	2.19	3.28	3.17
Jan-92	65	2.29	2.04	3.25	3.47
Jul-92	71	2.28	2.10	3.16	3.35
Apr-94	92	1.80	2.07	2.82	3.15
Oct-94	98	2.20	2.48	2.94	2.48
Apr-95	104	2.33	2.61	3.37	2.78

Table A-52. Serviceability Index, Greenville, IH 30, Section 8

Date	Time (Months)	Inside Lane Left	Inside Lane Right	Outside Lane Left	Outside Lane Right
May-87	9	3.47	3.47	4.34	4.40
Aug-88	24	2.89	2.98	3.71	3.97
Mar-89	31	3.44	3.36	3.96	3.98
Apr-90	44	3.66	3.68	3.64	3.61
Nov-90	51	2.69	2.69	3.48	3.44
Mar-91	55	2.79	2.89	3.38	3.62
Jul-91	59	3.02	3.08	3.94	4.04
Jan-92	65	2.90	2.91	3.50	3.51
Jul-92	71	2.81	2.94	3.44	3.43
Apr-94	92	2.69	2.86	2.85	3.18
Oct-94	98	2.97	2.52	3.39	3.17
Apr-95	104	3.23	2.85	3.50	3.59

Table A-53. International Roughness Index (m/km), Greenville, IH 30, Section 1

Date	Time (Months)	Outside Lane Right	Outside Lane Left	Inside Lane Right	Inside Lane Left
May-87	9	0.99	0.96	1.37	1.21
Aug-88	24	1.23	1.30	1.32	1.49
Mar-89	31	1.24	1.22	1.36	1.26
Apr-90	44	1.18	1.20	1.40	1.26
Nov-90	51	1.24	1.57	1.05	0.91
Mar-91	55	1.34	1.11	1.49	1.20
Jul-91	59	0.97	1.38	1.24	1.13
Jan-92	65	1.52	1.54	1.07	1.19
Jul-92	71	1.10	1.54	1.48	1.15
Apr-94	92	1.24	1.76	1.55	1.34
Oct-94	98	1.33	2.08	1.66	1.20
Apr-95	104	1.10	1.83	1.48	1.12

Table A-54. International Roughness Index (m/km), Greenville, IH 30, Section 2

Date	Time (Months)	Outside Lane Right	Outside Lane Left	Inside Lane Right	Inside Lane Left
May-87	9	0.70	0.76	0.83	1.03
Aug-88	24	0.78	1.03	1.03	1.36
Mar-89	31	0.89	0.89	0.99	1.10
Apr-90	44	0.87	0.94	1.15	1.23
Nov-90	51	1.02	1.34	1.25	1.35
Mar-91	55	1.25	1.42	1.20	1.34
Jul-91	59	0.92	1.38	1.05	1.35
Jan-92	65	1.35	1.33	1.40	1.39
Jul-92	71	1.12	1.87	1.35	1.57
Apr-94	92	1.26	2.11	1.42	1.82
Oct-94	98	1.43	2.62	1.54	1.66
Apr-95	104	1.07	1.85	1.30	1.38

Table A-55. International Roughness Index (m/km), Greenville, IH 30, Section 3

Date	Time (Months)	Outside Lane Right	Outside Lane Left	Inside Lane Right	Inside Lane Left
May-87	9	0.73	0.76	0.70	0.79
Aug-88	24	0.77	1.05	0.84	1.10
Mar-89	31	0.94	1.03	0.82	0.91
Apr-90	44	0.87	1.04	0.98	1.00
Nov-90	51	0.85	1.06	0.83	0.98
Mar-91	55	0.82	1.31	0.87	0.98
Jul-91	59	0.83	1.27	0.90	0.98
Jan-92	65	0.92	1.50	0.95	1.04
Jul-92	71	0.92	1.74	0.98	1.06
Apr-94	92	1.85	3.08	1.14	1.16
Oct-94	98	2.14	2.43	1.32	1.21
Apr-95	104	1.75	2.11	1.10	1.11

Table A-56. International Roughness Index (m/km), Greenville, IH 30, Section 4

Date	Time (Months)	Outside Lane Right	Outside Lane Left	Inside Lane Right	Inside Lane Left
May-87	9	0.85	0.93	0.90	1.03
Aug-88	24	1.12	1.33	1.13	1.41
Mar-89	31	1.13	1.12	0.93	1.06
Apr-90	44	1.24	1.38	1.41	1.09
Nov-90	51	1.28	1.35	1.16	1.28
Mar-91	55	1.37	1.59	1.49	1.49
Jul-91	59	1.48	1.84	1.41	1.50
Jan-92	65	1.60	1.94	1.48	1.42
Jul-92	71	1.65	2.33	1.53	1.49
Apr-94	92	2.81	3.33	1.36	1.64
Oct-94	98	3.27	3.64	1.65	1.49
Apr-95	104	2.77	3.01	1.63	1.44

Table A-57. International Roughness Index (m/km), Greenville, IH 30, Section 5

Date	Time (Months)	Inside Lane Left	Inside Lane Right	Outside Lane Left	Outside Lane Right
May-87	9	0.95	0.93	1.30	1.18
Aug-88	24	1.37	1.14	1.51	1.29
Mar-89	31	1.02	0.96	1.33	1.21
Apr-90	44	1.66	2.16	1.42	1.37
Nov-90	51	1.22	1.11	1.53	1.35
Mar-91	55	1.17	1.09	1.53	1.56
Jul-91	59	1.22	1.11	1.57	1.50
Jan-92	65	1.24	1.61	1.40	1.12
Jul-92	71	1.27	1.24	1.67	1.64
Apr-94	92	1.42	1.32	1.87	1.69
Oct-94	98	1.47	1.47	1.99	1.98
Apr-95	104	1.28	1.21	1.70	1.60

Table A-58. International Roughness Index (m/km), Greenville, IH 30, Section 6

Date	Time (Months)	Inside Lane Left	Inside Lane Right	Outside Lane Left	Outside Lane Right
May-87	9	1.17	1.28	1.18	1.00
Aug-88	24	1.50	1.37	1.45	1.07
Mar-89	31	1.15	1.05	1.28	1.16
Apr-90	44	1.38	1.41	1.26	1.22
Nov-90	51	1.38	1.39	1.41	1.31
Mar-91	55	1.36	1.29	1.30	1.27
Jul-91	59	1.31	1.33	1.39	1.21
Jan-92	65	1.04	0.90	1.47	0.97
Jul-92	71	1.44	1.42	1.43	1.42
Apr-94	92	1.44	1.40	1.52	1.51
Oct-94	98	1.45	1.67	1.60	1.69
Apr-95	104	1.34	1.43	1.40	1.31

Table A-59. International Roughness Index (m/km), Greenville, IH 30, Section 7

Date	Time (Months)	Inside Lane Left	Inside Lane Right	Outside Lane Left	Outside Lane Right
May-87	9	2.14	2.19	1.23	1.27
Aug-88	24	2.18	2.30	1.76	1.84
Mar-89	31	2.18	2.27	1.59	1.79
Apr-90	44	3.43	2.81	1.31	1.41
Nov-90	51	2.48	2.41	1.33	1.51
Mar-91	55	2.50	2.37	1.35	1.70
Jul-91	59	2.61	2.65	1.72	2.12
Jan-92	65	2.70	2.81	1.69	1.80
Jul-92	71	2.75	2.75	1.81	1.94
Apr-94	92	3.29	3.03	1.98	2.09
Oct-94	98	2.96	3.04	2.24	2.66
Apr-95	104	2.78	2.88	1.87	2.53

Table A-60. International Roughness Index (m/km), Greenville, IH 30, Section 8

Date	Time (Months)	Inside Lane Left	Inside Lane Right	Outside Lane Left	Outside Lane Right
May-87	9	1.90	2.01	1.09	1.01
Aug-88	24	2.34	2.31	1.48	1.28
Mar-89	31	1.92	2.04	1.20	1.21
Apr-90	44	1.61	1.67	1.51	1.52
Nov-90	51	2.40	2.40	1.44	1.53
Mar-91	55	2.49	2.31	1.59	1.42
Jul-91	59	2.24	2.19	1.30	1.20
Jan-92	65	2.33	2.29	1.52	1.48
Jul-92	71	2.41	2.22	1.59	1.66
Apr-94	92	2.43	2.18	1.93	1.60
Oct-94	98	2.24	2.64	1.76	1.82
Apr-95	104	2.02	2.43	1.63	1.46

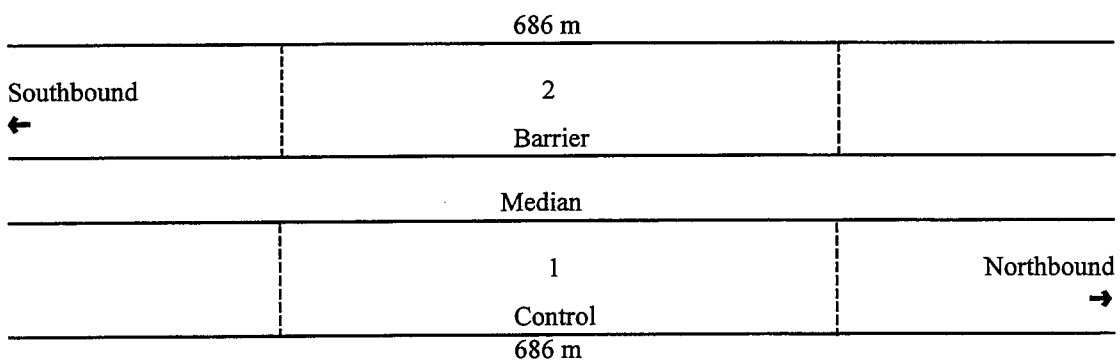

Figure A.5. Site Plan - San Antonio, US 281

Table A-61. Serviceability Index, San Antonio, US 281, Section 1

Date	Time (Months)	Outside Lane Right	Outside Lane Left	Center Lane Right	Center Lane Left	Inside Lane Right	Inside Lane Left
Aug-87	9	3.70	3.60	3.99	3.89	4.10	4.08
Jun-88	19	3.22	3.09	3.62	3.53	3.79	3.66
Oct-89	35	3.93	4.38	4.42	4.59	4.52	4.55
Apr-90	41	3.35	3.42	3.42	3.58	3.67	3.80
Nov-90	48	3.82	3.84	3.37	3.40	3.73	3.88
Apr-91	53	3.64	3.66	3.22	3.15	3.40	3.59
Aug-91	57	3.28	3.23	3.56	3.69	3.75	3.73
Jan-92	62	3.71	3.82	3.72	4.05	3.92	3.93
Jun-92	67	3.89	3.86	3.74	3.71	3.61	3.96
Apr-94	89	3.40	3.46	3.37	3.63	3.79	3.70
Feb-95	99	3.42	3.54	3.59	3.73	3.73	3.76

Table A-62. Serviceability Index, San Antonio, US 281, Section 2

Date	Time (Months)	Inside Lane Left	Inside Lane Right	Center Lane Left	Center Lane Right	Outside Lane Left	Outside Lane Right
Aug-87	9	2.98	3.35	3.25	3.51	3.50	3.47
Jun-88	19	2.64	2.99	2.87	3.03	2.87	2.86
Oct-89	35	3.51	3.46	3.99	3.88	3.25	2.95
Apr-90	41	2.83	3.15	3.01	3.09	3.48	3.47
Nov-90	48	2.80	3.14	3.26	3.16	2.68	2.98
Apr-91	53	3.04	3.17	3.20	3.12	2.60	2.96
Aug-91	57	2.65	2.98	2.87	3.21	3.38	3.45
Jan-92	62	2.58	2.91	2.94	3.05	3.23	3.20
Jun-92	67	3.00	3.15	3.25	3.16	2.44	2.86
Apr-94	89	3.35	3.62	3.88	3.89	3.89	3.64
Feb-95	99	3.52	3.79	4.05	4.04	3.95	3.73

Table A-63. International Roughness Index (m/km), San Antonio, US 281, Section 1

Date	Time (Months)	Outside Lane Right	Outside Lane Left	Center Lane Right	Center Lane Left	Inside Lane Right	Inside Lane Left
Aug-87	9	1.75	1.67	1.44	1.52	1.38	1.33
Jun-88	19	2.15	2.15	1.70	1.72	1.51	1.58
Oct-89	35	1.69	1.24	1.16	1.05	1.09	1.11
Apr-90	41	2.01	1.88	1.86	1.74	1.66	1.54
Nov-90	48	1.48	1.45	1.86	1.82	1.58	1.45
Apr-91	53	1.65	1.63	2.07	2.11	1.88	1.74
Aug-91	57	2.01	1.99	1.71	1.64	1.55	1.54
Jan-92	62	1.51	1.40	1.44	1.23	1.35	1.30
Jun-92	67	1.38	1.38	1.52	1.52	1.57	1.33
Apr-94	89	1.84	1.76	1.76	1.55	1.48	1.55
Feb-95	99	1.72	1.67	1.53	1.45	1.48	1.44

Table A-64. International Roughness Index (m/km), San Antonio, US 281, Section 2

Date	Time (Months)	Inside Lane Left	Inside Lane Right	Center Lane Left	Center Lane Right	Outside Lane Left	Outside Lane Right
Aug-87	9	2.48	2.10	2.17	1.96	1.92	1.98
Jun-88	19	2.72	2.29	2.42	2.24	2.40	2.47
Oct-89	35	1.82	1.86	1.43	1.43	1.92	2.17
Apr-90	41	2.53	2.20	2.26	2.12	1.82	1.85
Nov-90	48	2.29	2.09	1.94	2.04	2.63	2.34
Apr-91	53	2.22	2.14	1.99	2.06	2.75	2.35
Aug-91	57	2.69	2.31	2.26	2.04	1.84	1.86
Jan-92	62	2.76	2.40	2.17	2.19	1.93	2.00
Jun-92	67	2.23	2.15	1.95	2.01	2.92	2.43
Apr-94	89	1.88	1.68	1.47	1.46	1.43	1.56
Feb-95	99	1.70	1.51	1.32	1.31	1.35	1.44

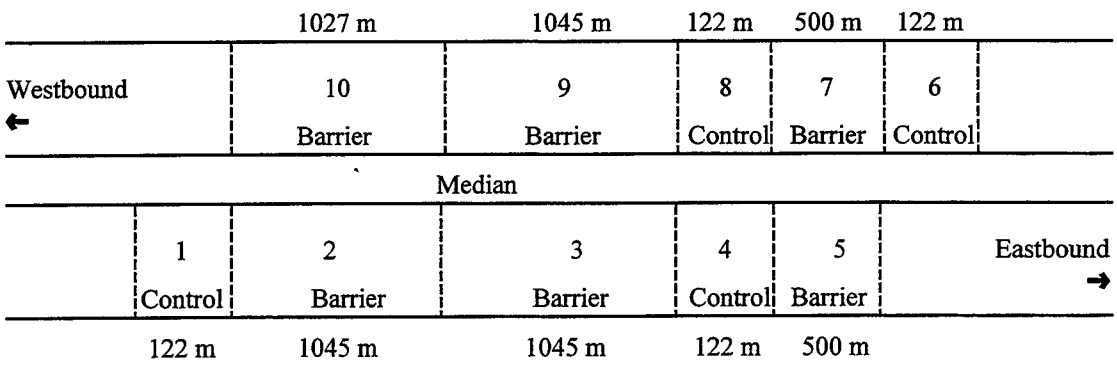

Figure A.6. Site Plan - San Antonio, IH 10

Table A-65. Serviceability Index, San Antonio, IH 10, Section 1

Date	Time (Months)	Outside Lane Right	Outside Lane Left	Center Lane Right	Center Lane Left	Inside Lane Right	Inside Lane Left
Aug-87	0	4.50	4.18	4.57	4.44	4.30	4.43
Jun-88	10	3.68	3.22	3.23	3.36	3.66	3.76
Oct-89	26	4.04	3.80	4.35	4.05	3.75	4.05
Mar-90	31	3.76	3.47	4.21	3.84	3.76	4.11
Nov-90	39	3.93	3.33	3.21	3.72	3.20	3.32
Mar-91	43	4.25	3.61	4.51	4.33	3.81	4.30
Aug-91	48	4.31	2.29	3.09	3.20	3.64	4.12
Jan-92	53	3.38	2.66	3.77	3.76	3.33	3.40
Jul-92	59	4.42	4.17	4.21	3.98	4.47	4.55
Apr-94	80	4.10	2.21	3.65	3.64	3.32	3.51
Feb-95	90	2.85	2.11	2.62	3.12	3.38	3.46

Table A-66. Serviceability Index, San Antonio, IH 10, Section 2

Date	Time (Months)	Outside Lane Right	Outside Lane Left	Center Lane Right	Center Lane Left	Inside Lane Right	Inside Lane Left
Aug-87	0	4.48	4.24	4.55	4.35	4.46	4.02
Jun-88	10	4.35	4.04	4.39	4.10	4.13	3.76
Oct-89	26	4.38	4.19	4.43	4.38	4.29	3.80
Mar-90	31	4.34	4.19	4.27	4.24	4.22	3.73
Nov-90	39	4.33	4.17	4.31	4.21	4.11	3.61
Mar-91	43	4.26	4.08	4.24	4.08	4.07	3.56
Aug-91	48	4.29	4.12	4.29	4.19	4.12	3.58
Jan-92	53	4.25	4.07	4.20	4.08	4.05	3.55
Jul-92	59	4.10	3.91	4.18	4.03	3.94	3.41
Apr-94	80	4.09	3.88	4.01	3.84	3.84	3.31
Feb-95	90	4.11	3.90	4.05	3.92	3.81	3.32

Table A-67. Serviceability Index, San Antonio, IH 10, Section 3

Date	Time (Months)	Outside Lane Right	Outside Lane Left	Center Lane Right	Center Lane Left	Inside Lane Right	Inside Lane Left
Aug-87	0	4.41	4.09	4.61	4.36	4.28	3.67
Jun-88	10	4.27	3.99	4.45	4.20	4.02	3.57
Oct-89	26	4.41	4.26	4.60	4.54	4.25	3.72
Mar-90	31	4.31	4.16	4.37	4.31	4.09	3.56
Nov-90	39	4.36	4.19	4.42	4.35	4.06	3.51
Mar-91	43	4.32	4.17	4.41	4.35	4.00	3.46
Aug-91	48	4.34	4.15	4.39	4.30	4.03	3.50
Jan-92	53	4.27	4.10	4.27	4.20	3.99	3.46
Jul-92	59	4.44	4.28	4.34	4.24	3.99	3.40
Apr-94	80	4.13	3.96	4.16	4.04	3.80	3.26
Feb-95	90	4.16	4.00	4.17	4.08	3.89	3.30

Table A-68. Serviceability Index, San Antonio, IH 10, Section 4

Date	Time (Months)	Outside Lane Right	Outside Lane Left	Center Lane Right	Center Lane Left	Inside Lane Right	Inside Lane Left
Aug-87	0	4.51	4.40	4.72	4.54	4.08	3.36
Jun-88	10	4.64	4.30	4.60	4.37	4.08	3.61
Oct-89	26	4.51	4.50	4.69	4.85	4.40	3.81
Mar-90	31	4.29	4.24	4.65	4.79	4.29	3.55
Nov-90	39	4.51	4.52	4.69	4.71	4.12	3.56
Mar-91	43	4.58	4.53	4.65	4.63	4.15	3.59
Aug-91	48	4.43	4.51	4.71	4.80	4.27	3.59
Jan-92	53	4.40	4.47	4.63	4.72	4.18	3.55
Jul-92	59	4.49	4.48	4.60	4.59	4.06	3.43
Apr-94	80	4.57	4.43	4.45	4.65	4.14	3.55
Feb-95	90	4.46	4.50	4.56	4.77	4.25	3.37

Table A-69. Serviceability Index, San Antonio, IH 10, Section 5

Date	Time (Months)	Outside Lane Right	Outside Lane Left	Center Lane Right	Center Lane Left	Inside Lane Right	Inside Lane Left
Aug-87	0	4.30	4.04	4.45	4.22	3.99	3.26
Jun-88	10	4.23	3.97	4.19	3.87	3.58	3.01
Oct-89	26	4.18	4.20	4.38	4.36	3.76	3.10
Mar-90	31	3.98	4.01	4.10	4.10	3.76	3.15
Nov-90	39	4.02	3.99	4.16	4.08	3.65	3.03
Mar-91	43	3.99	3.95	4.08	4.07	3.56	2.89
Aug-91	48	3.99	3.99	4.13	4.10	3.61	3.01
Jan-92	53	3.84	3.81	3.81	3.89	3.61	3.11
Jul-92	59	3.91	3.81	3.85	3.87	3.51	2.93
Apr-94	80	3.78	3.66	3.56	3.65	3.47	2.94
Feb-95	90	3.73	3.68	3.68	3.71	3.56	3.06

Table A-70. Serviceability Index, San Antonio, IH 10, Section 6

Date	Time (Months)	Inside Lane Left	Inside Lane Right	Center Lane Left	Center Lane Right	Outside Lane Left	Outside Lane Right
Aug-87	0	4.18	4.37	4.38	4.57	4.25	4.27
Jun-88	10	4.20	4.27	4.05	4.31	4.00	4.08
Oct-89	26	3.95	4.03	4.07	4.15	3.72	3.70
Mar-90	31	4.35	4.46	4.33	3.51	3.99	4.14
Nov-90	39	4.16	4.31	4.26	3.51	3.77	3.98
Mar-91	43	3.78	3.65	3.82	3.04	3.61	3.68
Aug-91	48	4.26	4.37	4.28	3.55	3.61	3.98
Jan-92	53	3.56	3.37	3.60	3.45	3.19	3.25
Jul-92	59	3.53	3.45	3.61	3.49	2.77	3.32
Apr-94	80	3.60	3.43	3.45	3.34	3.08	2.93
Feb-95	90	3.68	3.52	3.80	3.68	3.41	3.24

Table A-71. Serviceability Index, San Antonio, IH 10, Section 7

Date	Time (Months)	Inside Lane Left	Inside Lane Right	Center Lane Left	Center Lane Right	Outside Lane Left	Outside Lane Right
Aug-87	0	4.49	4.77	4.38	4.64	4.11	4.50
Jun-88	10	4.37	4.65	4.21	4.47	3.69	4.13
Oct-89	26	4.55	4.69	4.68	4.68	4.26	4.46
Mar-90	31	3.80	3.76	3.53	3.59	3.43	3.52
Nov-90	39	3.70	3.67	3.43	3.46	3.37	3.49
Mar-91	43	3.68	3.68	3.49	3.57	3.40	3.48
Aug-91	48	3.56	3.54	3.29	3.34	3.35	3.43
Jan-92	53	3.91	4.12	3.93	3.98	3.78	3.80
Jul-92	59	3.86	4.06	3.88	3.99	3.72	3.75
Apr-94	80	3.60	3.81	3.61	3.67	3.48	3.48
Feb-95	90	3.61	3.82	3.69	3.67	3.61	3.51

Table A-72. Serviceability Index, San Antonio, IH 10, Section 8

Date	Time (Months)	Inside Lane Left	Inside Lane Right	Center Lane Left	Center Lane Right	Outside Lane Left	Outside Lane Right
Aug-87	0	4.49	4.73	4.48	4.60	4.36	4.46
Jun-88	10	4.16	4.57	4.54	4.78	4.29	4.59
Oct-89	26	4.51	4.47	4.77	4.82	4.53	4.60
Mar-90	31	4.52	4.68	4.80	4.84	4.78	4.79
Nov-90	39	4.47	4.61	4.67	4.88	4.82	4.82
Mar-91	43	4.44	4.66	4.81	4.89	4.78	4.88
Aug-91	48	4.41	4.64	4.68	4.84	4.75	4.79
Jan-92	53	4.25	4.55	4.73	4.81	4.78	4.74
Jul-92	59	4.30	4.57	4.72	4.86	4.75	4.72
Apr-94	80	4.43	4.72	4.71	4.85	4.76	4.79
Feb-95	90	4.62	4.67	4.73	4.92	4.78	4.82

Table A-73. Serviceability Index, San Antonio, IH 10, Section 9

Date	Time (Months)	Inside Lane Left	Inside Lane Right	Center Lane Left	Center Lane Right	Outside Lane Left	Outside Lane Right
Aug-87	0	4.36	4.55	4.11	4.36	4.30	4.52
Jun-88	10	4.24	4.47	4.02	4.36	4.08	4.37
Oct-89	26	4.45	4.53	4.20	4.34	4.22	4.23
Mar-90	31	4.33	4.39	4.23	4.35	4.23	4.27
Nov-90	39	4.24	4.38	4.19	4.32	4.24	4.29
Mar-91	43	4.21	4.28	4.10	4.03	4.17	4.22
Aug-91	48	4.21	4.34	4.13	4.17	4.23	4.28
Jan-92	53	4.09	4.23	4.08	4.10	4.15	4.20
Jul-92	59	4.05	4.18	3.96	3.89	4.14	4.15
Apr-94	80	3.85	3.93	3.73	3.76	3.89	3.92
Feb-95	90	3.97	3.82	3.88	3.97	3.99	3.43

Table A-74. Serviceability Index, San Antonio, IH 10, Section 10

Date	Time (Months)	Inside Lane Left	Inside Lane Right	Center Lane Left	Center Lane Right	Outside Lane Left	Outside Lane Right
Aug-87	0	4.16	4.18	4.30	4.33	4.10	4.23
Jun-88	10	4.13	4.38	4.27	4.49	4.06	4.31
Oct-89	26	4.14	4.22	4.63	4.53	4.28	4.22
Mar-90	31	4.17	4.24	4.42	4.32	4.00	4.02
Nov-90	39	4.04	4.14	4.26	3.76	3.94	4.04
Mar-91	43	3.97	4.00	4.09	4.01	4.01	4.07
Aug-91	48	4.06	4.17	4.23	4.06	4.13	4.16
Jan-92	53	4.01	4.12	4.17	3.68	3.99	4.00
Jul-92	59	3.84	3.96	3.97	4.04	3.94	4.01
Apr-94	80	3.41	3.55	3.65	3.56	3.73	3.80
Feb-95	90	3.70	3.76	3.92	3.69	3.79	3.83

Table A-75. International Roughness Index (m/km), San Antonio, IH 10, Section 1

Date	Time (Months)	Outside Lane Right	Outside Lane Left	Center Lane Right	Center Lane Left	Inside Lane Right	Inside Lane Left
Aug-87	0	1.05	1.45	1.00	1.20	1.11	0.97
Jun-88	10	1.48	1.85	1.54	1.70	1.51	1.41
Oct-89	26	1.36	1.72	1.21	1.42	1.62	1.39
Mar-90	31	1.40	1.84	1.21	1.48	1.62	1.28
Nov-90	39	1.20	1.80	1.52	1.62	1.99	1.83
Mar-91	43	1.18	1.66	0.95	1.19	1.42	1.04
Aug-91	48	1.21	2.30	1.65	1.73	1.68	1.23
Jan-92	53	1.47	2.14	1.50	1.58	1.74	1.54
Jul-92	59	1.07	1.37	1.19	1.44	0.91	0.89
Apr-94	80	1.32	2.39	1.55	1.74	1.81	1.50
Feb-95	90	2.02	2.73	2.04	1.85	1.79	1.62

Table A-76. International Roughness Index (m/km), San Antonio, IH 10, Section 2

Date	Time	Outside Lane		Center Lane		Inside Lane	
	(Months)	Right	Left	Right	Left	Right	Left
Aug-87	0	1.00	1.28	0.93	1.15	1.09	1.54
Jun-88	10	1.12	1.40	1.06	1.35	1.31	1.65
Oct-89	26	1.09	1.35	1.08	1.16	1.16	1.59
Mar-90	31	1.09	1.34	1.17	1.22	1.20	1.63
Nov-90	39	1.11	1.34	1.14	1.25	1.27	1.69
Mar-91	43	1.16	1.44	1.20	1.33	1.31	1.76
Aug-91	48	1.14	1.38	1.17	1.31	1.25	1.71
Jan-92	53	1.18	1.43	1.24	1.38	1.31	1.74
Jul-92	59	1.28	1.54	1.25	1.43	1.41	1.88
Apr-94	80	1.31	1.60	1.39	1.55	1.45	1.86
Feb-95	90	1.30	1.56	1.34	1.51	1.47	1.84

Table A-77. International Roughness Index (m/km), San Antonio, IH 10, Section 3

Date	Time	Outside Lane		Center Lane		Inside Lane	
	(Months)	Right	Left	Right	Left	Right	Left
Aug-87	0	1.09	1.35	0.97	1.20	1.19	1.69
Jun-88	10	1.06	1.35	1.02	1.20	1.31	1.69
Oct-89	26	1.05	1.23	0.94	1.02	1.19	1.62
Mar-90	31	1.07	1.28	1.05	1.15	1.27	1.71
Nov-90	39	1.05	1.26	1.04	1.15	1.29	1.78
Mar-91	43	1.10	1.28	1.06	1.17	1.34	1.82
Aug-91	48	1.06	1.30	1.06	1.17	1.30	1.78
Jan-92	53	1.10	1.33	1.14	1.26	1.32	1.80
Jul-92	59	1.01	1.20	1.08	1.22	1.34	1.89
Apr-94	80	1.21	1.43	1.17	1.33	1.47	1.99
Feb-95	90	1.17	1.36	1.15	1.24	1.35	1.93

Table A-78. International Roughness Index (m/km), San Antonio, IH 10, Section 4

Date	Time	Outside Lane		Center Lane		Inside Lane	
	(Months)	Right	Left	Right	Left	Right	Left
Aug-87	0	1.00	1.21	0.86	1.01	1.36	2.04
Jun-88	10	0.94	1.19	0.97	1.16	1.34	1.74
Oct-89	26	1.07	1.13	0.94	0.82	1.10	1.63
Mar-90	31	1.22	1.27	0.97	0.87	1.18	1.81
Nov-90	39	1.09	1.14	0.88	1.00	1.32	1.81
Mar-91	43	1.05	1.10	0.96	1.01	1.28	1.74
Aug-91	48	1.15	1.11	0.90	0.88	1.22	1.80
Jan-92	53	1.20	1.19	0.93	0.96	1.31	1.82
Jul-92	59	1.04	1.26	0.98	1.06	1.34	1.91
Apr-94	80	1.09	1.19	1.08	1.04	1.32	1.76
Feb-95	90	1.13	1.17	1.01	0.91	1.29	1.95

Table A-79. International Roughness Index (m/km), San Antonio, IH 10, Section 5

Date	Time	Outside Lane		Center Lane		Inside Lane	
	(Months)	Right	Left	Right	Left	Right	Left
Aug-87	0	1.11	1.37	1.03	1.26	1.47	2.24
Jun-88	10	1.18	1.41	1.17	1.46	1.69	2.21
Oct-89	26	1.20	1.30	1.16	1.22	1.64	2.25
Mar-90	31	1.31	1.38	1.34	1.39	1.60	2.18
Nov-90	39	1.28	1.44	1.29	1.43	1.69	2.30
Mar-91	43	1.30	1.47	1.34	1.43	1.80	2.54
Aug-91	48	1.32	1.45	1.33	1.44	1.72	2.33
Jan-92	53	1.34	1.51	1.46	1.47	1.59	2.04
Jul-92	59	1.28	1.47	1.42	1.48	1.72	2.30
Apr-94	80	1.44	1.61	1.61	1.66	1.69	2.17
Feb-95	90	1.46	1.58	1.58	1.63	1.69	2.07

Table A-80. International Roughness Index (m/km), San Antonio, IH 10, Section 6

Date	Time (Months)	Inside Lane Left	Inside Lane Right	Center Lane Left	Center Lane Right	Outside Lane Left	Outside Lane Right
Aug-87	0	1.29	1.20	1.15	0.99	1.16	1.18
Jun-88	10	1.21	1.08	1.16	1.00	1.22	1.13
Oct-89	26	1.52	1.44	1.38	1.26	1.58	1.56
Mar-90	31	1.19	1.13	1.13	1.47	1.27	1.18
Nov-90	39	1.29	1.14	1.20	1.54	1.46	1.35
Mar-91	43	1.42	1.48	1.49	1.90	1.62	1.60
Aug-91	48	1.26	1.13	1.18	1.52	1.52	1.35
Jan-92	53	1.40	1.41	1.44	1.57	1.72	1.64
Jul-92	59	1.46	1.35	1.46	1.58	1.94	1.57
Apr-94	80	1.38	1.40	1.57	1.65	1.82	1.93
Feb-95	90	1.28	1.35	1.27	1.38	1.56	1.68

Table A-81. International Roughness Index (m/km), San Antonio, IH 10, Section 7

Date	Time (Months)	Inside Lane Left	Inside Lane Right	Center Lane Left	Center Lane Right	Outside Lane Left	Outside Lane Right
Aug-87	0	1.10	0.84	1.06	0.91	1.26	1.02
Jun-88	10	1.14	0.91	1.13	0.99	1.47	1.16
Oct-89	26	1.04	0.93	0.89	0.86	1.14	0.98
Mar-90	31	1.43	1.38	1.56	1.51	1.70	1.63
Nov-90	39	1.49	1.40	1.60	1.57	1.74	1.65
Mar-91	43	1.55	1.48	1.60	1.57	1.74	1.66
Aug-91	48	1.62	1.53	1.74	1.70	1.76	1.73
Jan-92	53	1.37	1.22	1.29	1.25	1.42	1.40
Jul-92	59	1.44	1.26	1.31	1.23	1.47	1.47
Apr-94	80	1.63	1.42	1.50	1.48	1.66	1.69
Feb-95	90	1.59	1.43	1.48	1.48	1.61	1.65

Table A-82. International Roughness Index (m/km), San Antonio, IH 10, Section 8

Date	Time	Inside Lane		Center Lane		Outside Lane	
	(Months)	Left	Right	Left	Right	Left	Right
Aug-87	0	1.11	0.94	0.95	0.87	1.08	1.02
Jun-88	10	1.36	0.93	0.93	0.77	1.13	0.93
Oct-89	26	1.07	1.07	0.86	0.76	0.99	0.89
Mar-90	31	1.11	0.94	0.79	0.75	0.83	0.85
Nov-90	39	1.15	0.97	0.94	0.69	0.80	0.72
Mar-91	43	1.17	0.97	0.82	0.72	0.89	0.76
Aug-91	48	1.19	0.97	0.95	0.75	0.81	0.79
Jan-92	53	1.38	1.05	0.83	0.74	0.77	0.81
Jul-92	59	1.27	1.05	0.85	0.70	0.87	0.83
Apr-94	80	1.21	0.89	0.95	0.79	0.84	0.78
Feb-95	90	1.02	0.88	0.88	0.65	0.77	0.76

Table A-83. International Roughness Index (m/km), San Antonio, IH 10, Section 9

Date	Time	Inside Lane		Center Lane		Outside Lane	
	(Months)	Left	Right	Left	Right	Left	Right
Aug-87	0	1.17	1.00	1.28	1.08	1.11	0.96
Jun-88	10	1.18	0.93	1.24	0.99	1.16	0.98
Oct-89	26	1.10	1.00	1.23	1.08	1.21	1.19
Mar-90	31	1.16	1.06	1.18	1.04	1.16	1.10
Nov-90	39	1.22	1.05	1.20	1.06	1.16	1.10
Mar-91	43	1.26	1.14	1.26	1.26	1.21	1.14
Aug-91	48	1.25	1.06	1.24	1.13	1.16	1.08
Jan-92	53	1.32	1.15	1.27	1.20	1.24	1.14
Jul-92	59	1.34	1.16	1.31	1.27	1.21	1.16
Apr-94	80	1.44	1.33	1.50	1.44	1.39	1.35
Feb-95	90	1.34	1.36	1.37	1.29	1.28	1.44

Table A-84. International Roughness Index (m/km), San Antonio, IH 10, Section 10

Date	Time (Months)	Inside Lane Left	Inside Lane Right	Center Lane Left	Center Lane Right	Outside Lane Left	Outside Lane Right
Aug-87	0	1.29	1.13	1.08	0.97	1.23	1.15
Jun-88	10	1.22	1.06	1.12	0.96	1.24	1.06
Oct-89	26	1.24	1.17	0.88	0.91	1.08	1.12
Mar-90	31	1.23	1.15	1.03	1.06	1.24	1.20
Nov-90	39	1.28	1.19	1.11	1.12	1.24	1.17
Mar-91	43	1.31	1.27	1.15	1.15	1.25	1.20
Aug-91	48	1.30	1.19	1.14	1.11	1.24	1.17
Jan-92	53	1.37	1.24	1.20	1.32	1.30	1.23
Jul-92	59	1.43	1.30	1.29	1.24	1.35	1.25
Apr-94	80	1.71	1.61	1.45	1.61	1.47	1.38
Feb-95	90	1.52	1.46	1.33	1.52	1.42	1.38

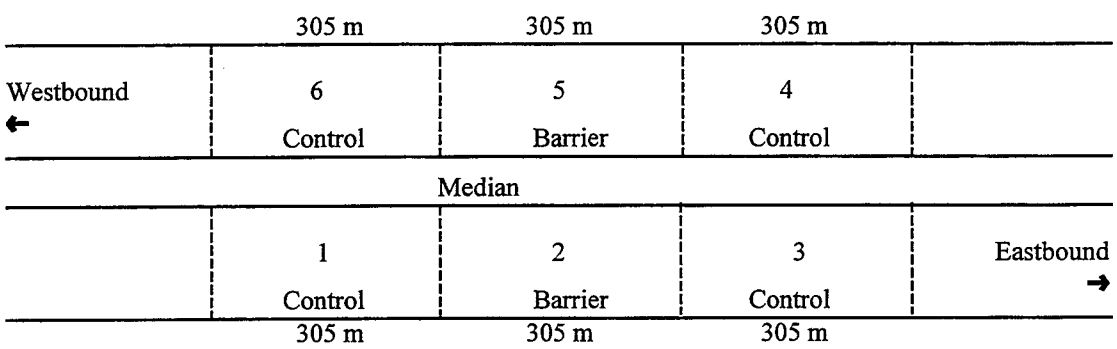

Figure A.7. Site Plan - Sierra Blanca, IH 10

Table A-85. Serviceability Index, Sierra Blanca, IH 10, Section 1

Date	Time (Months)	Outside Lane Right	Outside Lane Left	Inside Lane Right	Inside Lane Left
Oct-87	22	4.72	4.63	4.40	4.36
Jul-88	31	4.52	4.37	4.35	4.16
Dec-89	48	4.38	4.24	4.14	3.99
Apr-90	52	4.36	4.30	4.30	4.21
Nov-90	59	4.17	4.10	4.24	4.05
Mar-91	63	4.02	3.96	4.15	4.06
Aug-91	68	3.99	3.91	4.19	4.05
Jan-92	73	3.74	3.66	4.12	4.08
Jul-92	79	3.68	3.73	4.01	3.96

Table A-86. Serviceability Index, Sierra Blanca, IH 10, Section 2

Date	Time (Months)	Outside Lane Right	Outside Lane Left	Inside Lane Right	Inside Lane Left
Oct-87	22	4.82	4.57	4.35	4.19
Jul-88	31	4.74	4.44	3.99	3.81
Dec-89	48	4.44	4.20	3.64	3.62
Apr-90	52	4.44	4.14	3.92	3.83
Nov-90	59	4.30	3.97	3.52	3.44
Mar-91	63	4.21	3.84	3.41	3.31
Aug-91	68	4.07	3.68	3.29	3.26
Jan-92	73	4.00	3.74	3.15	3.11
Jul-92	79	3.83	3.50	3.04	2.93

Table A-87. Serviceability Index, Sierra Blanca, IH 10, Section 3

Date	Time (Months)	Outside Lane Right	Outside Lane Left	Inside Lane Right	Inside Lane Left
Oct-87	22	4.84	4.63	4.64	4.50
Jul-88	31	4.83	4.60	4.50	4.34
Dec-89	48	4.70	4.48	4.27	4.14
Apr-90	52	4.81	4.63	4.32	4.23
Nov-90	59	4.62	4.40	4.10	3.95
Mar-91	63	4.55	4.33	3.90	3.78
Aug-91	68	4.45	4.28	3.88	3.72
Jan-92	73	4.32	4.10	3.62	3.46
Jul-92	79	4.13	3.80	3.39	3.26

Table A-88. Serviceability Index, Sierra Blanca, IH 10, Section 4

Date	Time (Months)	Inside Lane Left	Inside Lane Right	Outside Lane Left	Outside Lane Right
Oct-87	22	4.74	4.82	4.30	4.66
Jul-88	31	4.49	4.69	4.17	4.66
Dec-89	48	4.67	4.73	4.20	4.56
Apr-90	52	4.58	4.71	4.15	4.58
Nov-90	59	4.63	4.66	4.21	4.60
Mar-91	63	4.59	4.72	4.20	4.59
Aug-91	68	4.58	4.71	4.18	4.59
Jan-92	73	4.61	4.64	4.23	4.42
Jul-92	79	4.51	4.71	4.15	4.46

Table A-89. Serviceability Index, Sierra Blanca, IH 10, Section 5

Date	Time (Months)	Inside Lane Left	Inside Lane Right	Outside Lane Left	Outside Lane Right
Oct-87	22	4.39	4.50	4.12	4.46
Jul-88	31	4.20	4.36	4.23	4.59
Dec-89	48	4.22	4.17	4.08	4.40
Apr-90	52	4.22	4.23	4.10	4.42
Nov-90	59	4.01	3.94	3.85	4.31
Mar-91	63	4.03	3.96	3.86	4.24
Aug-91	68	4.06	3.93	3.78	4.19
Jan-92	73	4.00	3.85	3.77	4.22
Jul-92	79	3.90	3.84	3.58	4.16

Table A-90. Serviceability Index, Sierra Blanca, IH 10, Section 6

Date	Time (Months)	Inside Lane Left	Inside Lane Right	Outside Lane Left	Outside Lane Right
Oct-87	22	4.43	4.55	4.49	4.70
Jul-88	31	4.36	4.64	4.52	4.77
Dec-89	48	4.34	4.43	4.42	4.65
Apr-90	52	4.46	4.59	4.49	4.70
Nov-90	59	4.34	4.35	4.35	4.52
Mar-91	63	4.26	4.36	4.26	4.54
Aug-91	68	4.23	4.34	4.29	4.51
Jan-92	73	4.23	4.28	4.19	4.52
Jul-92	79	4.18	4.29	4.19	4.47

Table A-91. International Roughness Index (m/km), Sierra Blanca, IH 10, Section 1

Date	Time (Months)	Outside Lane Right	Outside Lane Left	Inside Lane Right	Inside Lane Left
Oct-87	22	0.84	0.83	0.99	1.03
Jul-88	31	0.95	1.03	1.05	1.22
Dec-89	48	1.11	1.23	1.23	1.38
Apr-90	52	1.14	1.17	1.12	1.18
Nov-90	59	1.25	1.23	1.13	1.26
Mar-91	63	1.36	1.34	1.21	1.30
Aug-91	68	1.37	1.34	1.16	1.26
Jan-92	73	1.49	1.47	1.19	1.22
Jul-92	79	1.54	1.46	1.30	1.37

Table A-92. International Roughness Index (m/km), Sierra Blanca, IH 10, Section 2

Date	Time (Months)	Outside Lane Right	Outside Lane Left	Inside Lane Right	Inside Lane Left
Oct-87	22	0.78	0.99	1.26	1.38
Jul-88	31	0.87	1.10	1.51	1.64
Dec-89	48	1.14	1.31	1.79	1.79
Apr-90	52	1.17	1.35	1.57	1.63
Nov-90	59	1.25	1.48	1.87	1.95
Mar-91	63	1.28	1.54	1.98	2.07
Aug-91	68	1.42	1.71	2.07	2.10
Jan-92	73	1.46	1.65	2.18	2.26
Jul-92	79	1.63	1.88	2.29	2.38

Table A-93. International Roughness Index (m/km), Sierra Blanca, IH 10, Section 3

Date	Time (Months)	Outside Lane Right	Outside Lane Left	Inside Lane Right	Inside Lane Left
Oct-87	22	0.71	0.89	0.93	1.01
Jul-88	31	0.73	0.96	1.04	1.15
Dec-89	48	0.86	0.97	1.24	1.29
Apr-90	52	0.79	0.88	1.20	1.21
Nov-90	59	0.93	1.06	1.36	1.41
Mar-91	63	0.98	1.12	1.48	1.56
Aug-91	68	1.07	1.15	1.52	1.59
Jan-92	73	1.15	1.27	1.82	1.92
Jul-92	79	1.30	1.50	1.94	2.01

Table A-94. International Roughness Index (m/km), Sierra Blanca, IH 10, Section 4

Date	Time (Months)	Inside Lane Left	Inside Lane Right	Outside Lane Left	Outside Lane Right
Oct-87	22	0.86	0.80	1.30	0.98
Jul-88	31	1.05	0.86	1.34	0.97
Dec-89	48	0.92	0.86	1.32	1.09
Apr-90	52	0.98	0.87	1.36	1.06
Nov-90	59	0.97	0.93	1.30	1.05
Mar-91	63	1.00	0.88	1.34	1.05
Aug-91	68	0.99	0.88	1.35	1.08
Jan-92	73	0.96	0.95	1.29	1.20
Jul-92	79	1.07	0.90	1.38	1.15

Table A-95. International Roughness Index (m/km), Sierra Blanca, IH 10, Section 5

Date	Time (Months)	Inside Lane Left	Inside Lane Right	Outside Lane Left	Outside Lane Right
Oct-87	22	1.17	1.00	1.31	1.01
Jul-88	31	1.25	1.10	1.27	0.95
Dec-89	48	1.25	1.23	1.34	1.11
Apr-90	52	1.25	1.17	1.34	1.09
Nov-90	59	1.35	1.35	1.45	1.13
Mar-91	63	1.36	1.30	1.45	1.19
Aug-91	68	1.32	1.31	1.50	1.22
Jan-92	73	1.37	1.38	1.50	1.20
Jul-92	79	1.44	1.36	1.61	1.23

Table A-96. International Roughness Index (m/km), Sierra Blanca, IH 10, Section 6

Date	Time (Months)	Inside Lane Left	Inside Lane Right	Outside Lane Left	Outside Lane Right
Oct-87	22	1.15	0.97	1.04	0.88
Jul-88	31	1.22	0.92	0.99	0.81
Dec-89	48	1.19	1.07	1.08	0.90
Apr-90	52	1.12	0.96	1.04	0.87
Nov-90	59	1.15	1.14	1.10	0.95
Mar-91	63	1.24	1.10	1.16	0.96
Aug-91	68	1.24	1.12	1.15	0.97
Jan-92	73	1.23	1.17	1.22	0.97
Jul-92	79	1.27	1.17	1.23	0.99

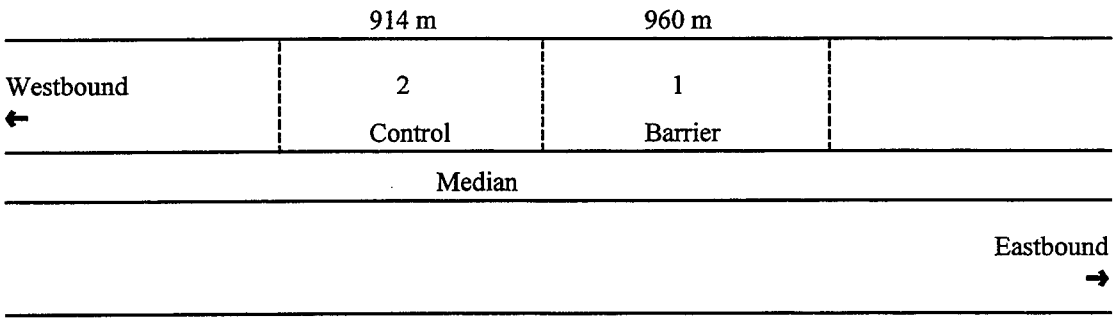

Figure A.8. Site Plan - Seguin, IH 10

Table A-97. Serviceability Index, Seguin, IH 10, Section 1

Date	Time (Months)	Outside Lane Right	Outside Lane Left	Inside Lane Right	Inside Lane Left
Sep-89	10	4.76	4.74	4.68	4.68
May-90	18	4.71	4.79	4.68	4.64
Dec-90	25	4.59	4.64	4.61	4.51
Mar-91	28	4.53	4.62	4.56	4.47
Jul-91	32	4.77	4.71	4.69	4.69
Jan-92	38	4.59	4.53	4.49	4.47
Jul-92	44	4.63	4.52	4.37	4.34
Apr-94	65	4.37	4.38	4.11	4.04
Feb-95	75	4.63	4.43	4.20	4.17

Table A-98. Serviceability Index, Seguin, IH 10, Section 2

Date	Time (Months)	Outside Lane Right	Outside Lane Left	Inside Lane Right	Inside Lane Left
Jul-91	32	4.74	4.69	4.60	4.49
Jan-92	38	4.46	4.56	4.49	4.38
Jul-92	44	4.52	4.61	4.67	4.55
Apr-94	65	4.53	4.39	4.44	4.28
Feb-95	75	4.63	4.48	4.54	4.42

Table A-99. International Roughness Index (m/km), Seguin, IH 10, Section 1

Date	Time (Months)	Outside Lane Right	Outside Lane Left	Inside Lane Right	Inside Lane Left
Sep-89	10	0.76	0.79	0.83	0.81
May-90	18	0.82	0.76	0.84	0.85
Dec-90	25	0.85	0.84	0.82	0.92
Mar-91	28	0.89	0.85	0.87	0.95
Jul-91	32	0.71	0.81	0.81	0.83
Jan-92	38	0.85	0.93	0.92	0.96
Jul-92	44	0.78	0.91	0.97	1.02
Apr-94	65	1.06	1.09	1.09	1.18
Feb-95	75	0.82	1.07	1.01	1.09

Table A-100. International Roughness Index (m/km), Seguin, IH 10, Section 2

Date	Time (Months)	Outside Lane Right	Outside Lane Left	Inside Lane Right	Inside Lane Left
Jul-91	32	0.77	0.79	0.84	0.90
Jan-92	38	0.92	0.85	0.89	0.98
Jul-92	44	0.86	0.85	0.76	0.86
Apr-94	65	0.88	0.94	0.91	1.01
Feb-95	75	0.74	0.87	0.81	0.90

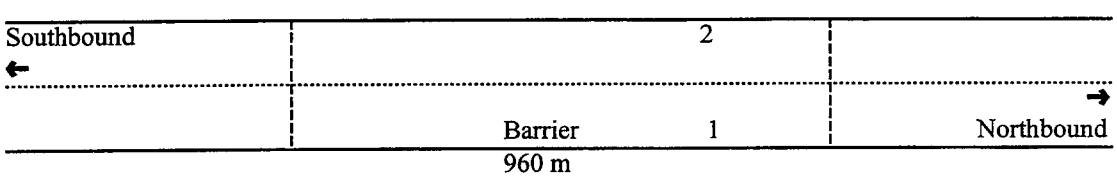

Figure A.9. Site Plan - Converse, FM 1516

Table A-101. Serviceability Index, Converse, FM 1516

Date	Time (Months)	Northbound Right	Northbound Left	Southbound Left	Southbound Right
May-90	6	4.23	4.67	4.92	4.65
Dec-90	13	4.07	4.54	4.76	4.47
Apr-91	17	4.00	4.53	4.72	4.41
Jul-91	20	4.00	4.53	4.74	4.42
Jan-92	26	3.99	4.47	4.78	4.37
Jun-92	31	3.57	4.31	4.61	3.98
Apr-94	53	3.02	3.83	4.13	3.37
Feb-95	63	2.78	3.59	3.55	2.97

Table A-102. International Roughness Index (m/km), Converse, FM 1516

Date	Time (Months)	Northbound Right	Northbound Left	Southbound Left	Southbound Right
May-90	6	1.32	0.91	0.67	0.91
Dec-90	13	1.38	0.97	0.77	1.06
Apr-91	17	1.46	0.98	0.81	1.11
Jul-91	20	1.44	0.97	0.79	1.08
Jan-92	26	1.44	0.98	0.74	1.10
Jun-92	31	1.79	1.13	0.90	1.42
Apr-94	53	2.28	1.45	1.24	1.91
Feb-95	63	2.52	1.71	1.67	2.30

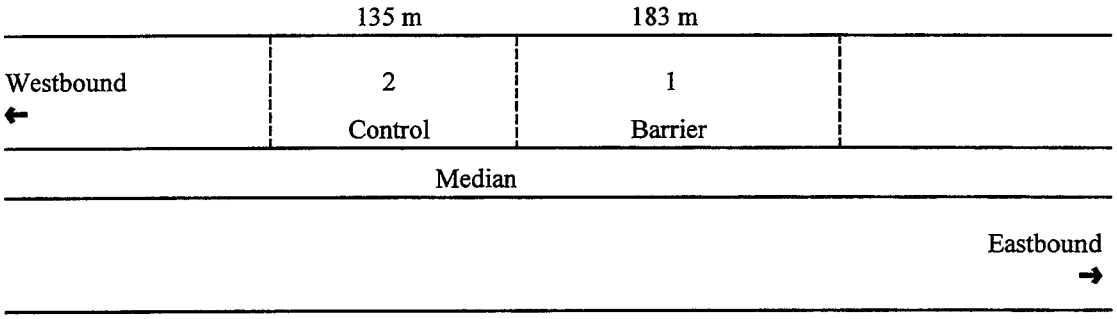

Figure A.10. Site Plan - Dallas, IH 635

Table A-103. Serviceability Index, Dallas, IH 635, Section 1

Date	Time (Months)	Outside Lane Right	Outside Lane Left	Center Lane Right	Center Lane Left	Inside Lane Right	Inside Lane Left
Nov-90	2	3.43	3.68	3.86	3.95	4.11	4.05
Mar-91	6	3.35	3.56	3.70	3.79	4.02	3.98
Jul-91	10	3.52	3.76	3.92	3.97	4.14	4.11
Jan-92	16	3.34	3.53	3.66	3.71	3.94	3.95
Jul-92	22	3.24	3.46	3.53	3.52	3.66	3.65
Apr-94	43	2.97	3.13	3.14	3.07	3.44	3.30
Oct-94	49	3.00	3.24	3.27	3.35	3.23	3.36
Apr-95	55	2.72	3.49	3.52	3.65	3.66	3.72

Table A-104. Serviceability Index, Dallas, IH 635, Section 2

Date	Time (Months)	Outside Lane Right	Outside Lane Left	Center Lane Right	Center Lane Left	Inside Lane Right	Inside Lane Left
Nov-90	2	4.07	4.09	3.18	3.43	4.54	4.58
Mar-91	6	3.71	3.96	3.11	3.37	4.56	4.54
Jul-91	10	3.62	3.71	2.91	2.88	4.22	4.41
Jan-92	16	3.88	3.99	3.19	3.40	4.53	4.51
Jul-92	22	3.56	3.68	3.05	3.10	4.46	4.52
Apr-94	43	3.03	2.96	2.93	2.79	4.14	3.59
Oct-94	49	2.58	2.47	2.28	2.39	3.67	3.88
Apr-95	55	1.98	2.66	2.01	2.77	3.97	4.13

Table A-105. International Roughness Index (m/km), Dallas, IH 635, Section 1

Date	Time (Months)	Outside Lane Right	Outside Lane Left	Center Lane Right	Center Lane Left	Inside Lane Right	Inside Lane Left
Nov-90	2	1.70	1.49	1.27	1.31	1.21	1.26
Mar-91	6	1.79	1.59	1.38	1.44	1.23	1.31
Jul-91	10	1.67	1.47	1.28	1.36	1.18	1.21
Jan-92	16	1.83	1.65	1.47	1.52	1.32	1.37
Jul-92	22	1.96	1.73	1.61	1.69	1.47	1.52
Apr-94	43	2.33	2.09	1.79	1.93	1.61	1.73
Oct-94	49	2.21	1.87	1.87	1.77	1.77	1.65
Apr-95	55	2.49	1.75	1.65	1.56	1.50	1.47

Table A-106. International Roughness Index (m/km), Dallas, IH 635, Section 2

Date	Time (Months)	Outside Lane Right	Outside Lane Left	Center Lane Right	Center Lane Left	Inside Lane Right	Inside Lane Left
Nov-90	2	1.37	1.36	1.41	1.44	1.01	0.99
Mar-91	6	1.52	1.33	1.52	1.43	0.98	1.01
Jul-91	10	1.78	1.78	1.94	1.88	1.17	1.06
Jan-92	16	1.53	1.55	1.60	1.54	1.00	1.03
Jul-92	22	1.70	1.62	1.80	1.72	1.06	1.07
Apr-94	43	2.24	2.24	2.41	2.49	1.38	1.64
Oct-94	49	2.46	2.62	2.73	2.71	1.81	1.61
Apr-95	55	3.04	2.49	3.07	2.30	1.44	1.24

APPENDIX B

REGRESSION COEFFICIENTS FOR VERTICAL MOVEMENT

Table B-1. Coefficient ξ_1 for Pavement Width of 9.0 m

Thornthwaite Moisture Index	Suction Compression Index	Barrier Depth 0	90 cm	150 cm	240 cm
-46.5	0.04	0.697	0.667	0.644	0.538
-21.3	0.04	0.624	0.566	0.531	0.478
-11.3	0.04	0.478	0.438	0.406	0.368
14.8	0.04	0.398	0.376	0.372	0.338
26.8	0.04	0.371	0.353	0.342	0.327
-46.5	0.06	0.786	0.746	0.734	0.607
-21.3	0.06	0.660	0.597	0.561	0.486
-11.3	0.06	0.471	0.421	0.388	0.342
14.8	0.06	0.410	0.381	0.374	0.339
26.8	0.06	0.393	0.377	0.354	0.343
-46.5	0.08	0.848	0.806	0.787	0.654
-21.3	0.08	0.692	0.621	0.580	0.497
-11.3	0.08	0.486	0.422	0.386	0.327
14.8	0.08	0.440	0.413	0.404	0.353
26.8	0.08	0.439	0.419	0.403	0.387
-46.5	0.10	0.902	0.857	0.844	0.701
-21.3	0.10	0.723	0.632	0.589	0.485
-11.3	0.10	0.500	0.430	0.387	0.308
14.8	0.10	0.510	0.470	0.452	0.410
26.8	0.10	0.516	0.503	0.481	0.452

Table B-2. Coefficient ξ_1 for Pavement Width of 12.6 m

Thornthwaite Moisture Index	Suction Compression Index	Barrier Depth 0	90 cm	150 cm	240 cm
-46.5	0.04	0.614	0.568	0.545	0.462
-21.3	0.04	0.545	0.501	0.469	0.427
-11.3	0.04	0.425	0.397	0.364	0.338
14.8	0.04	0.372	0.353	0.344	0.314
26.8	0.04	0.351	0.336	0.327	0.318
-46.5	0.06	0.688	0.636	0.613	0.514
-21.3	0.06	0.569	0.512	0.486	0.428
-11.3	0.06	0.407	0.360	0.340	0.304
14.8	0.06	0.374	0.351	0.334	0.310
26.8	0.06	0.374	0.354	0.339	0.322
-46.5	0.08	0.744	0.682	0.668	0.559
-21.3	0.08	0.589	0.520	0.492	0.429
-11.3	0.08	0.403	0.354	0.320	0.281
14.8	0.08	0.404	0.376	0.355	0.324
26.8	0.08	0.419	0.392	0.382	0.349
-46.5	0.10	0.795	0.734	0.713	0.602
-21.3	0.10	0.591	0.516	0.483	0.407
-11.3	0.10	0.409	0.349	0.314	0.264
14.8	0.10	0.462	0.420	0.395	0.359
26.8	0.10	0.494	0.459	0.438	0.395

Table B-3. Coefficient ξ_1 for Pavement Width of 16.2 m

Thornthwaite Moisture Index	Suction Compression Index	Barrier Depth 0	90 cm	150 cm	240 cm
-46.5	0.04	0.523	0.477	0.470	0.402
-21.3	0.04	0.487	0.448	0.425	0.393
-11.3	0.04	0.381	0.361	0.330	0.314
14.8	0.04	0.348	0.331	0.318	0.295
26.8	0.04	0.329	0.316	0.318	0.304
-46.5	0.06	0.590	0.543	0.526	0.451
-21.3	0.06	0.491	0.447	0.431	0.385
-11.3	0.06	0.348	0.316	0.301	0.279
14.8	0.06	0.346	0.321	0.307	0.294
26.8	0.06	0.348	0.330	0.320	0.300
-46.5	0.08	0.635	0.588	0.569	0.488
-21.3	0.08	0.494	0.445	0.429	0.383
-11.3	0.08	0.339	0.301	0.281	0.253
14.8	0.08	0.364	0.337	0.325	0.298
26.8	0.08	0.386	0.361	0.345	0.322
-46.5	0.10	0.680	0.627	0.615	0.529
-21.3	0.10	0.484	0.426	0.408	0.356
-11.3	0.10	0.330	0.286	0.267	0.232
14.8	0.10	0.411	0.372	0.350	0.314
26.8	0.10	0.449	0.412	0.385	0.349

Table B-4. Coefficient ξ_1 for Pavement Width of 23.4 m

Thornthwaite Moisture Index	Suction Compression Index	Barrier Depth 0	90 cm	150 cm	240 cm
-46.5	0.04	0.386	0.371	0.364	0.326
-21.3	0.04	0.397	0.379	0.363	0.351
-11.3	0.04	0.327	0.314	0.293	0.284
14.8	0.04	0.308	0.299	0.286	0.275
26.8	0.04	0.298	0.291	0.291	0.282
-46.5	0.06	0.439	0.416	0.410	0.370
-21.3	0.06	0.384	0.366	0.364	0.337
-11.3	0.06	0.278	0.261	0.261	0.250
14.8	0.06	0.290	0.277	0.274	0.266
26.8	0.06	0.303	0.291	0.278	0.272
-46.5	0.08	0.479	0.450	0.445	0.403
-21.3	0.08	0.374	0.354	0.354	0.330
-11.3	0.08	0.252	0.237	0.226	0.214
14.8	0.08	0.297	0.282	0.275	0.257
26.8	0.08	0.323	0.303	0.292	0.279
-46.5	0.10	0.512	0.488	0.484	0.434
-21.3	0.10	0.347	0.322	0.328	0.299
-11.3	0.10	0.235	0.214	0.202	0.183
14.8	0.10	0.313	0.284	0.268	0.250
26.8	0.10	0.349	0.318	0.301	0.275

Table B-5. Coefficient ξ_1 for Pavement Width of 34.2 m

Thornthwaite Moisture Index	Suction Compression Index	Barrier Depth 0	90 cm	150 cm	240 cm
-46.5	0.04	0.303	0.303	0.303	0.280
-21.3	0.04	0.344	0.342	0.335	0.326
-11.3	0.04	0.287	0.285	0.273	0.271
14.8	0.04	0.275	0.273	0.269	0.265
26.8	0.04	0.271	0.269	0.273	0.267
-46.5	0.06	0.341	0.335	0.341	0.324
-21.3	0.06	0.319	0.315	0.324	0.311
-11.3	0.06	0.234	0.232	0.236	0.233
14.8	0.06	0.254	0.249	0.247	0.247
26.8	0.06	0.265	0.260	0.253	0.254
-46.5	0.08	0.370	0.370	0.374	0.351
-21.3	0.08	0.304	0.299	0.308	0.299
-11.3	0.08	0.204	0.198	0.190	0.188
14.8	0.08	0.241	0.237	0.237	0.228
26.8	0.08	0.265	0.256	0.252	0.250
-46.5	0.10	0.398	0.398	0.406	0.385
-21.3	0.10	0.269	0.265	0.277	0.265
-11.3	0.10	0.173	0.169	0.167	0.159
14.8	0.10	0.224	0.213	0.208	0.202
26.8	0.10	0.252	0.240	0.232	0.228

Table B-6. Coefficient ξ_1 for Pavement Width of 45.0 m

Thornthwaite Moisture Index	Suction Compression Index	Barrier Depth 0	90 cm	150 cm	240 cm
-46.5	0.04	0.273	0.280	0.288	0.273
-21.3	0.04	0.330	0.330	0.326	0.321
-11.3	0.04	0.276	0.278	0.268	0.266
14.8	0.04	0.269	0.267	0.265	0.262
26.8	0.04	0.264	0.264	0.269	0.264
-46.5	0.06	0.312	0.318	0.324	0.312
-21.3	0.06	0.304	0.306	0.314	0.306
-11.3	0.06	0.225	0.224	0.228	0.228
14.8	0.06	0.241	0.240	0.241	0.243
26.8	0.06	0.251	0.251	0.247	0.250
-46.5	0.08	0.341	0.346	0.355	0.341
-21.3	0.08	0.286	0.288	0.298	0.293
-11.3	0.08	0.189	0.188	0.183	0.185
14.8	0.08	0.225	0.225	0.228	0.223
26.8	0.08	0.247	0.243	0.243	0.243
-46.5	0.10	0.373	0.377	0.385	0.373
-21.3	0.10	0.251	0.253	0.265	0.257
-11.3	0.10	0.159	0.159	0.160	0.155
14.8	0.10	0.197	0.194	0.192	0.192
26.8	0.10	0.220	0.217	0.217	0.215

Table B-7. Coefficient ξ_2 for Pavement Width of 9.0 m

Thornthwaite Moisture Index	Suction Compression Index	Barrier Depth 0	90 cm	150 cm	240 cm
-46.5	0.04	0.3554	0.3172	0.0588	0.1671
-21.3	0.04	0.6700	0.5750	0.4929	0.5474
-11.3	0.04	0.7886	0.7106	0.6749	0.7596
14.8	0.04	0.7391	0.5289	0.5174	0.5822
26.8	0.04	0.6899	0.5325	0.5013	0.5574
-46.5	0.06	0.4424	0.3721	0.0830	0.2438
-21.3	0.06	0.6855	0.6383	0.5768	0.6497
-11.3	0.06	0.8505	0.7488	0.7464	0.8216
14.8	0.06	0.7507	0.6135	0.5660	0.6153
26.8	0.06	0.7510	0.4671	0.4995	0.5399
-46.5	0.08	0.4665	0.3438	0.0673	0.1318
-21.3	0.08	0.7304	0.6720	0.5809	0.6967
-11.3	0.08	0.9045	0.8275	0.7921	0.8917
14.8	0.08	0.7730	0.5728	0.5628	0.6465
26.8	0.08	0.6756	0.4488	0.5059	0.5496
-46.5	0.10	0.4556	0.3400	0.1106	0.1458
-21.3	0.10	0.7872	0.6972	0.6516	0.7663
-11.3	0.10	0.9325	0.8418	0.8203	0.9456
14.8	0.10	0.7398	0.5491	0.5986	0.7050
26.8	0.10	0.6135	0.4509	0.4893	0.5695

Table B-8. Coefficient ξ_2 for Pavement Width of 12.6 m

Thornthwaite Moisture Index	Suction Compression Index	Barrier Depth 0	90 cm	150 cm	240 cm
-46.5	0.04	0.5841	0.4939	0.3256	0.4174
-21.3	0.04	0.7961	0.7212	0.6588	0.6762
-11.3	0.04	0.9029	0.8271	0.7916	0.8537
14.8	0.04	0.8504	0.6911	0.6909	0.7256
26.8	0.04	0.8236	0.7097	0.6860	0.7142
-46.5	0.06	0.5952	0.5155	0.3244	0.3251
-21.3	0.06	0.8429	0.7701	0.6836	0.7699
-11.3	0.06	0.9545	0.8551	0.8471	0.9003
14.8	0.06	0.8508	0.7509	0.6952	0.7665
26.8	0.06	0.8484	0.6502	0.6729	0.6769
-46.5	0.08	0.6091	0.4715	0.3438	0.3682
-21.3	0.08	0.8763	0.7952	0.7197	0.7996
-11.3	0.08	1.0065	0.9445	0.8928	0.9683
14.8	0.08	0.8827	0.7153	0.7210	0.7835
26.8	0.08	0.8003	0.6286	0.6494	0.6654
-46.5	0.10	0.6208	0.4978	0.3223	0.3657
-21.3	0.10	0.9093	0.8281	0.7713	0.8482
-11.3	0.10	1.0336	0.9511	0.9386	1.0104
14.8	0.10	0.8314	0.7042	0.6998	0.7436
26.8	0.10	0.7190	0.5928	0.5373	0.6576

Table B-9. Coefficient ξ_2 for Pavement Width of 16.2 m

Thornthwaite Moisture Index	Suction Compression Index	Barrier Depth 0	90 cm	150 cm	240 cm
-46.5	0.04	0.6798	0.5945	0.5257	0.4749
-21.3	0.04	0.8661	0.7768	0.7125	0.6874
-11.3	0.04	0.9456	0.8634	0.8150	0.8368
14.8	0.04	0.8770	0.7251	0.7486	0.7545
26.8	0.04	0.8613	0.7854	0.7455	0.7014
-46.5	0.06	0.6848	0.6154	0.4986	0.4856
-21.3	0.06	0.9025	0.8137	0.7247	0.7317
-11.3	0.06	0.9983	0.9004	0.8679	0.9281
14.8	0.06	0.9049	0.7900	0.7821	0.8056
26.8	0.06	0.8710	0.6990	0.6490	0.7108
-46.5	0.08	0.6750	0.6067	0.4860	0.4612
-21.3	0.08	0.9392	0.8410	0.7619	0.7863
-11.3	0.08	1.0546	0.9755	0.9267	0.9689
14.8	0.08	0.9112	0.7639	0.7575	0.7710
26.8	0.08	0.7928	0.6849	0.6178	0.7156
-46.5	0.10	0.6831	0.5893	0.4963	0.4802
-21.3	0.10	0.9822	0.8761	0.7891	0.8479
-11.3	0.10	1.0845	0.9926	0.9579	1.0145
14.8	0.10	0.8590	0.7481	0.7140	0.7545
26.8	0.10	0.7103	0.6132	0.6536	0.6515

Table B-10. Coefficient ξ_2 for Pavement Width of 23.4 m

Thornthwaite Moisture Index	Suction Compression Index	Barrier Depth 0	90 cm	150 cm	240 cm
-46.5	0.04	0.8165	0.7732	0.6999	0.6290
-21.3	0.04	0.9090	0.8119	0.7208	0.6776
-11.3	0.04	0.9832	0.8724	0.8536	0.8106
14.8	0.04	0.8957	0.7609	0.7788	0.7673
26.8	0.04	0.9071	0.8073	0.5868	0.6976
-46.5	0.06	0.8231	0.7664	0.6980	0.6281
-21.3	0.06	0.9722	0.8661	0.7690	0.7303
-11.3	0.06	1.0446	0.9378	0.8759	0.8963
14.8	0.06	0.9304	0.8209	0.7797	0.7353
26.8	0.06	0.8673	0.6800	0.6400	0.7105
-46.5	0.08	0.8233	0.7557	0.6848	0.6224
-21.3	0.08	1.0177	0.9069	0.8076	0.7825
-11.3	0.08	1.1038	1.0092	0.9290	0.9373
14.8	0.08	0.9382	0.7964	0.7343	0.7519
26.8	0.08	0.7873	0.6875	0.7016	0.6889
-46.5	0.10	0.8186	0.7553	0.6847	0.6060
-21.3	0.10	1.0697	0.9606	0.8538	0.8362
-11.3	0.10	1.1429	1.0494	0.9944	1.0018
14.8	0.10	0.8914	0.8038	0.7833	0.8132
26.8	0.10	0.7358	0.7056	0.7390	0.7332

Table B-11. Coefficient ξ_2 for Pavement Width of 34.2 m

Thornthwaite Moisture Index	Suction Compression Index	Barrier Depth 0	90 cm	150 cm	240 cm
-46.5	0.04	0.9659	0.9084	0.8550	0.7626
-21.3	0.04	0.9535	0.8684	0.8004	0.7317
-11.3	0.04	0.9970	0.8850	0.8807	0.8431
14.8	0.04	0.9073	0.7901	0.8204	0.8015
26.8	0.04	0.9153	0.7911	0.6295	0.7128
-46.5	0.06	0.9633	0.9065	0.8518	0.7713
-21.3	0.06	1.0200	0.9185	0.8244	0.7874
-11.3	0.06	1.0645	0.9711	0.8880	0.8783
14.8	0.06	0.9583	0.8579	0.7787	0.7437
26.8	0.06	0.8720	0.7273	0.7270	0.7478
-46.5	0.08	0.9623	0.8991	0.8442	0.7580
-21.3	0.08	1.0636	0.9636	0.8665	0.8202
-11.3	0.08	1.1194	1.0341	0.9690	0.9375
14.8	0.08	0.9763	0.8519	0.7983	0.7972
26.8	0.08	0.8486	0.7795	0.7801	0.7556
-46.5	0.10	0.9557	0.8912	0.8365	0.7558
-21.3	0.10	1.1214	1.0244	0.9197	0.8728
-11.3	0.10	1.1814	1.0928	1.0393	1.0130
14.8	0.10	1.0296	0.9614	0.9330	0.9130
26.8	0.10	0.9260	0.9007	0.9032	0.8699

Table B-12. Coefficient ξ_2 for Pavement Width of 45.0 m

Thornthwaite Moisture Index	Suction Compression Index	Barrier Depth 0	90 cm	150 cm	240 cm
-46.5	0.04	1.0147	0.9581	0.9110	0.8414
-21.3	0.04	0.9734	0.9008	0.8485	0.7982
-11.3	0.04	1.0025	0.9132	0.9088	0.8719
14.8	0.04	0.9334	0.8364	0.8610	0.8424
26.8	0.04	0.9333	0.8318	0.7097	0.7746
-46.5	0.06	1.0082	0.9538	0.9109	0.8409
-21.3	0.06	1.0273	0.9487	0.8706	0.8401
-11.3	0.06	1.0564	0.9839	0.9134	0.9015
14.8	0.06	0.9734	0.8901	0.8301	0.8013
26.8	0.06	0.8975	0.7902	0.7939	0.8045
-46.5	0.08	1.0049	0.9486	0.9048	0.8339
-21.3	0.08	1.0634	0.9838	0.9084	0.8676
-11.3	0.08	1.1056	1.0365	0.9878	0.9606
14.8	0.08	0.9982	0.9008	0.8578	0.8550
26.8	0.08	0.9030	0.8469	0.8445	0.8188
-46.5	0.10	0.9954	0.9416	0.8977	0.8260
-21.3	0.10	1.1092	1.0326	0.9529	0.9091
-11.3	0.10	1.1544	1.0851	1.0411	1.0162
14.8	0.10	1.0815	1.0157	0.9863	0.9564
26.8	0.10	1.0167	0.9774	0.9620	0.9261

Table B-13. Coefficient ξ_3 for Pavement Width of 9.0 m

Thornthwaite Moisture Index	Suction Compression Index	Barrier Depth 0	90 cm	150 cm	240 cm
-46.5	0.04	2.2566	1.9955	1.6932	1.8018
-21.3	0.04	2.4001	2.1157	2.2395	2.4438
-11.3	0.04	2.0422	2.1203	2.1554	2.5220
14.8	0.04	2.2195	2.3378	2.4186	2.6594
26.8	0.04	2.1691	2.2330	2.3504	2.6468
-46.5	0.06	2.3573	1.8919	1.9439	1.8439
-21.3	0.06	2.3808	2.2429	2.5221	2.6322
-11.3	0.06	2.0790	2.2475	2.4901	2.6835
14.8	0.06	2.1541	2.2523	2.4894	2.6205
26.8	0.06	2.1834	2.2458	2.1735	2.3228
-46.5	0.08	2.3817	1.9547	1.8580	1.8853
-21.3	0.08	2.4848	2.3931	2.6612	2.7898
-11.3	0.08	2.1095	2.2321	2.4145	2.5681
14.8	0.08	2.2167	2.4331	2.4718	2.5586
26.8	0.08	2.2497	2.1298	2.0805	2.2050
-46.5	0.10	2.3685	1.9179	1.9477	1.8728
-21.3	0.10	2.7422	2.5384	2.8712	2.8678
-11.3	0.10	2.2579	2.4355	2.5575	2.5657
14.8	0.10	2.6312	2.4582	2.5339	2.8302
26.8	0.10	2.4176	2.2405	2.0801	2.0499

Table B-14. Coefficient ξ_3 for Pavement Width of 12.6 m

Thornthwaite Moisture Index	Suction Compression Index	Barrier Depth 0	90 cm	150 cm	240 cm
-46.5	0.04	2.3978	1.8231	1.5987	1.8247
-21.3	0.04	2.8008	2.5280	2.5762	2.9363
-11.3	0.04	2.6985	2.7820	2.7138	3.4367
14.8	0.04	3.1595	3.1039	3.0111	3.6982
26.8	0.04	3.0522	2.9897	3.2813	3.8021
-46.5	0.06	2.3725	1.7872	1.6265	1.7484
-21.3	0.06	2.8999	2.6084	2.8805	3.2932
-11.3	0.06	2.8014	2.7176	3.2392	3.7098
14.8	0.06	2.8554	2.9264	2.9641	3.6684
26.8	0.06	3.0531	2.8351	2.9320	2.9125
-46.5	0.08	2.4270	1.7754	1.7332	1.7988
-21.3	0.08	3.1217	2.7528	3.0169	3.5195
-11.3	0.08	2.8250	2.9343	3.0164	3.8470
14.8	0.08	3.0499	3.0806	2.9870	3.5851
26.8	0.08	3.1007	2.6020	2.6986	2.5727
-46.5	0.10	2.4599	1.8412	1.7305	1.8518
-21.3	0.10	3.3050	2.9377	3.2522	3.6642
-11.3	0.10	3.2681	3.2089	3.3714	4.2504
14.8	0.10	3.4362	3.0014	3.0018	3.3785
26.8	0.10	3.2238	2.3949	2.2301	2.3081

Table B-15. Coefficient ξ_3 for Pavement Width of 16.2 m

Thornthwaite Moisture Index	Suction Compression Index	Barrier Depth 0	90 cm	150 cm	240 cm
-46.5	0.04	2.1697	1.5492	1.5252	1.6560
-21.3	0.04	3.2979	2.7317	2.8387	3.3034
-11.3	0.04	3.3560	3.2537	3.0829	4.1736
14.8	0.04	4.1444	3.6811	3.4964	4.5820
26.8	0.04	3.8612	3.5473	4.1897	4.4218
-46.5	0.06	2.1915	1.6306	1.4949	1.6462
-21.3	0.06	3.3071	2.7990	3.0790	3.6135
-11.3	0.06	3.4357	3.1917	3.7432	5.0562
14.8	0.06	3.7147	3.3463	3.5575	4.8743
26.8	0.06	3.6833	3.2009	3.2646	3.3612
-46.5	0.08	2.2076	1.6548	1.5183	1.6449
-21.3	0.08	3.5346	2.9376	3.2602	4.0094
-11.3	0.08	3.8134	3.4884	3.8500	5.3672
14.8	0.08	3.6956	3.3509	3.5386	4.2863
26.8	0.08	3.4642	2.8076	2.5611	2.9248
-46.5	0.10	2.2484	1.6578	1.5889	1.7417
-21.3	0.10	3.9121	3.0145	3.4212	4.2855
-11.3	0.10	4.0853	3.8044	4.3774	6.7795
14.8	0.10	4.0172	3.2253	3.1968	3.6121
26.8	0.10	3.2769	2.3800	2.1009	2.2763

Table B-16. Coefficient ξ_3 for Pavement Width of 23.4 m

Thornthwaite Moisture Index	Suction Compression Index	Barrier Depth 0	90 cm	150 cm	240 cm
-46.5	0.04	1.8124	1.8644	1.6398	1.6490
-21.3	0.04	2.8502	2.6750	2.3399	2.5232
-11.3	0.04	3.9648	3.4731	3.5180	3.6964
14.8	0.04	3.6360	2.9903	3.1700	3.6949
26.8	0.04	4.1574	3.8971	2.4239	3.2570
-46.5	0.06	1.9003	1.8057	1.6293	1.6752
-21.3	0.06	2.8293	2.6396	2.4841	2.6016
-11.3	0.06	3.4446	3.1226	3.4661	4.6243
14.8	0.06	3.2652	2.8890	3.1059	3.0612
26.8	0.06	3.3851	2.3639	2.1484	2.8175
-46.5	0.08	1.9574	1.7519	1.5896	1.6806
-21.3	0.08	2.8520	2.6052	2.4600	2.7732
-11.3	0.08	3.4719	3.4412	2.9080	3.7854
14.8	0.08	3.1120	2.4643	2.2605	2.4936
26.8	0.08	2.4331	2.0401	2.1224	2.2487
-46.5	0.10	1.9262	1.8184	1.6545	1.6278
-21.3	0.10	2.8122	2.4638	2.4220	2.7902
-11.3	0.10	3.3457	3.0791	2.8212	3.7225
14.8	0.10	2.2464	1.8758	1.8083	2.0950
26.8	0.10	1.8010	1.6261	1.7539	1.7393

Table B-17. Coefficient ξ_3 for Pavement Width of 34.2 m

Thornthwaite Moisture Index	Suction Compression Index	Barrier Depth 0	90 cm	150 cm	240 cm
-46.5	0.04	1.9670	2.0404	1.8746	1.8013
-21.3	0.04	3.0723	3.0140	2.8087	2.7188
-11.3	0.04	4.1922	3.4758	3.9566	4.3355
14.8	0.04	3.5036	2.9660	3.6116	4.2887
26.8	0.04	4.1822	3.4239	2.4493	3.2375
-46.5	0.06	1.9469	1.9067	1.8451	1.9922
-21.3	0.06	2.9999	2.7133	2.5810	2.8856
-11.3	0.06	3.8132	3.5947	3.4333	4.3022
14.8	0.06	3.4145	2.9878	2.7126	2.9047
26.8	0.06	2.9132	2.2504	2.3721	2.9557
-46.5	0.08	1.9471	1.9847	1.8694	1.9094
-21.3	0.08	3.0562	2.7246	2.5185	2.8528
-11.3	0.08	3.8837	3.4569	2.8166	3.4032
14.8	0.08	2.6726	2.2180	2.1446	2.4297
26.8	0.08	2.0628	1.9423	2.0671	2.3131
-46.5	0.10	1.9186	1.9423	1.8873	2.0138
-21.3	0.10	2.9842	2.6864	2.4534	2.8137
-11.3	0.10	3.4354	3.0901	2.9948	3.8241
14.8	0.10	1.8226	1.7299	1.7657	2.0024
26.8	0.10	1.5256	1.5649	1.6876	1.8957

Table B-18. Coefficient ξ_3 for Pavement Width of 45.0 m

Thornthwaite Moisture Index	Suction Compression Index	Barrier Depth 0	90 cm	150 cm	240 cm
-46.5	0.04	2.2954	2.4533	2.3856	2.4869
-21.3	0.04	3.8369	3.6632	3.5214	3.5794
-11.3	0.04	5.1518	4.3532	5.0121	5.2675
14.8	0.04	4.5094	3.7037	4.6049	5.4170
26.8	0.04	5.0955	4.2079	3.1610	4.1662
-46.5	0.06	2.3575	2.4783	2.3737	2.5814
-21.3	0.06	3.7841	3.5641	3.2450	3.7582
-11.3	0.06	4.9088	4.5087	4.1304	5.2300
14.8	0.06	3.9953	3.5756	3.4064	3.7150
26.8	0.06	3.2445	2.7591	3.0435	3.7825
-46.5	0.08	2.3955	2.4530	2.3968	2.5731
-21.3	0.08	3.8117	3.5139	3.2359	3.7074
-11.3	0.08	4.7381	4.2856	3.6414	4.6214
14.8	0.08	3.1572	2.7273	2.7254	3.2130
26.8	0.08	2.4397	2.4058	2.6503	2.9594
-46.5	0.10	2.4572	2.4981	2.4011	2.6282
-21.3	0.10	3.7456	3.4620	3.1147	3.5674
-11.3	0.10	4.2879	3.8868	3.8754	5.0690
14.8	0.10	2.1400	2.1429	2.2044	2.5882
26.8	0.10	1.7914	1.9233	2.1838	2.4021

APPENDIX C

DESORPTION COEFFICIENTS

Desorption coefficients relate the volumetric water content to the matric suction of soil. Jayatilaka et al. (1992) presented desorption relationships in terms of gravimetric water content for 17 soil samples collected from different pavement sections in Texas. In that study, the measurements of soil suction were made using a pressure plate apparatus. The desorption relationship used in this study is that proposed by Gardner as given in Equation 5.2. Since the Gardner's desorption expression needs the volumetric water content, the measured gravimetric water contents need to be converted to the volumetric water contents. In this appendix, relationships are derived to convert gravimetric water content to volumetric water content, desorption coefficients are estimated for 14 different expansive clay soil samples of CH soil groups of the Unified Soil Classification System, and desorption coefficients extracted from the literature for other groups of soils are tabulated.

DERIVATION

In this section, equations are derived to estimate Gardner's desorption coefficients from gravimetric water content versus suction relationships. The assumptions necessary for the derivation are as follows.

1. When the volumetric water content is equal to the field capacity (θ_{fc}) of that soil, the suction of soil is equal to 2.0 pF (Lytton 1994).
2. The volumetric water content at the field capacity is equal to 0.88 times the volumetric water content at saturation (Lytton 1994).
3. Dry density of soil at the field capacity and at saturation are equal.

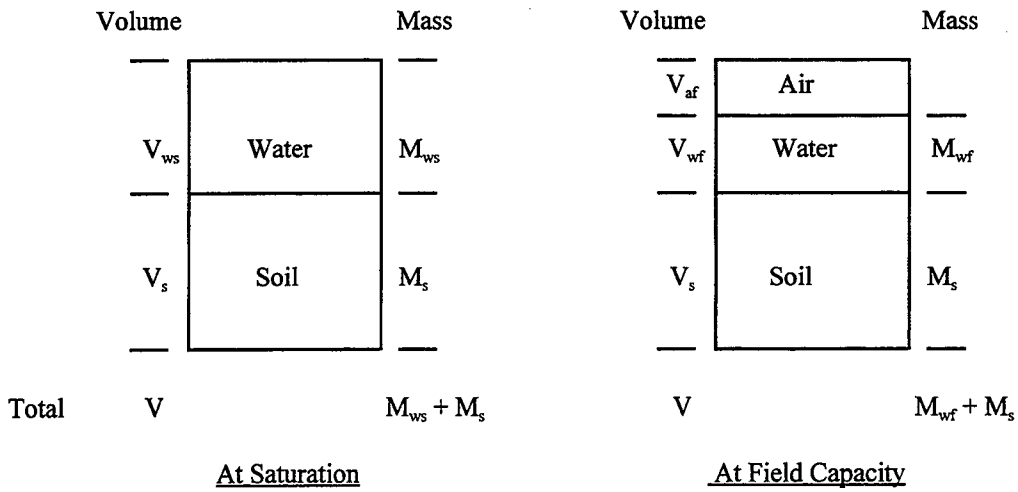

Figure C.1. Phase Diagrams for Saturated and Field Capacity Conditions

The gravimetric water contents at saturation and at field capacity are given by (Figure C.1):

$$w_s = \frac{M_{ws}}{M_s} \tag{C.1}$$

$$w_f = \frac{M_{wf}}{M_s} \tag{C.2}$$

where

w_s, w_f	=	gravimetric water contents at saturation and at field capacity,
M_{ws}, M_{wf}	=	mass of water at saturation and at field capacity, and
M_s	=	mass of soil solids.

The volumetric water contents at saturation and at field capacity are given by:

$$\theta_s = \frac{V_{ws}}{V} = \frac{\gamma_w M_{ws}}{V} \tag{C.3}$$

$$\theta_f = \frac{V_{wf}}{V} = \frac{\gamma_w M_{wf}}{V} \tag{C.4}$$

where

θ_s, θ_f	=	volumetric water contents at saturation and at field capacity,
V	=	total volume of soil sample,
V_{ws}, V_{wf}	=	volume of water at saturation and at field capacity, and
γ_w	=	density of water.

Applying assumption 2 ($\theta_f = 0.88\ \theta_s$) to Equations C.3 and C.4, the following relationship is obtained.

$$M_{wf} = 0.88 M_{ws} \tag{C.5}$$

Solving Equations C.1, C.2, and C.5 the following relationship between gravimetric water contents at saturation and at field capacity is obtained.

$$w_f = 0.88 w_s \tag{C.6}$$

The dry density of soil sample at saturation (γ_d) is given by:

$$\gamma_d = \frac{M_s}{V} = \frac{G\gamma_w V_s}{V} = G\gamma_w \frac{(V - V_{ws})}{V} = G\gamma_w(1 - \theta_s) \tag{C.7}$$

where

G	=	specific gravity of soil solids, and
V_s	=	volume of soil solids.

The gravimetric water content at saturation is given by:

$$w_s = \frac{M_{ws}}{M_s} = \frac{M_{ws}/V}{M_s/V} = \frac{\gamma_w V_{ws}/V}{M_s/V} = \frac{\gamma_w \theta_s}{\gamma_d} \tag{C.8}$$

Equating γ_d from Equations C.7 and C.8:

$$G\gamma_w(1 - \theta_s) = \frac{\gamma_w \theta_s}{w_s} \tag{C.9}$$

Rearranging Equation C.9, the following expression for θ_s is obtained.

$$\theta_s = \frac{Gw_s}{1 + Gw_s} \tag{C.10}$$

A typical plot of suction versus gravimetric water content is shown in Figure C.2. The absolute value of the slope of the straight line (S) is given by:

$$S = \frac{I - 2}{w_f} = \frac{I - 2}{0.88\, w_s} \tag{C.11}$$

where

I = intercept of the straight line.

Substituting w_s from Equation C.11 into Equation C.10, the following expression for θ_s is obtained.

$$\theta_s = \frac{G(I - 2)}{0.88\, S + G(I - 2)} \tag{C.12}$$

Substituting θ_s from Equation C.12 into Equation C.7, an expression for dry density at saturation (γ_d) is obtained as follows.

$$\gamma_d = \frac{0.88\, G\gamma_w S}{0.88\, S + G(I - 2)} \tag{C.13}$$

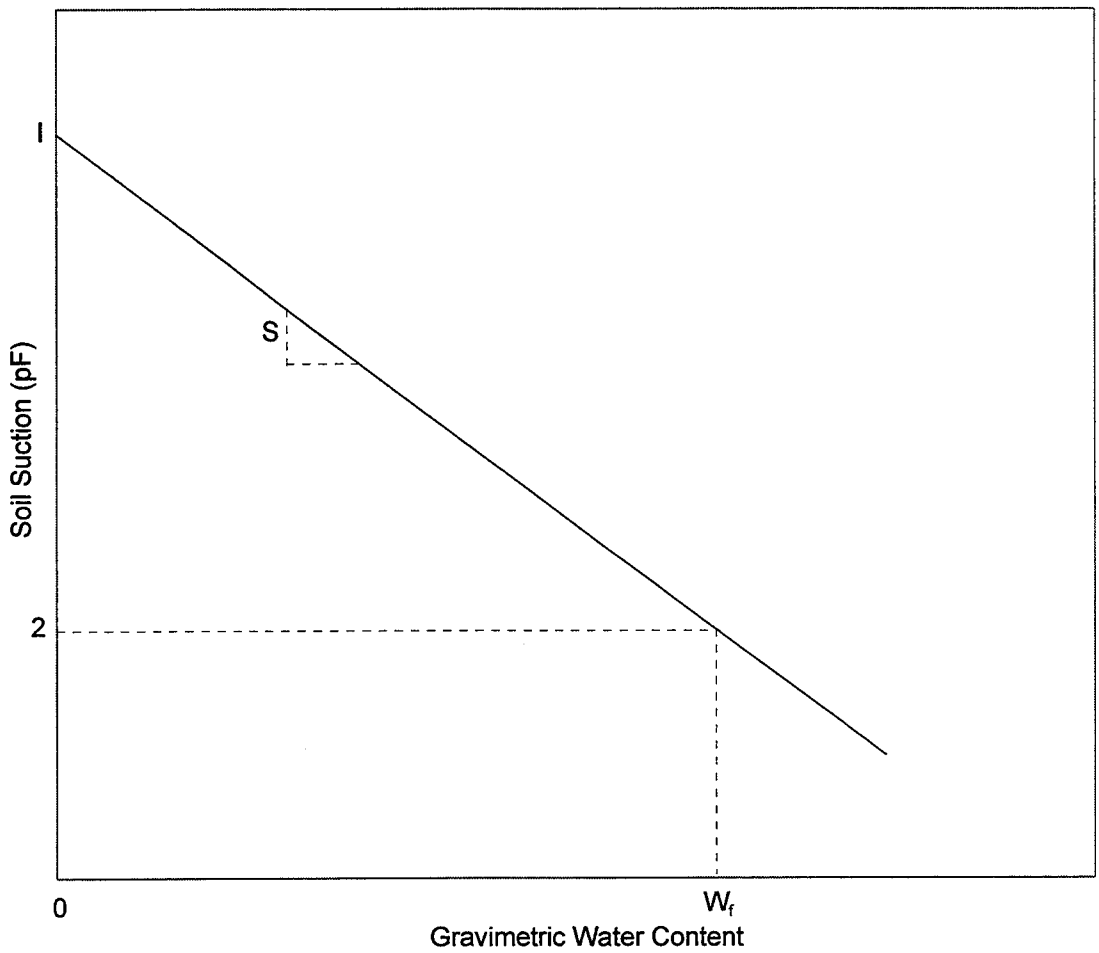

Figure C.2. A Typical Plot of Soil Suction Vs. Gravimetric Water Content

Assuming the dry density and the suction at field capacity are equal to γ_d, and 2.0 pF, respectively, a relationship can be derived to estimate the volumetric moisture content at any level of suction (Figure C.3).

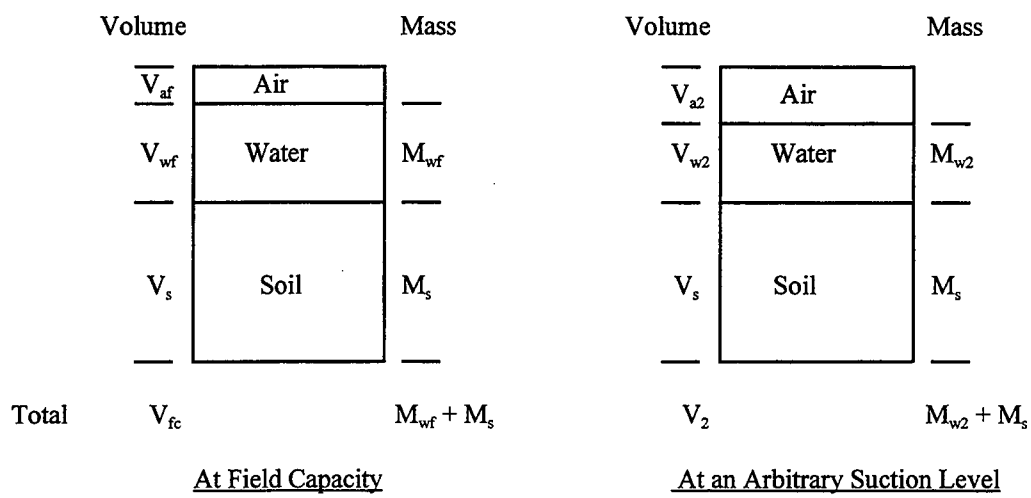

Figure C.3. Phase Diagrams for Field Capacity and Arbitrary Suction Conditions

At field capacity:

$$\frac{V_{fc}}{M_s} = \frac{1}{\gamma_d} \tag{C.14}$$

where

V_{fc} = total volume of soil sample at field capacity, and

M_s = mass of soil solids.

At an arbitrary suction level, the total volume of soil sample (V_2) is given by:

$$V_2 = \frac{V_{w2}}{\theta_2} = \frac{M_{w2} / \gamma_w}{\theta_2} \tag{C.15}$$

where

V_{w2} = volume of water at an arbitrary suction level,

θ_2 = volumetric water content at the arbitrary suction level, and

M_{w2} = mass of water at the arbitrary suction level.

Dividing Equation C.15 by M_s:

$$\frac{V_2}{M_s} = \left(\frac{M_{w2}}{M_s}\right) \cdot \left(\frac{1}{\gamma_w \theta_2}\right) = \frac{w_2}{\gamma_w \theta_2} \tag{C.16}$$

where

w_2 = gravimetric water content at the arbitrary suction level.

Dividing Equation C.16 by Equation C.14:

$$\frac{V_2}{V_{fc}} = \frac{w_2 \gamma_d}{\gamma_w \theta_2} \tag{C.17}$$

When there is no overburden pressure, Equation 2.10 becomes:

$$\frac{\Delta V}{V} = -\gamma_h \log_{10}\left(\frac{h_f}{h_i}\right) \tag{C.18}$$

Taking initial and final conditions to be the field capacity and the arbitrary point, respectively, Equation C.18 can be written as:

$$\frac{\Delta V}{V_{fc}} = -\gamma_h (pF_2 - pF_{fc}) \tag{C.19}$$

where

ΔV = change in volume,

γ_h = suction compression index, and

pF_2, pF_{fc} = suction in pF units at the arbitrary point and at field capacity, respectively.

The volume of soil sample at the arbitrary suction level (V_2) can be written as:

$$V_2 = V_{fc} + \Delta V \tag{C.20}$$

Substituting ΔV from Equation C.19 into Equation C.20, the following equation can be obtained.

$$\frac{V_2}{V_{fc}} = 1 - \gamma_h(pF_2 - pF_{fc}) \tag{C.21}$$

Solving Equations C.17 and C.21, the following equation to estimate the volumetric water content at the arbitrary suction level (θ_2) can be obtained.

$$\theta_2 = \frac{\gamma_d w_2}{\gamma_w[1 - \gamma_h(pF_2 - pF_{fc})]} \tag{C.22}$$

ESTIMATION OF DESORPTION COEFFICIENTS FOR SOME SOIL SAMPLES

The Gardner's desorption coefficients for 14 different soil samples are estimated in this section using the relationships derived in the previous section. The absolute values of slope and the intercepts of plots of soil suction versus gravimetric water content, specific gravities, and suction compression indices (SCI) of these soil samples are shown in Table C-1.

The nonlinear desorption relationship given in Equation 5.2 can be linearized as follows.

$$\log_{10} h = \frac{1}{x}\log_{10}\left(\frac{1}{a}\right) + \frac{1}{x}\log_{10}\left(\frac{n - \theta}{\theta}\right) \tag{C.23}$$

For each soil sample, the porosity (n) which is numerically equal to θ_s was calculated from Equation C.12. The volumetric water content (θ) for each data point was calculated from Equation C.22. Linear regression was performed on data using $\log_{10}$ h as the dependant variable and $\log_{10}$ [(n-θ)/ θ] as the independent variable. Regression results are tabulated in Table C-2.

Table C-1. Data to Estimate Desorption Coefficients

Soil Sample	Slope (S)	Intercept (I)	Specific gravity (G)	SCI
BH1(0-3)	8.01	5.92	2.76	0.10
BH1(4-7)	8.15	5.94	2.78	0.10
BH1(7-10)	7.98	5.93	2.82	0.10
BH4(0-4)	7.25	5.67	2.71	0.09
BH4(5-7)	6.95	5.60	2.75	0.08
BH5(0-3)	7.16	5.78	2.69	0.07
BH5(4-6)	7.41	5.61	2.68	0.07
BH5(6-10)	9.59	5.60	2.71	0.04
BH8(2-3)	10.16	5.83	2.77	0.06
BH8(4-6)	8.22	5.84	2.75	0.08
BH8(6-9)	7.84	5.92	2.77	0.09
BH11(0-3)	10.55	5.74	2.70	0.08
BH11(3-7)	7.76	6.02	2.81	0.08
BH11(7-10)	5.84	5.87	2.75	0.11

Table C-2. Regression Results of Soil Suction Versus Volumetric Water Content

Soil Sample	Slope of Straight Line (m)	Intercept of Straight Line (c)	R^2
BH1(0-3)	3.5239	4.0143	0.97
BH1(4-7)	3.4450	3.8798	0.98
BH1(7-10)	3.0579	3.9470	0.89
BH4(0-4)	3.3710	3.8269	0.98
BH4(5-7)	3.4824	3.6358	0.95
BH5(0-3)	2.5301	3.9372	0.98
BH5(4-6)	2.6992	4.1145	0.88
BH5(6-10)	2.6960	4.1986	0.95
BH8(2-3)	2.5625	3.9033	0.99
BH8(4-6)	2.6070	4.0103	0.95
BH8(6-9)	2.7155	4.1155	0.99
BH11(0-3)	2.7315	4.1758	0.96
BH11(3-7)	2.7490	4.1972	0.96
BH11(7-10)	2.7260	4.1852	0.94

Desorption coefficients can be estimated from the following equations:

$$x = \frac{1}{m} \tag{C.24}$$

$$a = 10^{-\frac{c}{m}} \tag{C.25}$$

where

m = slope of the straight line obtained from regression,

c = intercept of the straight line obtained from regression, and

a, x = desorption coefficients.

Desorption coefficients obtained are tabulated in Table C-3.

Table C-3. Gardner's Desorption Coefficients for CH Soils

Soil Sample	No.	Unified Soil Classification	n	a	x
BH1(0-3)	CH1	CH	0.606	0.0296	0.3661
BH1(4-7)	CH2	CH	0.604	0.0297	0.3638
BH1(7-10)	CH3	CH	0.612	0.0292	0.3668
BH4(0-4)	CH4	CH	0.609	0.0726	0.2838
BH4(5-7)	CH5	CH	0.618	0.0748	0.2903
BH5(0-3)	CH6	CH	0.617	0.0512	0.3270
BH5(4-6)	CH7	CH	0.597	0.0732	0.2966
BH5(6-10)	CH8	CH	0.536	0.0904	0.2872
BH8(2-3)	CH9	CH	0.543	0.0300	0.3902
BH8(4-6)	CH10	CH	0.594	0.0290	0.3836
BH8(6-9)	CH11	CH	0.612	0.0305	0.3683
BH11(0-3)	CH12	CH	0.521	0.0278	0.3952
BH11(3-7)	CH13	CH	0.623	0.0299	0.3705
BH11(7-10)	CH14	CH	0.674	0.0277	0.3709

The linear regression performed on the porosity for the 14 soil samples resulted the following relationship:

$$n = 0.0027\ (\%LL) + 0.4111 \qquad n = 14 \qquad R^2 = 0.87 \tag{C.26}$$

where

LL = liquid limit of soil.

Table C.4 shows the Gardner's desorption coefficients extracted from the literature for various groups of soils (Lytton et al. 1989).

Table C-4. Gardner's Desorption Coefficients for Various Groups of Soils

No.	Unified Soil Classification	n	a	x
GM-GC1	GM-GC	0.296	0.004	0.637
GM1	GM	0.206	0.152	0.269
GM2	GM	0.276	0.040	0.648
GM3	GM	0.311	0.066	0.251
GM4	GM	0.378	0.043	0.478
GP1	GP	0.203	0.065	0.550
GW1	GW	0.307	0.039	0.302
GW2	GW	0.416	0.596	0.318
GW3	GW	0.355	0.309	0.319
SM-SC1	SM-SC	0.396	0.013	0.770
SM1	SM	0.284	0.016	0.562
SM2	SM	0.382	0.001	1.023
SM3	SM	0.544	0.110	0.339
SM4	SM	0.396	0.039	0.468
SM5	SM	0.384	0.015	0.835
SM6	SM	0.506	0.011	0.671
SM7	SM	0.419	0.023	0.549
SM8	SM	0.454	0.208	0.436
SM9	SM	0.419	0.010	0.835
SM10	SM	0.450	0.018	0.806
SM11	SM	0.531	0.029	0.745
SM12	SM	0.684	0.042	0.501
SP-SM1	SP-SM	0.365	0.048	0.769
SP-SM2	SP-SM	0.368	0.095	0.613
SP1	SP	0.416	0.055	0.790
SP2	SP	0.424	0.024	0.951
SP3	SP	0.450	0.042	0.900
SP4	SP	0.372	0.076	0.665
SP5	SP	0.368	0.053	0.809
SW-SP1	SW-SP	0.296	0.012	1.082
SW1	SW	0.355	0.162	0.585
SW2	SW	0.399	0.000	1.982
SW3	SW	0.278	0.111	0.616

Table C-4. (Continued)

No.	Unified Soil Classification	n	a	x
CL1	CL	0.542	0.065	0.417
CL2	CL	0.383	0.000	0.976
CL3	CL	0.440	0.004	0.610
CL4	CL	0.379	0.000	0.957
CL5	CL	0.452	0.018	0.523
CL6	CL	0.491	0.000	1.910
CL7	CL	0.447	0.000	1.593
CL8	CL	0.493	0.028	0.344
CL9	CL	0.360	6.9E-6	1.551
CL10	CL	0.341	0.024	0.359
CL11	CL	0.293	0.064	0.247
CL12	CL	0.493	0.004	0.474
ML-OL1	ML-OL	0.632	0.064	0.535
ML-OL2	ML-OL	0.469	0.000	1.362
ML-CL1	ML-CL	0.409	0.066	0.365
ML-CL2	ML-CL	0.391	0.013	0.634
ML-CL3	ML-CL	0.392	0.001	1.052
ML1	ML	0.504	0.003	1.054
ML2	ML	0.516	0.000	1.257
ML3	ML	0.528	0.032	0.681
ML4	ML	0.609	0.065	0.411
ML5	ML	0.468	0.000	1.019
ML6	ML	0.452	0.000	1.474
ML7	ML	0.439	0.012	0.575
ML8	ML	0.462	0.003	0.973
ML9	ML	0.377	0.022	0.707
ML10	ML	0.684	0.038	0.610
ML11	ML	0.376	0.031	0.722
ML12	ML	0.451	0.000	2.059

APPENDIX D

VERTICAL MOVEMENT AT TEST SECTIONS

Table D-1. Estimated Vertical Movements (cm) at Test Sections

Test Site	Section	Outside Lane		Center Lane		Inside Lane	
		Right	Left	Right	Left	Right	Left
General McMullen	1 - 6	5.4832	4.1478	3.5448	3.1478	2.9803	2.8923
IH 37	1, 6, 7, 12	5.2344	3.9912	3.2997	2.9087	2.6897	2.5732
	2 - 5, 8 - 11	3.4046	2.9348	2.6482	2.4765	2.3775	2.3244
Greenville	1	0.3981	0.3970	-	-	0.3981	0.4175
	2	0.4194	0.4172	-	-	0.4194	0.4430
	5, 6	1.3018	1.2831	-	-	1.3018	1.4516
	7, 8	1.4356	1.4121	-	-	1.4356	1.6149
US 281	1	4.8341	3.7923	3.2236	2.9136	2.7532	2.6800
	2	3.4122	2.9751	2.7184	2.5727	2.4963	2.4618
San Antonio, IH 10	1, 4, 6, 8	5.4602	4.1544	3.4304	3.0221	2.7941	2.6730
	2, 3, 5, 7, 9, 10	3.5428	3.0525	2.7533	2.5739	2.4703	2.4147
Sierra Blanca	1, 3, 4, 6	0.6216	0.6063	-	-	0.6216	0.6806
	2	0.7498	0.7355	-	-	0.7498	0.7915
	5	0.7482	0.7338	-	-	0.7482	0.7898
Seguin	1	3.4961	3.4508	-	-	3.4762	3.7990
	2	5.8021	5.6204	-	-	5.7275	6.8396
Converse	1, 2	3.7140	3.5828	-	-	-	-
Dallas	1	2.7154	2.6626	2.6601	2.6602	2.6687	2.7772
	2	3.4272	3.2472	3.2298	3.2307	3.2753	3.5882

APPENDIX E

REGRESSION COEFFICIENTS FOR ROUGHNESS

Table E-1. Coefficient ρ_s

Test Site	Section	Outside Lane		Center Lane		Inside Lane	
		Right	Left	Right	Left	Right	Left
Greenville	1	-	-	-	-	343.26	340.44
	2	-	-	-	-	98.75	94.71
	5	170.68	173.69	-	-	112.88	98.72
	6	184.56	187.67	-	-	319.73	298.58
	7	72.55	77.78	-	-	-	-
	8	76.62	81.96	-	-	-	-
San Antonio, IH 10	1	-	-	33.28	93.40	86.51	112.91
	2	248.57	272.39	199.32	227.88	-	-
	3	345.56	427.40	288.48	324.31	210.66	219.78
	4	505.80	714.01	453.96	526.37	320.45	338.70
	5	170.11	248.06	133.51	162.38	161.40	170.64
	6	-	-	61.70	133.39	108.74	121.35
	7	70.19	113.55	69.56	95.30	79.73	88.61
	8	-	-	-	-	-	-
	9	191.32	285.63	200.12	230.19	186.76	198.49
	10	210.22	286.39	126.36	155.52	179.62	187.94
Sierra Blanca	1	89.22	92.22	-	-	271.71	260.53
	2	-	-	-	-	35.20	29.74
	3	184.31	187.09	-	-	74.23	66.08
	4	430.67	433.43	-	-	406.23	395.40
	5	172.64	173.67	-	-	-	-
	6	335.52	338.11	-	-	281.02	272.30
Seguin	1	256.79	263.66	-	-	193.22	157.68
	2	255.26	298.85	-	-	355.30	213.21
Converse	1	50.63	83.94	-	-	-	-
	2	52.52	84.03	-	-	-	-
Dallas	1	68.42	77.65	-	-	68.57	52.84
	2	25.98	46.87	-	-	135.89	74.61

Table E-2. Coefficient ρ_i

Test Site	Section	Outside Lane		Center Lane		Inside Lane	
		Right	Left	Right	Left	Right	Left
Greenville	1	-	-	-	-	372.64	366.56
	2	-	-	-	-	238.88	231.48
	5	274.01	279.79	-	-	288.82	260.65
	6	338.33	345.54	-	-	373.82	329.32
	7	182.73	190.93	-	-	124.05	70.84
	8	189.85	197.06	-	-	241.05	185.19
San Antonio, IH 10	1	-	-	116.08	201.44	144.57	183.89
	2	313.16	363.61	267.49	317.36	296.88	311.31
	3	603.37	757.75	472.59	527.39	-	-
	4	497.96	915.45	642.91	780.62	348.56	387.97
	5	324.47	465.03	252.32	308.42	316.46	333.47
	6	-	-	149.54	290.16	391.31	428.42
	7	150.30	227.77	163.59	220.51	189.25	207.76
	8	-	-	-	-	-	-
	9	354.17	510.50	382.76	454.88	373.01	393.49
	10	372.66	528.81	252.79	314.82	324.21	338.43
Sierra Blanca	1	155.04	161.63	-	-	421.19	400.41
	2	-	-	-	-	77.33	66.91
	3	244.59	250.17	-	-	115.46	99.52
	4	518.05	524.86	-	-	585.63	563.48
	5	377.58	381.32	-	-	-	-
	6	461.22	464.89	-	-	433.28	414.42
Seguin	1	339.79	349.01	-	-	419.84	345.86
	2	587.66	638.14	-	-	919.54	625.22
Converse	1	71.29	140.26	-	-	-	-
	2	79.52	139.19	-	-	-	-
Dallas	1	82.53	98.22	-	-	139.99	114.21
	2	-	-	-	-	185.88	112.64

APPENDIX F

ROUGHNESS MODEL CONSTANTS

Table F-1. Roughness Model Constants B_s and B_i

Test Site	Section	B_S			B_i		
		Outside	Center	Inside	Outside	Center	Inside
Greenville	1	-	-	145.36	-	-	313.40
	2	-	-	171.19	-	-	313.56
	5	160.96	-	94.53	309.09	-	188.05
	6	166.31	-	141.19	385.56	-	297.06
	7	222.55	-	-	348.94	-	296.77
	8	227.23	-	-	306.81	-	311.54
San Antonio, IH 10	1	-	147.24	218.00	-	209.06	324.69
	2	48.58	159.20	-	102.90	277.98	259.53
	3	166.92	199.72	173.02	314.87	305.46	-
	4	159.45	177.35	150.70	319.72	337.28	325.43
	5	158.98	160.93	166.19	286.68	312.71	305.94
	6	-	175.58	104.13	-	344.40	306.44
	7	88.44	143.48	159.71	158.01	317.28	332.91
	8	-	-	-	-	-	-
	9	192.35	167.61	210.97	318.85	402.01	368.35
	10	155.35	162.54	149.64	318.48	345.76	255.76
Sierra Blanca	1	196.08	-	189.49	430.72	-	352.20
	2	-	-	130.94	-	-	249.88
	3	181.70	-	138.14	364.71	-	270.17
	4	180.39	-	183.56	445.10	-	375.42
	5	71.53	-	-	259.72	-	-
	6	169.28	-	147.80	239.87	-	319.66
Seguin	1	151.66	-	110.10	203.53	-	229.18
	2	239.90	-	127.77	277.82	-	264.65
Converse	1	253.89	-	-	525.69	-	-
	2	240.17	-	-	454.80	-	-
Dallas	1	174.81	-	144.98	297.16	-	237.60
	2	116.06	-	195.85	-	-	234.07

APPENDIX G

EXAMPLE PROBLEMS

EXAMPLE 1

Given

Depth of root zone	=	244 cm
Number of soil layers to depth of root zone	=	4
Mean Thornthwaite Moisture Index	=	-12.5
Width of Pavement	=	1219 cm
Distance to right wheel path from the center	=	274 cm
Initial PSI - northbound, right wheel	=	4.3
Initial PSI - southbound, right wheel	=	4.75
Initial IRI - northbound, right wheel	=	1.25 m/km
Initial IRI - southbound, right wheel	=	0.86 m/km
Traffic - analysis period (C)	=	20 years
ADT in one direction when t = 0	=	1250
ADT in one direction when t = C	=	2750
80 kN single axles when t = C	=	702,000
Structural Number (SN)	=	15.24 cm (6.0 in)
Resilient modulus of subgrade soil	=	36544.13 kN/ m^2
	=	5300 lbf/ in^2
Depth of vertical moisture barrier	=	244 cm
Reliability - for AASHTO model	=	95%
- for B_s and B_i	=	95%

Layer thicknesses, liquid limits, plasticity indices % clay, and % fine clay are as in Table 3-3.

Desorption parameters are given in Table 5-2.

Find

PSI and IRI versus time for right wheel path of both northbound and southbound lanes.

Solution

Vertical movement (from modified MOPREC program) = 9.98 cm

Amplitude of moisture depth (from modified MOPREC program) = 12.21 cm

From Equations 4.37 through 4.39,

$$\xi_1 = 2.0144 - 0.0238*9.98 - 0.000892*244 - 0.1611*\log_e(12.21) - 0.1936*\log_e(1219/2) + 0.4016*9.98/12.21 + 0.00005336*9.98*(-12.5) + 0.00004112*12.21*244$$

$$= 0.3588$$

$$\xi_2 = -1.2924 + 0.0332*9.98 + 0.004651*(-12.5) - 0.002591*244 + 0.321*\log_e(1219/2) + 0.000006077*(244)^2 - 0.2634*9.98/12.21 - 0.001172*9.98*(-12.5) + 0.00005722*12.21*244$$

$$= 0.8700$$

$$\xi_3 = \exp[1.0725 - 0.07346*9.98 + 0.008762*(-12.5) - 0.003529*244 + 0.00000852*(244)^2 - 0.001458*9.98*(-12.5) + 0.000121*9.98*(1219/2) + 0.000156*12.21*244]$$

$$= 3.5201$$

Vertical movement at the right wheel path (from Equation 4.36)

$$= 9.98*0.3588*\exp[(0.8700*274/609.5)^{3.5201}]$$

$$= 3.714 \text{ cm}$$

For 95 percent reliability, Z = 1.645

$$B_s = 162.87 + 40.99*1.645 = 230.29855$$

$$B_i = 306.66 + 72.83*1.645 = 426.46535$$

80 kN single-axle load applications for 40 years (from Equation 5.11)

$$= 702{,}000/[(20*(1250 + 2750)]*[2*1250*40 + (2750 - 1250)*40^2/20]$$

$$= 1{,}930{,}500$$

From Equation 5.13

$$\lambda = [0.4 + 1094/(6 + 1)^{5.19}]*[\log_{10}(1930500) - 9.36*\log_{10}(6 + 1) + 8.27 - 2.32*\log_{10}(5300) + 1.645*0.35]$$

$$= -0.63143$$

From Equation 5.17 and 5.25

$$A_s = 480*[\log_e(10^{0.63143})]^{(1/0.6)}$$

$$= 895.6487$$

$$A_i = 480*[\log_e\{3.01/\{8.4193*\exp(-0.4664*(4.2 - 2.7*(10^{-0.63143}))) - 1.19\}\}]^{(1/0.55)}$$

$$= 1707.634$$

From Equations 5.6 and 5.7

$$\rho_s = 895.6487 - 230.29855*3.714 = 40.3199$$

$$\rho_i = 1707.634 - 426.46535*3.714 = 123.7412$$

Roughness equations (from Equations 5.4 and 5.5)

Northbound lane

$$PSI = 4.3 - (4.3 - 1.5)\exp[-(40.3199/t)^{0.6}]$$

$$IRI = 1.25 + (4.2 - 1.25)\exp[-(123.7412/t)^{0.55}]$$

Southbound lane

$$PSI = 4.75 - (4.75 - 1.5)\exp[-(40.3199/t)^{0.6}]$$

$$IRI = 0.86 + (4.2 - 0.86)\exp[-(123.7412/t)^{0.55}]$$

Predicted roughness with time is shown in Table G-1. A plots of predicted and measured roughness are shown in Figures 5.4 and 5.5.

Table G-1. Predicted Roughness with Time, Converse FM 1516

Time (months)	Northbound		Southbound	
	PSI	IRI	PSI	IRI
6	4.18	1.26	4.61	0.88
13	3.91	1.34	4.30	0.97
17	3.78	1.40	4.14	1.03
20	3.69	1.44	4.04	1.08
26	3.54	1.53	3.87	1.18
31	3.43	1.60	3.74	1.25
53	3.10	1.85	3.36	1.54
63	3.00	1.94	3.24	1.64

EXAMPLE 2

Given

Initial PSI	=	4.2
Initial IRI	=	1.19 m/km
Structural Number (SN)	=	16.84 cm (6.63 in)
Resilient modulus of subgrade soil	=	36544.13 kN/ m^2
		5300 lbf/ in^2
Barrier depths	=	0, 91, 152, 244 cm
Swell rate constant (AASHTO 1993)	=	0.13
Swelling probability (AASHTO 1993)	=	100
Potential Vertical Rise (AASHTO 1993)	=	10.16 cm (4 in)

Other data are as in Example 1.

Find

Change in PSI and IRI versus time for right wheel path for four vertical moisture barrier depths using the new model and for the no barrier condition using the AASHTO model.

Solution

New Model

Vertical movement (from modified MOPREC program) = 9.98 cm

Amplitude of moisture depth (from modified MOPREC program) = 12.21 cm

The parameters ξ_1, ξ_2, and ξ_3 are calculated as in the Example 1. The results are tabulated in Table G-2.

Table G-2. Vertical Movement Parameters for Different Barrier Depths

Barrier Depth (cm)	ξ_1	ξ_2	ξ_3	Vertical Movement at Wheel Path (cm)
0	0.4540	0.9700	3.1509	4.8736
91	0.4185	0.8481	2.9165	4.4341
152	0.3947	0.8228	2.9969	4.1432
244	0.3588	0.8700	3.5201	3.7140

For 95 percent reliability, Z = 1.645

$$B_s = 162.87 + 40.99 * 1.645 = 230.29855$$

$$B_i = 306.66 + 72.83 * 1.645 = 426.46535$$

80 kN single-axle load applications for 40 years (from Equation 5.11)

$$= 702{,}000/[(20*(1250 + 2750)]*[2*1250*40 + (2750 - 1250)*40^2 /20]$$

$$= 1{,}930{,}500$$

From Equation 5.13

$$\lambda = [0.4 + 1094/(6.63 + 1)^{5.19}]*[\log_{10}(1{,}930{,}500) - 9.36*\log_{10}(6.63 +1) + 8.27 - 2.32*\log_{10}(5300) + 1.645*0.35]$$

$$= - 0.75861$$

From Equation 5.17

$$A_s = 480*[\log_e (10^{0.75861})]^{(1/0.6)}$$
$$= 1216.086$$

From Equation 5.25

$$A_i = 480*[\log_e \{3.01/\{8.4193*\exp(-0.4664*(4.2 - 2.7*(10^{-0.75861}))) - 1.19\}\}]^{(1/0.55)}$$
$$= 2259.202$$

From Equations 5.6 and 5.7,

For no barrier condition, $\rho_s = 1216.086 - 230.29855*4.8736 = 93.7029$

$\rho_i = 2259.202 - 426.46535*4.8736 = 180.7808$

For 91 cm deep barrier, $\rho_s = 1216.086 - 230.29855*4.4341 = 194.9191$

$\rho_i = 2259.202 - 426.46535*4.4341 = 368.2123$

For 152 cm deep barrier, $\rho_s = 1216.086 - 230.29855*4.1432 = 261.9129$

$\rho_i = 2259.202 - 426.46535*4.1432 = 492.2711$

For 244 cm deep barrier, $\rho_s = 1216.086 - 230.29855*3.7140 = 360.7571$

$\rho_i = 2259.202 - 426.46535*3.7140 = 675.3100$

Change in roughness (from Equations 5.15 and 5.23),

For no barrier condition,

$$\Delta PSI = (4.2 - 1.5) *\exp[- (93.7029/ t)^{0.6}]$$
$$\Delta IRI = (4.2 - 1.19)* \exp[- (180.7808/ t)^{0.55}]$$

For no 91 cm deep barrier,

$$\Delta PSI = (4.2 - 1.5)* \exp[- (194.9191/ t)^{0.6}]$$
$$\Delta IRI = (4.2 - 1.19)* \exp[- (368.2123/ t)^{0.55}]$$

For no 152 cm deep barrier,

$$\Delta PSI = (4.2 - 1.5) * \exp[- (261.9129/ t)^{0.6}]$$

$$\Delta IRI = (4.2 - 1.19) * \exp[- (492.2711/ t)^{0.55}]$$

For no 244 cm deep barrier,

$$\Delta PSI = (4.2 - 1.5) * \exp[- (360.7571/ t)^{0.6}]$$

$$\Delta IRI = (4.2 - 1.19) * \exp[- (675.3100/ t)^{0.55}]$$

where t is in months. Change in roughness versus time for different barrier depths are shown in Figures 5.6 and 5.7.

AASHTO model

For no barrier condition,

From Equation 5.14,

$$\Delta PSI_w = (4.2 - 1.5) * 10^{\lambda}$$

Note: λ is not a constant but varies with time. For t = 40 years, λ = - 0.75861

From Equation 2.27

$$\Delta PSI_{sw} = 0.00335 * 4 * 100 * [1 - \exp(- 0.13\ t)]$$

Then the total change in PSI (ΔPSI_t)

$$\Delta PSI_t = (4.2 - 1.5) * 10^{\lambda} + 0.00335 * 4 * 100 * [1 - \exp(- 0.13\ t)]$$

where t is in years. λ needs to be calculated for each t, using Equations 5.11 and 5.13, as shown in Example 1.

Then the PSI at any time t is given by

$$PSI = 4.2 - \Delta PSI_t$$

From Equation 5.18,

$$IRI = 8.4193 * \exp[- 0.4664 * (4.2 - \Delta PSI_t)]$$

Then the total change in IRI (ΔIRI_t)

$$\Delta IRI_t = 8.4193*\exp[-0.4664*(4.2 - \Delta PSI_t)] - 1.19$$

The AASHTO model and the new model are compared in Figures 5.8 and 5.9.

EXAMPLE 3

Given

Depth of root zone		=	244 cm
Number of soil layers to depth of root zone		=	4
Mean Thornthwaite Moisture Index		=	-12.5
Width of Pavement		=	1219 cm
Distance to right wheel path from the center		=	274 cm
Initial PSI - northbound, right wheel		=	4.2
Traffic -	analysis period, C	=	20 years
	ADT in one direction when t = 0	=	1250
	ADT in one direction when t = C	=	2750
	80 kN single axles when t = C	=	702,000
Structural Number (SN)		=	16.51 cm (6.5 in)
Resilient modulus of subgrade soil		=	36544.13 kN/ m^2
		=	5300 lbf/ in^2
Reliability -	for AASHTO model	=	95%
-	for B_s and B_i	=	95%
Allowable terminal serviceability after 10 years		=	3.5

Layer thicknesses, liquid limits, plasticity indices % clay, and % fine clay are as in Table 3-3.

Desorption parameters are given in Table 5-2.

Find

Find the minimum depth of vertical moisture barrier required.

Solution

Vertical movement (from modified MOPREC program) = 9.98 cm

Amplitude of moisture depth (from modified MOPREC program) = 12.21 cm

The loss of serviceabilities for barrier depths of 0 cm, 30 cm, 60 cm, 90 cm, 120 cm, 150 cm, 180 cm, 210 cm, and 240 cm are calculated. The parameters ξ_1, ξ_2, and ξ_3 are calculated as in the Example 1. The results are tabulated in Table G-3.

Table G-3. Vertical Movement Parameters for Different Barrier Depths

Barrier Depth (cm)	ξ_1	ξ_2	ξ_3	Vertical Movement at Wheel Path (cm)
0	0.4540	0.9700	3.1509	4.8736
30	0.4423	0.9187	3.0241	4.7281
60	0.4306	0.8784	2.9473	4.5832
90	0.4189	0.8489	2.9168	4.4389
120	0.4072	0.8304	2.9312	4.2953
150	0.3955	0.8229	2.9912	4.1527
180	0.3838	0.8263	3.0996	4.0112
210	0.3721	0.8406	3.2616	3.8710
240	0.3604	0.8658	3.4851	3.7324

For 95 percent reliability, Z = 1.645

$$B_s = 162.87 + 40.99 * 1.645 = 230.29855$$

80 kN single-axle load applications for 40 years (from Equation 5.11)

$$= 702{,}000/[(20*(1250 + 2750)]*[2*1250*40 + (2750 - 1250)*40^2 /20]$$

$$= 1{,}930{,}500$$

From Equation 5.13

$$\lambda = [0.4 + 1094/(6.5 + 1)^{5.19}]*[\log_{10}(1{,}930{,}500) - 9.36*\log_{10}(6.5 +1) + 8.27 - 2.32*\log_{10}(5300) + 1.645*0.35]$$

$$= - 0.73322$$

From Equation 5.17

$$A_s = 480*[\log_e (10^{0.73322})]^{(1/0.6)}$$

$$= 1149.0025$$

From Equations 5.6 and 5.15,

For no barrier condition, $\rho_s = 1149.0025 - 230.29855*4.8736 = 26.6210$

$\Delta PSI = (4.2 - 1.5) *\exp[- (26.6210/ t)^{0.6}]$

For $t = 10$ years = 120 months,

$\Delta PSI = 2.7*\exp[- (26.6210/120)^{0.6}] = 1.80$

For 30 cm deep barrier, $\rho_s = 1149.0025 - 230.29855*4.7281 = 60.1327$

$\Delta PSI = (4.2 - 1.5) *\exp[- (60.1327/ t)^{0.6}]$

For $t = 10$ years = 120 months,

$\Delta PSI = 2.7*\exp[- (60.1327/120)^{0.6}] = 1.39$

For 60 cm deep barrier, $\rho_s = 1149.0025 - 230.29855*4.5832 = 93.4973$

$\Delta PSI = (4.2 - 1.5) *\exp[- (93.4973/ t)^{0.6}]$

For $t = 10$ years = 120 months,

$\Delta PSI = 2.7*\exp[- (93.4973/120)^{0.6}] = 1.14$

For 90 cm deep barrier, $\rho_s = 1149.0025 - 230.29855*4.4389 = 126.7268$

$\Delta PSI = (4.2 - 1.5) *\exp[- (126.7268/ t)^{0.6}]$

For $t = 10$ years = 120 months,

$\Delta PSI = 2.7*\exp[- (126.7268/120)^{0.6}] = 0.96$

For 120 cm deep barrier, $\rho_s = 1149.0025 - 230.29855*4.2953 = 159.7903$

$\Delta PSI = (4.2 - 1.5) *\exp[- (159.7903/ t)^{0.6}]$

For $t = 10$ years = 120 months,

$\Delta PSI = 2.7*\exp[- (159.7903/120)^{0.6}] = 0.82$

For 150 cm deep barrier, ρ_s = 1149.0025 - 230.29855*4.1527 = 192.6404

ΔPSI = (4.2 - 1.5) *exp[- (192.6404/ t)$^{0.6}$]

For t = 10 years = 120 months,

ΔPSI = 2.7*exp[- (192.6404/120)$^{0.6}$] = 0.72

For 180 cm deep barrier, ρ_s = 1149.0025 - 230.29855*4.0112 = 225.2279

ΔPSI = (4.2 - 1.5) *exp[- (225.2279/ t)$^{0.6}$]

For t = 10 years = 120 months,

ΔPSI = 2.7*exp[- (225.2279/120)$^{0.6}$] = 0.63

For 210 cm deep barrier, ρ_s = 1149.0025 - 230.29855*3.8710 = 257.5075

ΔPSI = (4.2 - 1.5) *exp[- (257.5075/ t)$^{0.6}$]

For t = 10 years = 120 months,

ΔPSI = 2.7*exp[- (257.5075/120)$^{0.6}$] = 0.56

For 240 cm deep barrier, ρ_s = 1149.0025 - 230.29855*3.7324 = 289.4383

ΔPSI = (4.2 - 1.5) *exp[- (289.4383/ t)$^{0.6}$]

For t = 10 years = 120 months,

ΔPSI = 2.7*exp[- (289.4383/120)$^{0.6}$] = 0.50

Allowable loss of serviceability in 10 years = 4.2 - 3.5 = 0.7

Minimum depth of barrier required = 180 cm

APPENDIX H

PRES - COMPUTER PROGRAM DOCUMENTATION

INTRODUCTION

The computer program PRES is a model to estimate the development of roughness in flexible pavements built on expansive soil subgrades. The program calculates the roughness in terms of Serviceability Index (SI) and International Roughness Index(IRI) for 20 years in one-year intervals from the date of initial construction or the date of rehabilitation. It is capable of calculating roughness in any given wheel path for pavements of up to 10 lanes in width. The program simulates the field conditions by accounting for the climatic, lateral drainage and longitudinal slope conditions, subgrade soil properties, structural properties of the pavement, and traffic. It is written in FORTRAN language. At present, the PRES program can only be run using the DOS operating system.

The roughness model first estimates the total vertical movement (the total of shrinkage and swelling) in a single column of soil at the edge of the pavement using the subgrade soil properties given in the input file. This is achieved by estimating extreme suction profiles for the given locality using the Thornthwaite Moisture Index and desorption parameters of subgrade soil. The total vertical movement in any given wheel path is then calculated using a set of regression equations. A sigmoidal model is used to describe the development of roughness over time. In the roughness model, the roughness development with time due to expansive clay activity for a wheel path is represented by a single parameter which is calculated from a regression equation using the total vertical movement estimated for that wheel path. The other parameter in the roughness model is related to the development of roughness due to traffic and is calculated from the AASHTO model.

This appendix describes how to set up the input file and run this program. A complete description of input variables is included. Also, sample input and output files are included. A listing of the program is also included in this appendix.

RUNNING PRES

In order to run the program, the file pres.exe and a data file are needed. The files may be stored either in the hard disk of the computer or in a floppy disk. Making the directory where the PRES program is located as the current directory, the program can be run by typing pres and pressing the ENTER button as in the example below.

C:\>pres ↵

Then the following command is appeared in the screen.

ENTER NAME OF THE INPUT FILE

At this prompt, the name of the input file should be given. If the input file is in the current directory, only the name of the input file is required. If the input file is in some other directory, the file name including the path should be given as in the example below.

A:\>pres.dat ↵

Following entering the input file name the following command will appear in the screen.

ENTER NAME OF THE OUTPUT FILE

At this prompt, the name of the output file should be given including the path as in the example below.

A:\>pres.out ↵

After the completion of running the program, the results will be stored in the output file. From this point, it can be printed out or transferred to a graphical software for plotting.

THE INPUT FILE

The input file for PRES is a simple nonformatted list of the input data. Values can be entered as real numbers or integers. Data should be entered in the input file in the order of the card numbers given in the input guide. Data in one card can be entered in more than one

line. However, the order of the data given in the input guide should be preserved. Data for a new card number should always be started in a new line.

Input Guide

Card 1 Program Identification Data and Title. Format (20A4).

This data should comprise one line of alphanumeric characters up to a maximum of 80 characters.

Card 2 NLAY, ICEC.

NLAY Number of subgrade soil layers up to the depth of root zone. Maximum number of layers that can be entered is 10.

ICEC A flag to indicate whether the cation exchange capacity is given in the input file. If the data is entered in the input file, ICEC = 1. If the data is not entered in the data file, ICEC = 0.

Card 3A TH(I), XLL(I), PI(I), CLAY(I), FINE(I), AWL(I), XWL(I), TSAT(I), I = 1, NLAY

This card is read when ICEC = 0 in card 2. Card is repeated NLAY times as new lines. The sum of thicknesses of subgrade soil layers ($\sum$ TH(I)) should be equal to the depth of root zone. The first layer should be the top layer of the soil profile. Data for other layers should be in the order they are in the profile. The last layer should be the bottom layer of the profile.

TH(I) Thickness of subgrade soil layer "I" in m.

XLL(I) Liquid Limit (%) of subgrade soil layer "I."

PI(I) Plasticity Index (%) of subgrade soil layer "I."

CLAY(I) Clay content (% passing No. 200 sieve) of subgrade soil layer "I."

FINE(I) Fine clay content (% less than 2 microns) of subgrade soil layer "I."

AWL(I) Gardner's desorption constant "a" of subgrade soil layer "I."

XWL(I) Gardner's desorption constant "x" of subgrade soil layer "I."

TSAT(I) Porosity of subgrade soil layer "I."

In this case, the cation exchange capacity is estimated from Equation 2.16. The larger value estimated from the two expressions in Equation 2.16 is used for the cation exchange capacity.

Card 3B TH(I), XLL(I), PI(I), CLAY(I), FINE(I), CEC(I), AWL(I), XWL(I), TSAT(I), I = NLAY

This card is read when ICEC = 1 in card 2. Card is repeated NLAY times as new lines. The sum of thicknesses of subgrade soil layers ($\sum$ TH(I)) should be equal to the depth of root zone. The first layer should be the top layer of the soil profile. Data for other layers should be in the order they are in the profile. The last layer should be the bottom layer of the profile.

CEC(I) Cation exchange capacity of subgrade soil layer "I" in meq/100 g.

Other parameters are as in Card 3A.

Card 4 TIM, ZR

TIM Mean Thornthwaite Moisture Index at the site (from Figure 3.1).

ZR Depth of root zone at the site in m.

Card 5 IFLG1, IFLG2

IFLG1 A flag to give the longitudinal slope condition. IFLG1 should be equal to 1, 2, or 3 as follows.

"Flat" slope condition	-	1
"Hill" slope condition	-	2
"Valley" slope condition	-	3

IFLG2 A flag to give the lateral drainage condition. IFLG1 should be equal to 1, 2, or 3 as follows.

"Negative" drainage condition	-	1
"Zero" drainage condition	-	2
"Positive" drainage condition	-	3

Card 6 NELEM(I), I = 1, NLAY

For accurate estimation of suction profiles and the vertical movement, each layer of soil should be divided into several sub layers. Total number of sub layers ($\sum$ NELEM(I)) should not exceed 95. Data may be entered in a single line.

NELEM(I) Number of sub layers of subgrade soil layer "I."

Card 7 WDTH, NBD, NWL

WDTH Width of the pavement in m.

NBD Number of barrier depths are used in the analysis. Maximum number of barrier depths that can be used is 10.

NWL Number of wheel paths. Maximum number of wheel paths that can be used is 20.

Card 8 BDEP(I), I = 1, NBD

Data may be entered in a single line.

BDEP(I) Barrier depth of barrier number "I" in m.

Card 9 DIST(I), I = 1, NWL

Data may be entered in a single line.

DIST(I) Distance to wheel path number "I" from the center of pavement in m.

Card 10 IR

IR Flag to indicate the units of roughness. IR = 1 is used to obtain roughness in terms of Serviceability Index, and IR = 2 is used to obtain roughness in terms of International Roughness Index. If the roughness is required both in terms of Serviceability Index and International Roughness Index, IR should be equal to 3.

Card 11A FSI(I), I = 1, NWL

This card is read when either IR = 1 or IR = 3 in card 9. Data may be entered in a single line.

FSI(I) Initial Serviceability Index (soon after the construction or rehabilitation) of the wheel path number "I." Typical value for FSI is 4.2.

Card 11B FIRI(I), I = 1, NWL

This card is read when either IR = 2 or IR = 3 in card 10. Data may be entered in a single line.

FIRI(I) Initial International Roughness Index (soon after the construction or rehabilitation) of the wheel path number "I" in m/ km. Typical value for FIRI is 1.19

Card 12 SN, RESM

SN Structural number (AASHTO) of the pavement section in mm.

RESM Resilient Modulus of the subgrade in kN/ m^2.

Card 13 C(I), RZ(I), RC(I), TC(I), I = 1, NWL

Card is repeated NWL times as new lines. In entering data, the same order that used in Card 9 should be used.

C(I) Traffic analysis period of the wheel path number "I" in years.

RZ(I) Average daily traffic (ADT) of the wheel path number "I" at the beginning of analysis period.

RC(I) Average daily traffic (ADT) of the wheel path number "I" at the end of analysis period.

TC(I) Cumulative 80 kN single load applications on the wheel path number "I" at the end of analysis period.

Card 14 RELA, RELB

The percent reliability that can be used is 50, 60, 70, 75, 80, 85, 90, 95, 97, and 99.

RELA Percent reliability for the AASHTO model to calculate the serviceability loss due to traffic.

RELB Percent reliability for the roughness constants B_s and B_i.

THE OUTPUT FILE

One output file is generated by the program. Name of the file is given by the user. The output file gives the input data with appropriate names and headings so that the user can check the input data entered in the input file. Following the input data, the results of the analysis are provided.

SAMPLE INPUT FILE

```
CONVERSE, FM 1516
   4  0
  .915    50.4  31.6  83.4  40.6  .0278  .3952  .521
  .61     83.4  54    89.8  48    .0299  .3705  .623
  .61     72.9  49.4  89.4  46.7  .0297  .3638  .604
  .305    80    51.3  90.3  52.3  .0299  .3705  .623
  -12.5    2.44
  1  1
  15  10  10   5
  12.19    4    4
  0  .91  1.52  2.44
  2.74   .91   .91   2.74
  3
  4.2   4.2   4.20  4.20
  1.19  1.19  1.19  1.19
  168.402  36544.132
  20  1250  2750  702000
  20  1250  2750  702000
  20  1250  2750  702000
  20  1250  2750  702000
  95  95
```

SAMPLE OUTPUT FILE

CONVERSE, FM 1516

OUTPUT FILE - PRES

DATA

LAYER # 1

THICKNESS	=	.92 m
SOIL PROPERTIES		
LIQUID LIMIT (%)	=	50.40
PLASTICITY INDEX (%)	=	31.60
PERCENT PASSING # 200	=	83.40
PERCENT FINE CLAY	=	40.60
CATION EXCHANGE CAPACITY	=	35.70 meq/100 g
DESORPTION CURVE "AWL" VALUE	=	.0278
DESORPTION CURVE "XWL" VALUE	=	.3952
DESORPTION CURVE "POROSITY" VALUE	=	.5210

LAYER # 2

THICKNESS	=	.61 m
SOIL PROPERTIES		
LIQUID LIMIT (%)	=	83.40
PLASTICITY INDEX (%)	=	54.00
PERCENT PASSING # 200	=	89.80
PERCENT FINE CLAY	=	48.00
CATION EXCHANGE CAPACITY	=	56.51 meq/100 g
DESORPTION CURVE "AWL" VALUE	=	.0299
DESORPTION CURVE "XWL" VALUE	=	.3705
DESORPTION CURVE "POROSITY" VALUE	=	.6230

LAYER # 3

THICKNESS	=	.61 m
SOIL PROPERTIES		
LIQUID LIMIT (%)	=	72.90
PLASTICITY INDEX (%)	=	49.40
PERCENT PASSING # 200	=	89.40
PERCENT FINE CLAY	=	46.70
CATION EXCHANGE CAPACITY	=	49.98 meq/100 g
DESORPTION CURVE "AWL" VALUE	=	.0297
DESORPTION CURVE "XWL" VALUE	=	.3638
DESORPTION CURVE "POROSITY" VALUE	=	.6040

LAYER # 4

THICKNESS	=	.31 m
SOIL PROPERTIES		
LIQUID LIMIT (%)	=	80.00
PLASTICITY INDEX (%)	=	51.30
PERCENT PASSING # 200	=	90.30
PERCENT FINE CLAY	=	52.30
CATION EXCHANGE CAPACITY	=	54.40 meq/100 g
DESORPTION CURVE "AWL" VALUE	=	.0299
DESORPTION CURVE "XWL" VALUE	=	.3705
DESORPTION CURVE "POROSITY" VALUE	=	.6230

ELEMENT DATA

LAYER NO.	LAYER THICK.(m)	NO. OF ELEMENTS
1	.92	15
2	.61	10
3	.61	10
4	.31	5

ENVIRONMENTAL AND GEOMETRICAL DATA

MEAN THORNTHWAITE MOISTURE INDEX	=	-12.50
ROOT DEPTH	=	2.44 m
WIDTH OF PAVEMENT	=	12.19 m

BARRIER DATA

NO.	BARRIER DEPTH (m)

1	.00
2	.91
3	1.52
4	2.44

WHEEL PATH DATA

NO.	DIST. FROM THE CENTER OF PAVEMENT (m)
1	2.74
2	.91
3	.91
4	2.74

INITIAL ROUGHNESS

WHEEL PATH NO.	SI	IRI (m/km)
1	4.20	1.19
2	4.20	1.19
3	4.20	1.19
4	4.20	1.19

STRUCTURAL PROPERTIES OF PAVEMENT

STRUCTURAL NUMBER	=	168.4020 mm
RESILIENT MODULUS	=	36544.13 kPa

TRAFFIC DATA

WHEEL PATH NO. 1

TRAFFIC ANALYSIS PERIOD	=	20.0 Years
ADT IN ONE DIRECTION WHEN T=0	=	1250.0
ADT IN ONE DIRECTION WHEN T=C	=	2750.0
80 KN SINGLE AXLES WHEN T=C	=	702000.0

WHEEL PATH NO. 2

TRAFFIC ANALYSIS PERIOD	=	20.0 Years
ADT IN ONE DIRECTION WHEN T=0	=	1250.0
ADT IN ONE DIRECTION WHEN T=C	=	2750.0
80 KN SINGLE AXLES WHEN T=C	=	702000.0

WHEEL PATH NO. 3

TRAFFIC ANALYSIS PERIOD	=	20.0 Years
ADT IN ONE DIRECTION WHEN T=0	=	1250.0
ADT IN ONE DIRECTION WHEN T=C	=	2750.0
80 KN SINGLE AXLES WHEN T=C	=	702000.0

WHEEL PATH NO. 4

TRAFFIC ANALYSIS PERIOD	=	20.0 Years
ADT IN ONE DIRECTION WHEN T=0	=	1250.0
ADT IN ONE DIRECTION WHEN T=C	=	2750.0
80 KN SINGLE AXLES WHEN T=C	=	702000.0

RELIABILITY

FOR TRAFFIC	=	95.0
FOR ROUGHNESS CONSTANTS Bs AND Bi	=	95.0

RESULTS

SUCTION COMPRESSION INDEX (SCI)

LAYER NO.	SCI
1	.0794
2	.0871
3	.0851
4	.0944

DEPTH OF AVAILABLE MOISTURE dam	=	31.95 cm
STD. DEVIATION OF THORNTHWAITE MOISTURE INDEX	=	14.19
MAXIMUM TMI AT THE SITE	=	12.35
MINIMUM TMI AT THE SITE	=	-37.35

MEAN EXPECTED SOIL MOISTURE DEPTH AT SITE = 9.62 cm
MAX. EXPECTED SOIL MOISTURE DEPTH AT SITE = 30.22 cm
MIN. EXPECTED SOIL MOISTURE DEPTH AT SITE = .00 cm
AMPLITUDE OF MOISTURE DEPTH = 12.21 cm

MATRIX POTENTIAL OF SOIL AT FIELD CAPACITY = 2.00
MOISTURE CONTENT OF SOIL AT MEAN pF = .3145
MATRIX POTENTIAL OF SOIL AT MEAN TMI = 3.87

TOTAL POTENTIAL VERTICAL SWELLING = 8.06 cm
TOTAL POTENTIAL VERTICAL SHRINKAGE = 1.92 cm
TOTAL 1-D VERTICAL MOVEMENT = 9.98 cm

BARRIER DEPTH = .00 cm
PARAMETERS FOR VERTICAL MOVEMENT
XI-1 = .4540
XI-2 = .9700
XI-3 = 3.1509

EQUATION FOR 2D VERTICAL MOVEMENT
VM = 4.53 * EXP((.9700 * d/D) ** 3.1509)

VERTICAL MOVEMENT

DISTANCE FROM CENTER ,d, (cm)	VERTICAL MOVEMENT, VM, (cm)
274.0	4.8736
91.0	4.5401
91.0	4.5401
274.0	4.8736

WHEEL PATH NO. 1
DISTANCE FROM CENTER OF THE PAVEMENT = 274.00cm

ROUGHNESS CONSTANTS
THE COEFFICIENT ,As = 1216.0848
THE COEFFICIENT ,Bs = 230.2985
THE COEFFICIENT ,Rhos = 93.7032
THE COEFFICIENT ,Ai = 2259.1998
THE COEFFICIENT ,Bi = 426.4654
THE COEFFICIENT ,Rhoi = 180.7808

ESTIMATED ROUGHNESS WITH TIME

YEAR	SERVICEABILITY INDEX	INTERNATIONAL ROUGHNESS INDEX (m/km)
0	4.20	1.19
1	4.11	1.23
2	3.92	1.33
3	3.74	1.46
4	3.59	1.57
5	3.47	1.67
6	3.36	1.76
7	3.27	1.85
8	3.19	1.92
9	3.12	1.99
10	3.06	2.05
11	3.00	2.11
12	2.95	2.16
13	2.91	2.21
14	2.87	2.25
15	2.83	2.29
16	2.79	2.33
17	2.76	2.37
18	2.73	2.41
19	2.70	2.44
20	2.67	2.47

WHEEL PATH NO. 2

DISTANCE FROM CENTER OF THE PAVEMENT = 91.00cm

ROUGHNESS CONSTANTS

THE COEFFICIENT ,As	= 1216.0848
THE COEFFICIENT ,Bs	= 230.2985
THE COEFFICIENT ,Rhos	= 170.5160
THE COEFFICIENT ,Ai	= 2259.1998
THE COEFFICIENT ,Bi	= 426.4654
THE COEFFICIENT ,Rhoi	= 323.0223

ESTIMATED ROUGHNESS WITH TIME

YEAR	SERVICEABILITY INDEX	INTERNATIONAL ROUGHNESS INDEX (m/km)
0	4.20	1.19
1	4.18	1.20
2	4.09	1.24
3	3.99	1.30
4	3.88	1.36
5	3.78	1.43
6	3.70	1.50
7	3.61	1.56
8	3.54	1.62
9	3.48	1.67
10	3.41	1.73
11	3.36	1.78
12	3.31	1.82
13	3.26	1.87
14	3.22	1.91
15	3.17	1.95
16	3.14	1.99
17	3.10	2.02
18	3.07	2.05
19	3.03	2.09
20	3.00	2.12

WHEEL PATH NO. 3

DISTANCE FROM CENTER OF THE PAVEMENT = 91.00cm

ROUGHNESS CONSTANTS

THE COEFFICIENT ,As	= 1216.0848
THE COEFFICIENT ,Bs	= 230.2985
THE COEFFICIENT ,Rhos	= 170.5160
THE COEFFICIENT ,Ai	= 2259.1998
THE COEFFICIENT ,Bi	= 426.4654
THE COEFFICIENT ,Rhoi	= 323.0223

ESTIMATED ROUGHNESS WITH TIME

YEAR	SERVICEABILITY INDEX	INTERNATIONAL ROUGHNESS INDEX (m/km)
0	4.20	1.19
1	4.18	1.20
2	4.09	1.24
3	3.99	1.30
4	3.88	1.36
5	3.78	1.43
6	3.70	1.50
7	3.61	1.56
8	3.54	1.62
9	3.48	1.67
10	3.41	1.73
11	3.36	1.78
12	3.31	1.82
13	3.26	1.87
14	3.22	1.91
15	3.17	1.95
16	3.14	1.99
17	3.10	2.02
18	3.07	2.05
19	3.03	2.09

20	3.00	2.12

WHEEL PATH NO. 4
DISTANCE FROM CENTER OF THE PAVEMENT = 274.00cm

ROUGHNESS CONSTANTS

THE COEFFICIENT ,As	= 1216.0848
THE COEFFICIENT ,Bs	= 230.2985
THE COEFFICIENT ,Rhos	= 93.7032
THE COEFFICIENT ,Ai	= 2259.1998
THE COEFFICIENT ,Bi	= 426.4654
THE COEFFICIENT ,Rhoi	= 180.7808

ESTIMATED ROUGHNESS WITH TIME

YEAR	SERVICEABILITY INDEX	INTERNATIONAL ROUGHNESS INDEX (m/km)
0	4.20	1.19
1	4.11	1.23
2	3.92	1.33
3	3.74	1.46
4	3.59	1.57
5	3.47	1.67
6	3.36	1.76
7	3.27	1.85
8	3.19	1.92
9	3.12	1.99
10	3.06	2.05
11	3.00	2.11
12	2.95	2.16
13	2.91	2.21
14	2.87	2.25
15	2.83	2.29
16	2.79	2.33
17	2.76	2.37
18	2.73	2.41
19	2.70	2.44
20	2.67	2.47

BARRIER DEPTH = 91.00 cm
PARAMETERS FOR VERTICAL MOVEMENT

XI-1	=	.4185
XI-2	=	.8481
XI-3	=	2.9165

EQUATION FOR 2D VERTICAL MOVEMENT

```
VM =  4.18 * EXP((   .8481 * d/D) **   2.9165)
```

VERTICAL MOVEMENT

DISTANCE FROM CENTER ,d, (cm)	VERTICAL MOVEMENT, VM, (cm)
274.0	4.4341
91.0	4.1857
91.0	4.1857
274.0	4.4341

WHEEL PATH NO. 1
DISTANCE FROM CENTER OF THE PAVEMENT = 274.00cm

ROUGHNESS CONSTANTS

THE COEFFICIENT ,As	= 1216.0848
THE COEFFICIENT ,Bs	= 230.2985
THE COEFFICIENT ,Rhos	= 194.9140
THE COEFFICIENT ,Ai	= 2259.1998
THE COEFFICIENT ,Bi	= 426.4654
THE COEFFICIENT ,Rhoi	= 368.2024

ESTIMATED ROUGHNESS WITH TIME

YEAR	SERVICEABILITY INDEX	INTERNATIONAL ROUGHNESS INDEX (m/km)
0	4.20	1.19
1	4.19	1.19
2	4.12	1.22
3	4.03	1.27
4	3.93	1.33
5	3.84	1.39
6	3.76	1.45
7	3.69	1.51
8	3.62	1.56
9	3.55	1.61
10	3.49	1.66
11	3.44	1.71
12	3.39	1.75
13	3.34	1.80
14	3.30	1.84
15	3.25	1.87
16	3.22	1.91
17	3.18	1.94
18	3.15	1.98
19	3.11	2.01
20	3.08	2.04

WHEEL PATH NO. 2
DISTANCE FROM CENTER OF THE PAVEMENT = 91.00cm

ROUGHNESS CONSTANTS

THE COEFFICIENT ,As	= 1216.0848
THE COEFFICIENT ,Bs	= 230.2985
THE COEFFICIENT ,Rhos	= 252.1287
THE COEFFICIENT ,Ai	= 2259.1998
THE COEFFICIENT ,Bi	= 426.4654
THE COEFFICIENT ,Rhoi	= 474.1522

ESTIMATED ROUGHNESS WITH TIME

YEAR	SERVICEABILITY INDEX	INTERNATIONAL ROUGHNESS INDEX (m/km)
0	4.20	1.19
1	4.19	1.19
2	4.16	1.21
3	4.09	1.24
4	4.02	1.28
5	3.95	1.32
6	3.88	1.37
7	3.81	1.42
8	3.75	1.46
9	3.69	1.51
10	3.63	1.55
11	3.58	1.59
12	3.53	1.63
13	3.49	1.67
14	3.45	1.70
15	3.41	1.74
16	3.37	1.77
17	3.33	1.80
18	3.30	1.83
19	3.27	1.86
20	3.24	1.89

WHEEL PATH NO. 3
DISTANCE FROM CENTER OF THE PAVEMENT = 91.00cm

ROUGHNESS CONSTANTS

THE COEFFICIENT ,As	= 1216.0848
THE COEFFICIENT ,Bs	= 230.2985
THE COEFFICIENT ,Rhos	= 252.1287
THE COEFFICIENT ,Ai	= 2259.1998

THE COEFFICIENT ,Bi = 426.4654
THE COEFFICIENT ,Rhoi = 474.1522

ESTIMATED ROUGHNESS WITH TIME

YEAR	SERVICEABILITY INDEX	INTERNATIONAL ROUGHNESS INDEX (m/km)
0	4.20	1.19
1	4.19	1.19
2	4.16	1.21
3	4.09	1.24
4	4.02	1.28
5	3.95	1.32
6	3.88	1.37
7	3.81	1.42
8	3.75	1.46
9	3.69	1.51
10	3.63	1.55
11	3.58	1.59
12	3.53	1.63
13	3.49	1.67
14	3.45	1.70
15	3.41	1.74
16	3.37	1.77
17	3.33	1.80
18	3.30	1.83
19	3.27	1.86
20	3.24	1.89

WHEEL PATH NO. 4
DISTANCE FROM CENTER OF THE PAVEMENT = 274.00cm

ROUGHNESS CONSTANTS
THE COEFFICIENT ,As = 1216.0848
THE COEFFICIENT ,Bs = 230.2985
THE COEFFICIENT ,Rhos = 194.9140
THE COEFFICIENT ,Ai = 2259.1998
THE COEFFICIENT ,Bi = 426.4654
THE COEFFICIENT ,Rhoi = 368.2024

ESTIMATED ROUGHNESS WITH TIME

YEAR	SERVICEABILITY INDEX	INTERNATIONAL ROUGHNESS INDEX (m/km)
0	4.20	1.19
1	4.19	1.19
2	4.12	1.22
3	4.03	1.27
4	3.93	1.33
5	3.84	1.39
6	3.76	1.45
7	3.69	1.51
8	3.62	1.56
9	3.55	1.61
10	3.49	1.66
11	3.44	1.71
12	3.39	1.75
13	3.34	1.80
14	3.30	1.84
15	3.25	1.87
16	3.22	1.91
17	3.18	1.94
18	3.15	1.98
19	3.11	2.01
20	3.08	2.04

BARRIER DEPTH = 152.00 cm
PARAMETERS FOR VERTICAL MOVEMENT
XI-1 = .3947
XI-2 = .8228

XI-3 = 2.9969

EQUATION FOR 2D VERTICAL MOVEMENT

VM = 3.94 * EXP((.8228 * d/D) ** 2.9969)

VERTICAL MOVEMENT

DISTANCE FROM CENTER ,d, (cm)	VERTICAL MOVEMENT, VM, (cm)
274.0	4.1432
91.0	3.9455
91.0	3.9455
274.0	4.1432

WHEEL PATH NO. 1

DISTANCE FROM CENTER OF THE PAVEMENT = 274.00cm

ROUGHNESS CONSTANTS

THE COEFFICIENT ,As	= 1216.0848
THE COEFFICIENT ,Bs	= 230.2985
THE COEFFICIENT ,Rhos	= 261.9038
THE COEFFICIENT ,Ai	= 2259.1998
THE COEFFICIENT ,Bi	= 426.4654
THE COEFFICIENT ,Rhoi	= 492.2537

ESTIMATED ROUGHNESS WITH TIME

YEAR	SERVICEABILITY INDEX	INTERNATIONAL ROUGHNESS INDEX (m/km)
0	4.20	1.19
1	4.20	1.19
2	4.16	1.21
3	4.10	1.23
4	4.03	1.27
5	3.96	1.31
6	3.89	1.36
7	3.83	1.40
8	3.77	1.45
9	3.71	1.49
10	3.65	1.53
11	3.60	1.57
12	3.55	1.61
13	3.51	1.65
14	3.47	1.68
15	3.43	1.72
16	3.39	1.75
17	3.36	1.78
18	3.32	1.81
19	3.29	1.84
20	3.26	1.87

WHEEL PATH NO. 2

DISTANCE FROM CENTER OF THE PAVEMENT = 91.00cm

ROUGHNESS CONSTANTS

THE COEFFICIENT ,As	= 1216.0848
THE COEFFICIENT ,Bs	= 230.2985
THE COEFFICIENT ,Rhos	= 307.4337
THE COEFFICIENT ,Ai	= 2259.1998
THE COEFFICIENT ,Bi	= 426.4654
THE COEFFICIENT ,Rhoi	= 576.5656

ESTIMATED ROUGHNESS WITH TIME

YEAR	SERVICEABILITY INDEX	INTERNATIONAL ROUGHNESS INDEX (m/km)
0	4.20	1.19
1	4.20	1.19
2	4.17	1.20
3	4.13	1.22
4	4.07	1.25
5	4.01	1.28

6	3.95	1.32
7	3.89	1.36
8	3.84	1.40
9	3.79	1.43
10	3.73	1.47
11	3.69	1.51
12	3.64	1.54
13	3.60	1.58
14	3.56	1.61
15	3.52	1.64
16	3.48	1.67
17	3.45	1.70
18	3.42	1.73
19	3.38	1.76
20	3.35	1.79

WHEEL PATH NO. 3
DISTANCE FROM CENTER OF THE PAVEMENT = 91.00cm

ROUGHNESS CONSTANTS

THE COEFFICIENT ,As	= 1216.0848
THE COEFFICIENT ,Bs	= 230.2985
THE COEFFICIENT ,Rhos	= 307.4337
THE COEFFICIENT ,Ai	= 2259.1998
THE COEFFICIENT ,Bi	= 426.4654
THE COEFFICIENT ,Rhoi	= 576.5656

ESTIMATED ROUGHNESS WITH TIME

YEAR	SERVICEABILITY INDEX	INTERNATIONAL ROUGHNESS INDEX (m/km)
0	4.20	1.19
1	4.20	1.19
2	4.17	1.20
3	4.13	1.22
4	4.07	1.25
5	4.01	1.28
6	3.95	1.32
7	3.89	1.36
8	3.84	1.40
9	3.79	1.43
10	3.73	1.47
11	3.69	1.51
12	3.64	1.54
13	3.60	1.58
14	3.56	1.61
15	3.52	1.64
16	3.48	1.67
17	3.45	1.70
18	3.42	1.73
19	3.38	1.76
20	3.35	1.79

WHEEL PATH NO. 4
DISTANCE FROM CENTER OF THE PAVEMENT = 274.00cm

ROUGHNESS CONSTANTS

THE COEFFICIENT ,As	= 1216.0848
THE COEFFICIENT ,Bs	= 230.2985
THE COEFFICIENT ,Rhos	= 261.9038
THE COEFFICIENT ,Ai	= 2259.1998
THE COEFFICIENT ,Bi	= 426.4654
THE COEFFICIENT ,Rhoi	= 492.2537

ESTIMATED ROUGHNESS WITH TIME

YEAR	SERVICEABILITY INDEX	INTERNATIONAL ROUGHNESS INDEX (m/km)
0	4.20	1.19
1	4.20	1.19

2	4.16	1.21
3	4.10	1.23
4	4.03	1.27
5	3.96	1.31
6	3.89	1.36
7	3.83	1.40
8	3.77	1.45
9	3.71	1.49
10	3.65	1.53
11	3.60	1.57
12	3.55	1.61
13	3.51	1.65
14	3.47	1.68
15	3.43	1.72
16	3.39	1.75
17	3.36	1.78
18	3.32	1.81
19	3.29	1.84
20	3.26	1.87

BARRIER DEPTH = 244.00 cm

PARAMETERS FOR VERTICAL MOVEMENT

XI-1 = .3588

XI-2 = .8700

XI-3 = 3.5201

EQUATION FOR 2D VERTICAL MOVEMENT

VM = 3.58 * EXP((.8700 * d/D) ** 3.5201)

VERTICAL MOVEMENT

DISTANCE FROM CENTER ,d, (cm)	VERTICAL MOVEMENT, VM, (cm)
274.0	3.7140
91.0	3.5828
91.0	3.5828
274.0	3.7140

WHEEL PATH NO. 1

DISTANCE FROM CENTER OF THE PAVEMENT = 274.00cm

ROUGHNESS CONSTANTS

THE COEFFICIENT ,As = 1216.0848

THE COEFFICIENT ,Bs = 230.2985

THE COEFFICIENT ,Rhos = 360.7496

THE COEFFICIENT ,Ai = 2259.1998

THE COEFFICIENT ,Bi = 426.4654

THE COEFFICIENT ,Rhoi = 675.2956

ESTIMATED ROUGHNESS WITH TIME

YEAR	SERVICEABILITY INDEX	INTERNATIONAL ROUGHNESS INDEX (m/km)
0	4.20	1.19
1	4.20	1.19
2	4.18	1.20
3	4.15	1.21
4	4.11	1.23
5	4.06	1.26
6	4.01	1.29
7	3.95	1.32
8	3.90	1.35
9	3.86	1.38
10	3.81	1.42
11	3.77	1.45
12	3.72	1.48
13	3.68	1.51
14	3.64	1.54
15	3.61	1.57

16	3.57	1.60
17	3.54	1.63
18	3.51	1.65
19	3.48	1.68
20	3.45	1.70

WHEEL PATH NO. 2
DISTANCE FROM CENTER OF THE PAVEMENT = 91.00cm

ROUGHNESS CONSTANTS

THE COEFFICIENT ,As	= 1216.0848
THE COEFFICIENT ,Bs	= 230.2985
THE COEFFICIENT ,Rhos	= 390.9640
THE COEFFICIENT ,Ai	= 2259.1998
THE COEFFICIENT ,Bi	= 426.4654
THE COEFFICIENT ,Rhoi	= 731.2466

ESTIMATED ROUGHNESS WITH TIME

YEAR	SERVICEABILITY INDEX	INTERNATIONAL ROUGHNESS INDEX (m/km)
0	4.20	1.19
1	4.20	1.19
2	4.19	1.19
3	4.16	1.21
4	4.12	1.22
5	4.08	1.25
6	4.03	1.27
7	3.98	1.30
8	3.94	1.33
9	3.89	1.36
10	3.85	1.39
11	3.80	1.42
12	3.76	1.45
13	3.72	1.48
14	3.69	1.51
15	3.65	1.54
16	3.62	1.56
17	3.58	1.59
18	3.55	1.62
19	3.52	1.64
20	3.49	1.67

WHEEL PATH NO. 3
DISTANCE FROM CENTER OF THE PAVEMENT = 91.00cm

ROUGHNESS CONSTANTS

THE COEFFICIENT ,As	= 1216.0848
THE COEFFICIENT ,Bs	= 230.2985
THE COEFFICIENT ,Rhos	= 390.9640
THE COEFFICIENT ,Ai	= 2259.1998
THE COEFFICIENT ,Bi	= 426.4654
THE COEFFICIENT ,Rhoi	= 731.2466

ESTIMATED ROUGHNESS WITH TIME

YEAR	SERVICEABILITY INDEX	INTERNATIONAL ROUGHNESS INDEX (m/km)
0	4.20	1.19
1	4.20	1.19
2	4.19	1.19
3	4.16	1.21
4	4.12	1.22
5	4.08	1.25
6	4.03	1.27
7	3.98	1.30
8	3.94	1.33
9	3.89	1.36
10	3.85	1.39
11	3.80	1.42

12	3.76	1.45
13	3.72	1.48
14	3.69	1.51
15	3.65	1.54
16	3.62	1.56
17	3.58	1.59
18	3.55	1.62
19	3.52	1.64
20	3.49	1.67

WHEEL PATH NO. 4
DISTANCE FROM CENTER OF THE PAVEMENT = 274.00cm

ROUGHNESS CONSTANTS

THE COEFFICIENT ,As	= 1216.0848
THE COEFFICIENT ,Bs	= 230.2985
THE COEFFICIENT ,Rhos	= 360.7496
THE COEFFICIENT ,Ai	= 2259.1998
THE COEFFICIENT ,Bi	= 426.4654
THE COEFFICIENT ,Rhoi	= 675.2956

ESTIMATED ROUGHNESS WITH TIME

YEAR	SERVICEABILITY INDEX	INTERNATIONAL ROUGHNESS INDEX (m/km)
0	4.20	1.19
1	4.20	1.19
2	4.18	1.20
3	4.15	1.21
4	4.11	1.23
5	4.06	1.26
6	4.01	1.29
7	3.95	1.32
8	3.90	1.35
9	3.86	1.38
10	3.81	1.42
11	3.77	1.45
12	3.72	1.48
13	3.68	1.51
14	3.64	1.54
15	3.61	1.57
16	3.57	1.60
17	3.54	1.63
18	3.51	1.65
19	3.48	1.68
20	3.45	1.70

LISTING OF THE PRES PROGRAM

```
C*********************************************************************
C     PRES.FOR  A PROGRAM TO CALCULATE PAVEMENT ROUGHNESS IN TERMS OF
C     SERVICEABILITY INDEX AND INTERNATIONAL ROUGHNESS INDEX AT
C     DIFFERENT WHEEL PATHS GIVEN THE MEAN THORNTHWAITE MOISTURE INDEX,
C     SOIL PROPERTIES, GEOMETRY OF THE PAVEMENT, TRAFFIC, INITIAL
C     ROUGHNESS, AND DEPTH OF VERTICAL MOISTURE BARRIERS.
C*********************************************************************
      IMPLICIT REAL*8(A-H,O-Z)
      CHARACTER INFILE*12
      CHARACTER OUTFILE*12
      DIMENSION SUMDH(2)
      INTEGER TITLE(40)
      COMMON/DES/TSAT(10),AWL(10),XWL(10)
      COMMON/TDES/TS,AAWL,XXWL
      COMMON/IFL/IFLG1,IFLG2
      COMMON/SUCI/GAMMH(10)
      COMMON/ROOT/ZR
      COMMON/NPROF1/NLAY
      COMMON/NPROF2/NELEM(10)
      COMMON/PROF/TH(10)
      COMMON/SUCTION/DELPF(96,2),Z(96),ZM(96),PFAVG(96,2)
      COMMON/GEO1/BDEP(10),DIST(20)
      COMMON/GEO2/WDTH
      COMMON/NGEO/NWL
      COMMON/SP/XLL(10),PI(10),CLAY(10),FINE(10),CEC(10)
      COMMON/VMOVE/H2D(20)
      COMMON/PR/FSI(20),FIRI(20),SN,RM
      COMMON/NPR/IR
      COMMON/TR/C(20),RZ(20),RC(20),TC(20)
      COMMON/REL/RELA,RELB
      COMMON/ROU/SI(0:25),RI(0:25)
C
      WRITE(6,'(A)')'  ENTER NAME OF THE INPUT FILE'
      READ(6,'(A)')INFILE
      WRITE(6,'(A)')'  ENTER NAME OF THE OUTPUT FILE'
      READ(6,'(A)')OUTFILE
      OPEN(UNIT=4,FILE=INFILE,STATUS='OLD')
      OPEN(UNIT=5,FILE=OUTFILE,STATUS='NEW')
C
      READ(4,'(20A4)')(TITLE(I),I=1,20)
      WRITE(5,14)(TITLE(I),I=1,20)
   14 FORMAT(20A4)
C
      READ(4,*) NLAY,ICEC
C
      DO 36 I=1,NLAY
      IF (ICEC.EQ.0) THEN
      READ(4,*) TH(I),XLL(I),PI(I),CLAY(I),FINE(I)
     *,AWL(I),XWL(I),TSAT(I)
      CEC1=(XLL(I)-PI(I))**1.17
      CEC2=(XLL(I))**0.912
      IF(CEC1.GE.CEC2) THEN
      CEC(I)=CEC1
      ELSE
      CEC(I)=CEC2
      ENDIF
      ELSE
      READ(4,*) TH(I),XLL(I),PI(I),CLAY(I),FINE(I),CEC(I)
     *,AWL(I),XWL(I),TSAT(I)
      ENDIF
   36 CONTINUE
C
      READ(4,*) TIM,ZR
C
      READ(4,*) IFLG1,IFLG2
C
      READ(4,*) (NELEM(I),I=1,NLAY)
C
```

```
      READ(4,*) WDTH,NBD,NWL
C
      READ(4,*) (BDEP(I),I=1,NBD)
C
      READ(4,*) (DIST(I),I=1,NWL)
C
      READ(4,*) IR
C
      IF(IR.EQ.1) THEN
      READ(4,*) (FSI(I),I=1,NWL)
      ELSE
      IF(IR.EQ.2) THEN
      READ(4,*) (FIRI(I),I=1,NWL)
      ELSE
      READ(4,*) (FSI(I),I=1,NWL)
      READ(4,*) (FIRI(I),I=1,NWL)
      ENDIF
      ENDIF
C
      READ(4,*) SN,RESM
C
      DO 20 I=1,NWL
      READ(4,*) C(I),RZ(I),RC(I),TC(I)
   20 CONTINUE
C
      READ(4,*) RELA,RELB
C
      WRITE(5,'(/A)')
     *' OUTPUT FILE - PRES'
C
      WRITE(5,'(/A)') '              DATA'
C
      DO 66 I=1,NLAY
      WRITE(5,'(/A,I5)') '             LAYER #',I
      WRITE(5,'(A,F8.2,A)')
     *'  THICKNESS                              = ',TH(I),' m'
      WRITE(5,'(A)') '         SOIL PROPERTIES'
      WRITE(5,'(A,F8.2/,A,F8.2/,A,F8.2/,A,F8.2/,A,F8.2,A)')
     *'  LIQUID LIMIT (%)                       = ',XLL(I),
     *'  PLASTICITY INDEX (%)                   = ',PI(I),
     *'  PERCENT PASSING # 200                  = ',CLAY(I),
     *'  PERCENT FINE CLAY                      = ',FINE(I),
     *'  CATION EXCHANGE CAPACITY               = ',CEC(I),' meq/100 g'
      WRITE(5,'(A,F8.4/,A,F8.4/,A,F8.4)')
     *'  DESORPTION CURVE "AWL" VALUE           = ',AWL(I),
     *'  DESORPTION CURVE "XWL" VALUE           = ',XWL(I),
     *'  DESORPTION CURVE "POROSITY" VALUE      = ',TSAT(I)
   66 CONTINUE
C
      WRITE(5,'(/A)') '                ELEMENT DATA'
      WRITE(5,'(A)') '  LAYER NO.   LAYER THICK.(m)   NO. OF ELEMENTS'
      DO 76 I=1,NLAY
      WRITE(5,'(2X,I5,10X,F6.2,15X,I5)') I,TH(I),NELEM(I)
   76 CONTINUE
C
      WRITE(5,'(/A)') '            ENVIRONMENTAL AND GEOMETRICAL DATA'
      WRITE(5,'(A,F8.2/,A,F8.2,A/,A,F8.2,A)')
     *'  MEAN THORNTHWAITE MOISTURE INDEX       = ',TIM,
     *'  ROOT DEPTH                             = ',ZR,' m',
     *'  WIDTH OF PAVEMENT                      = ',WDTH,' m'
C
      WRITE(5,'(/A)') '        BARRIER DATA'
      WRITE(5,'(A)') '   NO.       BARRIER DEPTH (m)'
      DO 86 I=1,NBD
      WRITE(5,'(I5,10X,F8.2)') I,BDEP(I)
   86 CONTINUE
C
      WRITE(5,'(/A)') '      WHEEL PATH DATA'
```

```
      WRITE(5,'(A)') '   NO.   DIST. FROM THE CENTER OF PAVEMENT (m)'
      DO 96 I=1,NWL
      WRITE(5,'(I5,10X,F8.2)') I,DIST(I)
   96 CONTINUE
C
      WRITE(5,'(/A)') '       INITIAL ROUGHNESS'
      IF(IR.EQ.1) THEN
      WRITE(5,'(A)') ' WHEEL PATH NO.        SI'
      DO 12 I=1,NWL
      WRITE(5,'(4X,I3,12X,F6.2)') I,FSI(I)
   12 CONTINUE
      ELSE
      IF(IR.EQ.2) THEN
      WRITE(5,'(A)') ' WHEEL PATH NO.        IRI (m/km)'
      DO 22 I=1,NWL
      WRITE(5,'(4X,I3,12X,F6.2)') I,FIRI(I)
   22 CONTINUE
      ELSE
      WRITE(5,'(A)') ' WHEEL PATH NO.        SI            IRI (m/km)'
      DO 32 I=1,NWL
      WRITE(5,'(4X,I3,12X,F6.2,7X,F6.2)') I,FSI(I),FIRI(I)
   32 CONTINUE
      ENDIF
      ENDIF
C
      WRITE(5,'(/A)') '       STRUCTURAL PROPERTIES OF PAVEMENT'
      WRITE(5,'(A,F8.4,A/,A,F12.2,A)')
     *'  STRUCTURAL NUMBER                          = ',SN,' mm',
     *'  RESILIENT MODULUS                          = ',RESM,' kPa'
C
      WRITE(5,'(/A)') '       TRAFFIC DATA'
      DO 42 I=1,NWL
      WRITE(5,'(/A,I3)') '                WHEEL PATH NO. ',I
      WRITE(5,'(A,F6.1,A/,A,F12.1/,A,F12.1/,A,F15.1)')
     *'  TRAFFIC ANALYSIS PERIOD                    = ',C(I),' Years',
     *'  ADT IN ONE DIRECTION WHEN T=0              = ',RZ(I),
     *'  ADT IN ONE DIRECTION WHEN T=C              = ',RC(I),
     *'  80 KN SINGLE AXLES WHEN T=C                = ',TC(I)
   42 CONTINUE
C
      WRITE(5,'(/A)') '       RELIABILITY'
      WRITE(5,'(A,F4.1/,A,F4.1)')
     *'  FOR TRAFFIC                                = ',RELA,
     *'  FOR ROUGHNESS CONSTANTS Bs AND Bi          = ',RELB
C
      DO 18 I=1,NLAY
      TH(I)=TH(I)*100.0
   18 CONTINUE
C
      ZR=ZR*100.0
      WDTH=WDTH*100.0
      RM=RESM/6.8951193
      SN=SN/25.4
C
      DO 28 I=1,NBD
      BDEP(I)=BDEP(I)*100.0
   28 CONTINUE
C
      DO 38 I=1,NWL
      DIST(I)=DIST(I)*100.0
   38 CONTINUE
C
      DO 17 I=1,NLAY
      CALL SOILP(I,AC,CEAC)
C
      IF(CEAC.GT.3.0.OR.AC.GT.3.0) THEN
      WRITE(5,'(/A,A,I3,A)')
     *'Error in soil properties or soil properties out of',
```

```
     *' range in layer #',I,'.'
      GOTO 500
      ENDIF
C
   17 CONTINUE
C
      SUM1=0.0
      SUM2=0.0
      SUM3=0.0
      DO 27 I=1,NLAY
      SUM1=SUM1+TSAT(I)*TH(I)
      SUM2=SUM2+AWL(I)*TH(I)
      SUM3=SUM3+XWL(I)*TH(I)
   27 CONTINUE
      TS=SUM1/ZR
      AAWL=SUM2/ZR
      XXWL=SUM3/ZR
C
      CALL THORNTH(TIM,SIGT,TIMX,TIMN)
C
      PFCAP=2.0
      PFROOT=4.5
      P1=10.0**PFCAP
      P2=10.0**PFROOT
      THET1=TS/(1.+AAWL*(P1**XXWL))
      THET2=TS/(1.+AAWL*(P2**XXWL))
      WDFCAP=ZR*(THET1-THET2)/2.0
      DM = WDTMI(TIM,WDFCAP)
      ADM=TIAMPL(TIM,WDFCAP)
      DMX = WDTMI(TIMX,WDFCAP)+ADM
      DMN = WDTMI(TIMN,WDFCAP)-ADM
      IF(DMX.GT.WDFCAP) THEN
      DMX=WDFCAP
      ENDIF
      IF(DMN.LT.0) THEN
      DMN=0
      ENDIF
C
      TFCAP=TS/(1+AAWL*(100.0**XXWL))
      TROOT=THET2
      ZC=WDFCAP/(TFCAP-TROOT)
      ZTIM=DM
      TZERO=ZTIM/ZC+TROOT
      PF0=DLOG10(((TS-TZERO)/(AAWL*TZERO))**(1./XXWL))
C
C     Call the subroutine to determine the change in pF with depth
C     for the two states of potential wetting and drying.
C
      CALL REX3(DM,DMX,DMN,TZERO,PFROOT,NEL,TIM)
C
C     Now determine the change in H due to the changes in pF with depth
C     shrink and swell calculations.
C
      CALL DELTAH(SUMDH,DELH)
C
      WRITE(5,'(//A)')
     *'              RESULTS'
C
      WRITE(5,'(/A/,A)')
     *' SUCTION COMPRESSION INDEX (SCI)',
     *'  LAYER NO.        SCI'
      WRITE(5,'(3X,I5,8X,F6.4)')(I,GAMMH(I),I=1,NLAY)
C
      WRITE(5,'(/A,F6.2,A/,A,F6.2/,A,F7.2/,A,F7.2)')
     *'  DEPTH OF AVAILABLE MOISTURE  dam                  = ',WDFCAP,' cm',
     *'  STD. DEVIATION OF THORNTHWAITE MOISTURE INDEX =',SIGT,
     *'  MAXIMUM TMI AT THE SITE                           =',TIMX,
     *'  MINIMUM TMI AT THE SITE                           =',TIMN
```

```
C
      WRITE(5,'(/A,F6.2,A/,A,F6.2,A/,A,F6.2,A/,A,F6.2,A)')
     *'  MEAN EXPECTED SOIL MOISTURE DEPTH AT SITE      =',DM,' cm',
     *'  MAX. EXPECTED SOIL MOISTURE DEPTH AT SITE      =',DMX,' cm',
     *'  MIN. EXPECTED SOIL MOISTURE DEPTH AT SITE      =',DMN,' cm',
     *'  AMPLITUDE OF MOISTURE DEPTH                    =',ADM,' cm'
C
      WRITE(5,'(/A,F6.2/,A,F6.4/,A,F6.2)')
     *'  MATRIX POTENTIAL OF SOIL AT FIELD CAPACITY     = ',PFCAP,
     *'  MOISTURE CONTENT OF SOIL AT MEAN pF            = ',TZERO,
     *'  MATRIX POTENTIAL OF SOIL AT MEAN TMI           = ',PF0
C
      WRITE(5,'(/A,F6.2,A/,A,F6.2,A/,A,F6.2,A)')
     *'  TOTAL POTENTIAL VERTICAL SWELLING  =',SUMDH(1),' cm',
     *'  TOTAL POTENTIAL VERTICAL SHRINKAGE =',SUMDH(2),' cm',
     *'  TOTAL 1-D VERTICAL MOVEMENT        =',DELH,' cm'
C
      DO 43 I=1,NBD
      WRITE(5,'(//A,F8.2,A)')
     *'          BARRIER DEPTH   =',BDEP(I),' cm'
C
      CALL VERT2D(I,DELH,TIM,ADM,AL,RO,BT)
C
      IF(AL.LE.0.0.OR.RO.LE.0.0.OR.BT.LE.0.0) THEN
      WRITE(5,'(/A,A)')
     *'Negative Parameters for Vertical Movement.  Data Out of Range',
     *'.'
      GOTO 500
      ENDIF
C
      WRITE(5,'(A/,A,F8.4/,A,F8.4/,A,F8.4)')
     *'  PARAMETERS FOR VERTICAL MOVEMENT',
     *'     XI-1     = ',AL,
     *'     XI-2     = ',RO,
     *'     XI-3     = ',BT
C
      XXX=DELH*AL
      WRITE(5,'(/A/,A,F6.2,A,F8.4,A,F8.4,A,F8.4,A)')
     *'       EQUATION FOR 2D VERTICAL MOVEMENT',
     *'  VM =',XXX,' * EXP((',RO,' * d/D) ** ',BT,')'
C
      WRITE(5,'(/A/,A)')
     *'                    VERTICAL MOVEMENT',
     *'  DISTANCE FROM CENTER ,d, (cm)     VERTICAL MOVEMENT, VM, (cm)'
C
      WRITE(5,'(10X,F8.1,25X,F8.4)')(DIST(L),H2D(L),L=1,NWL)
C
      DO 30 J=1,NWL
      CALL ROUGH(J,AS,AI,BS,BI,ROS,ROI)
C
      WRITE(5,'(//A,I3)')
     *'      WHEEL PATH NO. ',J
      WRITE(5,'(A,F8.2,A)')
     *' DISTANCE FROM CENTER OF THE PAVEMENT     = ',DIST(J),'cm'
      WRITE(5,'(/A)')
     *'   ROUGHNESS CONSTANTS'
      IF(IR.EQ.1.OR.IR.EQ.3) THEN
      WRITE(5,'(A,F10.4/,A,F10.4/,A,F10.4)')
     *' THE COEFFICIENT ,As                      =',AS,
     *' THE COEFFICIENT ,Bs                      =',BS,
     *' THE COEFFICIENT ,Rhos                    =',ROS
      IF(ROS.LE.0.0) THEN
      WRITE(5,'(/A)')
     *'Negative RhoS. Increase Structural Number and/or barrier depth.'
      GOTO 500
      ENDIF
      ENDIF
C
```

```
      IF(IR.EQ.2.OR.IR.EQ.3) THEN
      WRITE(5,'(A,F10.4/,A,F10.4/,A,F10.4)')
     *' THE COEFFICIENT ,Ai                          =',AI,
     *' THE COEFFICIENT ,Bi                          =',BI,
     *' THE COEFFICIENT ,Rhoi                        =',ROI
      IF(ROI.LE.0.0) THEN
      WRITE(5,'(/A)')
     *'Negative RhoI. Increase Structural Number and/or barrier depth.'
      GOTO 500
      ENDIF
      ENDIF
C
      WRITE(5,'(/A)')
     *'            ESTIMATED ROUGHNESS WITH TIME'
C
      IF(IR.EQ.1) THEN
      WRITE(5,'(A)')
     *' YEAR    SERVICEABILITY INDEX'
      WRITE(5,'(1X,I3,11X,F6.2)')(JJ,SI(JJ),JJ=0,20)
      ELSE
      IF(IR.EQ.2) THEN
      WRITE(5,'(A)')
     *' YEAR    INTERNATIONAL ROUGHNESS INDEX (m/km)'
      WRITE(5,'(1X,I3,16X,F6.2)')(JJ,RI(JJ),JJ=0,20)
      ELSE
      WRITE(5,'(A)')
     *'YEAR  SERVICEABILITY INDEX  INTERNATIONAL ROUGHNESS INDEX (m/km)'
      WRITE(5,'(1X,I3,11X,F6.2,22X,F6.2)')(JJ,SI(JJ),RI(JJ),JJ=0,20)
      ENDIF
      ENDIF
   30 CONTINUE
   43 CONTINUE
C
  500 CONTINUE
C
      STOP
      END
C
C***********************************************************************
      SUBROUTINE ROUGH(J,AS,AI,BS,BI,ROS,ROI)
C***********************************************************************
C     CALCULATE ROUGHNESS
C***********************************************************************
C
      IMPLICIT REAL*8(A-H,O-Z)
      COMMON/VMOVE/H2D(20)
      COMMON/PR/FSI(20),FIRI(20),SN,RM
      COMMON/NPR/IR
      COMMON/TR/C(20),RZ(20),RC(20),TC(20)
      COMMON/REL/RELA,RELB
      COMMON/ROU/SI(0:25),RI(0:25)
      DIMENSION IREL(10),ZREL(10)
      DATA IREL/50,60,70,75,80,85,90,95,97,99/,
     *ZREL/0.0,0.2533,0.5244,0.6745,0.8418,1.0365,1.2817,1.645,
     *1.8814,2.3267/
C
      DO 10 JJ=1,10
      IF(IREL(JJ).EQ.RELA) ZA=ZREL(JJ)
      IF(IREL(JJ).EQ.RELB) ZB=ZREL(JJ)
   10 CONTINUE
C
C
      XLAMDA1=0.4+1094.0/((SN+1.)**5.19)
      XLAMDA2=-9.36*DLOG10(SN+1.)+8.27-2.32*DLOG10(RM)+ZA*0.35
      W18=(TC(J)*(2.*RZ(J)*40.+(RC(J)-RZ(J))*1600./
     *C(J)))/(C(J)*(RZ(J)+RC(J)))
      XLAMDA=XLAMDA1*(DLOG10(W18)+XLAMDA2)
C
```

```
      IF(IR.EQ.1.OR.IR.EQ.3) THEN
      BS=162.87+40.99*ZB
      AS1=10.**(-XLAMDA)
      AS=480.*((DLOG(AS1))**(1./0.6))
      ROS=AS-BS*H2D(J)
      IF(ROS.LE.0.0) GOTO 400
      SI(0)=FSI(J)
      ENDIF
      IF(IR.EQ.2.OR.IR.EQ.3) THEN
      BI=306.66+72.83*ZB
      AI1=-.4664*(4.2-2.7*(10.**XLAMDA))
      AI=480.*((DLOG(3.01/(8.4193*DEXP(AI1)-1.19)))**(1./.55))
      ROI=AI-BI*H2D(J)
      IF(ROI.LE.0.0) GOTO 400
      RI(0)=FIRI(J)
      ENDIF
C
      DO 60 M=1,20
      XM=12.*M
      IF(IR.EQ.1.OR.IR.EQ.3) THEN
      SI(M)=FSI(J)-(FSI(J)-1.5)*DEXP(-((ROS/XM)**0.6))
      ENDIF
      IF(IR.EQ.2.OR.IR.EQ.3) THEN
      RI(M)=FIRI(J)+(4.2-FIRI(J))*DEXP(-((ROI/XM)**0.55))
      ENDIF
   60 CONTINUE
C
  400 CONTINUE
      RETURN
      END
C
C***********************************************************************
      SUBROUTINE SOILP(I,AC,CEAC)
C***********************************************************************
C     Determine the suction compression index.
C***********************************************************************

      IMPLICIT REAL*8(A-H,O-Z)
      COMMON/SUCI/GAMMH(10)
      COMMON/SP/XLL(10),PI(10),CLAY(10),FINE(10),CEC(10)
C
      IF (CLAY(I).EQ.0.0.OR.FINE(I).EQ.0.0) THEN
      AC=0.0
      CEAC=0.0
      PFINE=0.0
      ELSE
      PFINE=100.0*FINE(I)/CLAY(I)
      AC=PI(I)/PFINE
      CEAC=CEC(I)/PFINE
      ENDIF
C
      IF(CEAC.GT.3.0.OR.AC.GT.3.0) GOTO 16
C
      IF(CEAC.LT.0.175.AND.AC.LT.0.4) THEN
      SCI100=0.0
      GOTO 12
      ENDIF
      IF(CEAC.LT.0.23.AND.AC.GE.0.4) THEN
      SCI100=0.0
      GOTO 12
      ENDIF
C
      IF(CEAC.LT.0.4.AND.AC.LT.0.4) THEN
      SCI100=0.033
      GOTO 12
      ENDIF
      IF(CEAC.LE.1.0.AND.AC.LT.0.4) THEN
      SCI100=0.061
```

```
      GOTO 12
      ENDIF
      IF(CEAC.LT.0.5.AND.AC.LE.3.0) THEN
      SCI100=0.061
      GOTO 12
      ENDIF
      IF(CEAC.LE.1.0.AND.AC.LT.0.6) THEN
      SCI100=0.096
      GOTO 12
      ENDIF
      IF(CEAC.LT.2.5.AND.AC.LT.0.4) THEN
      SCI100=0.033
      GOTO 12
      ENDIF
      IF(CEAC.LT.1.5.AND.AC.LT.0.6) THEN
      SCI100=0.033
      GOTO 12
      ENDIF
      IF(CEAC.LT.2.5.AND.AC.LT.0.6) THEN
      SCI100=0.096
      GOTO 12
      ENDIF
      IF(CEAC.LT.1.5.AND.AC.LE.3.0) THEN
      SCI100=0.163
      GOTO 12
      ENDIF
      IF(CEAC.LE.3.0.AND.AC.LE.3.0) THEN
      SCI100=0.220
      ENDIF
   12 GAMMH(I)=SCI100*PFINE/100
C
   16 CONTINUE
      RETURN
      END
C
C*********************************************************************
      SUBROUTINE THORNTH(TIM,SIGT,TIMX,TIMN)
C*********************************************************************
      IMPLICIT REAL*8(A-H,O-Z)
      DIMENSION IYRS(9),ZRPY(9)
      DATA IYRS/20,25,30,35,40,45,50,75,100/,
     *ZRPY/1.645,1.7511,1.8338,1.90214,1.96,2.0096,
     *2.054,2.21667,2.32667/
C
      SIGT=.2833*TIM+17.73
C
      IRPY=25
      ZZ=1.7511
      TIMX=TIM+SIGT*ZZ
      TIMN=TIM-SIGT*ZZ
C
      RETURN
      END
C
C*********************************************************************
      SUBROUTINE VERT2D(I,H,T,AD,AL,RO,BT)
C*********************************************************************
      IMPLICIT REAL*8(A-H,O-Z)
      DIMENSION A1(8),R1(9),B1(8),A2(8),R2(9),B2(8)
      COMMON/GEO1/BDEP(10),DIST(20)
      COMMON/GEO2/WDTH
      COMMON/NGEO/NWL
      COMMON/VMOVE/H2D(20)
      DATA A1/2.0144,-.0238,-.000892,-.1611,-.1936,.4016,
     *     .00005336,.00004112/
      DATA R1/-1.2924,.0332,.004651,-.002591,.321,.000006077,-.2634,
     *     -.001172,.00005722/
      DATA B1/1.0725,-.07346,.008762,-.003529,.00000852,-.001458,
```

```
     *      .000121,.000156/
      DATA A2/.9061,-.03515,-.00015,.04483,-.0924,.3332,.00005867
     *      ,.000006405/
      DATA R2/-.4083,.02936,-.002136,-.001454,.1701,.000002259,
     *      -.1412,-.000186,.00002022/
      DATA B2/1.4566,-.08179,.0175,-.002933,.000008001,-.003066,
     *      .00002585,.00009203/
C
      AL1=A1(1)+A1(2)*H+A1(3)*BDEP(I)+A1(4)*DLOG(AD)+
     *    A1(5)*DLOG(WDTH/2.0)+A1(6)*(H/AD)+A1(7)*(H*T)+
     *    A1(8)*(AD*BDEP(I))
C
      RO1=R1(1)+R1(2)*H+R1(3)*T+R1(4)*BDEP(I)+R1(5)*
     *    DLOG(WDTH/2.0)+R1(6)*((BDEP(I))**2)+R1(7)*(H/AD)+
     *    R1(8)*(H*T)+R1(9)*((BDEP(I))*AD)
C
      BT1=B1(1)+B1(2)*H+B1(3)*T+B1(4)*(BDEP(I))+B1(5)*
     *    ((BDEP(I))**2)+B1(6)*(H*T)+B1(7)*(H*WDTH/2.0)+
     *    B1(8)*((BDEP(I))*AD)
C
      AL2=A2(1)+A2(2)*H+A2(3)*BDEP(I)+A2(4)*DLOG(AD)+
     *    A2(5)*DLOG(WDTH/2.0)+A2(6)*(H/AD)+A2(7)*(H*T)+
     *    A2(8)*(AD*BDEP(I))
C
      RO2=R2(1)+R2(2)*H+R2(3)*T+R2(4)*BDEP(I)+R2(5)*
     *    DLOG(WDTH/2.0)+R2(6)*((BDEP(I))**2)+R2(7)*(H/AD)+
     *    R2(8)*(H*T)+R2(9)*((BDEP(I))*AD)
C
      BT2=B2(1)+B2(2)*H+B2(3)*T+B2(4)*(BDEP(I))+B2(5)*
     *    ((BDEP(I))**2)+B2(6)*(H*T)+B2(7)*(H*WDTH/2.0)+
     *    B2(8)*((BDEP(I))*AD)
C
      IF (WDTH.LE.1800.0) THEN
       AL=AL1
       RO=RO1
       BT=DEXP(BT1)
      ELSE
C
      IF (WDTH.GE.2200.0) THEN
       AL=AL2
       RO=RO2
       BT=DEXP(BT2)
      ELSE
C
       BT1=DEXP(BT1)
       BT2=DEXP(BT2)
       AL=(AL1*(2200.0-WDTH)+AL2*(WDTH-1800.0))/400.0
       RO=(RO1*(2200.0-WDTH)+RO2*(WDTH-1800.0))/400.0
       BT=(BT1*(2200.0-WDTH)+BT2*(WDTH-1800.0))/400.0
       ENDIF
       ENDIF
C
      IF(AL.LE.0.0.OR.RO.LE.0.0.OR.BT.LE.0.0) GOTO 61
      DO 24 K=1,NWL
      VERTM=H*AL*DEXP((RO*2*DIST(K)/WDTH)**BT)
      H2D(K)=VERTM
   24 CONTINUE
C
   61 CONTINUE
C
      RETURN
      END
C*********************************************************************
      SUBROUTINE DELTAH(SUMDH,DELH)
C*********************************************************************
      IMPLICIT REAL*8(A-H,O-Z)
      DIMENSION SUMDH(2)
      COMMON/NPROF1/NLAY
```

```
      COMMON/NPROF2/NELEM(10)
      COMMON/PROF/TH(10)
      COMMON/SUCTION/DELPF(96,2),Z(96),ZM(96),PFAVG(96,2)
      COMMON/SUCI/GAMMH(10)
C
      DO 20 J=1,2
      SUMDH(J)=0.
      IF(J.EQ.1) F=0.8
      IF(J.EQ.2) F=0.5
      iii=0
      do 28 jj=1,nlay
      do 38 k=1,nelem(jj)
      i=iii+k
      OBC=0.
      DELZ=Z(I+1)-Z(I)
      DELPF(I,J)=DELPF(I,J)*GAMMH(jj)
      IF(ZM(I).LT.40.) GOTO 200
      SIGMAF=ZM(I)*(1.+2.*ZK0(PFAVG(I,J)))/3.
      gamms=1.2*gammh(jj)
      OBC=GAMMS*DLOG10(SIGMAF/40.)
      IF((SIGMAF/40.).LT.1) OBC=0.
      DELPF(I,J)=DELPF(I,J)-OBC
      IF(DELPF(I,J).LT.0) DELPF(I,J)=0.
  200 CONTINUE
      SUMDH(J)=F*DELZ*DELPF(I,J)+SUMDH(J)
   38 continue
      iii=i
   28 continue
   20 CONTINUE
      delh=sumdh(1)+sumdh(2)
C
      RETURN
      END
C***********************************************************************
      SUBROUTINE REX3(DM,DMX,DMN,TZERO,PFROOT,NEL,TIM)
C***********************************************************************
C     REX3.FOR A PROGRAM TO CALCULATE THE pF DISTRIBUTION WITH DEPTH
C     ASSUMING A Root EXtraction FUNCTION AND DESORPTION CURVE.
C
C     TSAT = SATURATED VOLUMETRIC MOISTURE CONTENT
C     THETA(I) = MOISTURE CONTENT OF THE ith LAYER
C     PF(I) = SUCTION IN pF OF THE ith LAYER
C     DTIM = TIME STEP
C     TZERO = EQUILIBRIUM MOISTURE CONTENT OF PROFILE
C     ZR = DEPTH OF THE ROOT ZONE cms
C     DW = MOISTURE DEPTH REMOVED DURING ONE TIME STEP.
C***********************************************************************
      IMPLICIT REAL*8(A-H,O-Z)
      DIMENSION THETA(96),PF(96)
      DIMENSION THOUT(96,0:50),PFOUT(96,0:50)
      COMMON/TDES/TS,AAWL,XXWL
      COMMON/ROOT/ZR
      COMMON/SUCTION/DELPF(96,2),Z(96),ZM(96),PFAVG(96,2)
      COMMON/NPROF1/NLAY
      COMMON/NPROF2/NELEM(10)
      COMMON/PROF/TH(10)
      DATA PF1/100.0/,PF2/300./
C
      CALL IMDF1(DM,DMX,TZERO,THETA,NEL,TIM)
C
      IP=0
      SDW=0.
      IFLW=0
      PF3=10.**PFROOT
C
      AWZ=DMX-DMN
      DIFFD=DMX-DM
C
```

```
      JJJ=0
      DO 9 J=1,NLAY
      DO 11 M=1,NELEM(J)
      I=JJJ+M
      PF(I)=FPF(TS,AAWL,XXWL,THETA(I),0)
      PFOUT(I,0)=DLOG10(PF(I))
      THOUT(I,0)=THETA(I)
   11 CONTINUE
      JJJ=I
    9 CONTINUE
C
      DO 500 ISTEP=1,9999999
C
C     Calculate the change in total soil moisture depth at the
C     current time step, given the functional form.
C
      QW=0.1
C
C     Determine the change in moisture depth for each soil layer
C
      JJJ=0
      DO 19 J=1,NLAY
      DO 21 M=1,NELEM(J)
      I=JJJ+M
      IF(PF(I).LE.PF2) ALPH=1.
      IF(PF(I).GT.PF2.AND.PF(I).LE.PF3) ALPH=(PF3-PF(I))/(PF3-PF2)
      IF(PF(I).GT.PF3) ALPH=0.
      DELZ=Z(I+1)-Z(I)
      DW=ALPH*2.*QW*(DELZ-(Z(I+1)**2-Z(I)**2)/(2.*ZR))/ZR
      IF(DW.LT.0.) dw=0.
      SDW=SDW+DW
      THETA(I)=THETA(I)-DW/DELZ
      PF(I)=FPF(TS,AAWL,XXWL,THETA(I),0)
   21 CONTINUE
      JJJ=I
   19 CONTINUE
C
C     Obtain the the water depth/pF vector when the water depth has
C     reached the mean value and also when the dry state has been
C     reached.  At this point we exit the moisture extraction loop.
C
      IF(SDW.GE.DIFFD.AND.IFLW.EQ.0) THEN
      IP=IP+1
      JWET=IP
      IFLW=1
      DO 6 I=1,NEL
      THOUT(I,IP)=THETA(I)
    6 PFOUT(I,IP)=DLOG10(PF(I))
      ENDIF
C
      IF(SDW.GE.AWZ) THEN
      IP=IP+1
      JDRY=IP
      DO 7 I=1,NEL
      THOUT(I,IP)=THETA(I)
    7 PFOUT(I,IP)=DLOG10(PF(I))
      GOTO 600
      ENDIF
C
  500 CONTINUE
C
  600 CONTINUE
C
      DO 80 I=1,NEL
      DELPF(I,1)=PFOUT(I,JWET)-PFOUT(I,0)
      DELPF(I,2)=PFOUT(I,JDRY)-PFOUT(I,JWET)
      PFAVG(I,1)=(PFOUT(I,0)+PFOUT(I,JWET))/2.
      PFAVG(I,2)=(PFOUT(I,JWET)+PFOUT(I,JDRY))/2.
```

```
   80 CONTINUE
C
      RETURN
      END
C***********************************************************************
      SUBROUTINE IMDF1(DM,DMX,TZERO,THETA,NEL,TIM)
C***********************************************************************
C     Determine the initial moisture profile.
C***********************************************************************
      IMPLICIT REAL*8(A-H,O-Z)
      DIMENSION THETA(96),PFS(3,3)
      COMMON/ROOT/ZR
      COMMON/TDES/TS,AAWL,XXWL
      COMMON/IFL/IFLG1,IFLG2
      COMMON/NPROF1/NLAY
      COMMON/NPROF2/NELEM(10)
      COMMON/PROF/TH(10)
      COMMON/SUCTION/DELPF(96,2),Z(96),ZM(96),PFAVG(96,2)
      DATA PFS/2.0,2.3,2.0,
     *         2.2,2.5,2.2,
     *         2.3,2.6,2.3/
C
      z(1)=0.0
      zz=0.0
      jjj=1
      do 8 i=1,nlay
      do 18 j=1,nelem(I)
      jj=jjj+j
      z(jj)=zz+th(I)/nelem(I)
      zz=z(jj)
   18 continue
      jjj=jj
    8 continue
      nel=jjj-1
c
      DO 12 I=1,nel
      zm(i)=(z(i+1)+z(i))/2.
   12 continue
c
      DO 29 I=1,3
      DO 19 J=1,3
      IF(IFLG1.EQ.I.AND.IFLG2.EQ.J) THEN
      TFCAPP=PFS(I,J)
      ENDIF
   19 CONTINUE
   29 CONTINUE
      IF(TIM.GE.10.0) THEN
      TFCAPP=TFCAPP
      ELSE
      IF(TIM.GE.-20.0) THEN
      TFCAPP=TFCAPP+.2
      ELSE
      TFCAPP=TFCAPP+.4
      ENDIF
      ENDIF
C
      TFCAPP=10.0**TFCAPP
      TFCAPP=TS/(1+AAWL*(TFCAPP**XXWL))
C
      DIFFD=DMX-DM
      TMAX=2.*DIFFD/ZR+TZERO
C
      IF(TMAX.GT.TFCAPP) THEN
C
C     If the new moisture depth ZMAX produces a moisture content at the
C     surface TMAX that is greater than the field capacity moisture
C     TFCAP then determine the depth of soil at field capacity ZFCAP
C     then calculate the distribution of THETA with depth, a weighted
```

```
C     average procedure is used in the layer in which ZFCAP occurs.
C
      DIFFT=TFCAPP-TZERO
      ZFCAP=(DIFFD/DIFFT)*2.-ZR
C
      do 120 i=1,nel
      DZ=Z(I+1)-Z(I)
      DELTZ=DIFFT/(ZR-ZFCAP)
      IF(ZFCAP.GT.Z(I+1)) THEN
      THETA(I)=TFCAPP
      GOTO 120
      ENDIF
      IF(ZFCAP.GT.Z(I).AND.ZFCAP.LT.Z(I+1)) THEN
      DTHETA=0.5*(Z(I+1)-ZFCAP)*DELTZ
      T=TFCAPP-DTHETA
      THETA(I)=(T*(Z(I+1)-ZFCAP)+TFCAPP*(ZFCAP-Z(I)))/DZ
      GOTO 120
      ENDIF
      DTHETA=((Z(I+1)+Z(I))/2.-ZFCAP)*DELTZ
      THETA(I)=TFCAPP-DTHETA
      IF(ZM(I).GT.ZR) THETA(I)=TZERO
  120 CONTINUE
      ELSE
C
C     Condition where ZMAX does not produce a moisture content at
C     the surface that is greater than the moisture content at field
C     capacity.
C
      DO 125 I=1,nel
      DTHETA=ZM(I)*(TMAX-TZERO)/ZR
      THETA(I)=TMAX-DTHETA
      IF(ZM(I).GT.ZR) THETA(I)=TZERO
  125 CONTINUE
      ENDIF
C
      RETURN
      END
C***********************************************************************
      FUNCTION ZK0(APF)
C***********************************************************************
      IMPLICIT REAL*8(A-H,O-Z)
      IF(APF.LT.3.) ZK0=1.0
      IF(APF.GT.4.5) ZK0=0.
      IF(APF.GE.3.AND.APF.LE.4.5) ZK0=1.-(1./1.5)*(APF-3.)
      RETURN
      END
C***********************************************************************
      FUNCTION FPF(TS,AAL,XXL,THET,KPF)
C***********************************************************************
      IMPLICIT REAL*8(A-H,O-Z)
C
      FPF=((TS-THET)/(AAL*THET))**(1/XXL)
      IF(KPF.EQ.1) FPF=DLOG10(FPF)
      RETURN
      END
C***********************************************************************
      FUNCTION WDTMI(T,WDFCAP)
C***********************************************************************
      IMPLICIT REAL*8(A-H,O-Z)
      DIMENSION S1(3),S2(3)
C
      DATA S1/.039337,.449079,.062651/
      DATA S2/1.357033,.30456,59.53593/
C
      GAMMA=S1(1)*WDFCAP+S2(1)
      D1=S1(2)*WDFCAP+S2(2)
      T1=S1(3)*WDFCAP+S2(3)
C
```

```
      TMI=T+60.
      WDTMI=WDFCAP/(1.+(WDFCAP-D1)/(D1*(TMI/T1)**GAMMA))
C
      RETURN
      END
C*********************************************************************
      FUNCTION TIAMPL(TA,WAT)
C*********************************************************************
      IMPLICIT REAL*8(A-H,O-Z)
      DIMENSION XB(4,4),XA(4)
      DATA XB/.007327, -.0001,-.23626, .034308,
     *   17.601, -19.000, -52.811,0.0000,
     *  .057207, .010000, .130077, 0.0000,
     *   16.104, -7.000, 39.558,  1.54771/
C
      DO 100 I=1,4
  100 XA(I)=XB(I,1)*WAT-XB(I,2)*DEXP(-XB(I,3)*WAT)+XB(I,4)
C
      A1=XA(1)
      A2=XA(2)
      A3=XA(3)
      A4=XA(4)
      TIAMPL=A4+A1*DEXP(-((TA-A2)/A3)**2)
C
      RETURN
      END
```

APPENDIX I

DESIGN AND CONSTRUCTION OF VERTICAL MOISTURE BARRIERS

SITE INVESTIGATION

Site investigation is essential before installing vertical moisture barriers in pavements. Sufficient information must be obtained to enable a safe and economic design. The primary objectives of the investigation are:

1. to determine the sequence, thickness and lateral extent of the soil strata, and
2. to collect representative samples of the soils for identification, classification, and for use in laboratory tests to determine relevant soil parameters.

Before the start of the comprehensive site investigation, a study of available geological maps and U.S. Soil Conservation Service county soil survey reports should be made and an inspection of the site and the surrounding area should be made on foot. Valuable information regarding the nature of subsurface soil conditions can be obtained by examining existing excavations, river banks, quarries, and road or railway cuts.

In dry weather, the surface of expansive soils is characterized by deep cracking. Maximum crack depth in a subgrade soil is a very important parameter in the design of vertical moisture barriers in pavements on expansive soils. If the rooting depth of resident vegetation is known, an estimate for the crack depth can be made. Generally, grass roots cause cracks to a depth of 4-8 ft. Where trees are growing or have a grown in the past, cracks penetrate to the depth of the root zone plus about 2 ft more. Root depths may be determined from borings by logging the samples taken for root fibers. The depth of the last sample where fibers were still found is an estimate of the root depth. Existing structures should be examined for signs of damage due to soil movement. As the drainage pattern in the area affects the availability of water to the subgrade, the drainage condition of the area should also

be obtained. Different longitudinal drainage conditions (normal, ponded, or slope) found along highway pavements are shown in Figure 129.

Based on the information obtained from the site visit, a comprehensive site investigation should be planned. Planning should include the determination of depth and location of borings. The number, location, and depth of boreholes should enable the basic soil layering structure of the site to be determined and significant irregularities in the subsurface conditions to be detected. The greater the degree of variability of the subsurface conditions, the greater the number of boreholes are required. Borings may be made in several stages. In the first stage, borings may be widely spaced. Based upon the findings from the initial borings, additional borings may be made between the initial borings to define the soil conditions in better detail. As a rule of thumb, borings should be placed every 100 m (or yards). They should be farther apart in uniform soils and closer together where the soil deposits are more variable. In order to carry out laboratory tests, it is recommended to collect Shelby tube soil samples at two foot intervals in all borings. Borings should be at least twice as deep as the expected depth of the moisture barrier.

For the samples collected from borings, the following laboratory tests should be carried out:

1. Atterberg limits,
2. percentage passing no. 200 sieve,
3. percent of fine clay (grain size less than 0.002 mm) from hydrometer analysis,
4. filter paper suction,
5. specific gravity of soil particles for use in the hydrometer test,
6. dry density,
7. natural moisture content,
8. laboratory suction using pressure plate apparatus (optional), and
9. cation exchange capacity (optional).

After an investigation has been completed and the results of laboratory tests are available, the subsurface conditions discovered in each borehole should be summarized in the

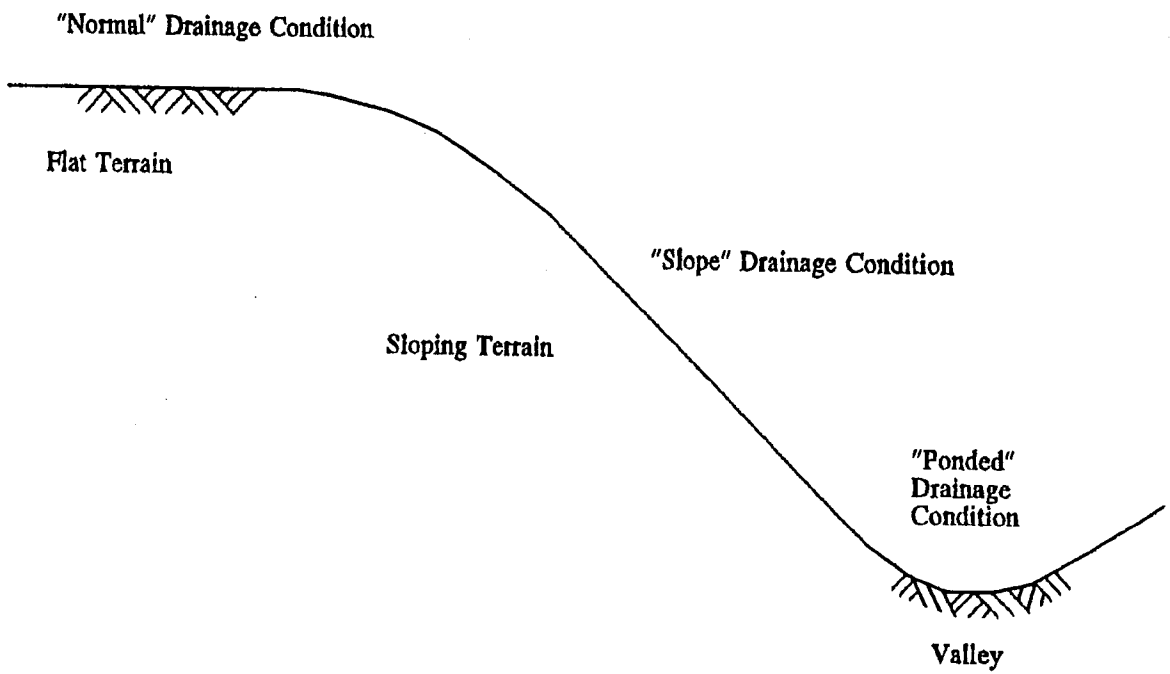

Figure 129. Types of Longitudinal Drainage Conditions along Highway Pavement.

form of a borehole log. The log is prepared with reference to a vertical scale. The following details should be shown in a borehole log:

1. location, boring number, date of boring, and elevation of the ground surface at the boring and datum used;
2. date started and completed and interruptions;
3. name of driller and soils engineer or technician;
4. any unusual conditions noted or any other conditions observed which might be pertinent;
5. a detailed description of each stratum and the levels of strata boundaries;
6. the level at which boring was terminated; and
7. results of laboratory or in situ tests.

In order to identify the locations where moisture barriers are effective, longitudinal profiles showing the three soil types (cracked or pervious, moderately cracked, and tight) should be drawn along the length of the project. A method of identifying these soils conditions is given below in this appendix. In reducing the development of roughness in pavements, vertical moisture barriers are effective only when the subgrade soil is moderately cracked (when the unsaturated permeability ranges between 0.00005 and 0.001 cm^2/sec). In cracked or highly pervious subgrade soils (when the unsaturated permeability is greater than 0.001 cm^2/sec) or tight subgrade soils (when the unsaturated permeability is less than 0.00005 cm^2/sec) vertical moisture barriers are not effective. Moisture barriers should be placed only where moderately cracked soils are shown on the longitudinal soil profile drawn along the length of the project.

METHOD OF ANALYSIS

1. Perform simple linear regression for the data obtained from laboratory suction tests using percentage gravimetric water content (as a decimal) as the independent variable and solid suction (pF) as the dependent variable and estimate the slope of the straight line. If the laboratory suction results are not available, the following equation can be used to estimate the slope of the straight line:

$$S = -20.288 + 0.1551\,(LL) - 0.1167\,(PI) + 0.0684\,(\#200) \qquad (34)$$

where,

S = Slope of the straight line (suction-water-content slope). This should be a negative number which ranges between 0 and -20.

LL = Liquid limit, in percent (a number between 0 and 100).

PI = Plasticity index, in percent (a number between 0 and 100).

#200 = Percentage passing the no. 200 sieve (a number between 0 and 100).

2. Estimate the activity and the cation exchange activity of the soils using the following relationships:

   Activity = PI% fine clay

   Cation Exchange activity = CEC/% fine clay

where,

PI = plasticity index,

CEC = cation exchange capacity, and

% fine clay = % passing 0.002 mm size/% passing #200.

Cation exchange capacity can be obtained directly from the cation exchange capacity test or from the following relationship:

$$CEC = (PL\%)^{1.17}\ \text{meq/100 gm} \qquad (35)$$

where,

PL = plastic limit, in percent.

3. Plot the activity and cation exchange activity of soils on McKeen's chart for the prediction of the suction compression index (SCI) and read the corresponding values of the suction compression index of soils with 100% fine clay content. The McKeen's chart is shown in Figure 130 and the values of SCI for each region in the chart is given in Table 55. Obtain the actual suction compression index for each soil sample by multiplying the suction compression index obtained from the chart by the fine clay percentage (as a decimal) of each soil sample.

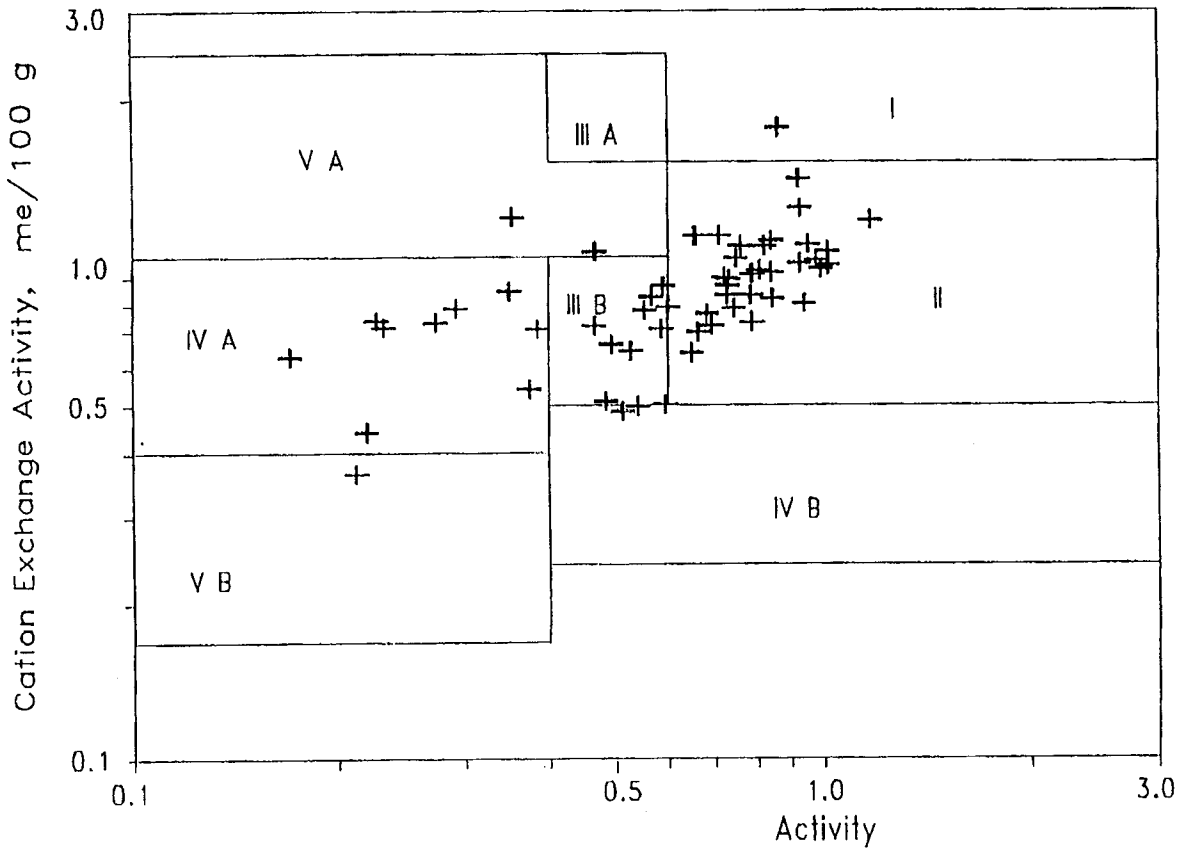

Figure 130. McKeen's Chart for the Prediction of Suction Compression Index.

Table 55. SCI Values from McKeen's Chart.

Region	SCI
I	0.220
II	0.163
III A	0.096
III B	0.096
IV A	0.061
IV B	0.061
V A	0.033
V B	0.033

4. Estimate the diffusion coefficient from the following relationship:

$$\alpha = 0.0029 - 0.000162\,(S) - 0.0122\,(SCI) \tag{36}$$

where,

α = diffusion coefficient (cm^2/sec),

S = suction-water-content slope (a negative number), and

SCI = suction compression index (a positive number between 0 and 0.22).

5. Estimate the unsaturated permeability from the following relationship:

$$P = \frac{\alpha \gamma_d}{|S| \gamma_w} \tag{37}$$

where,

α = diffusion coefficient (cm^2/sec),

γ_w = density of water,

γ_d = dry density of soil,

$|S|$ = absolute value of the suction-water-content slope, and

P = unsaturated permeability (cm^2/sec).

6. Determine the soil type (cracked or highly permeable, medium cracked or moderately permeable, or tightly closed cracks or minimally permeable) based on the estimated unsaturated permeability. The ranges of unsaturated permeability for each soil type are given in Table 56.

Table 56. Unsaturated Permeability in Different Soil Types.

Soil Type	Unsaturated Permeability (cm^2/sec)
Cracked or pervious	> 0.001
Medium cracked	0.00005 - 0.001
Tight	< 0.00005

7. Vertical moisture barriers are not effective in tight or cracked subgrade soils under any of the drainage conditions. They are effective in medium cracked soils in all climates and under all drainage conditions except for the following two conditions:
   1. extremely dry climates, and
   2. semi-arid climates under "ponded" drainage conditions.
8. In locations where vertical moisture barriers are effective, the depth of the barrier should be greater than or at least equal to the depth of the root zone. Where gravel or sand seams are present, vertical moisture barriers should go below those seams.
9. Using the subgrade soil investigation report and longitudinal soil profiles, determine the locations where moisture barriers are effective and the depth of the barrier needed for each location and provide vertical moisture barriers accordingly. However, it is not recommended to provide vertical moisture barriers less than 0.25 miles long.

GUIDELINES FOR THE CONSTRUCTION OF VERTICAL MOISTURE BARRIERS

1. The barrier should be placed along the edge of the paved surface of the roadway. The barrier should normally be 8 ft (2.4 m) deep. A greater depth may be required by site conditions revealed by the site investigation.
2. The fabric barrier should be placed at the inside edge of the trench excavated at the edge of the paved surface of the roadway. The trench should be backfilled with a graded material. The top one foot of the trench should consist of base materials or lean concrete.
3. Sand has been found to be a poor backfill material because it tends to settle after being placed, leaving a void beneath the trench cap. A good test for a candidate backfill material is to place it in a concrete cylinder mold and shake it. If it reduces volume due to the shaking, it will leave a void and should not be used. Lightweight aggregate has been found to be an acceptable backfill material in the Dallas district.
4. An impermeable asphalt concrete layer should be placed over the pavement and it should be extended beyond the barrier.
5. Construction joints including the lane-shoulder joint in the asphalt concrete layer should be properly sealed so that water does not penetrate to the subgrade from the surface.
6. Proper drainage should be maintained in the drainage ditches beside the roadway. In roadway sections where frequent maintenance is required to provide proper drainage, side ditches may be paved with concrete.
7. Whenever a crack appears in the pavement surface, it should be sealed immediately.